General Disclaimer

One or more of the Following Statements may affect this Document

- This document has been reproduced from the best copy furnished by the organizational source. It is being released in the interest of making available as much information as possible.

- This document may contain data, which exceeds the sheet parameters. It was furnished in this condition by the organizational source and is the best copy available.

- This document may contain tone-on-tone or color graphs, charts and/or pictures, which have been reproduced in black and white.

- This document is paginated as submitted by the original source.

- Portions of this document are not fully legible due to the historical nature of some of the material. However, it is the best reproduction available from the original submission.

Produced by the NASA Center for Aerospace Information (CASI)

(NASA-CR-150889) SPACE SHUTTLE PLUME SIMULATION APPLICATION. RESULTS AND MATH MODEL Final Report (Northrop Services, Inc., Huntsville, Ala.) 209 p HC A10/MF A01 CSCL 21H G3/16
N79-16055
Unclas
43314

SPACE SHUTTLE PLUME/SIMULATION APPLICATION

FINAL REPORT

RESULTS AND MATH MODEL

Prepared for:

NATIONAL AERONAUTICS AND SPACE ADMINISTRATION
GEORGE C. MARSHALL SPACE FLIGHT CENTER
Science and Engineering Directorate
Under Contract NAS8-32524

Prepared by:

NORTHROP SERVICES, INC.

P. O. Box 1484 Huntsville, Alabama 35807 (205) 837-0580

NSi

FOREWORD

This report presents the results of work performed by Northrop Services, Inc. Engineering Technology Group for the Marshall Space Flight Center under Contract NAS8-32524. The NASA technical monitors for this contract are Mr. K. Blackwell and Mr. J. Sims. The authors wish to acknowledge their valuable assistance, direction and contributions to the successful completion of this study.

TABLE OF CONTENTS

Section	Title	Page
	FOREWORD	ii
	SYMBOLS AND NOTATION	iii
I	INTRODUCTION	1-1
II	WIND TUNNEL MODEL	2-1
III	TEST CONDITIONS	3-1
IV	NOZZLE CALIBRATION	4-1
V	PLUME SIMULATION	5-1
VI	DATA ANALYSIS	6-1
VII	TEST RESULTS	7-1
VIII	BASE MATH MODEL	8-1
IX	FOREBODY MATH MODEL	9-1
X	CONCLUSIONS	10-1
XI	RECOMMENDATIONS	11-1
XII	REFERENCES	12-1
	APPENDIX	A-1

LIST OF ILLUSTRATIONS

Figure	Title	Page
2-1	IA119 MODEL INSTALLATION	2-2
2-2	FLOW THROUGH NOZZLE AIR SUPPLY STRUTS — IA119 MODEL	2-3
2-3	MPS NOZZLE (N_{104}) INTERNAL CONTOURS	2-4
2-4	SRB NOZZLE (N_{88}) INTERNAL CONTOURS	2-5
3-1	POWER VARIATION RUNS (M_∞ = 0.6)	3-3
3-2	POWER VARIATION RUNS (M_∞ = 0.8)	3-4
3-3	POWER VARIATION RUNS (M_∞ = 0.9)	3-5
3-4	POWER VARIATION RUNS (M_∞ = 0.95)	3-6
3-5	POWER VARIATION RUNS (M_∞ = 1.05)	3-7
3-6	POWER VARIATION RUNS (M_∞ = 1.10)	3-8
3-7	POWER VARIATION RUNS (M_∞ = 1.15)	3-9
3-8	POWER VARIATION RUNS (M_∞ = 1.25)	3-10
3-9	POWER VARIATION RUNS (M_∞ = 1.40)	3-11
3-10	SCHEDULE 6 ELEVON DEFLECTIONS	3-12
3-11a	ELEVON SCHEDULE	3-13
3-11b	ELEVON SCHEDULE	3-14
3-11c	ELEVON SCHEDULE	3-15
3-11d	ELEVON SCHEDULE	3-16
3-11e	ELEVON SCHEDULE	3-17
4-1	SSME NOZZLE CALIBRATION DATA	4-3
4-2	SRB NOZZLE CALIBRATION DATA	4-4
4-3	SRB NOZZLE CALIBRATION DATA	4-5
4-4	SRB NOZZLE CALIBRATION DATA	4-6
4-5	SRB NOZZLE CALIBRATION DATA	4-7
4-6	SRB NOZZLE CALIBRATION DATA	4-8
4-7	SRB NOZZLE CALIBRATION DATA	4-9
4-8	SRB NOZZLE CALIBRATION DATA	4-10
4-9	SRB NOZZLE CALIBRATION DATA	4-11
4-10	SRB NOZZLE CALIBRATION DATA	4-12
4-11	SRB NOZZLE CALIBRATION DATA	4-13

LIST OF ILLUSTRATIONS (Continued)

Figure	Title	Page
4-12	SRB NOZZLE CALIBRATION DATA	4-14
4-13	SRB NOZZLE CALIBRATION DATA	4-15
4-14	SRB NOZZLE CALIBRATION DATA	4-16
5-1	PROTOTYPE POSSIBILITY CURVE	5-3
5-2	SIMILARITY PARAMETER EXPONENT	5-4
5-3	PLUME FLOW FIELD AREAS	5-5
5-4	FAR FIELD DATA CORRELATION	5-6
5-5	SRB PROTOTYPE PLUME ANGLE	5-7
5-6	SRB PROTOTYPE PLUME RATIO OF SPECIFIC HEATS	5-8
5-7	SSME PROTOTYPE δ_j AND RATIO OF SPECIFIC HEATS	5-9
6-1	PLUME FLOW FIELD AREAS	6-8
6-2	IA119 MODEL ORBITER BASE CONFIGURATION	6-9
6-3	MODEL AND PROTOTYPE SSME EXTERNAL CONTOUR	6-10
6-4	ORBITER SSME NOZZLE PRESSURE INSTRUMENTATION	6-11
6-5	SSME NOZZLE HINGE MOMENT DEFINITION	6-12
6-6	SSME NOZZLE HINGE MOMENT NOMENCLATURE	6-13
6-7	ORBITER BASE PRESSURE INSTRUMENTATION	6-14
6-8	ORBITER BASE PLATE RELATIVE AREAS	6-15
6-9	OMS POD AREAS	6-16
6-10	ORBITER BODY FLAP PRESSURE INSTRUMENTATION	6-17
6-11	ORBITER FUSELAGE PRESSURE INSTRUMENTATION	6-18
6-12	ORBITER WING PRESSURE INSTRUMENTATION	6-19
6-13	ORBITER WING PRESSURE INSTRUMENTATION FOR WING POWER DELTAS	6-20
6-14	COMPARISON OF GAUGE AND PRESSURE DATA — WING NORMAL FORCE	6-21
6-15	COMPARISON OF GAUGE AND PRESSURE DATA — WING TORSION MOMENT	6-22
6-16	COMPARISON OF GAUGE AND PRESSURE DATA — WING BENDING MOMENT	6-23
6-17	COMPARISON OF GAUGE AND PRESSURE DATA — INBOARD ELEVON HINGE MOMENT	6-24

LIST OF ILLUSTRATIONS (Concluded)

Figure	Title	Page
6-18	COMPARISON OF GAUGE AND PRESSURE DATA — OUTBOARD ELEVON HINGE MOMENT	6-25
6-19	WING AND ELEVON FORCE AND MOMENT SIGN CONVENTION	6-26
6-20	VERTICAL TAIL INSTRUMENTATION LOCATION	6-27
6-21	VERTICAL TAIL AREAS	6-28
6-22	VERTICAL STABILIZER FORCE AND MOMENT SIGN CONVENTION	6-29
6-23	SRB BASE INSTRUMENTATION	6-30
6-24	SRB NOZZLE CONFIGURATION	6-31
6-25	SRB NOZZLE HEAT SHIELD AND COMPLIANCE RING	6-32
6-26	SRB NOZZLE HINGE MOMENT NOMENCLATURE	6-33
6-27	SRB FOREBODY INSTRUMENTATION	6-34
6-28	EXTERNAL TANK BASE PRESSURE INSTRUMENTATION LOCATION	6-35
8-1	ET BASE AXIAL FORCE	8-7
8-2	ET BASE PRESSURE COEFFICIENTS	8-8
8-3	TOTAL ORBITER BASE	8-9
8-4	EXTERNAL TANK BASE AXIAL FORCE	8-10
8-5	TOTAL BASE	8-11

LIST OF TABLES

Table	Title	Page
3-1	IA119 POWER ON-OFF DATA SETS (M_∞ = 0.6)	3-18
3-2	IA119 POWER ON-OFF DATA SETS (M_∞ = 0.8)	3-19
3-3	IA119 POWER ON-OFF DATA SETS (M_∞ = 0.9)	3-20
3-4	IA119 POWER ON-OFF DATA SETS (M_∞ = 0.95)	3-21
3-5	IA119 POWER ON-OFF DATA SETS (M_∞ = 1.05)	3-22
3-6	IA119 POWER ON-OFF DATA SETS (M_∞ = 1.10)	3-23
3-7	IA119 POWER ON-OFF DATA SETS (M_∞ = 1.15)	3-24
3-8	IA119 POWER ON-OFF DATA SETS (M_∞ = 1.25)	3-25
3-9	IA119 POWER ON-OFF DATA SETS (M_∞ = 1.40)	3-26
5-1	ASCENT TRAJECTORY AND SRB-SSME CHAMBER PRESSURE	5-10
6-1	SSME #1 PRESSURE INSTRUMENTATION LOCATION AND AREAS	6-36
6-2	SSME #2 PRESSURE INSTRUMENTATION LOCATION AND AREAS	6-37
6-3	SSME #3 PRESSURE INSTRUMENTATION LOCATION AND AREAS	6-38
6-4	ORBITER BASE PLATE PRESSURE INSTRUMENTATION LOCATION AND AREAS	6-39
6-5	ORBITER UPPER BODY FLAP PRESSURE INSTRUMENTATION LOCATION AND AREAS	6-40
6-6	ORBITER FOREBODY AND OMS POD INSTRUMENTATION LOCATION	6-41
6-7	RIGHT WING PRESSURE INSTRUMENTATION LOCATION AND AREAS	6-42
6-8	RIGHT ELEVON INBOARD PRESSURE INSTRUMENTATION LOCATION AND AREAS	6-43
6-9	RIGHT ELEVON OUTBOARD PRESSURE INSTRUMENTATION LOCATION AND AREAS	6-44
6-10	VERTICAL TAIL PRESSURE INSTRUMENTATION LOCATION AND AREAS	6-45
6-11	RIGHT SRB NOZZLE PRESSURE INSTRUMENTATION LOCATION AND AREAS	6-46
6-12	LEFT SRB FOREBODY PRESSURE INSTRUMENTATION LOCATION	6-47
6-13	EXTERNAL TANK BASE PRESSURE INSTRUMENTATION	6-48
6-14	REFERENCE DIMENSIONS	6-49
8-1	BASE AXIAL FORCE COEFFICIENT	8-12
8-2	BASE NORMAL FORCE COEFFICIENT	8-13
8-3	BASE PITCHING MOMENT COEFFICIENT	8-14

LIST OF TABLES (Continued)

Table	Title	Page
8-4	BASE AXIAL FORCE COEFFICIENT	8-15
8-5	BASE NORMAL FORCE COEFFICIENT	8-16
8-6	BASE PITCHING MOMENT COEFFICIENT	8-17
8-7	BASE AXIAL FORCE COEFFICIENT	8-18
8-8	BASE NORMAL FORCE COEFFICIENT	8-19
8-9	BASE PITCHING MOMENT COEFFICIENT	8-20
8-10	BASE AXIAL FORCE COEFFICIENT	8-21
8-11	BASE NORMAL FORCE COEFFICIENT	8-22
8-12	BASE PITCHING MOMENT COEFFICIENT	8-23
8-13	BASE AXIAL FORCE COEFFICIENT	8-24
8-14	BASE NORMAL FORCE COEFFICIENT	8-25
8-15	BASE PITCHING MOMENT COEFFICIENT	8-26
8-16	BASE COEFFICIENT PARTIALS	8-27
8-17	BASE AXIAL FORCE (LBS)	8-28
8-18	BASE NORMAL FORCE (LBS)	8-29
8-19	BASE PITCHING MOMENT	8-30
8-20	BASE AXIAL FORCE PARTIALS	8-31
8-21	BASE NORMAL FORCE PARTIALS	8-32
8-22	BASE PITCHING MOMENT PARTIALS	8-33
8-23	IA-119 BASE COEFFICIENT TOLERANCES	8-34
8-24	BASE MOMENT TOLERANCES	8-35
9-1	SSLV AND ORBITER POWER DELTA - NORMAL FORCE COEFFICIENT - FOREBODY	9-5
9-2	SSLV AND ORBITER POWER DELTA - NORMAL FORCE COEFFICIENT - FOREBODY INBOARD ELEVON GRADIENT - δ_{EI} GREATER THAN NOMINAL	9-7
9-3	SSLV AND ORBITER POWER DELTA - NORMAL FORCE COEFFICIENT - FOREBODY INBOARD ELEVON GRADIENT - δ_{EI} LESS THAN NOMINAL	9-9
9-4	SSLV AND ORBITER POWER DELTA - NORMAL FORCE COEFFICIENT - FOREBODY OUTBOARD ELEVON GRADIENT - δ_{EO} GREATER THAN NOMINAL	9-11

LIST OF TABLES (Concluded)

Table	Title	Page
9-5	SSLV AND ORBITER POWER DELTA - NORMAL FORCE COEFFICIENT - FOREBODY OUTBOARD ELEVON GRADIENT - δ_{E_O} LESS THAN NOMINAL.	9-13
9-6	SSLV AND ORBITER POWER DELTA - PITCHING MOMENT COEFFICIENT - FOREBODY	9-15
9-7	SSLV AND ORBITER POWER DELTA - PITCHING MOMENT COEFFICIENT - FOREBODY - INBOARD ELEVON GRADIENT - δ_{E_I} GREATER THAN NOMINAL	9-17
9-8	SSLV AND ORBITER POWER DELTA - PITCHING MOMENT COEFFICIENT - FOREBODY - INBOARD ELEVON GRADIENT - δ_{E_I} LESS THAN NOMINAL.	9-19
9-9	SSLV AND ORBITER POWER DELTA - PITCHING MOMENT COEFFICIENT - FOREBODY - OUTBOARD ELEVON GRADIENT - δ_{E_O} GREATER THAN NOMINAL	9-21
9-10	SSLV AND ORBITER POWER DELTA - PITCHING MOMENT COEFFICIENT - FOREBODY - OUTBOARD ELEVON GRADIENT - δ_{E_O} LESS THAN NOMINAL.	9-23
9-11	INBOARD ELEVON - HINGE MOMENT COEFFICIENT POWER DELTA. .	9-25
9-12	INBOARD ELEVON POWER DELTA - HINGE MOMENT COEFFICIENT INBOARD ELEVON GRADIENT - δ_{E_I} GREATER THAN NOMINAL . . .	9-27
9-13	INBOARD ELEVON POWER DELTA - HINGE MOMENT COEFFICIENT INBOARD ELEVON GRADIENT - δ_{E_I} LESS THAN NOMINAL.	9-29
9-14	INBOARD ELEVON POWER DELTA - HINGE MOMENT COEFFICIENT OUTBOARD ELEVON GRADIENT - δ_{E_O} GREATER THAN NOMINAL. . .	9-31
9-15	INBOARD ELEVON POWER DELTA - HINGE MOMENT COEFFICIENT OUTBOARD ELEVON GRADIENT - δ_{E_O} LESS THAN NOMINAL	9-33
9-16	VERTICAL TAIL SIDE FORCE POWER DELTA	9-35
9-17	VERTICAL TAIL BENDING MOMENT POWER DELTA	9-37
9-18	VERTICAL TAIL TORSION MOMENT POWER DELTA	9-39
9-19	FOREBODY FORCE COEFFICIENT TOLERANCES - SSLV AND ELEMENTS	9-41
9-20	FOREBODY MOMENT EQUATIONS - SSLV AND ELEMENTS.	9-42
9-21	FOREBODY FORCE TOLERANCES - COMPONENTS	9-43
9-22	FOREBODY MOMENT EQUATIONS - COMPONENTS	9-44

GENERAL NOMENCLATURE

SYMBOL	DEFINITION
ET	Space Shuttle external tank
O	Space Shuttle Orbiter
SRB	Space Shuttle Solid Rocket Booster
SSLV	Space Shuttle Launch Vehicle
Base	Locations on the Space Shuttle where the nozzle exhaust plumes are the primary influence in determining the local pressure environment
Components	Portions of the Orbiter; wing, body flap, etc.
Elements	Primary elements of the SSLV, Orbiter, ET, SRB's
Forebody	Locations on the Space Shuttle where the nozzle exhaust plumes are the secondary influence in determining the local pressure environments

TEST NOMENCLATURE

Symbol	Definition
General:	
C_A	Axial force coefficient
C_{B_V}	Vertical tail bending moment coefficient
C_{B_W}	Wing-root bending-moment coefficient
C_H	Hinge moment coefficient
$C_{H_{E_I}}$	Hinge-moment coefficient for inboard elevon.
$C_{H_{E_O}}$	Hinge-moment coefficient for outboard elevon.
C_ℓ	Rolling moment coefficient
C_M	Pitching moment coefficient
C_N	Normal force coefficient
C_{N_W}	Wing normal-force coefficient
C_{T_V}	Vertical tail torsion moment coefficient
C_{T_W}	Wing-root torsion-moment coefficient
C_Y	Side force coefficient
C_{Y_N}	Yawing moment coefficient
C_{Y_V}	Vertical tail shear force coefficient
L	Reference length, in. or ft. defined in Table 6-14
S	Reference area, ft^2 defined in Table 6-14
	SUBSCRIPTS
B	Base
F	Forebody - fuselage
C_P	Determined using power on pressure coefficient
DEL	Determined using power-on minus power-off delta pressure coefficient
O	Orbiter

TEST NOMENCLATURE

ET	ET
SRB	SRB
PON	Power On
POF	Power Off

GAS DYNAMIC NOMENCLATURE

Symbol	Definition
P_i	Pressure (absolute) at model surface tap i, psia
C_{P_i}	Pressure coefficient for model surface tap i.
ΔC_{P_i}	$C_{P_{Power\ On}} - C_{P_{Power\ Off}}$
P_{c_j}	Chamber pressure (absolute) for nozzle j, psia
P_{e_j}	Exit pressure (absolute) for nozzle j, psia
CPR_j	Chamber-pressure ratio for nozzle j
γ_j	Ratio of specific heats for nozzle J
$P_c/P_{\infty_{ORB}}$	SSME chamber to freestream pressure ratio
$P_c/P_{\infty_{SRB}}$	SRB chamber to freestream pressure ratio
P_c/P_e	Chamber to exit nozzle pressure ratio
P_c/P_{wall}	Chamber to nozzle wall pressure ratio
δ_j	Initial plume expansion angle
N	Exponent of ratio of specific heats and in similarity parameters

Deflections:

δ_{E_I}	Left inboard elevon setting, corrected for load deflection, deg.
δ_{E_O}	Left outboard elevon setting, corrected for load deflection, deg.
γ_{NJ}	Pitch-angle of nozzle-j axis in a plane parallel to the Orbiter plane-of-symmetry, deg.
γ_{N_j}	Pitch-angle of nozzle-j axis in a plane which yaws with the nozzle, deg.
ψ_{N_j}	Yaw-angle of nozzle-j axis in an Orbiter waterplane, deg.

Test Operations:

M	Freestream Mach number.
Re/ft	Freestream unit Reynolds number, ft^{-1}.
q	Freestream dynamic pressure, psf.
P_∞	Freestream static pressure, psia.
P_T	Freestream total pressure, psia.
T	Freestream static temperature, ^oR.
T_T	Freestream total temperature, ^oR.
α	Model angle-of-attack, deg.
β	Model angle-of-sideslip, deg.
$T_{T_{SRB}}$	SRB supply total temperature, ^oR.
$T_{T_{MPS}}$	MPS supply total temperature, ^oR.
$P_{c_{MPS}}$	MPS supply total pressure, psia.
$P_{c_{SRB}}$	SRB supply total pressure, psia.

REVISIONS			
REV SYM	DESCRIPTION	DATE	APPROVAL

Section I

INTRODUCTION

The analysis of pressure and gauge wind tunnel data from Space Shuttle wind tunnel test IA119 was performed to define the aerodynamic influence of the main propulsion system (MPS) and solid rocket booster (SRB) plumes on the total vehicle, elements, and components of the Space Shuttle vehicle during the transonic portion of ascent flight.

Wind tunnel test IA119 was a transonic test of a 0.02 scale model of the Space Shuttle launch vehicle. The wind tunnel test was conducted in the 11 x 11-foot section of the NASA/AMES Research Center Unitary Plan Wind Tunnel. Pressure data were obtained over the aft portions of the wind tunnel model in addition to wing and elevon gauge data.

Air was used as a simulant gas to develop the model exhaust plumes. A portion of the test was devoted to testing at various power levels. Data from the power level portion was used in conjunction with prototype base pressure possibility curves to evaluate nominal power levels to be used during the investigation of changes in model attitude, elevon deflection and nozzle gimbal angle. The simulation parameter used to develop nominal power levels was $[\delta_j \gamma_j^N]_{PROT} = [\delta_j \gamma_j^N]_{MODEL}$ where N varies with Mach number.

The plume induced aerodynamic loads were developed for the Space Shuttle base areas and forebody areas. The base areas include the orbiter base including nozzles, ET base and SRB base. The forebody includes the orbiter areas forward of the base, including the body flap, the wings and elevons, and ET and SRB areas forward of the base.

A math model of the plume induced aerodynamic characteristics was developed for a range of Mach numbers to match the forebody aerodynamic math model. The base aerodynamic characteristics are presented in terms of forces and moments versus attitude. Total vehicle base and forebody aerodynamic characteristics are presented in terms of aerodynamic coefficients for Mach number from 0.6 to 1.4. Element and component base and forebody aerodynamic characteristics are presented for Mach numbers of 0.6, 1.05, 1.1, 1.25 and 1.4. These Mach numbers

are compatible with defined forebody aerodynamic characteristics except for Mach 1.4. The forebody data is available at Mach 1.55. Base and forebody plume induced data is provided at Mach 1.4 because Mach 1.4 was the highest Mach number for which data is available at the present time.

Tolerances were developed for all plume induced aerodynamic characteristics. The tolerances are developed in terms of a math model and include simulation parameter uncertainties, model instrumentation uncertainties, model configuration uncertainties including tunnel-model support interference uncertainties and Reynolds number effects.

Section II

WIND TUNNEL MODEL

The wind tunnel model was a .02 scale space shuttle launch vehicle configuration. The wind tunnel model is designated - 88 OTS Configuration 140C (modified) Jet - Plume Integrated Space Shuttle Vehicle. The wind tunnel model is essentially the same as was used for an earlier Space Shuttle plume test IA19, conducted in 1974. The major difference being that the contoured SSME flow through nozzles were used during the IA119 test and conical SSME nozzles were used during the IA19 test. The orbiter model was the 140C model configuration which generally represents the OV101 orbiter mold lines. The OV102 mold lines have significant differences in the canopy contour, the wing section near the glove-wing fairing, and the elevon contour. Details of the model configuration can be obtained from the pretest report (reference 1).

The model was strut mounted as shown in Figure 2-1. Cold air was supplied through the strut to the SSME and SRB nozzles. An air supply strut was mounted between the ET and orbiter to supply air to the simulated SSME nozzles as shown in Figure 2-2. The SSME nozzles were contoured with an exit plane lip angle of 5 degrees. The SRB nozzles were conical with a lip angle of 27.5 degrees. Schematics of the SSME and SRB nozzle internal contour are presented in Figures 2-3 and 2-4. Calibration data for the nozzles are presented in Section IV. Details of the model configuration can be obtained from the pretest report (reference 1).

The left orbiter wing was strain-gauge instrumented to obtain wing shear forces, root bending moments and torsion moments. The inboard and outboard elevons on the left wing were also separately strain-gauge instrumented to obtain hinge moments. The right orbiter wing and elevons were pressure instrumented. All base, nozzle, and portions of each element forebody were pressure instrumented.

The flow through MPS nozzles and SRB nozzles were capable of being set at various gimbal-angle positions and several gimbal patterns were investigated. The inboard and outboard elevons were also capable of being set at various deflection angles and data were obtained for a series of elevon deflection combinations.

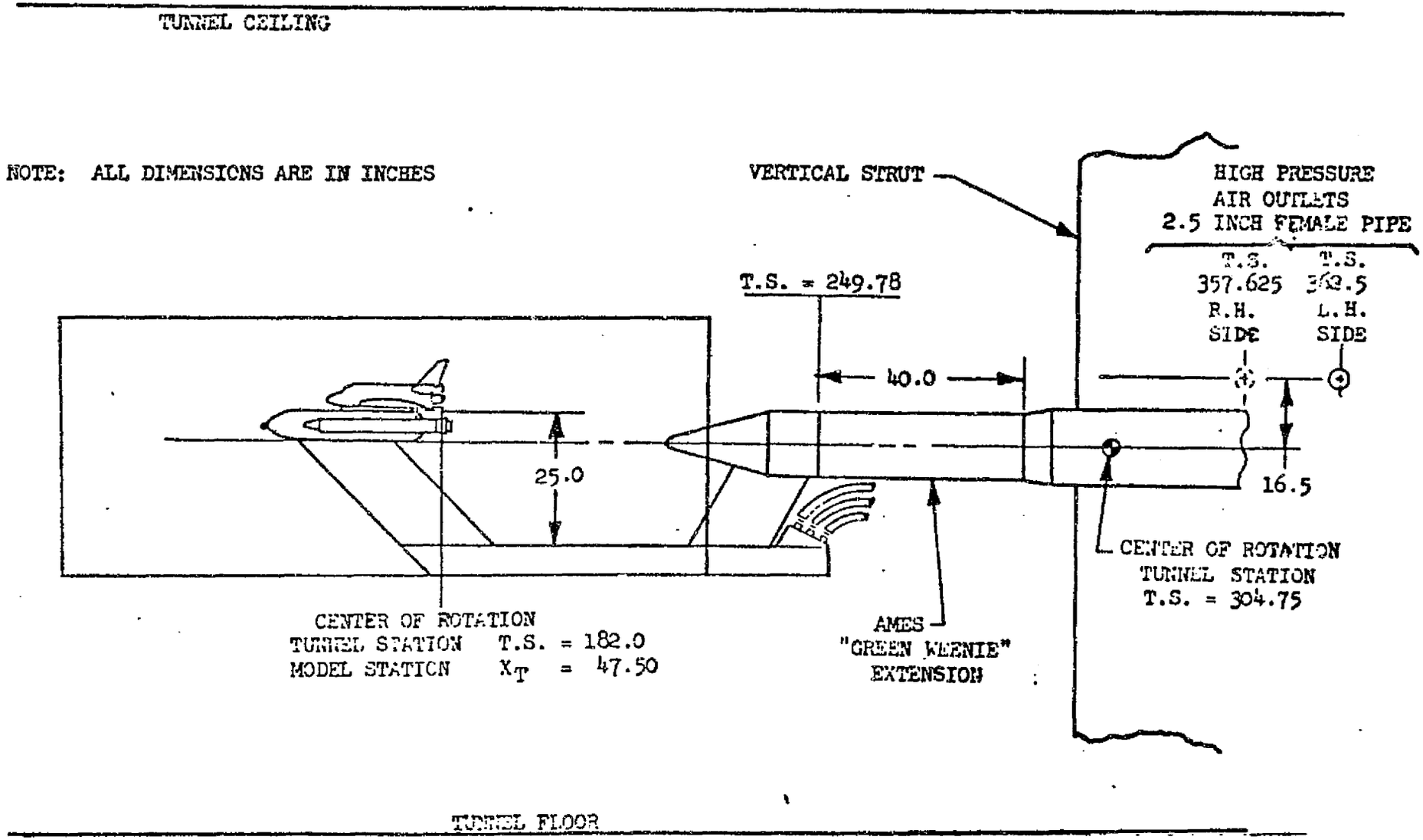

Figure 2-1. IA119 MODEL INSTALLATION

ORIGINAL PAGE IS
OF POOR QUALITY

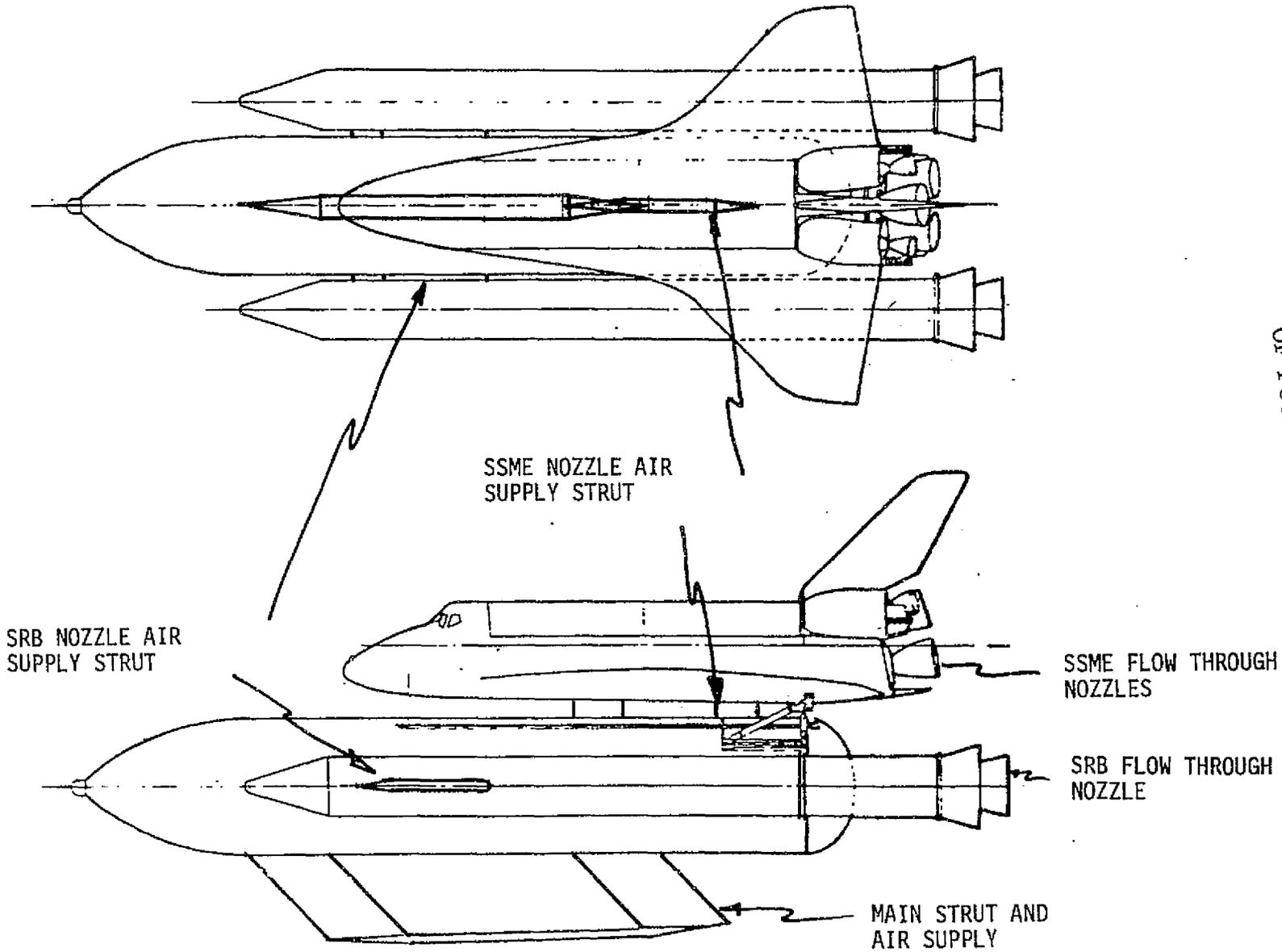

Figure 2-2. FLOW THROUGH NOZZLE AIR SUPPLY STRUTS — IA119 MODEL

ORIGINAL PAGE IS
OF POOR QUALITY

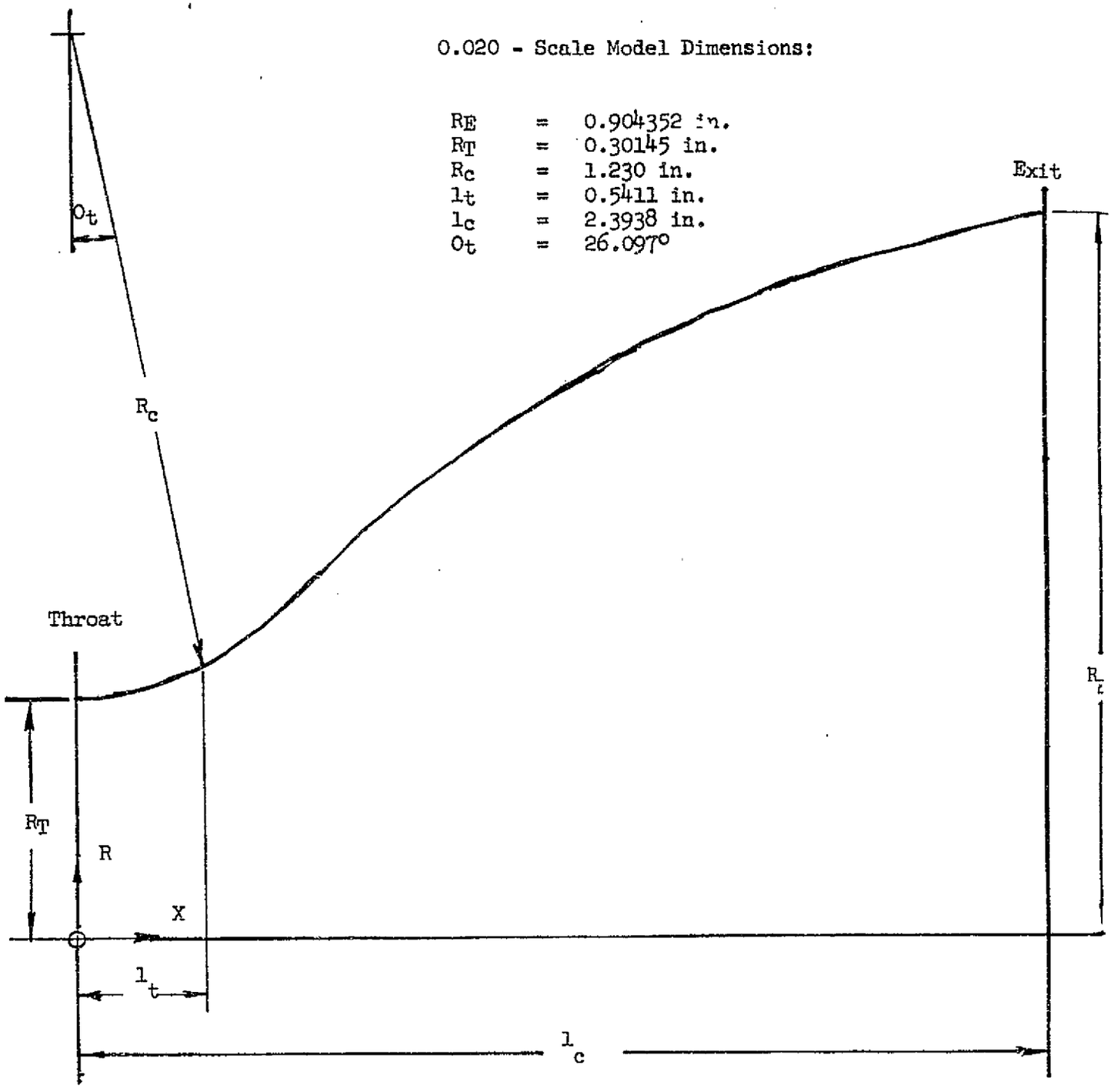

Figure 2-3. MPS NOZZLE (N_{104}) INTERNAL CONTOURS

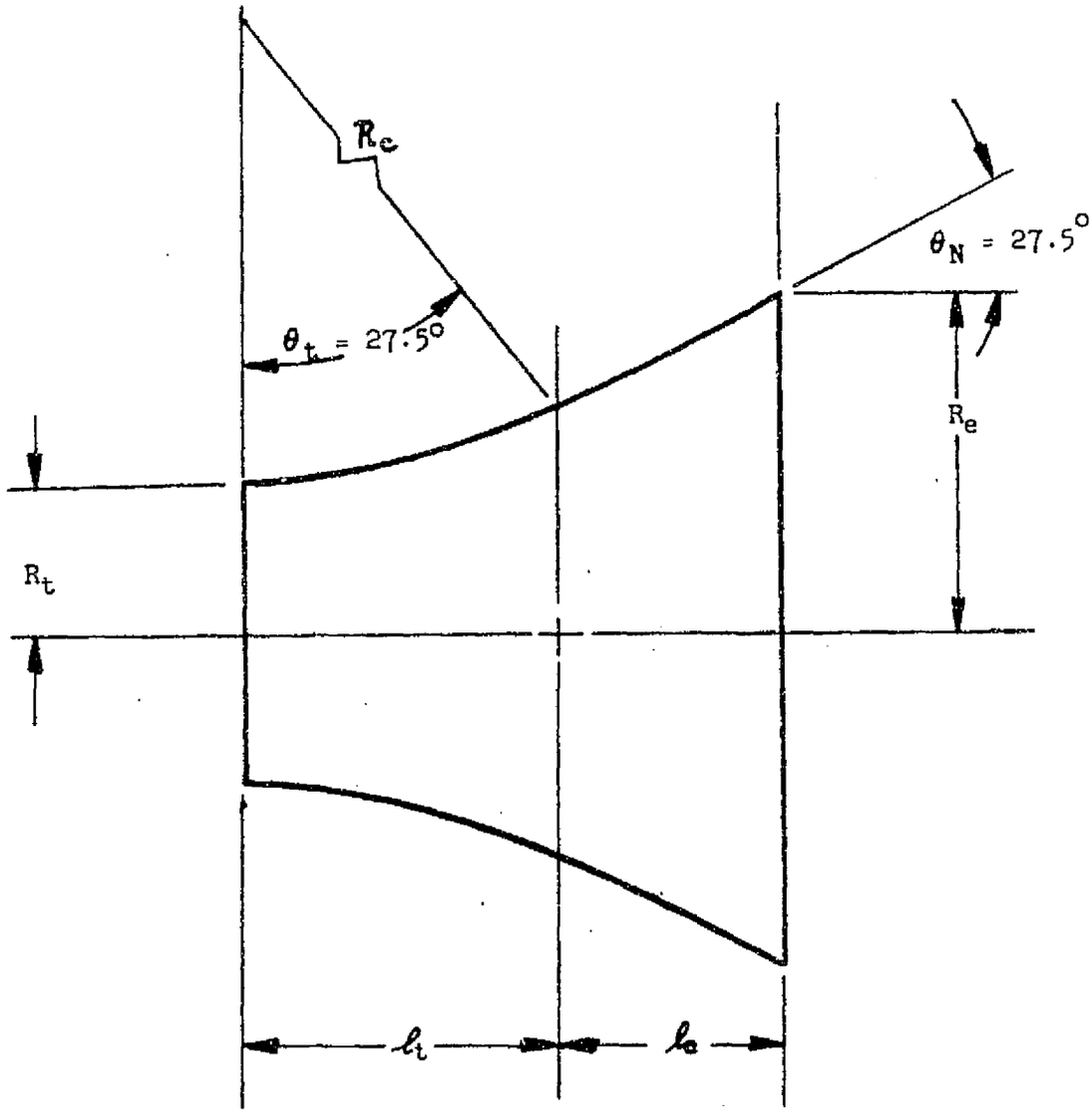

0.020 MODEL SCALE DIMENSIONS:

R_e = 1.44290 IN.

R_t = 0.6453 IN.

R_c = 2.9038 IN.

ℓ_t = 1.3408 IN.

ℓ_c = 0.9019 IN.

CONICAL NOZZLE $\varepsilon = 5$

Figure 2-4. SRB NOZZLE (N_{88}) INTERNAL CONTOURS

Section III

TEST CONDITIONS

The IA119 wind tunnel test program was essentially conducted in two parts. Part one was a power variation test at zero attitude, where chamber pressure of the MPS and SRB model nozzles was varied. Part two was a test program at a nominal power level that includes various elevon deflections, nozzle gimbal patterns, and attitudes.

Base pressure data, from the power variation test (Part 1), was evaluated at the test site along with prototype plume characteristics to evaluate the nominal model nozzle plume characteristics and model chamber pressures. (See Section V for plume simulation discussion). These tests were conducted at zero angle of attack and zero angle of sideslip. Tests were conducted for a series of Mach numbers from 0.6 to 1.4.

Part 2 of the test program consisted of testing the model using the nominal power levels developed in Part 1 over a range of attitudes and configurations (elevon deflections, gimbal angles, etc.). Data were obtained at nominal angles of attack of -8, -4, 0, and +4 degrees. The angles of sideslip were nominally 0, and ± 6 or ± 4 degrees.

The data analysis procedure required a power-on and a power-off run sequence. The power-on data was required to obtain the power-on base pressure environments. The power-off data is used to evaluate the influence of power on changes in local pressure environments for use in the analysis of forebody plume induced aerodynamic characteristics. The development of the forebody plume induced aerodynamic characteristics also required testing at positive and negative sideslip angles, because portions of the model forebody had pressure instrumentation on only one side of the model. Thus four sets of test data were required to develop the plume induced aerodynamic data. The power-on and power-off run data sets used for analysis are presented in Tables 3-1 through 3-9. These tables show the angle of sideslip schedule, the elevon deflections, and the nozzle gimbal angle run sets for each Mach number. The run numbers are arranged in terms of the model configuration at nominal power

levels (elevon deflection and gimbal angle), then the power variation run numbers, and then the roll 90 degrees run numbers.

Each power run number has a sequence slash number that denotes a particular MPS and SRB power level. Figures 3-1 through 3-9 show the power level for each power run-sequence combination. The square shows the nominal power value used for the testing of the various elevon settings and gimbal angles.

Tests were conducted at various elevon deflections corresponding to Schedule 6 and probable variations about schedule 6. Schedule 6 elevon deflections are presented in Figure 3-10. Plots of the various inboard and outboard elevon deflection angles evaluated during the test along with the nominal schedule 6 value are presented in Figures 3-11a through 3-11e. The elevon deflection closest to schedule 6 that was used to develop the plume induced aerodynamic data base is shown in each figure.

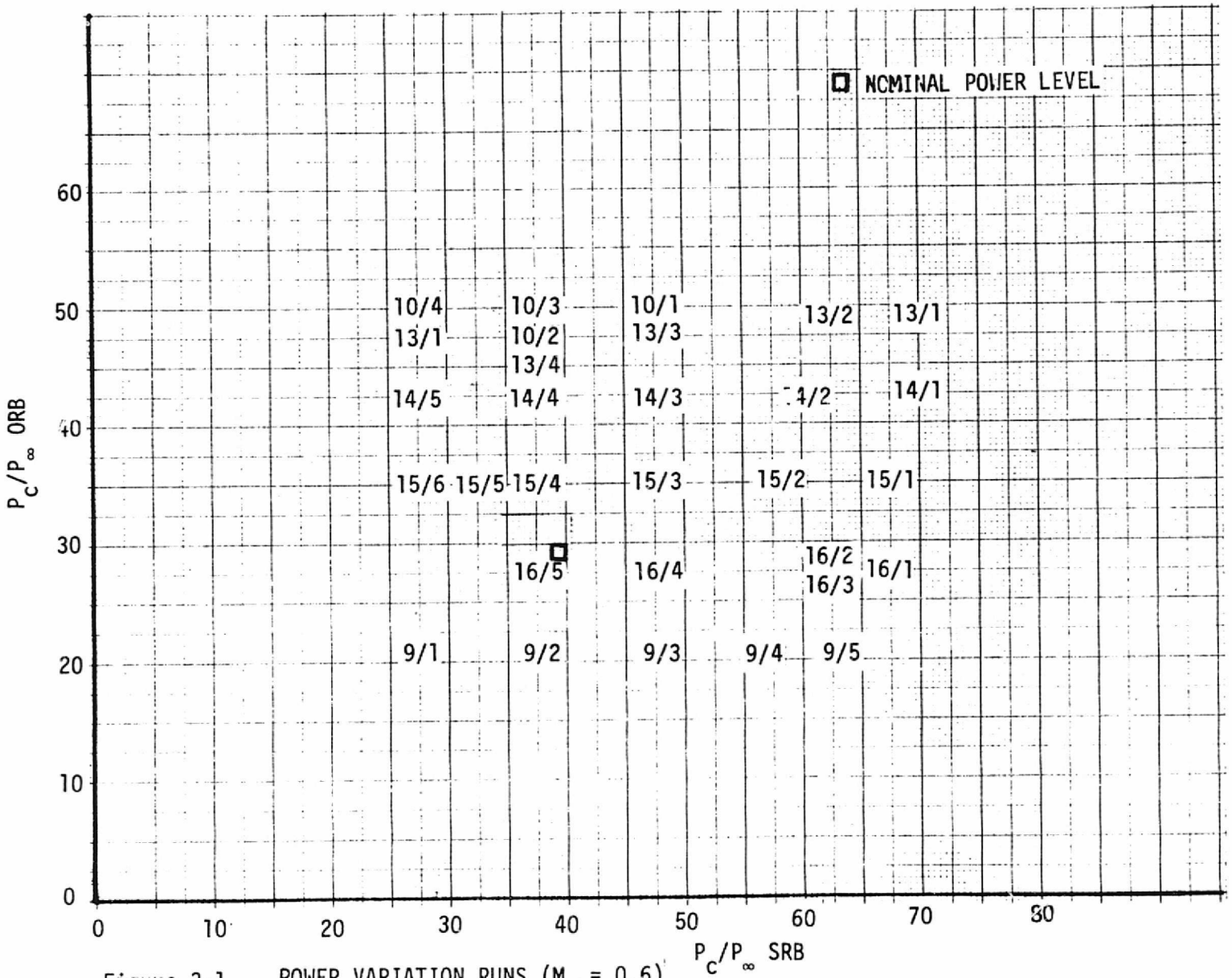

Figure 3-1 POWER VARIATION RUNS (M_∞ = 0.6)

ORIGINAL PAGE IS
OF POOR QUALITY

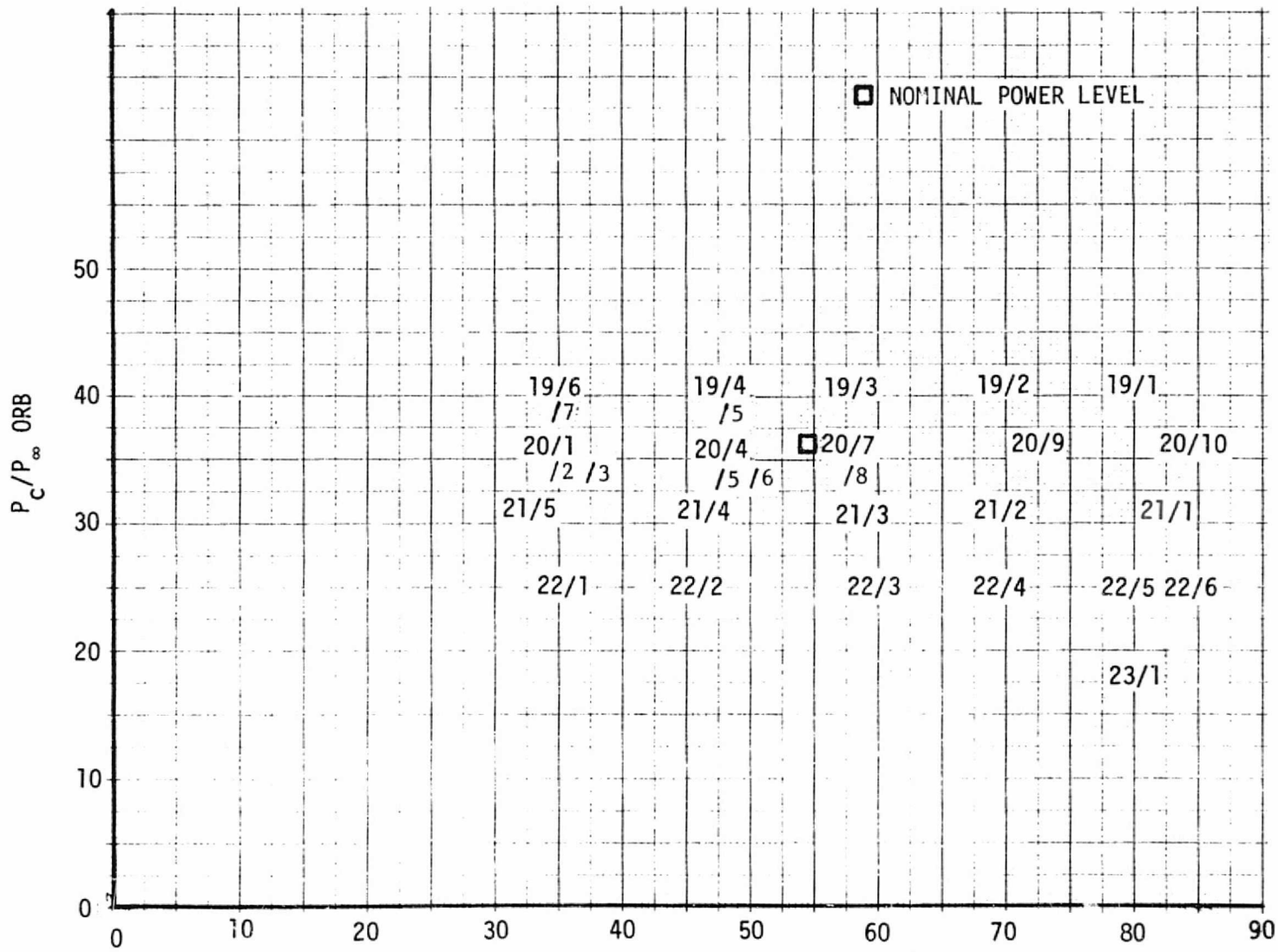

Figure 3-2 POWER VARIATION RUNS (M_∞ = 0.8)

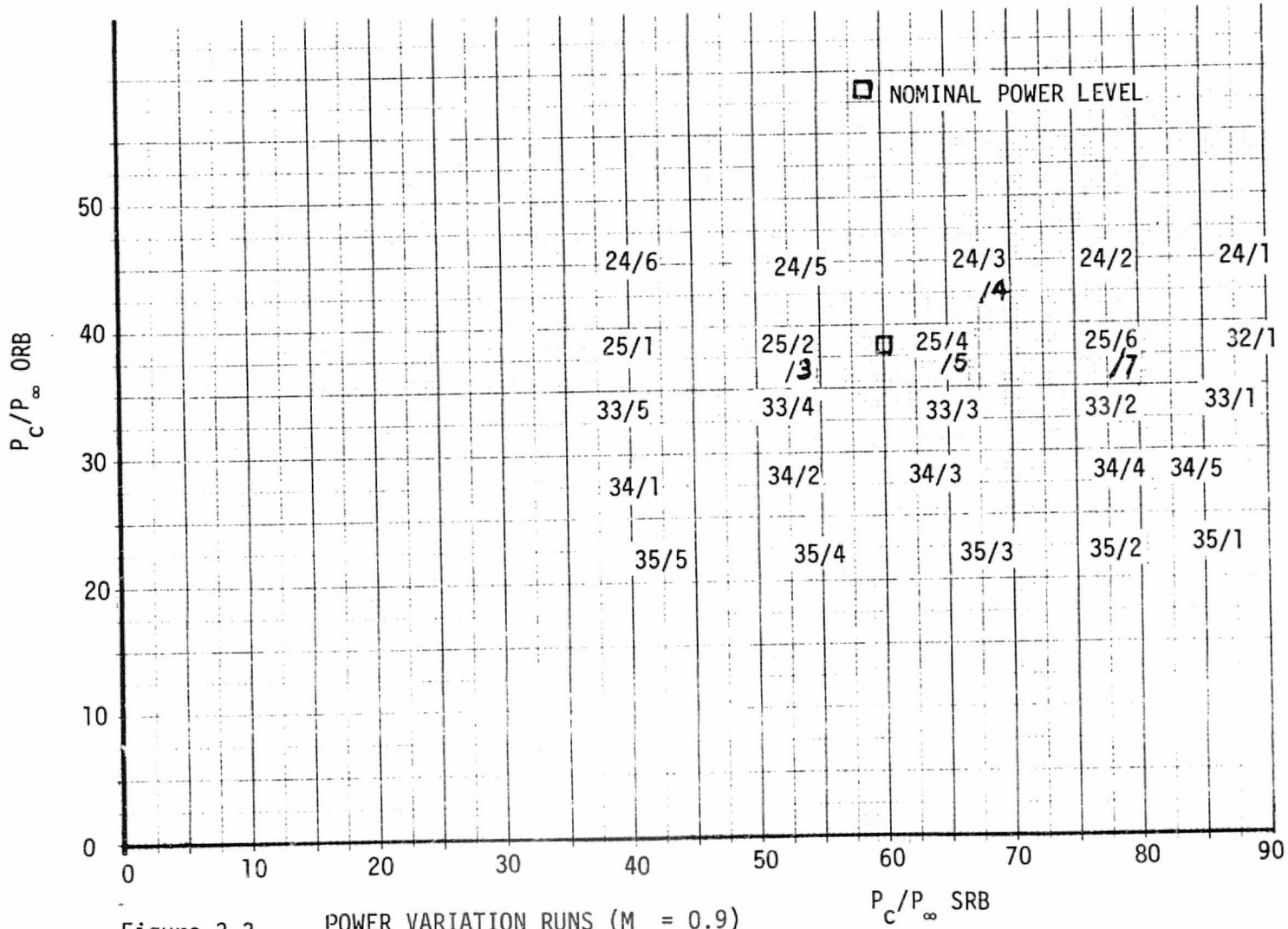

Figure 3-3 POWER VARIATION RUNS (M_∞ = 0.9)

ORIGINAL PAGE IS
OF POOR QUALITY

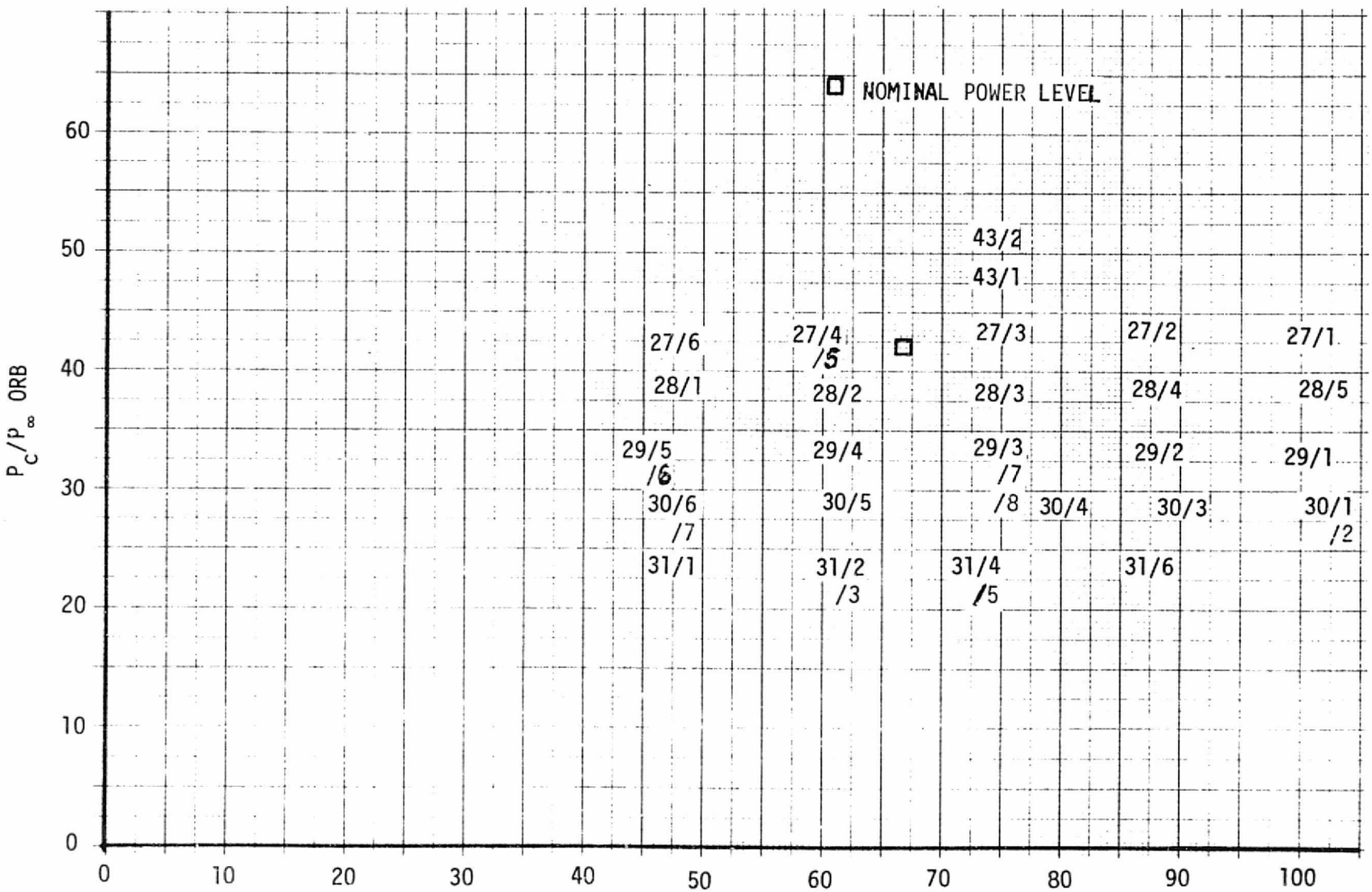

Figure 3-4 POWER VARIATION RUNS (M_∞ = 0.95)

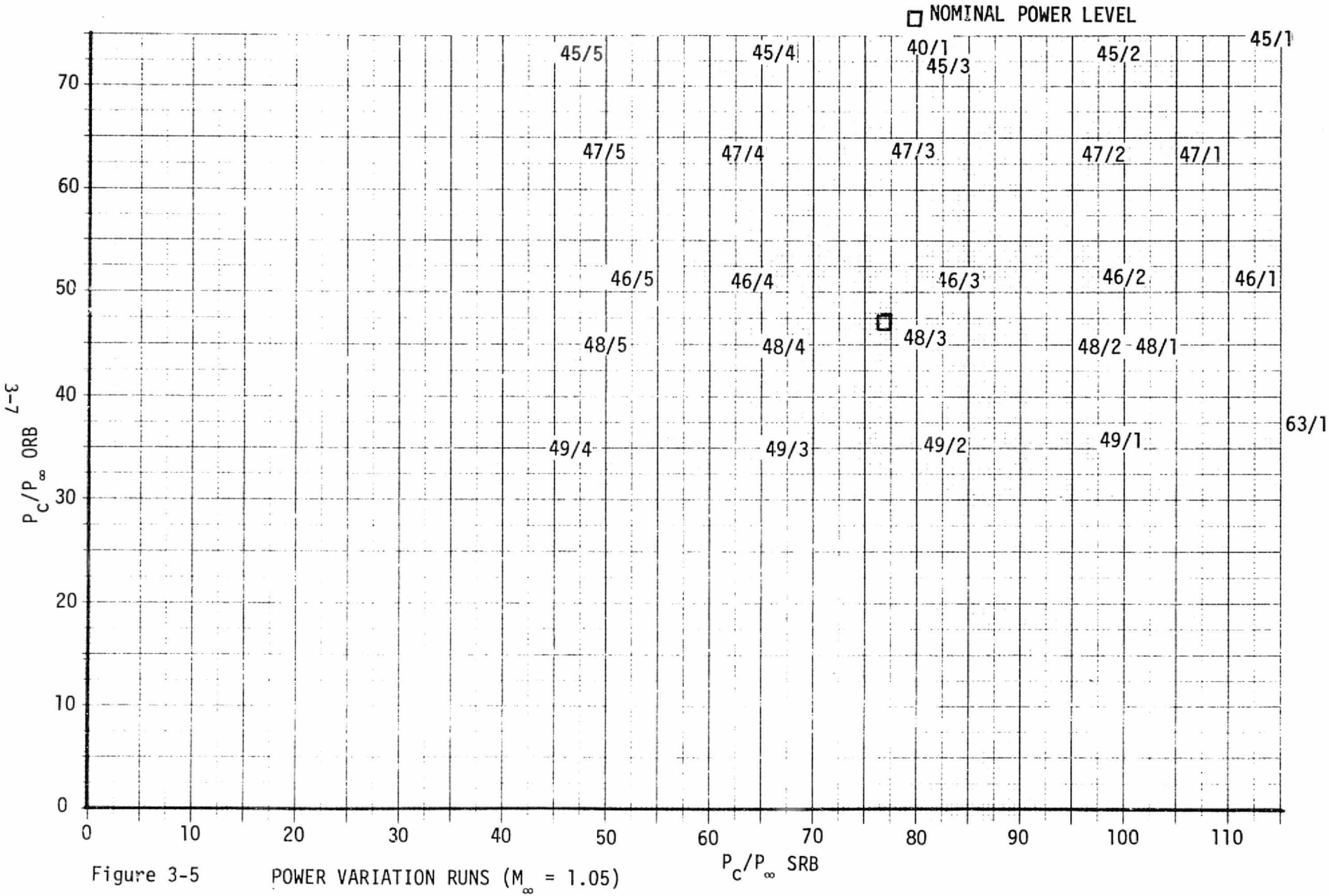

Figure 3-5 POWER VARIATION RUNS (M_∞ = 1.05)

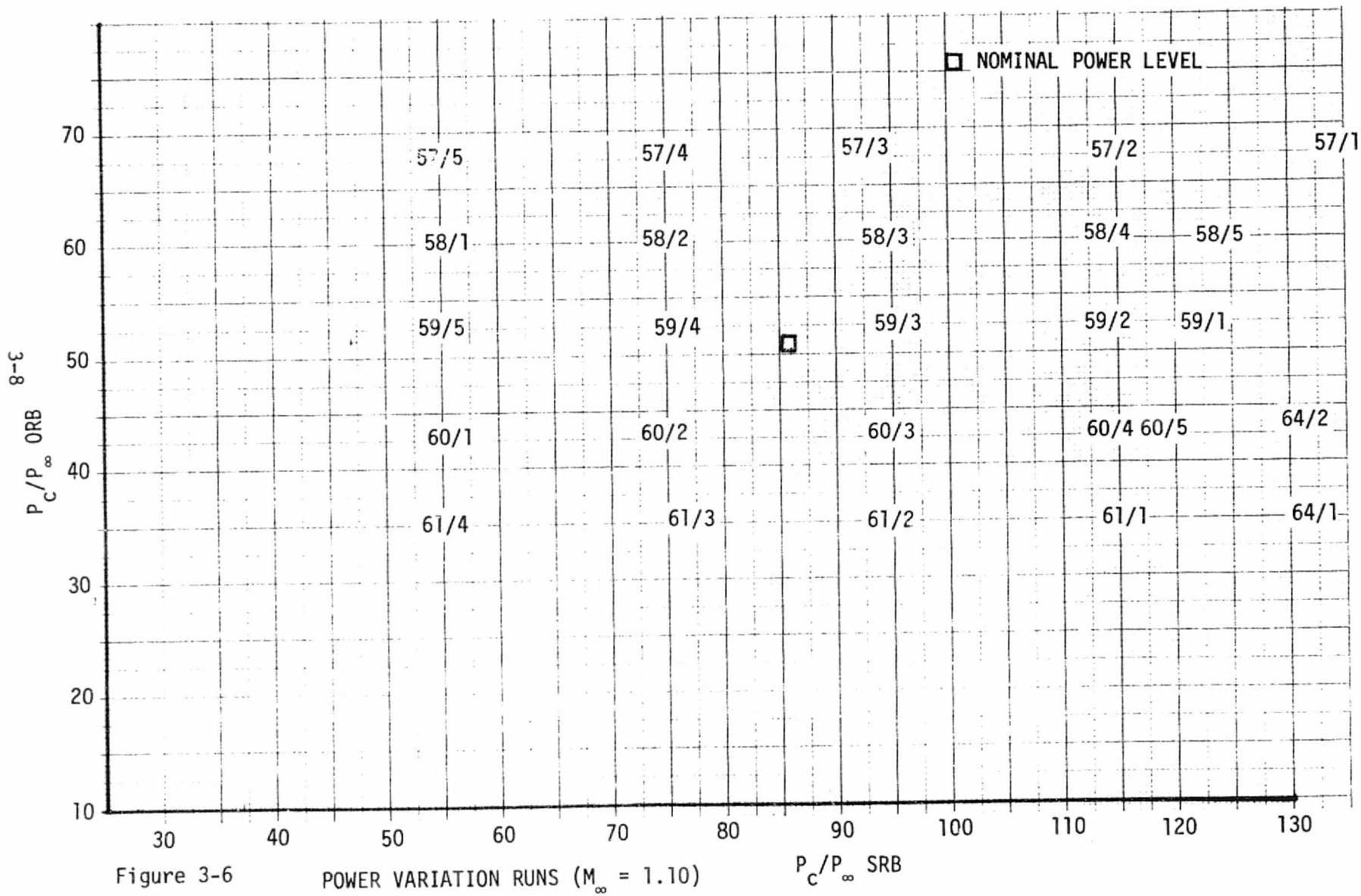

Figure 3-6 POWER VARIATION RUNS (M_∞ = 1.10)

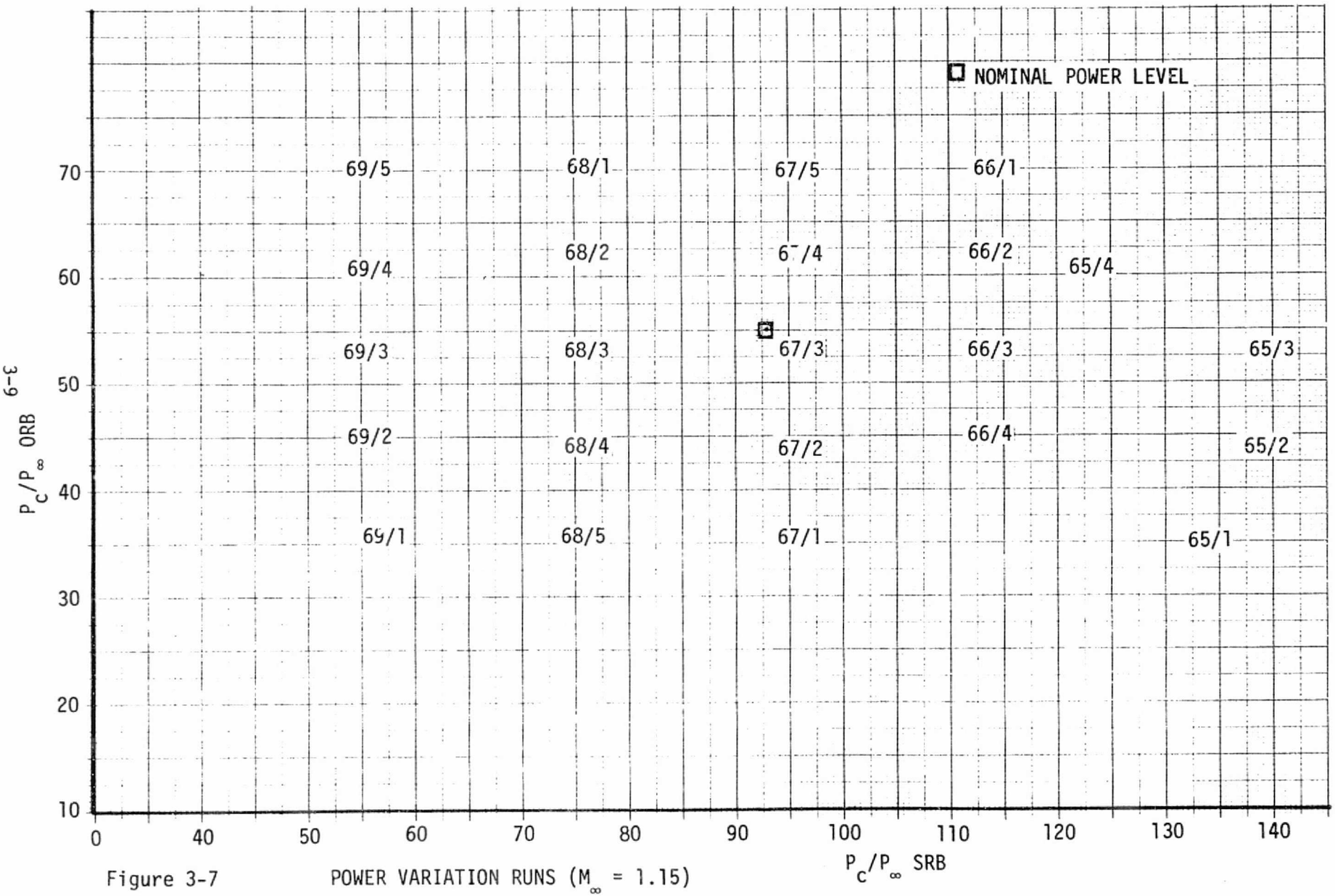

Figure 3-7 POWER VARIATION RUNS (M_∞ = 1.15)

ORIGINAL PAGE IS
OF POOR QUALITY

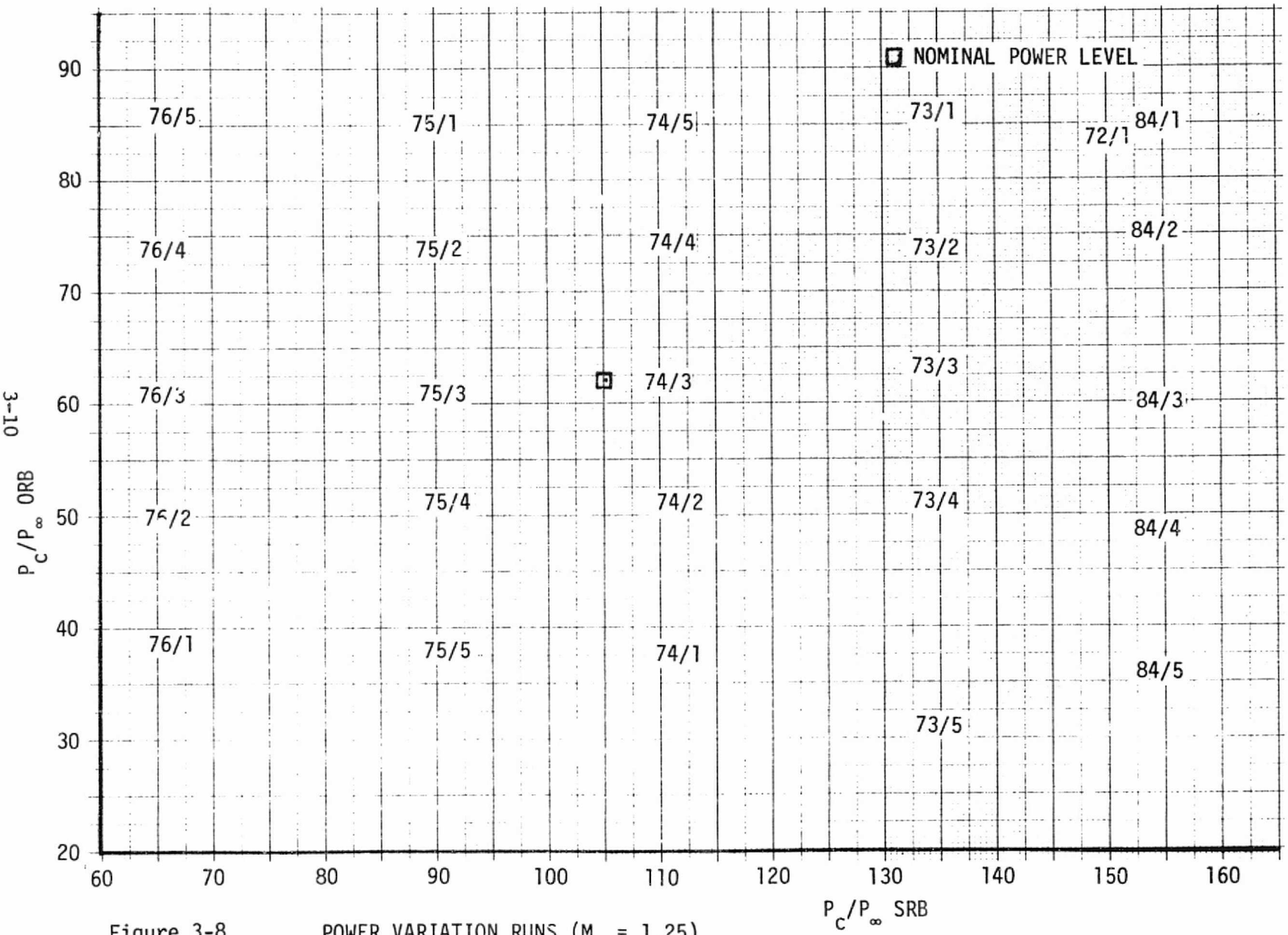

Figure 3-8 POWER VARIATION RUNS (M_∞ = 1.25)

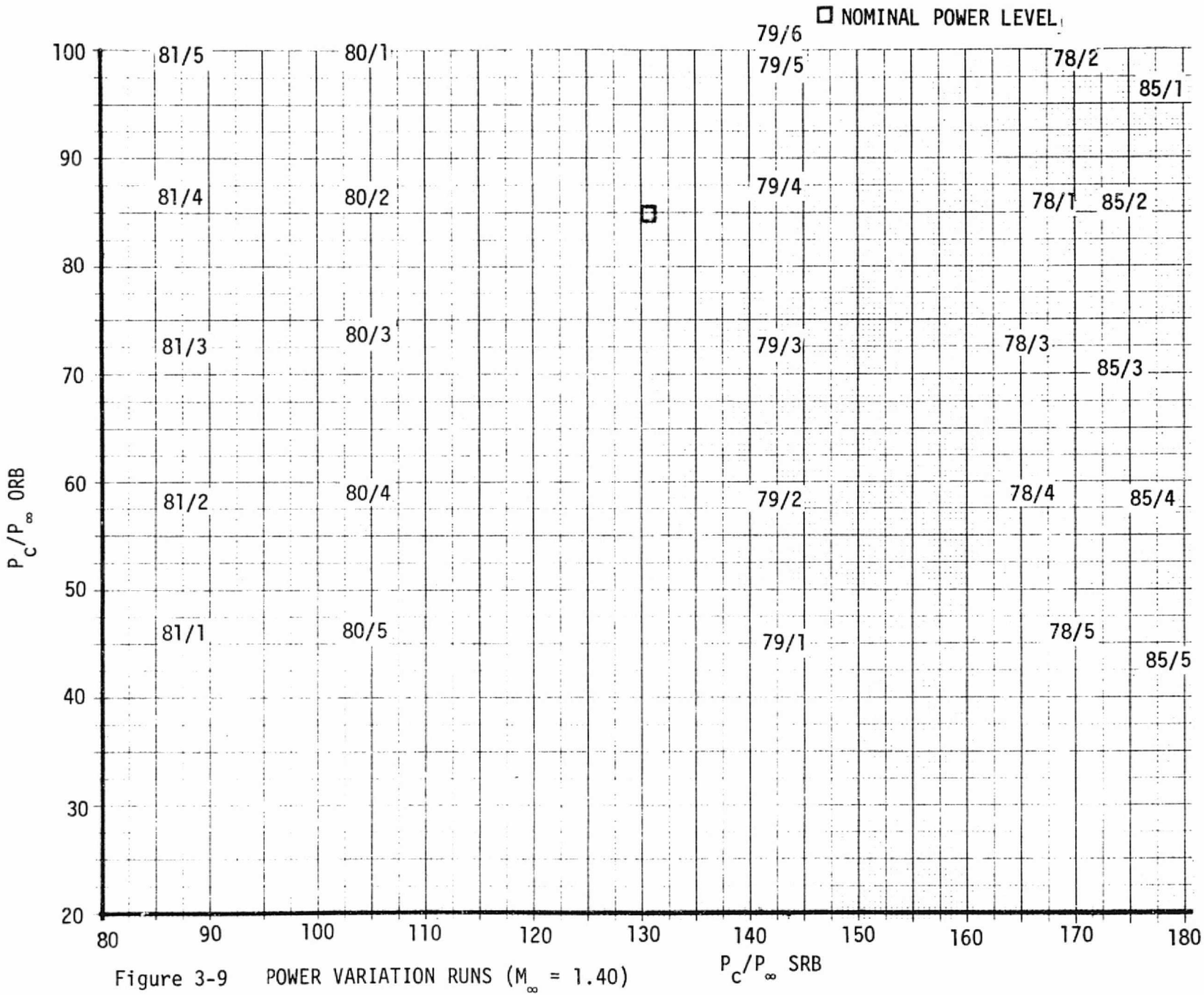

Figure 3-9 POWER VARIATION RUNS (M_∞ = 1.40)

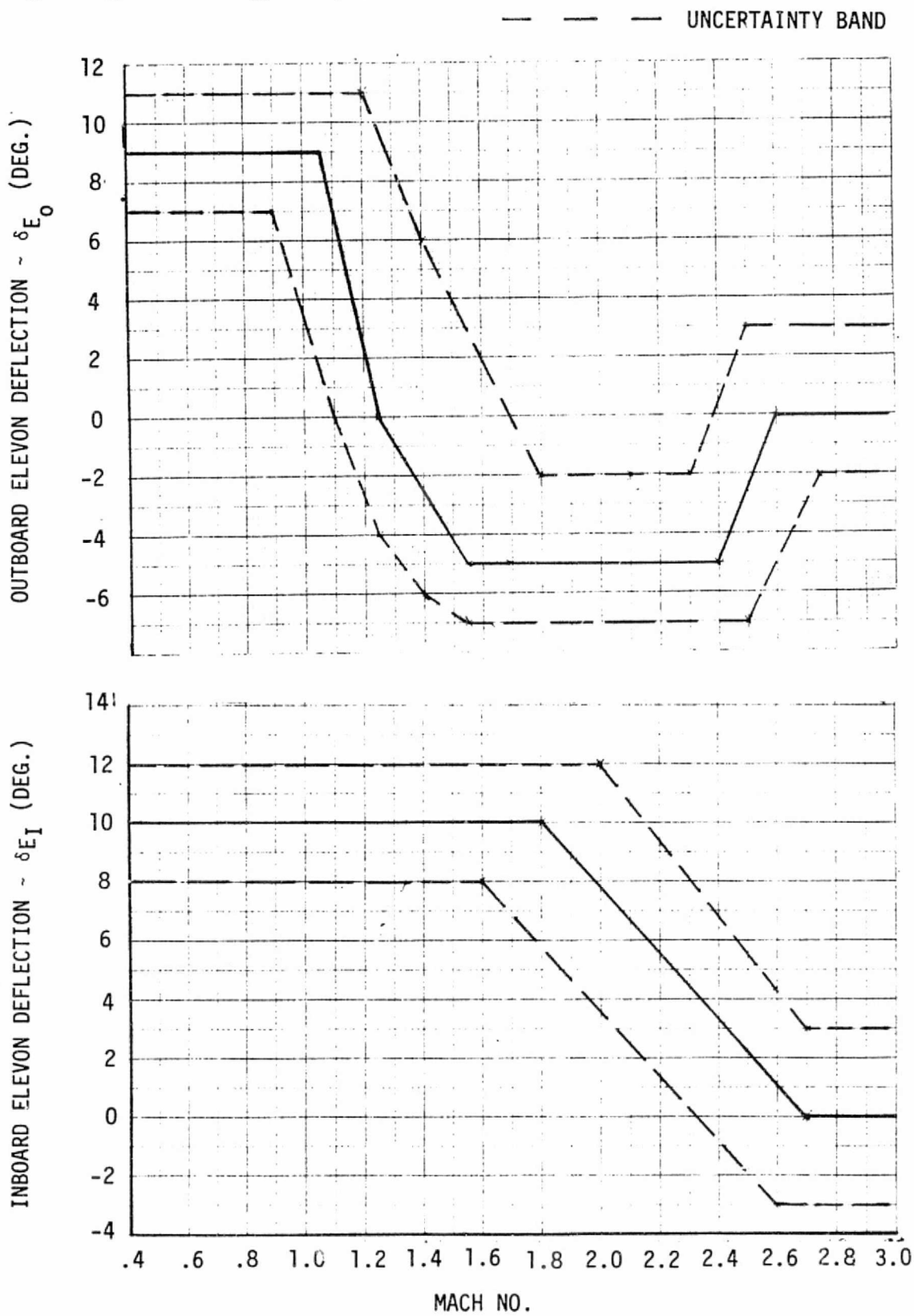

Figure 3-10. SCHEDULE 6 ELEVON DEFLECTIONS

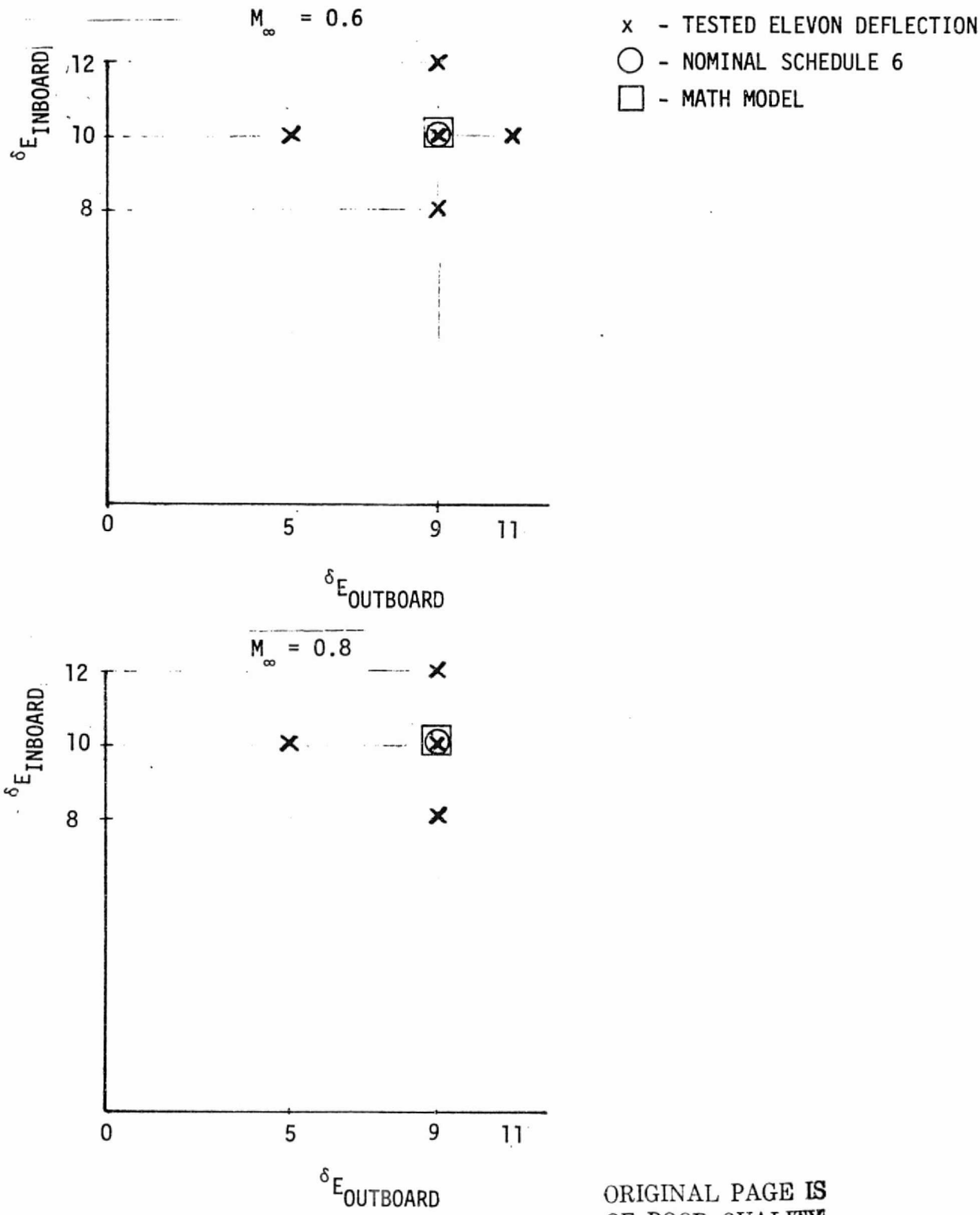

ORIGINAL PAGE IS
OF POOR QUALITY

Figure 3-11a. ELEVON SCHEDULE

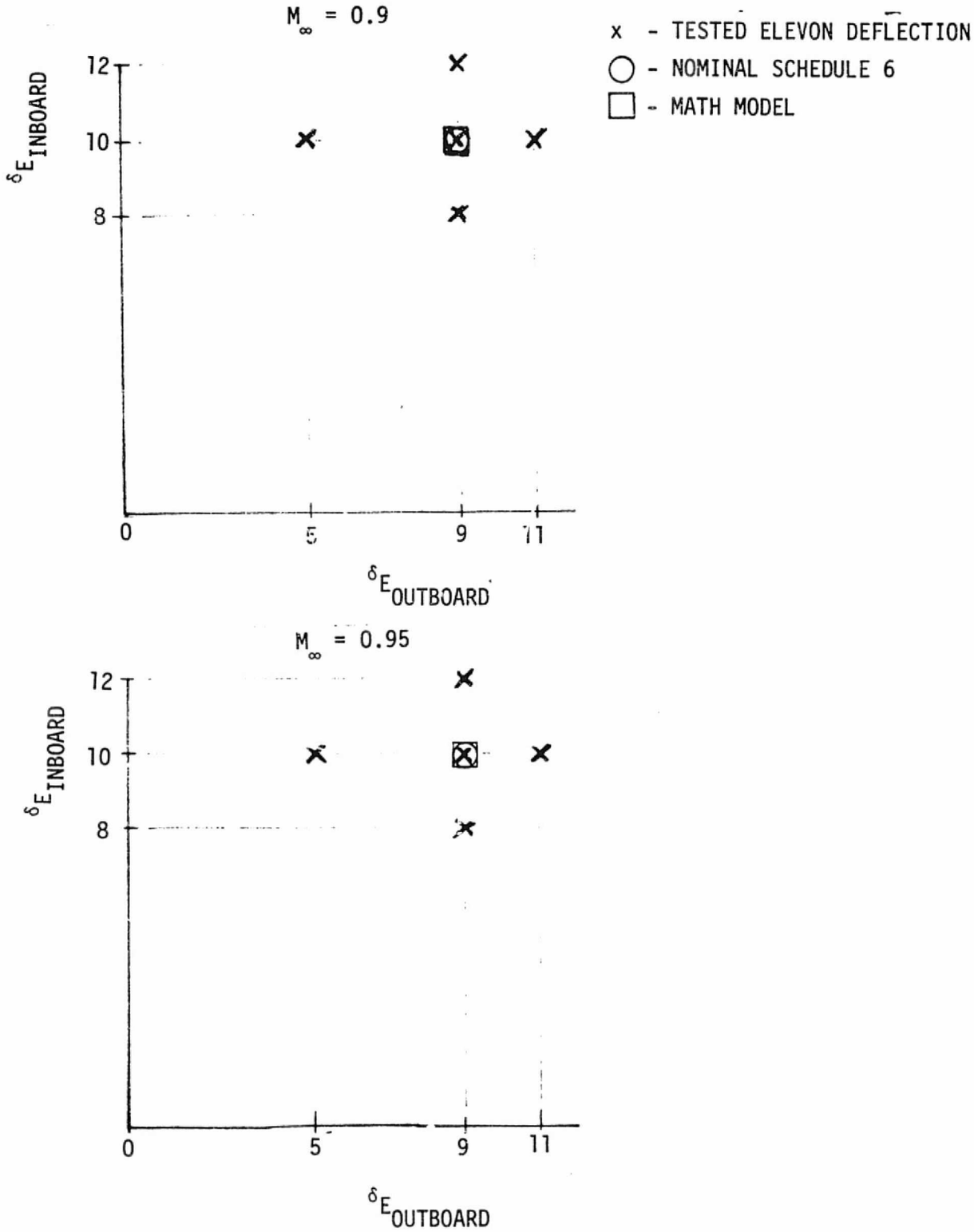

Figure 3-11b. ELEVON SCHEDULE

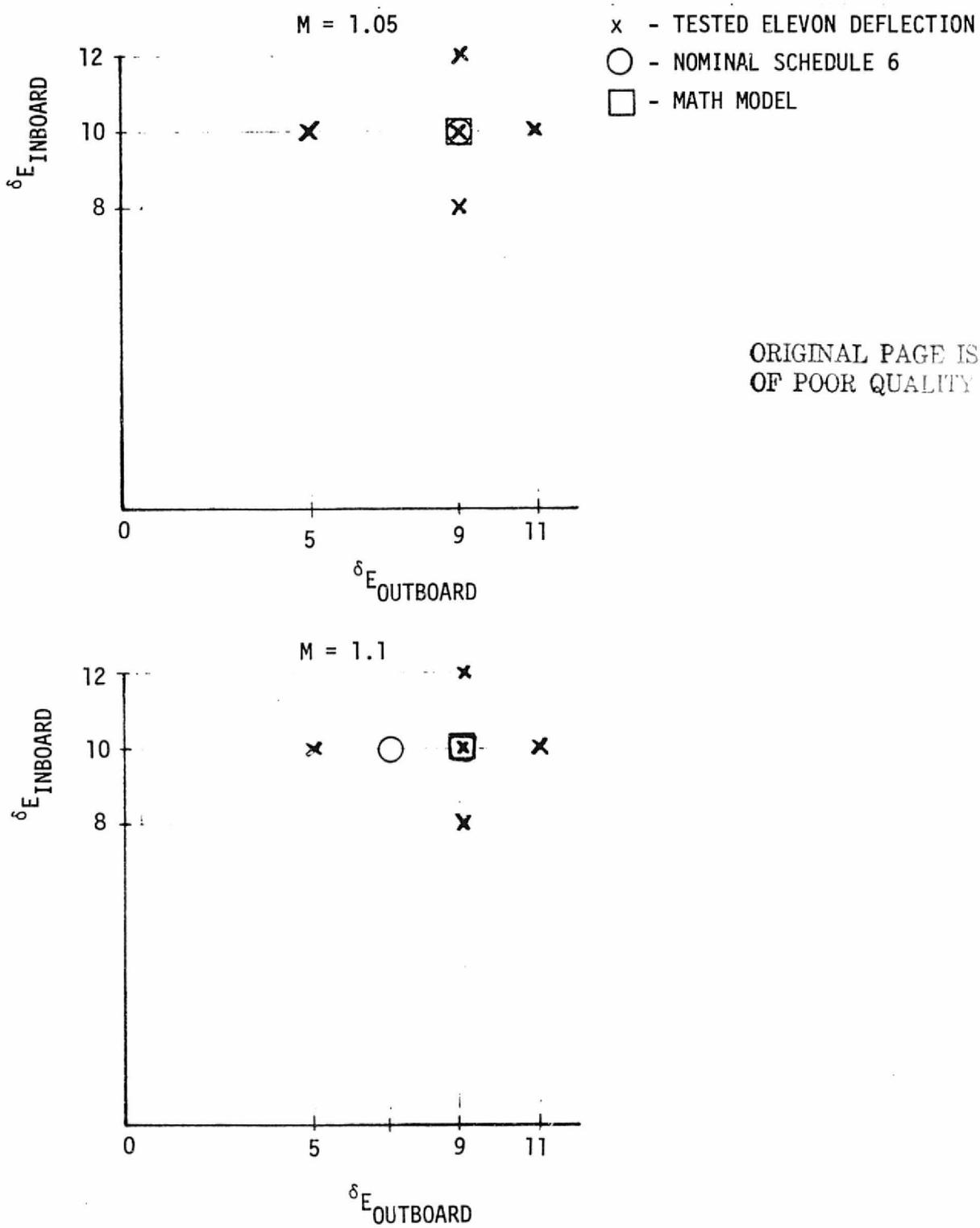

ORIGINAL PAGE IS
OF POOR QUALITY

Figure 3-11c. ELEVON SCHEDULE

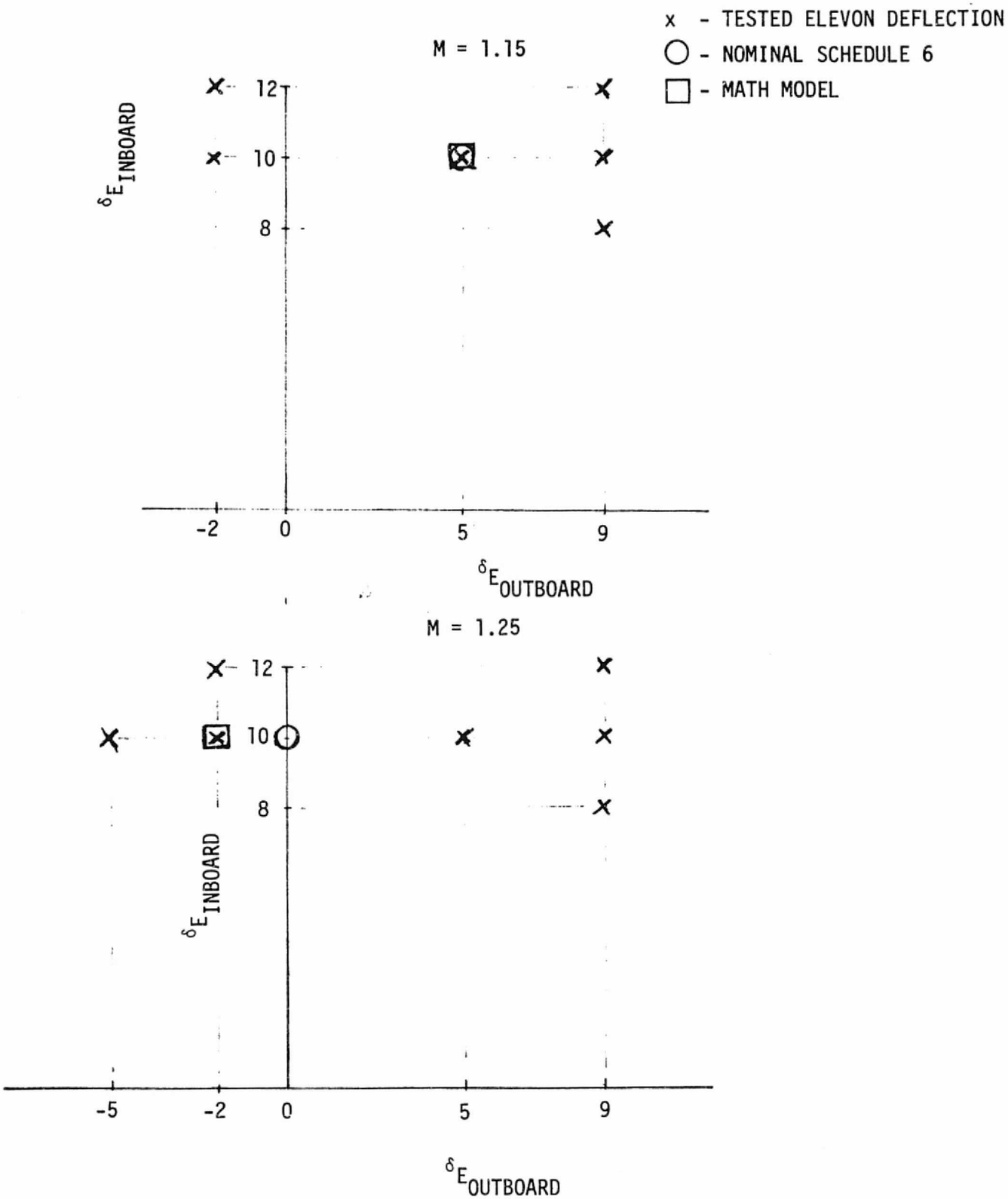

Figure 3-11d. ELEVON SCHEDULE

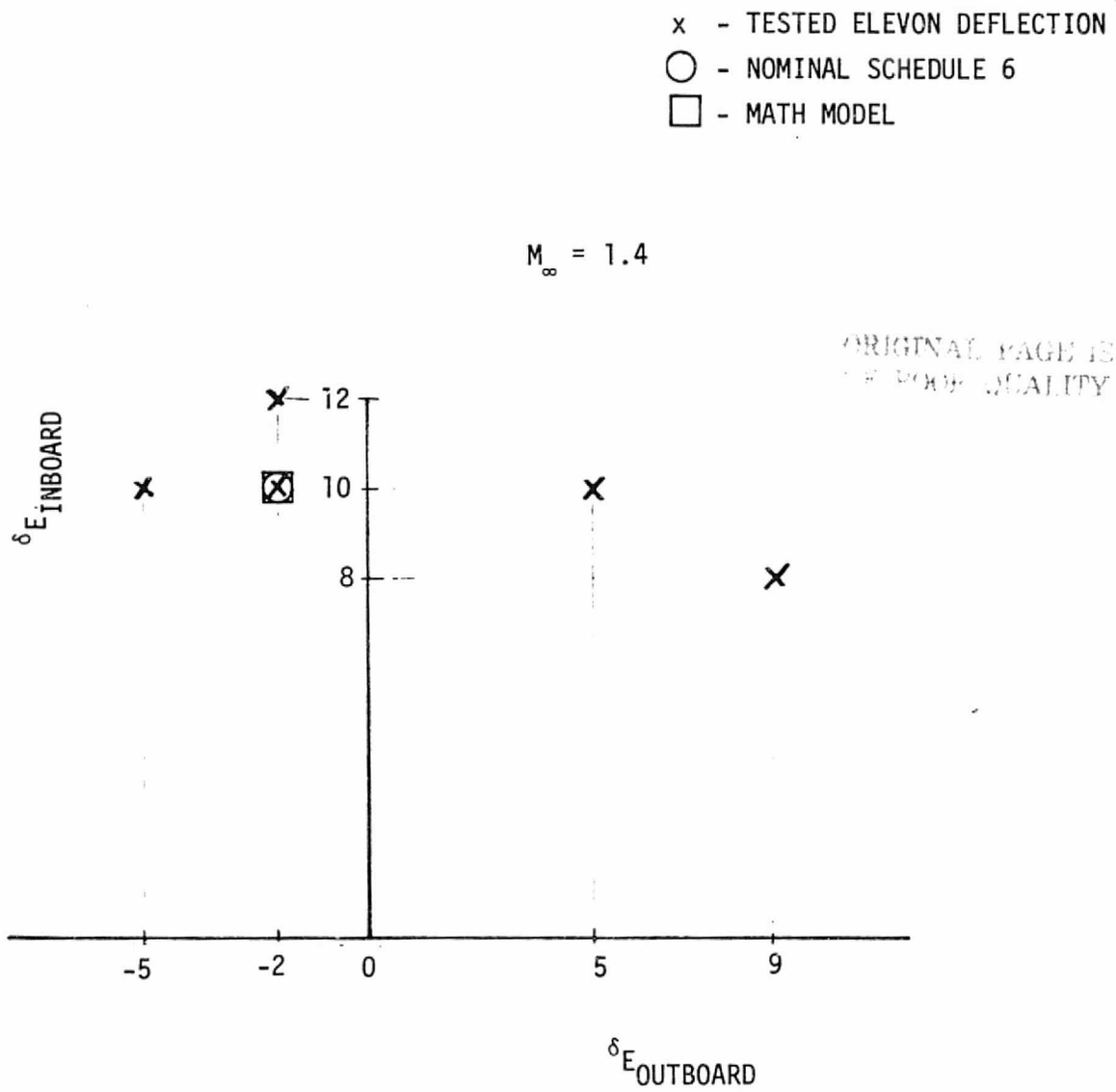

ORIGINAL PAGE IS
OF POOR QUALITY

Figure 3-11e. ELEVON SCHEDULE

Table 3-1.
IA119
POWER ON-OFF DATA SETS (M_∞ = 0.6)

	SRB/SSME				β					
α	POWER	-6	-4	-2	0	2	4	6	$\delta_{e_{10}}$	GIM
A	NN	155			154			153	10/9	N
A	OF OF	156			157			158	10/9	N
A	NN		274		273		272		10/11	N
A	OF OF		275		276		277		10/11	N
A	NN	166			167			168	10/5	N
A	OF OF	165			163			161	10/5	N
A	NN		626		625		624		8/9	N
A	OF OF		627		628		629		8/9	N
A	NN		282		280		281		12/9	N
A	OF OF		283		284		285		12/9	N
A	NN		429		430		431		10/9	GI
A	OF OF		428		427		426		10/9	GI
A	NN				482				10/9	G2
A	OF OF				483				10/9	G2
A	NN		489		488 } 1		487 } 2		10/9	G5
A	OF OF		490		491 }		492 }		10/9	G5
A	NN		569		568 } 1		567 } 3		10/9	G6
A	OF OF		570		571 }		572 }		10/9	G6
				POWER						
0	OF OF				53				10/9	N
↓	V N1				9-17				↓	↓
	↓ N2				16					
	N3				15					
	N4				14					
	N5				13					
				ROLL 90						
0	NN				649				10/5	N
0	OF OF				650				10/5	N

N = NOMINAL
OF = OFF
V = VARIABLE

1. α = 0 ONLY
2. α = -8, +4 ONLY
3. α = -8, 0, +4 ONLY

Table 3-2.
IA119
POWER ON-OFF DATA SETS (M_∞ = 0.8)

α	SRB/SSME POWER	β -6	-4	-2	0	2	4	6	$\delta_{e_{10}}$	GIM
A	NN	150			151			152	10/9	N
A	OF OF	149			148			147	10/9	N
A	NN		268		267		266		10/11	N
A	OF OF		269		270		271		10/11	N
A	NN	171			170			169	10/5	N
A	OF OF	172			173			174	10/5	N
A	NN		620		619		618		8/9	N
A	OF OF		621		622		623		8/9	N
A	NN		288		286		287		12/9	N
A	OF OF		289		290		291		12/9	N
A	NN		416		415		414		10/9	GI
A	OF OF		417		418		419		10/9	GI
A	NN		439		438		437		10/9	G2
A	OF OF		457		456		455		10/9	G2
A	NN		495		494 [1]		493 [2]		10/9	G5
A	OF OF		496		497		498		10/9	G5
A	NN		563		562 [1]		561 [2]		10/9	G6
A	OF OF		564		565		566		10/9	G6
	SRB/SSME			POWER						
0	OF OF				52				10/9	N
↓	V N1				23				↓	↓
	N2				22					
	N3				21					
	N4				20					
	↓ N5				19					
				ROLL						
0	NN				647				10/5	N
0	NN				648				10/5	N

N = NOMINAL
OF = OFF
V = VARIABLE

1. α = 0 ONLY
2. α = -8, +4 ONLY

Table 3-3.
IA119
POWER ON-OFF DATA SETS (M_∞ = 0.9)

α	SRB/SSME POWER	β -6	-4	-2	0	2	4	6	$\delta_{e_{10}}$	GIM
A	NN	143			142			141[3]	10/9	N
A	OF OF	144			145			146		N
A	NN		257		256		255		10/11	N
A	OF OF	264[x]	258	263[x]	259	262[x]	260	261[x]	10/11	N
A	OF OF				265				10/11	N
A	NN	183			184 [1]			185	10/5	N
A	OF OF	182	178		644/		176	175	10/5	N
A					131/ [4]				10/5	N
A					173				10/5	N
A	NN		614		613		612		8/9	N
A	OF OF		615		616		617		8/9	N
A	NN		294		293		292		12/9	N
A	OF OF		295		296		297		12/9	N
A	NN		390		389		388		10/9	GI
A	OF OF		391/ 393		392		400		10/9	GI
A	NN		466		465		464		10/9	G2
A	OF OF		467		468		469			G2
A	NN		501		500 [1]		499 [2]		10/9	G5
A	OF OF		502		503		504			G5
A	NN		557		556 [1]		555 [2]		10/9	G6
A	OF OF		558		559		560			G6
	SRB/SSME			POWER						
0	OF OF				51				10/9	N
↓	V N1				35				↓	↓
	N2				34					
	N3				33					
	N4				25/32					
	N5				24					
				ROLL						
0	NN				643				10/5	N
0	OF OF				644				10/5	N

N = NOMINAL
OF = OFF
V = VARIABLE

1. α = 0 ONLY
2. α = -8, +4 ONLY
3. α = 0, -8, -4 ONLY
4. α = +4 ONLY

Table 3-4.
IA119
POWER ON-OFF DATA SETS (M_∞ = 0.95)

	SRB/SSME	β								
α	POWER	-6	-4	-2	0	2	4	6	$\delta_{e_{10}}$	GIM
A	NN	138			137			136	10/9	N
A	OF OF	135			134			133	10/9	N
A	NN		249		248		247		10/11	N
A	OF OF		250		251/		252		10/11	N
					254					N
A	NN	188			187			186	10/5	N
A	OF OF	189			190			191	10/5	N
A	NN		608		607		606		8/9	N
A	OF OF		609		610		611		8/9	N
A	NN		301		299		298/		12/9	N
A							300			N
A	OF OF		302		303		304		12/9	N
A	NN		478		477		476		10/9	G2
A	OF OF		479		480		481		10/9	G2
				POWER						
0	OF OF				44				10/9	N
↓	V N1				31				↓	↓
	↓ N2				30					
	N3				29					
	N4				28					
	N5				27					
	N6				43					
	N7				43					
				ROLL						
0	NN				645				10/5	N
0	OF OF				646				10/5	N

N = NOMINAL
OF = OFF
V = VARIABLE

Table 3-5.
IA119
POWER ON-OFF DATA SETS (M_∞ = 1.05)

α	SRB/SSME POWER	β -6	-4	-2	0	2	4	6	$\delta_{e_{10}}$	GIM
A	NN	129			128			127	10/9	N
A	OF OF	130			131			132	10/9	N
A	NN		240		239[2]		238		10/11	N
A	OF OF		244		245[2]		246		10/11	N
A	NN	194			193			192	10/5	N
A	OF OF	195			196			197	10/5	N
A	NN		578		577		576		8/9	N
A	OF OF		579		580		581		8/9	N
A	NN		310		309[1]		308		12/9	N
A	OF OF		311		312		313		12/9	N
A	NN		394		395				10/9	GI
A	OF OF				398				10/9	GI
A	NN		444		443		442		10/9	G2
A	OF OF		445		446		447			G2
A	NN		507		506[3]		505[4]		10/9	G5
A	OF OF		508		509[3]		510[4]			G5
A	NN		533		532[3]		531[4]		10/9	G6
A	OF OF		534		535[3]		536[4]			G6
				POWER						
0	OF OF				50				10/9	N
	V N1				49					
	N2				48					
	N3				46					
	N4				47					
	N5				40/45					
					63					
				ROLL						
0	NN				633				10/5	N
0	OF OF				634				10/5	N

N = NOMINAL
OF = OFF
V = VARIABLE

1. α = 3.6°/4
2. α = 0, -4, +4 ONLY
3. α = 0 ONLY
4. α = -8, +4 ONLY

Table 3-6.
IA119
POWER ON-OFF DATA SETS (M_∞ = 1.10)

	SRB/SSME	β								
α	POWER	-6	-4	-2	0	2	4	6	$\delta_{e_{10}}$	GIM
A	NN	109			108			107	10/9	N
A	OF OF	110			111			112	10/9	N
A	NN	202			201			200	10/5	N
A	OF OF	203	204		205		206	207	10/5	N
A	NN		234		233		232		10/11	N
A	OF OF		235		236		237		10/11	N
A	NN		590		589		588		8/9	N
A	OF OF		591		592		593		8/9	N
A	NN		316		315		314		12/9	N
A	OF OF		317		318		319		12/9	N
A	NN		403		402		401		10/9	GI
A	OF OF		404		405		406		10/9	GI
A	NN		450		449		448		10/9	G2
A	OF OF		451/ 453		452		454		10/9	G2
A	NN		513		512[1]		511[2]		10/9	G5
A	OF OF		514		515		516		10/9	G5
A	NN		551		550[1]		549[2]		10/9	G6
A	OF OF		552		553		554		10/9	G6
				POWER						
0	OF OF				56				10/9	N
↓	V N1				61				↓	↓
↓	N2				60				↓	↓
↓	N3				59				↓	↓
↓	N4				58				↓	↓
↓	N5				57/64				↓	↓
				ROLL						
0	NN				635				10/5	N
0	OF OF				636				10/5	N

N = NOMINAL
OF = OFF
V = VARIABLE

1. α = 0 ONLY
2. α = -8, +4 ONLY

Table 3-7.
IA119
POWER ON-OFF DATA SETS (M_∞ = 1.15)

	SRB/SSME				β					
α	POWER	-6	-4	-2	0	2	4	6	$\delta_{e_{10}}$	GIM
A	NN	210			209			208	10/5	N
A	OF OF	211			212			213	10/5	N
A	NN	103			102			101	10/9	N
A	OF OF	104			105			106	10/9	N
A	NN		356		355		354		10/-2	N
A	OF OF		357		358		359		10/-2	N
A	NN		602		601		600		8/9	N
A	OF OF		603		604		605		8/9	N
A	NN		336		335		334		12/-2	N
A	OF OF		337		338		339		12/-2	N
A	NN		328		327		326		12/9	N
A	OF OF		329		330		331		12/9	N
A	NN		472		471		470		10/9	G2
A	OF OF		473		474		475		10/9	G2
				POWER						
0	OF OF				70				10/9	N
↓	N1 V				69				↓	↓
	N2 ↓				68					
	N3				67					
	N4				66					
	N5 ↓				65					
				ROLL						
0	NN				639				10/5	N
0	OF OF				640				10/5	N

N = NOMINAL
OF = OFF
V = VARIABLE

Table 3-8.
IA119
POWER ON-OFF DATA SETS (M_∞ = 1.25)

	SRB/SSME				β					
α	POWER	-6	-4	-2	0	2	4	6	δ_{e10}	GIM
A	NN		362		361		360		10/-2	N
A	OF OF		363		364		365		10/-2	N
A	NN		384		383		382		10/-5	N
A	OF OF		386		385		381		10/-5	N
A	NN	115			114			113	10/9	N
A	OF OF	116			117			120	10/9	N
A	NN	216			215			214	10/5	N
A	OF OF	217	218		219		220	221	10/5	N
A	NN		342		341		340		12/-2	N
A	OF OF		343		344		345		12/-2	N
A	NN		323		321		320		12/9	N
A	OF OF		322		324		325		12/9	N
A	NN		596		595		594		8/9	N
A	OF OF		597		598		599		8/9	N
A	NN		409		408		407		10/9	GI
A	OF OF		410		411		412		10/9	GI
A	NN		460		459		458		10/9	G2
A	OF OF		461		462		463		10/9	G2
A	NN		519		518 [1]		517		10/9	G5
A	OF OF		520		521 [1]		522		10/9	G5
A	NN		545		544 [1]				10/9	G6
A	OF OF		546		547 [1]				10/9	G6
				POWER						
0	OF OF				71				10/9	N
	N1 V				76					
	N2				75					
	N3				74					
	N4				73					
	N5				72/84					
				ROLL						
0	NN				641				10/5	N
0	OF OF				642				10/5	N

N = NOMINAL
OF = OFF
V = VARIABLE

1. α = 0, -8, +4 ONLY

Table 3-9.
IA119
POWER ON-OFF DATA SETS (M_∞ = 1.40)

α	SRB/SSME POWER	β -6	-4	-2	0	2	4	6	$\delta_{e_{10}}$	GIM
A	NN		368		367		366		10/-2	N
A	OF OF		369		370		371		10/-2	N
A	NN		376		375		374		10/-5	N
A	OF OF		378		379		380		10/-5	N
A	NN	224			223			222	10/5	N
A	OF OF	225	226		227		228	229	10/5	N
A	NN		584		583		582		8/9	N
A	OF OF		585		586		587		8/9	N
A	NN		348		347		346		12/-2	N
A	OF OF		349		350		351		12/-2	N
A	NN		422		421		413/		10/9	GI
A							420			GI
A	OF OF		423		424		425		10/9	GI
										GI
A	NN		435		434		433		10/9	G2
A	OF OF		436		440		441			G2
A	NN		525		524[1]		523[2]		10/9	G5
A	OF OF		526		527		528		10/9	G5
A	NN		539		538[3]		537[2]		10/9	G6
A	OF OF		540		541		542		10/9	G6
				POWER						
0	OF OF				77				10/9	N
	N1 V				81					
	N2				80					
	N3				79					
	N4				78					
	N5				85					
				ROLL						
0	NN				637				10/5	N
0	OF OF				638				10/5	N

N = NOMINAL
OF = OFF
V = VARIABLE

1. α = 0, -8, +4 ONLY
2. α = -8, +4 ONLY
3. α = 0 ONLY

Section IV

WIND TUNNEL MODEL NOZZLE CALIBRATION ANALYSIS

An analysis of the model nozzle calibration data was performed to determine nozzle flow characteristics for the evaluation of model power levels. A range of model power levels were required for the power level variation portion of the test. Model nozzle wall pressures and exit plane pressures were plotted and compared with MOC results to evaluate the nozzle flow characteristics and to evaluate chamber to exit pressure ratios. The chamber to exit pressure ratios were required to evaluate the model plume characteristics.

Initially it was anticipated that several model nozzle configurations would be used during the test program and thus a considerable amount of calibration data were evaluated. The test program ultimately used only the 2% contoured SSME nozzle configuration and the 2% conical SRB nozzle configuration. The nozzle calibration data and instrumentation layout was obtained from references 2 through 6. The nozzle calibration tests were conducted for the IA19 Space Shuttle plume test (reference 7). This test (IA19) used essentially the same model hardware as the IA119 test.

Summary model nozzle performance data are presented in Figures 4-1 and 4-2 for the SSME model nozzles and the SRB model nozzles respectively. The average chamber to exit plane pressure used for the model SSME nozzle was 49.5. The average chamber to exit plane pressure used for the SRB nozzle was 66.0. These values were used to develop pretest pressure ratios for each Mach number.

The SSME nozzle performance was close to the calibration data as shown in Figure 4-1. SSME nozzle number 2 was used to compute nozzle and SSME plume gas dynamic characteristics since the measured performance was closest to the calibration results. The SSME nozzle performance for chamber pressures near 300 psi was erratic indicating cases of nozzle flow separation. Conditions where the SSME nozzle chamber to exit pressure ratio dropped below 45 are noted for all data cases and the data was not used.

The SRB model nozzle performance was close to portions of the calibration data with little difference between the performance of the right and left SRB nozzles. The right SRB nozzle performance was used to calculate SRB model plume characteristics. The right SRB nozzle performance was closest to the nozzle calibration results. Model nozzle performance for chamber pressures less than 400 psi could experience nozzle wall flow separation for high ambient pressures (>9 psi). Data where the SRB nozzle chamber to exit pressure ratio was less than 60 was not used.

The SRB nozzle calibration data are presented in Figures 4-3 through 4-14. Difficulty was experienced in the analysis of the model SRB nozzle flow characteristics in evaluating an average chamber to exit plane pressure ratio. The near exit plane calibration data in Figures 4-11 through 4-14 show the large variation in exit plane pressure that was obtained during the nozzle calibration test. An analysis of the .01 scale SRB nozzle and the .02 scale SRB nozzle in conjunction with a MOC analysis indicated that a chamber to exit plane pressure ratio of 66 was the most representative. The post test analysis shown in Figure 4-2 shows that the pretest analysis produced a representative SRB model nozzle chamber to exit pressure ratio.

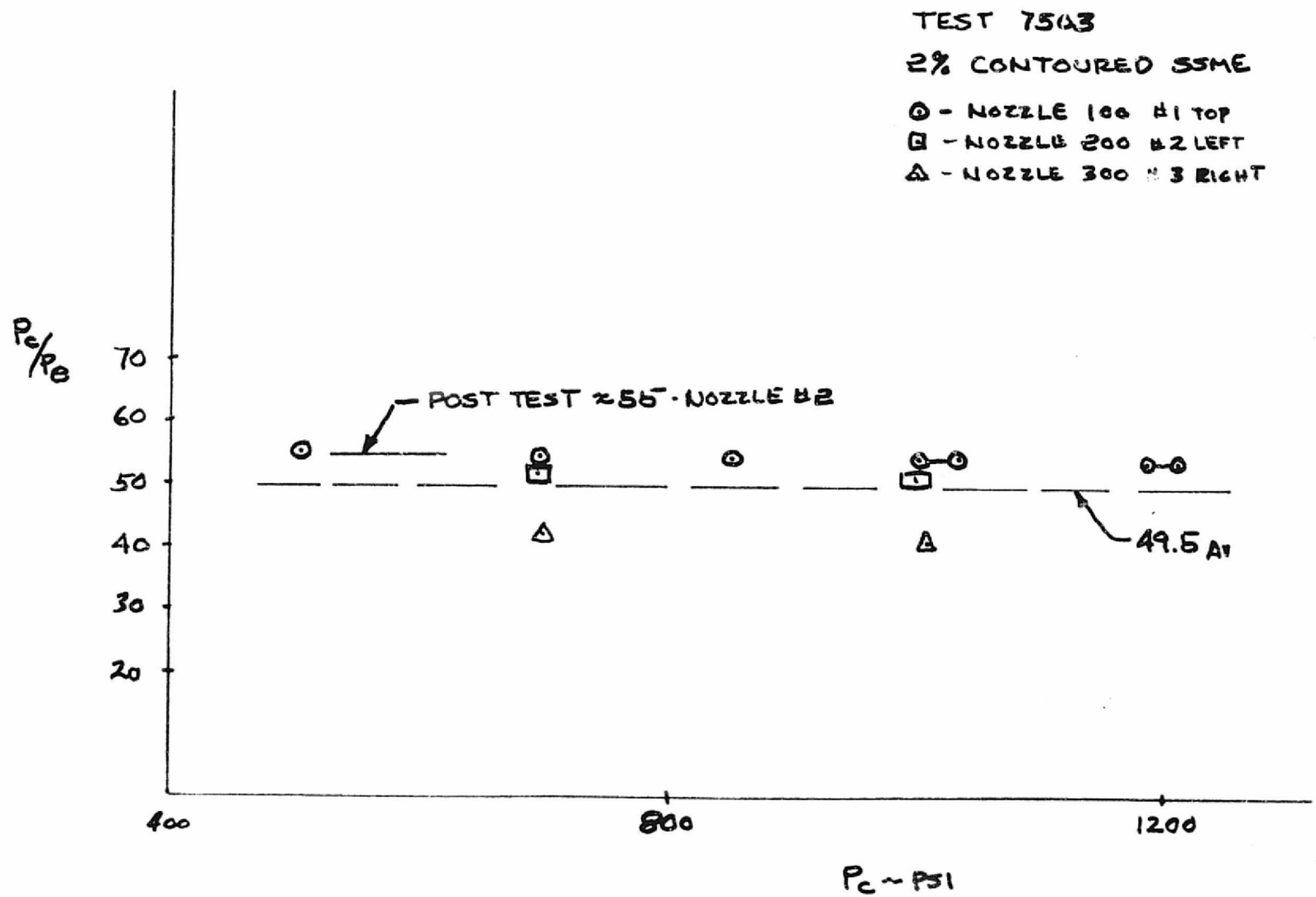

Figure 4-1. SSME NOZZLE CALIBRATION DATA

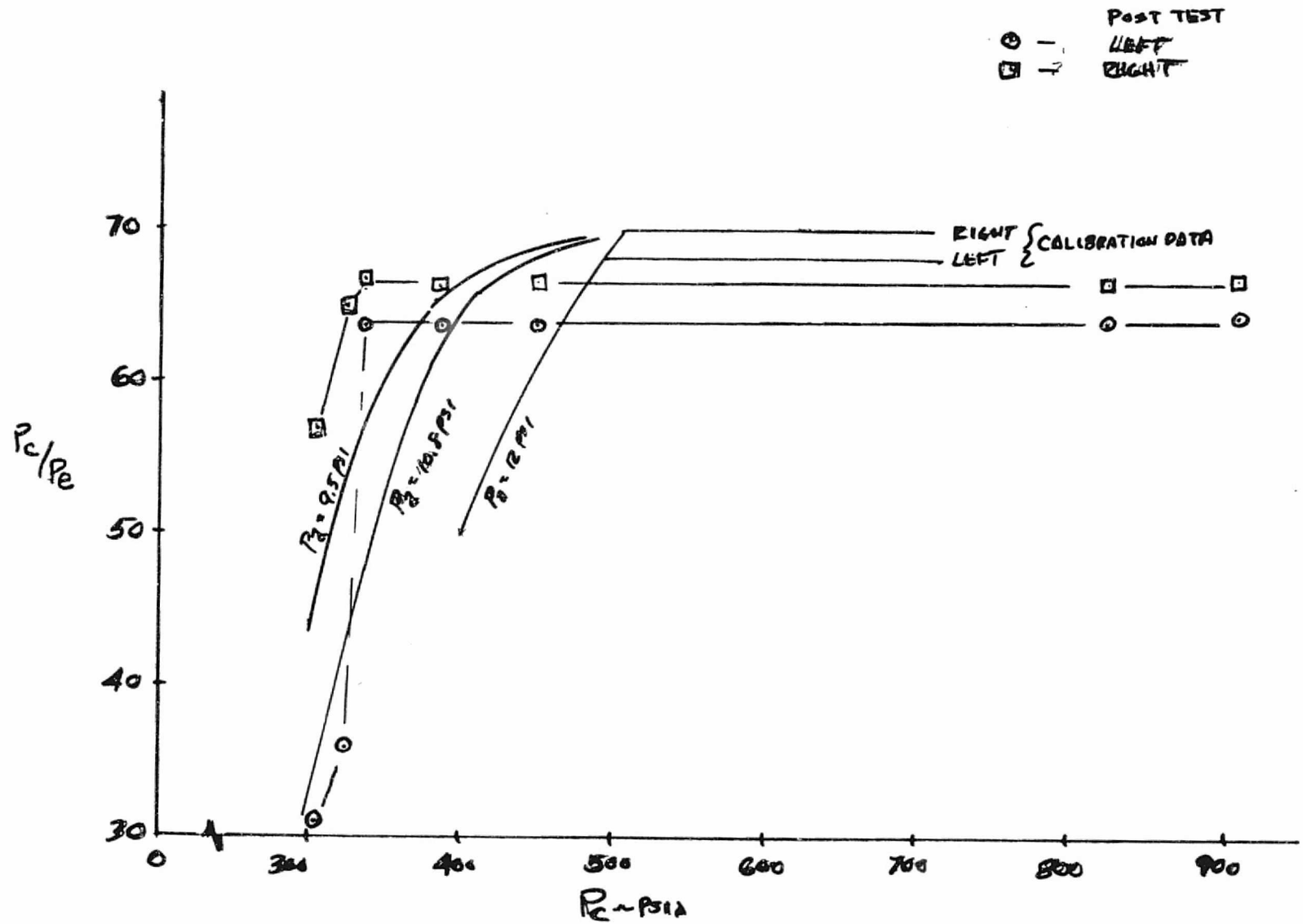

Figure 4-2. SRB NOZZLE CALIBRATION DATA

K•E 10 X 10 TO THE CENTIMETER 18 X 25 CM
KEUFFEL & ESSER CO. MADE IN U.S.A.

461510

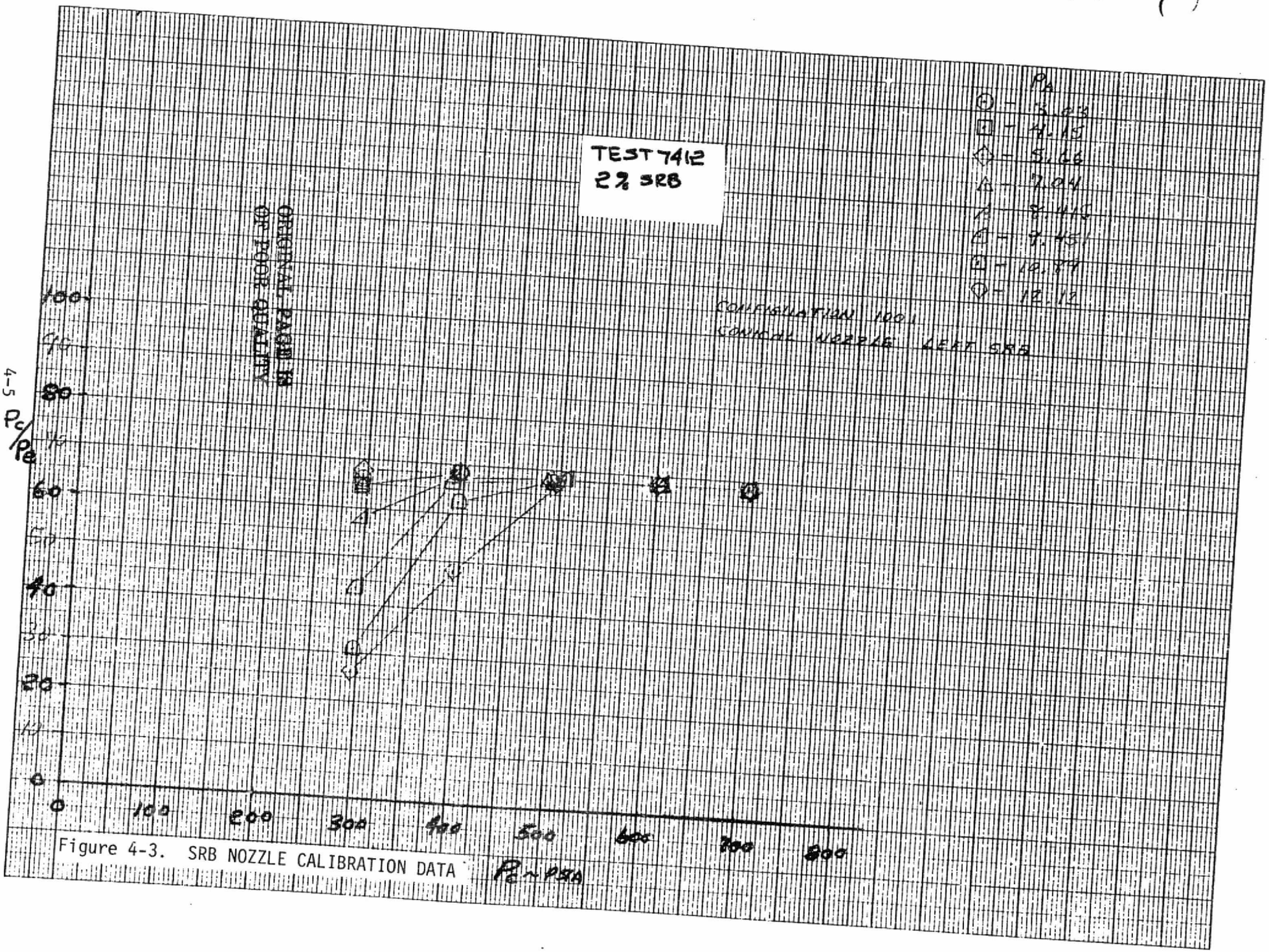

Figure 4-3. SRB NOZZLE CALIBRATION DATA

ORIGINAL PAGE IS
OF POOR QUALITY

K•E 10 X 10 TO THE CENTIMETER 18 X 25 CM
KEUFFEL & ESSER CO. MADE IN U.S.A.
46 1510

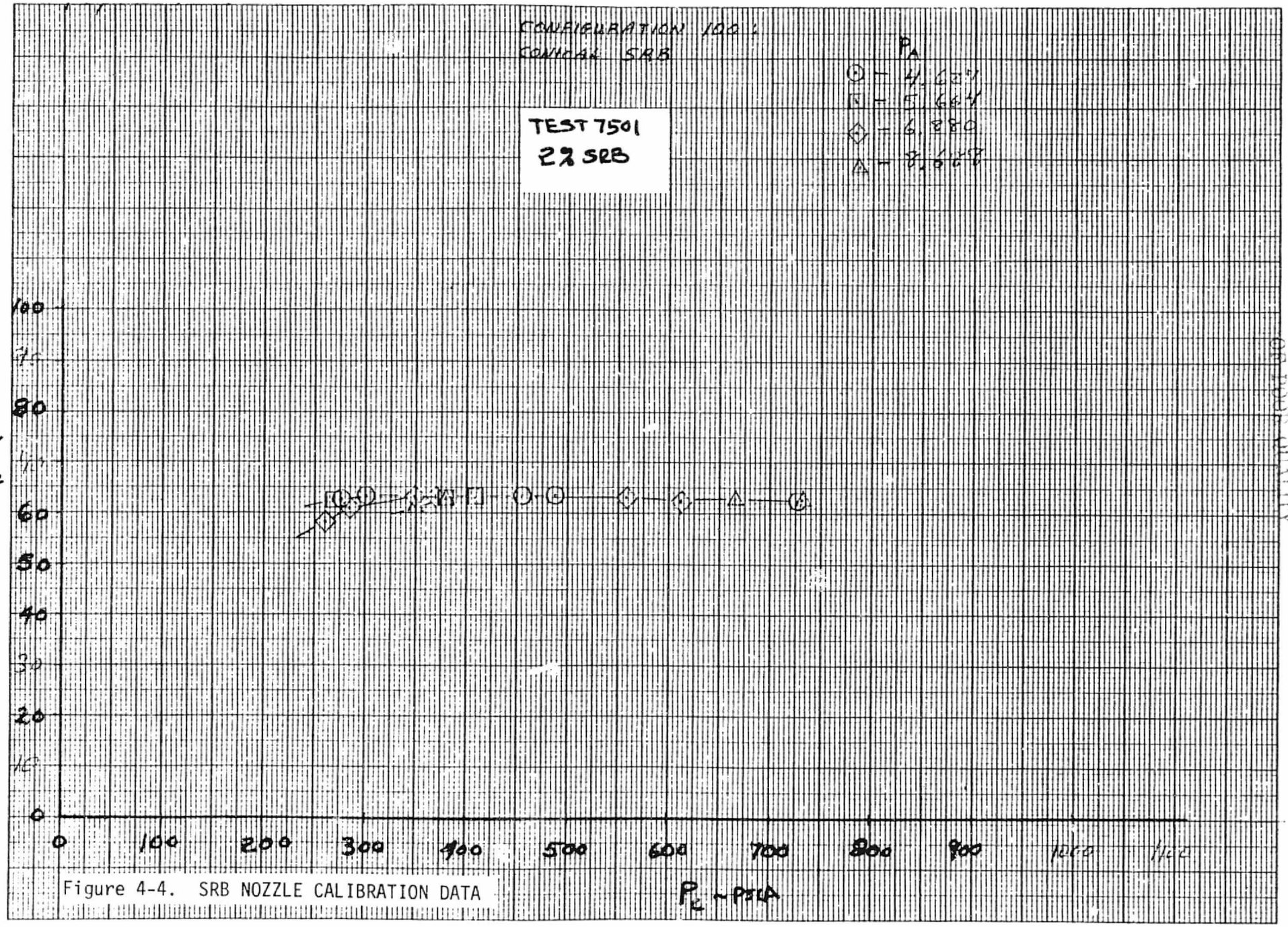

Figure 4-4. SRB NOZZLE CALIBRATION DATA

ORIGINAL PAGE IS
OF POOR QUALITY

K•E 10 X 10 TO THE CENTIMETER 18 X 25 CM
KEUFFEL & ESSER CO MADE IN U.S.A.
46 1510

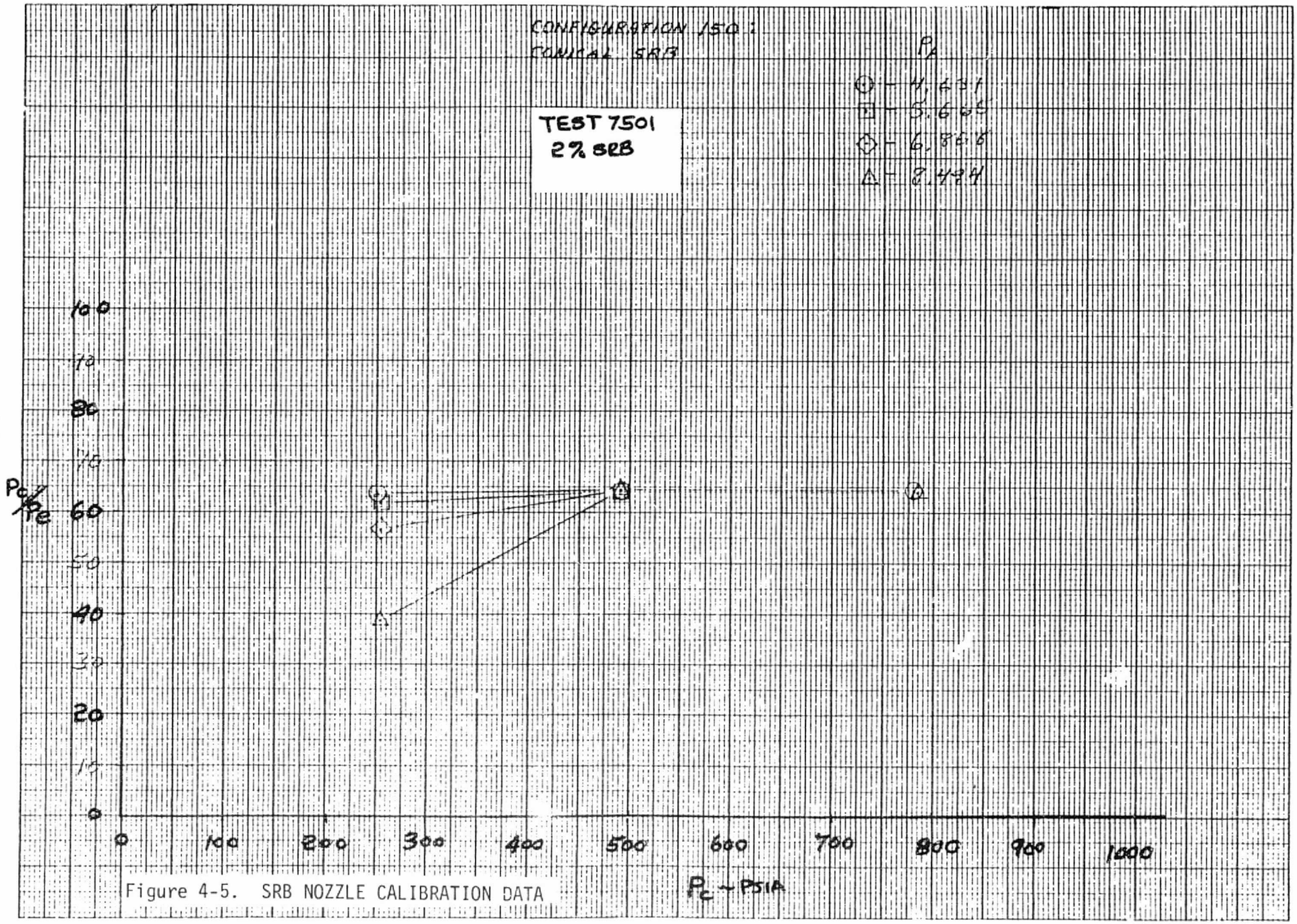

Figure 4-5. SRB NOZZLE CALIBRATION DATA

K•E 10 X 10 TO THE CENTIMETER 18 X 25 CM
KEUFFEL & ESSER CO. MADE IN U.S.A.
46 1510

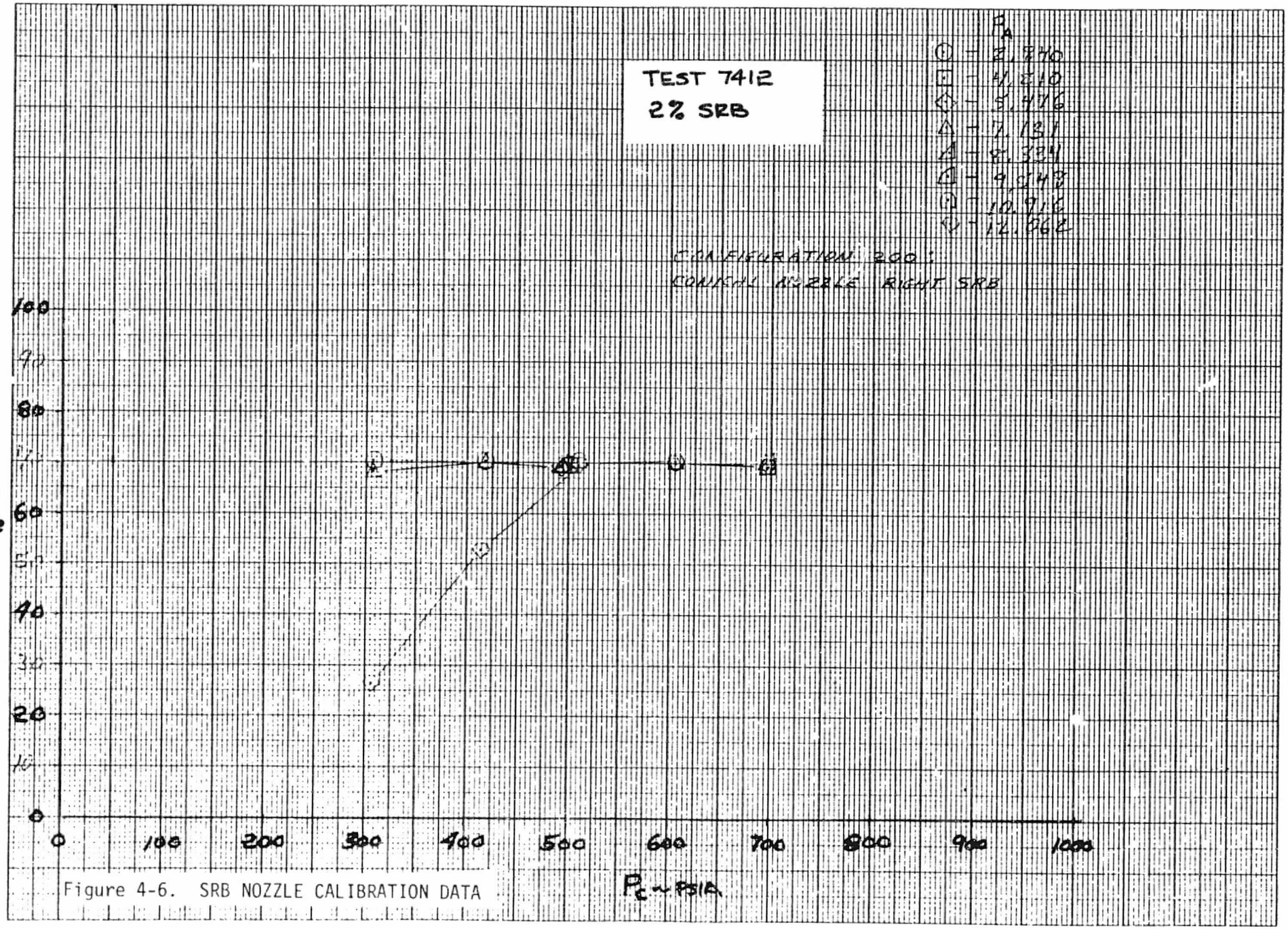

Figure 4-6. SRB NOZZLE CALIBRATION DATA

ORIGINAL PAGE IS
OF POOR QUALITY

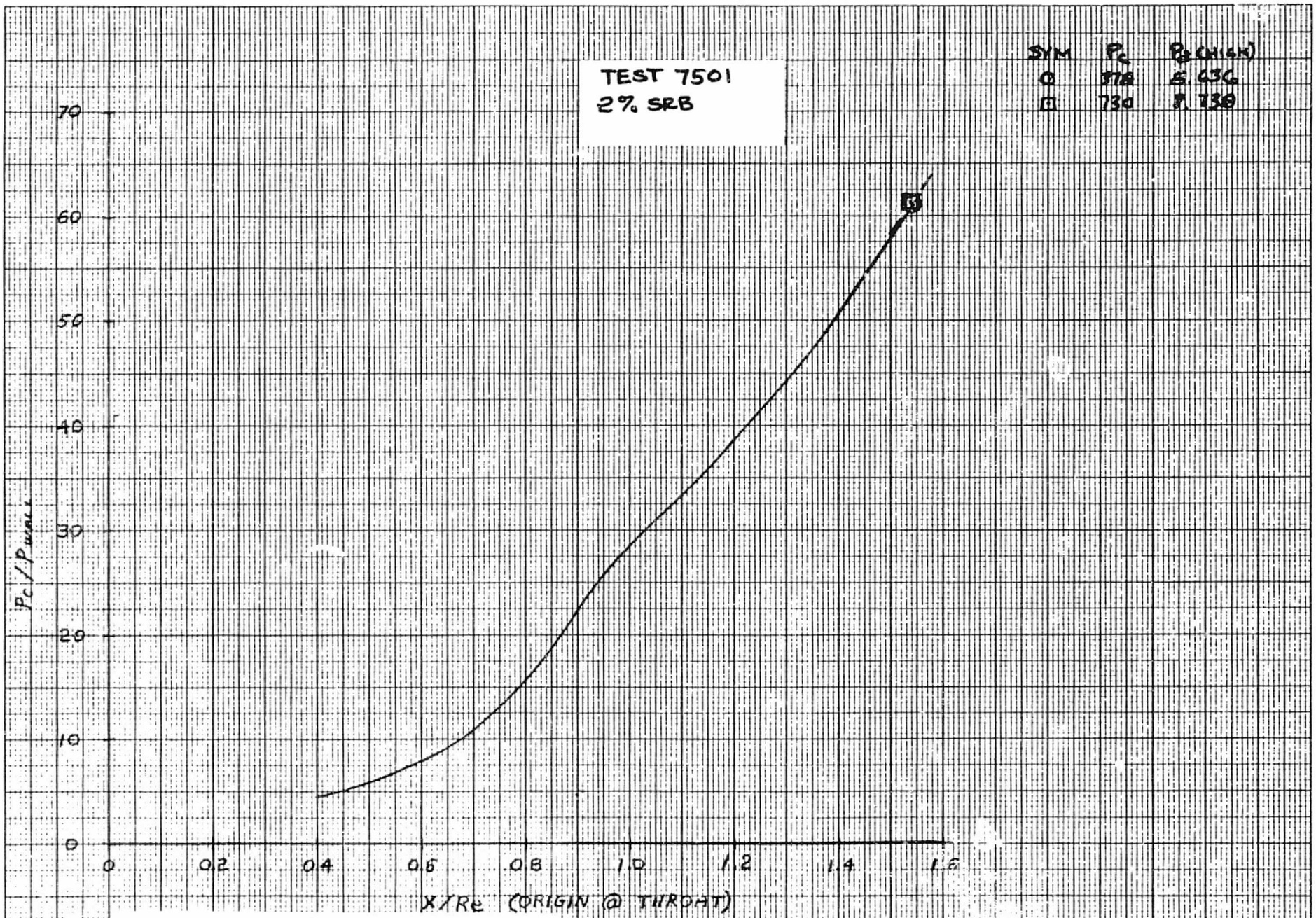

Figure 4-7. SRB NOZZLE CALIBRATION DATA

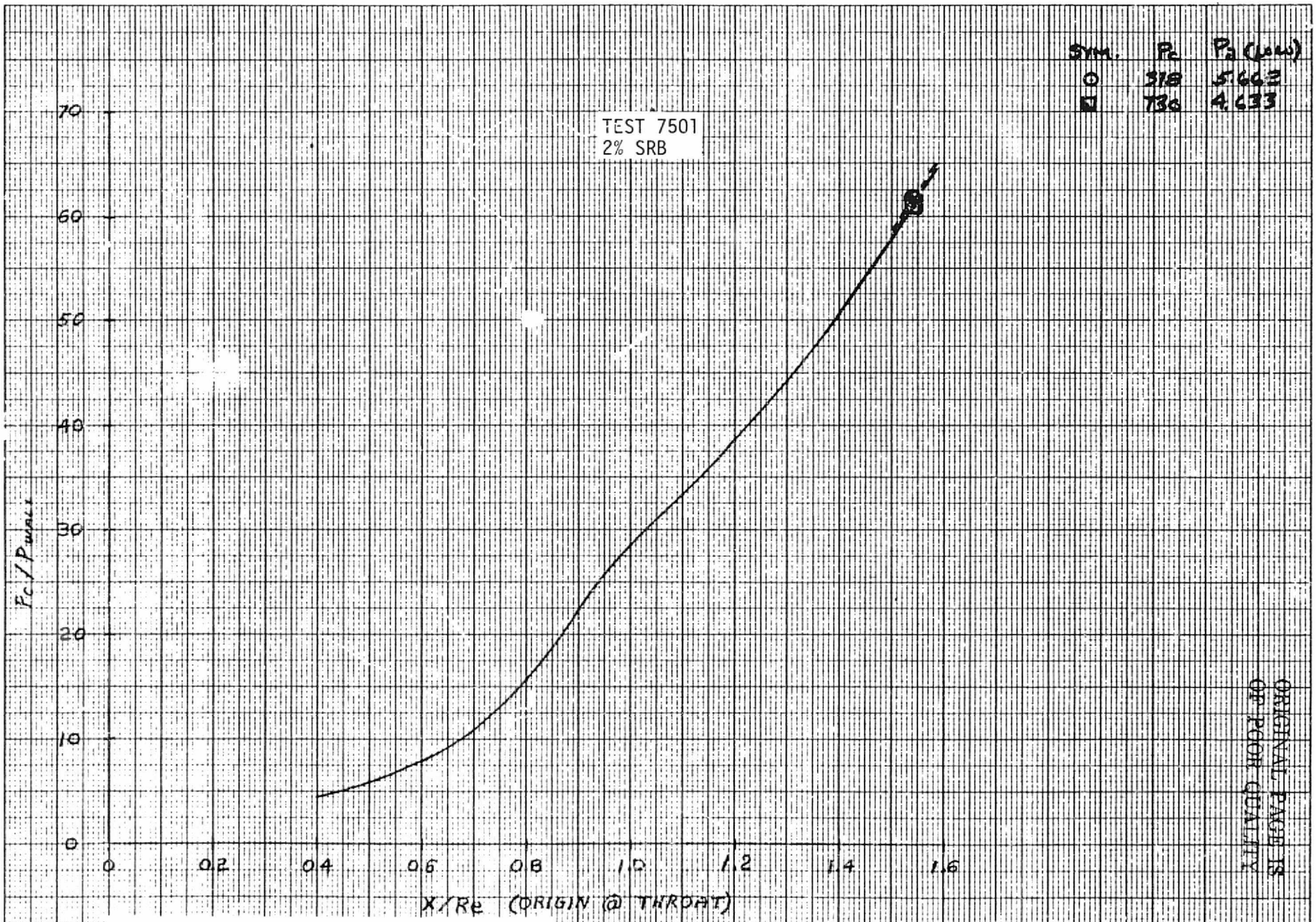

Figure 4-8. SRB NOZZLE CALIBRATION DATA

ORIGINAL PAGE IS OF POOR QUALITY

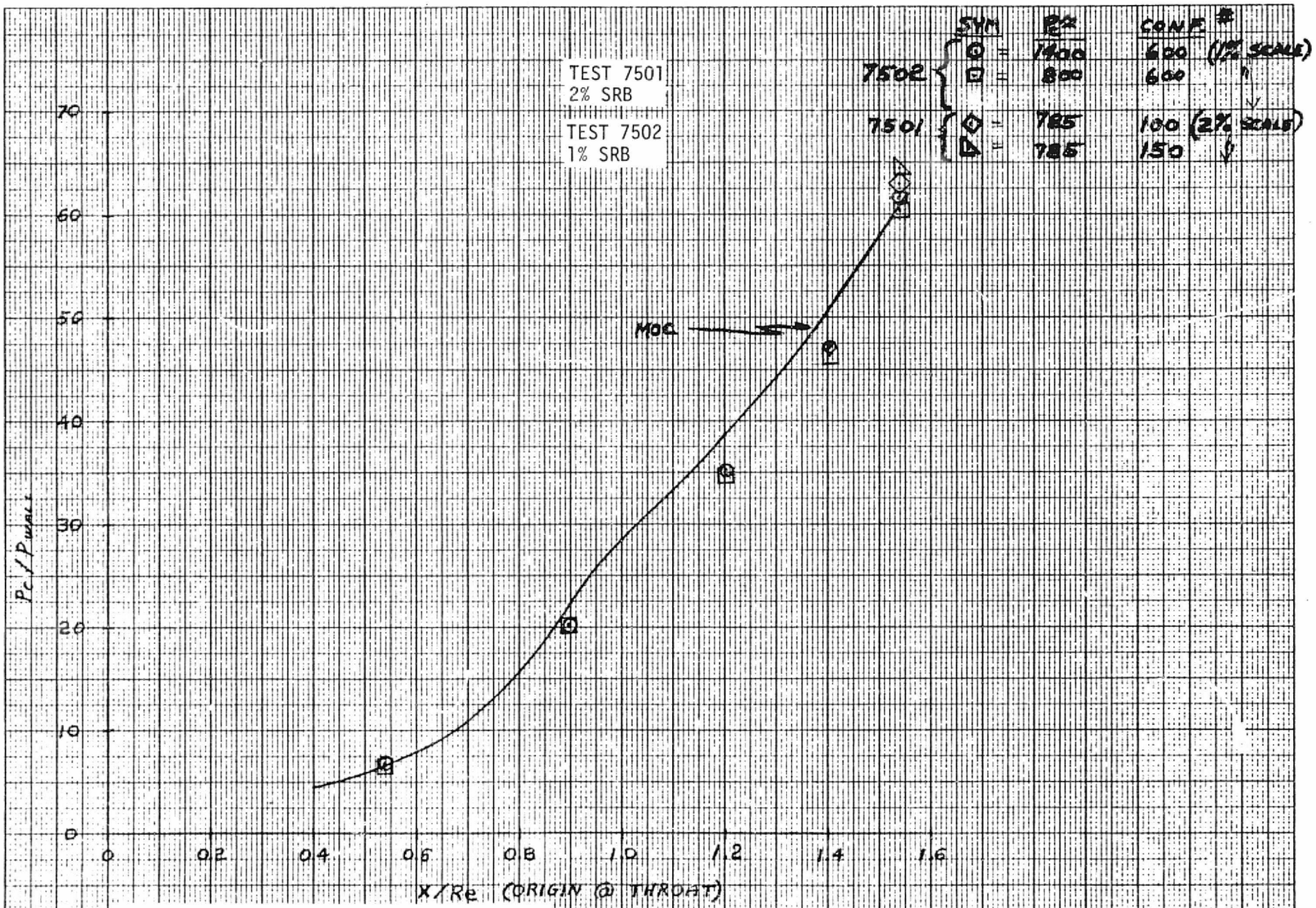

Figure 4-9. SRB NOZZLE CALIBRATION DATA

K•E 10 X 10 TO THE CENTIMETER 18 X 25 CM
KEUFFEL & ESSER CO. MADE IN U.S.A.

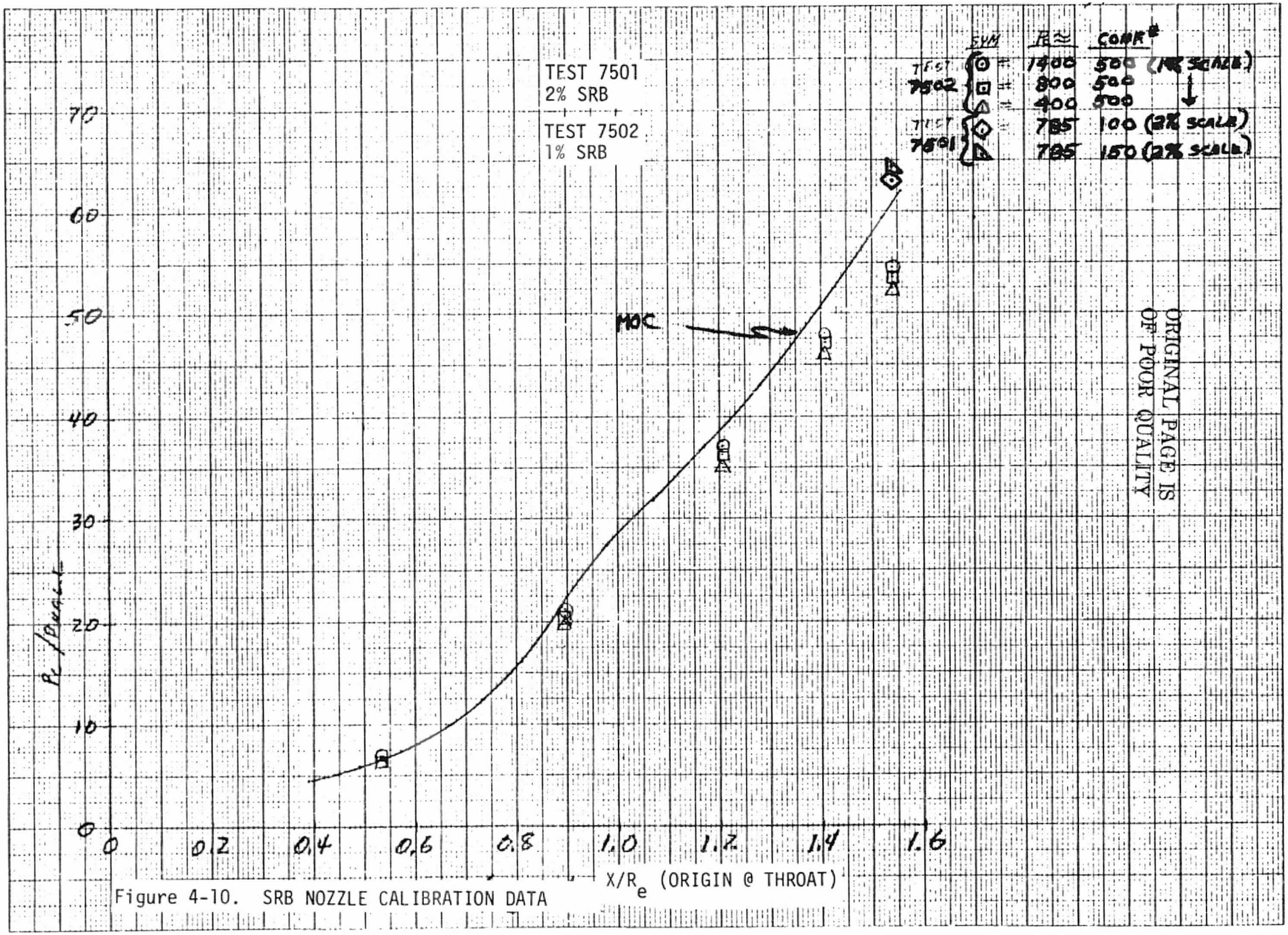

Figure 4-10. SRB NOZZLE CALIBRATION DATA

ORIGINAL PAGE IS
OF POOR QUALITY

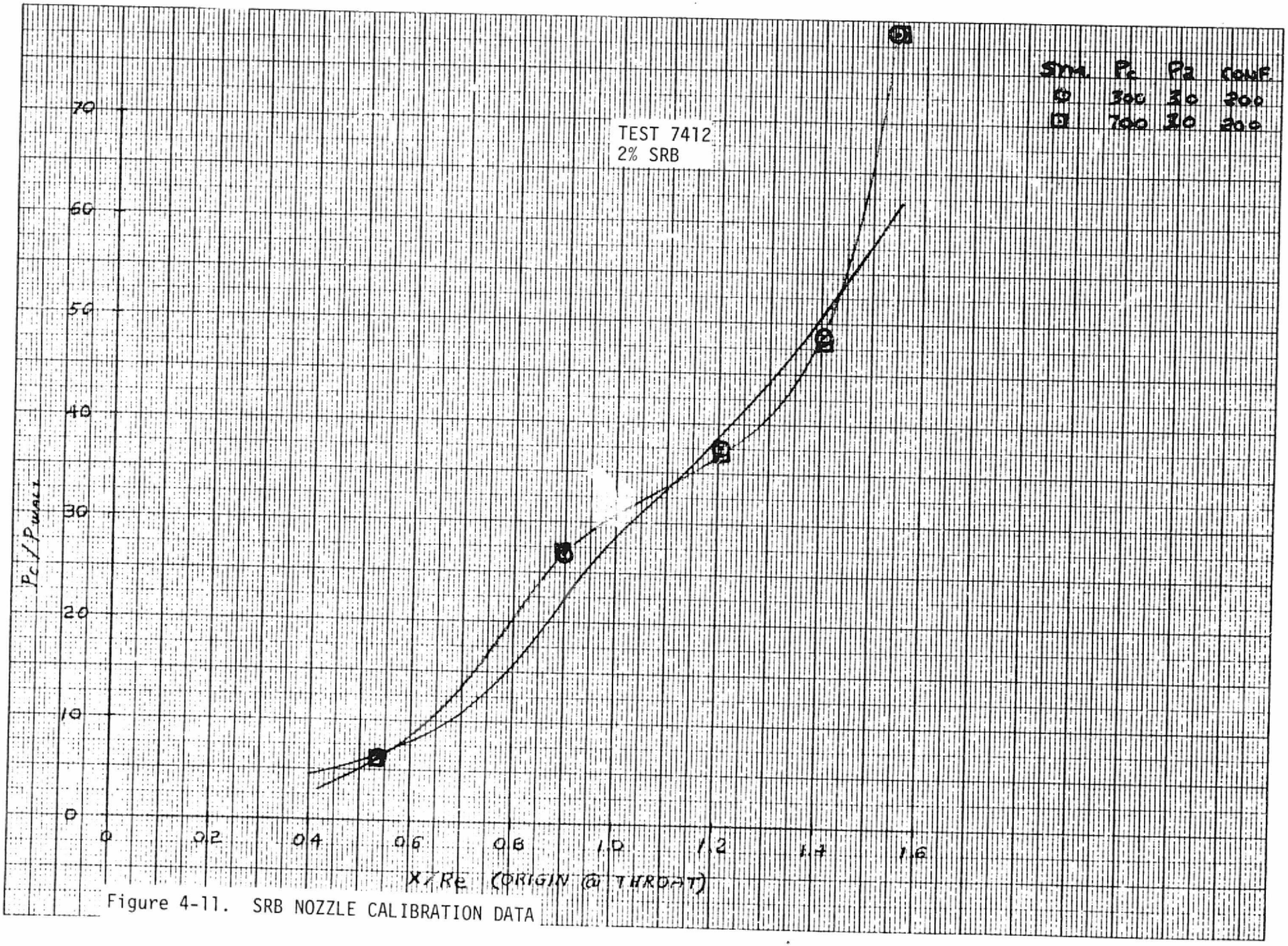

Figure 4-11. SRB NOZZLE CALIBRATION DATA

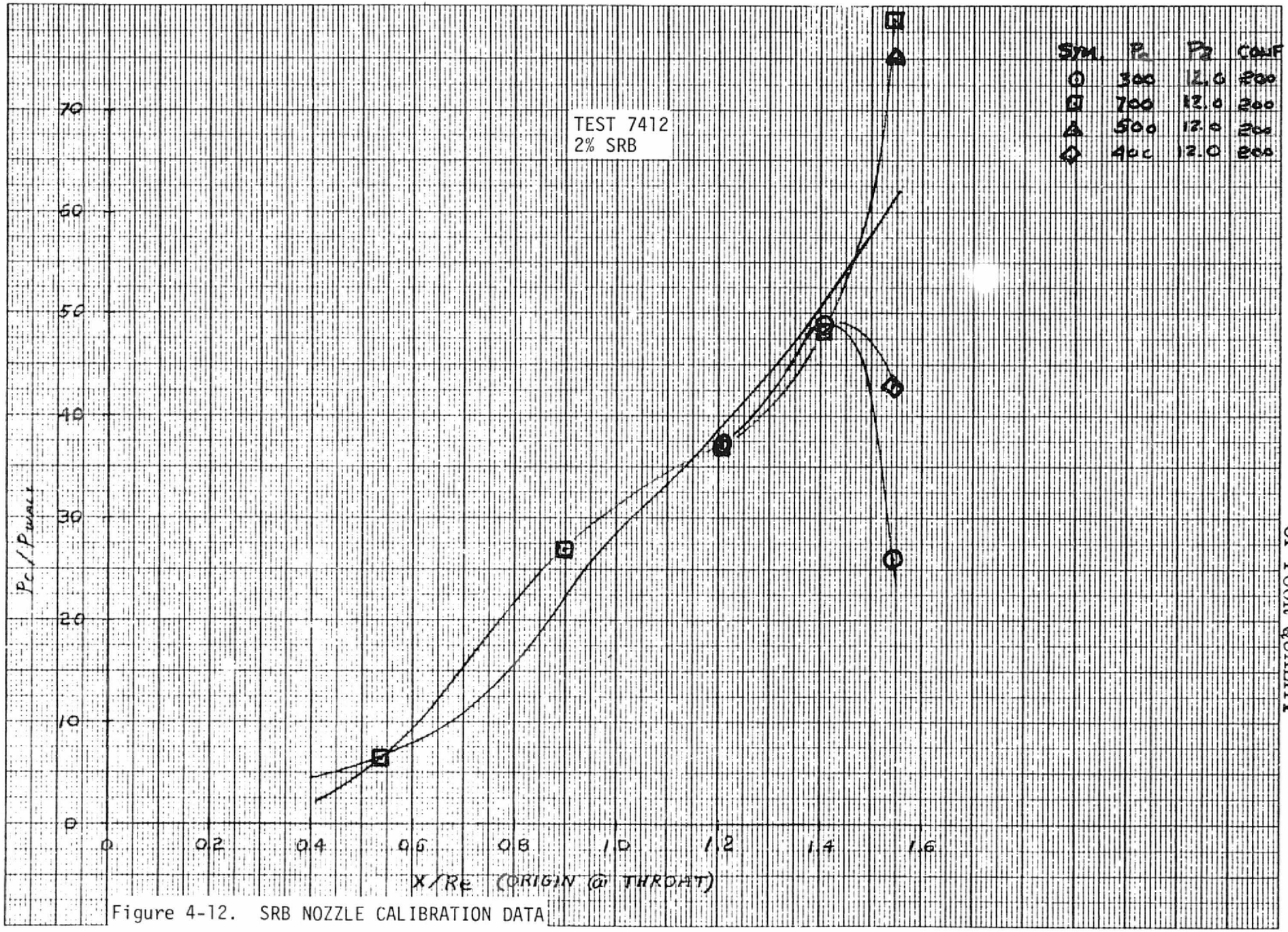

Figure 4-12. SRB NOZZLE CALIBRATION DATA

ORIGINAL PAGE IS
OF POOR QUALITY

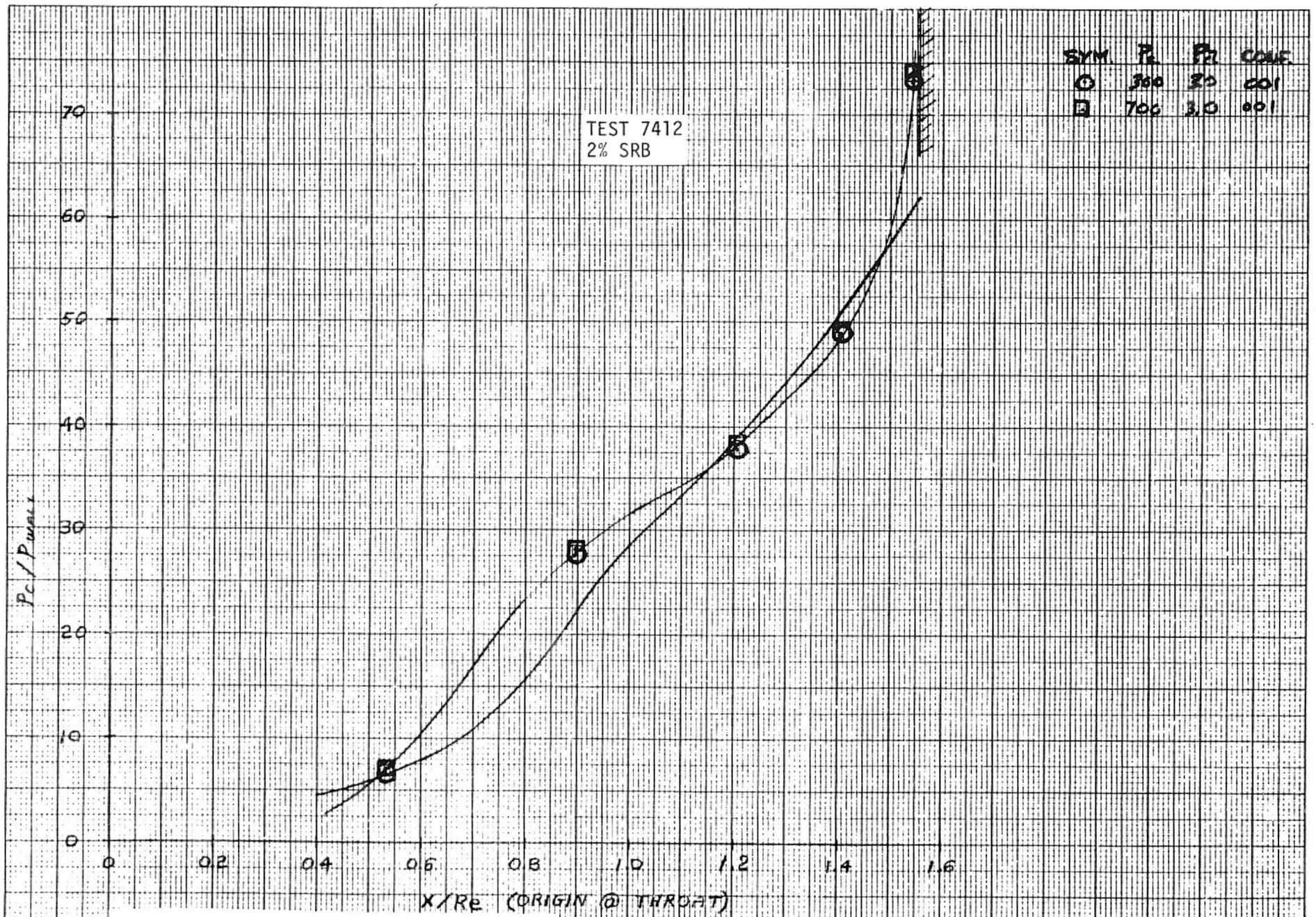

Figure 4-13. SRB NOZZLE CALIBRATION DATA

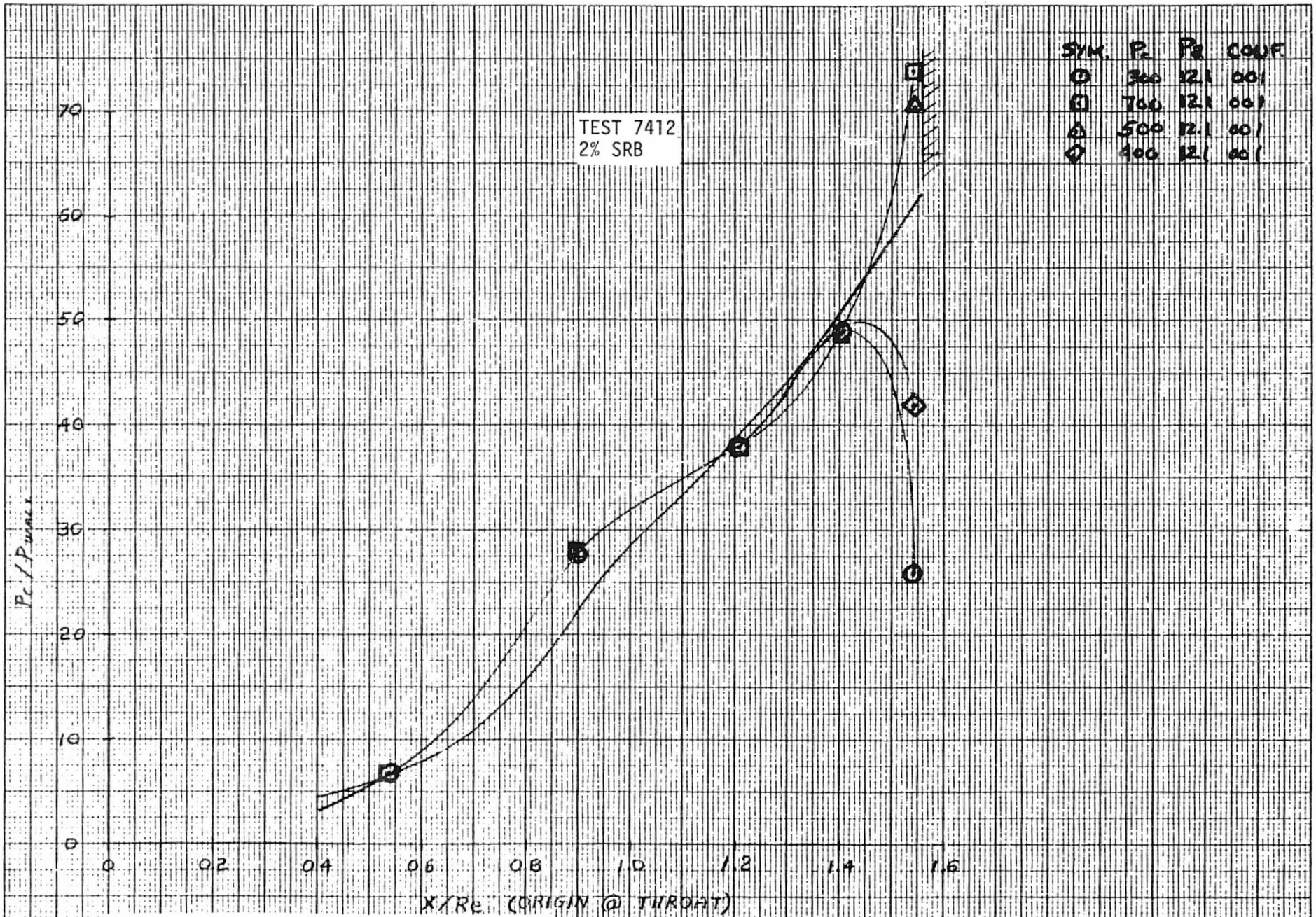

Figure 4-14. SRB NOZZLE CALIBRATION DATA

ORIGINAL PAGE IS
OF POOR QUALITY

Section V

PLUME SIMULATION

The Space Shuttle plumes were simulated using cold air flowing through model nozzles. The model plume characteristics required to develop base and forebody pressure environments were determined using an iteration procedure requiring the development of "PROTOTYPE POSSIBILITY CURVES". Prototype possibility curves are curves of base pressure or base pressure coefficient versus prototype plume characteristics. An example prototype possibility curve is shown in Figure 5-1. The curve is called possibility curve since it is developed for a range of possible prototype base pressure environments. These curves were developed prior to the wind tunnel test for both the SSME and SRB prototype nozzles. The SSME possibility curves were developed using possible orbiter base pressure coefficients and the SRB possibility curves were developed using SRB possible base pressure environments. During the power level portion of the test, model base pressure data are plotted on the prototype possibility curves as shown in Figure 5-1. The model power level is determined where the model pressure curve crosses the prototype pressure curve. An iteration procedure is used when there are two variables involved that influence the base pressure, i.e. SSME power level and SRB power level. The possibility curves and the model pressure data used to determine the nominal power levels at each Mach number are presented in the Appendix.

The form of the plume simulation equation used during the IA119 test program was the following (reference 8)

$$\delta_j \gamma_j^N \Big|_{PROT.} = \delta_j \gamma_j^N \Big|_{MODEL}$$

where N is a function of Mach number. A plot of N versus Mach number is shown in Figure 5-2 and was obtained from reference 9. This curve was developed by correlating the base pressure in the near field and the far field developed from cold gas air and CF_4 plumes. The plume induced near field and far field areas considered are shown in Figure 5-3. The model configurations used were single body single nozzle, single body triple nozzle and triple body configurations. The triple body configuration was similar to the ET-SRB space shuttle

configuration. The band on the curve represents the range of N for the various models used in the plume technology test (i.e., single body, triple body, etc.). The criteria used for correlation of the plume technology data was that the same base pressure occur for a five percent or less change in similarity parameter. The band represents the total spread of N for the various model and nozzle configurations considered in the plume technology program.

An example of the similarity parameter data correlation for the far field wing is presented in Figure 5-4. Figure 5-4 shows the wing plume induced normal force versus SSME similarity parameter. These curves show good general separation. The figure also shows that the wing plume induced increment in normal force is more sensitive to SRB power level than it is to SSME power level. The separation of the curves shows that the similarity parameter fits the data into distinct curves covering both positive and negative plume induced wing load conditions which shows good correlation and adds confidence to the similarity parameter used.

The similarity parameter $\delta_j \gamma_j^N$ requires the development of "PROTOTYPE POSSIBILITY CURVES" using prototype MPS and SRB plume characteristics. The δ_j and γ_j characteristics of the MPS and SRB plumes used to develop the prototype similarity parameter are presented in Figures 5-5 through 5-7. The SRB prototype plume characteristics presented in Figures 5-5 and 5-6 have been subsequently updated. The SRB plume angle shown in Figure 5.5 is approximately 1/2 a degree higher than the updated data. The "PROTOTYPE POSSIBILITY CURVES" are presented in the appendix.

The prototype plume characteristics are a function of the motor chamber pressure and altitude and are therefore dependent on the ascent trajectory. The 3A ascent trajectory characteristics were used as a reference trajectory. The ascent trajectory characteristics that influence the prototype plume characteristics are presented in Table 5-1.

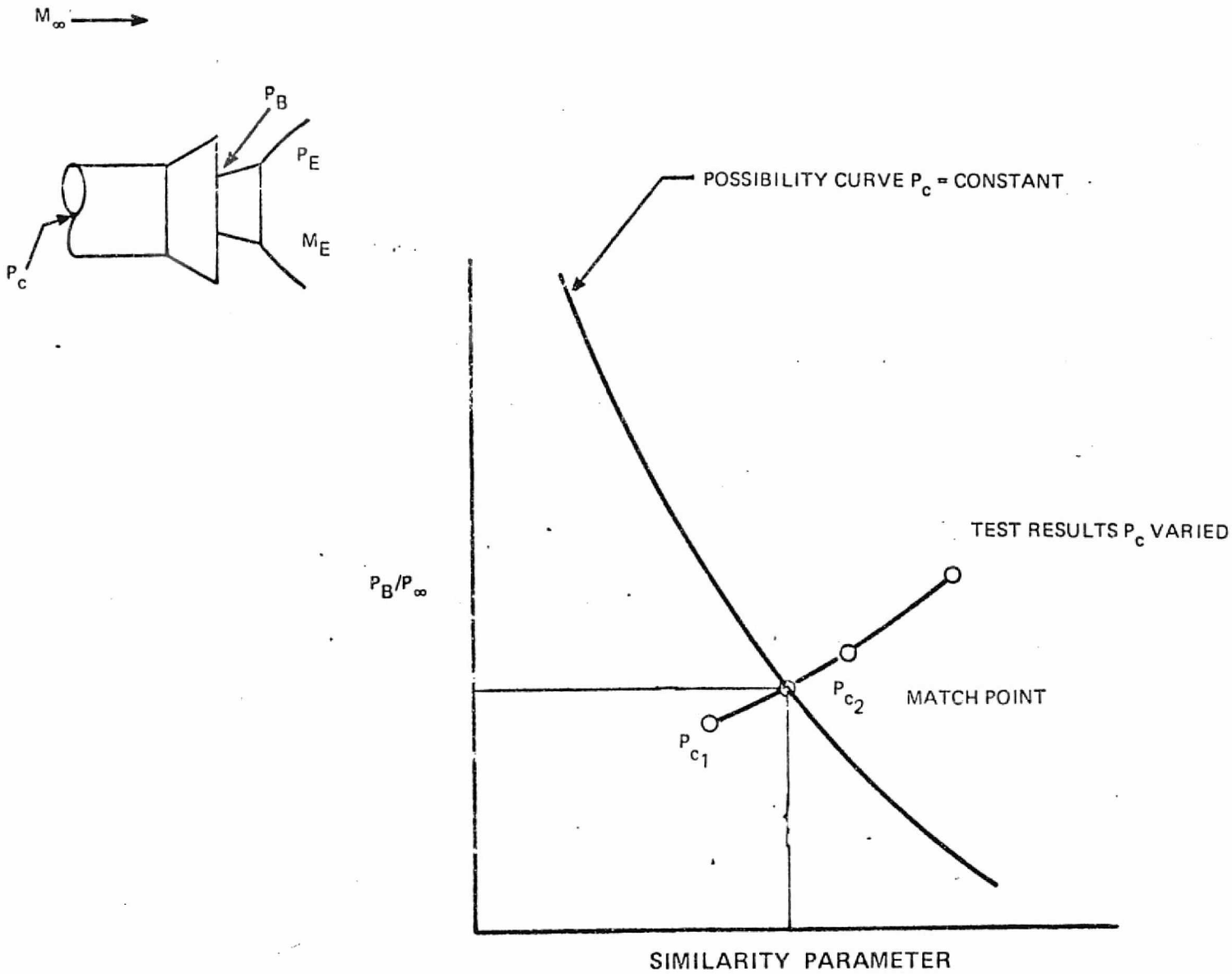

Figure 5-1. PROTOTYPE POSSIBILITY CURVE

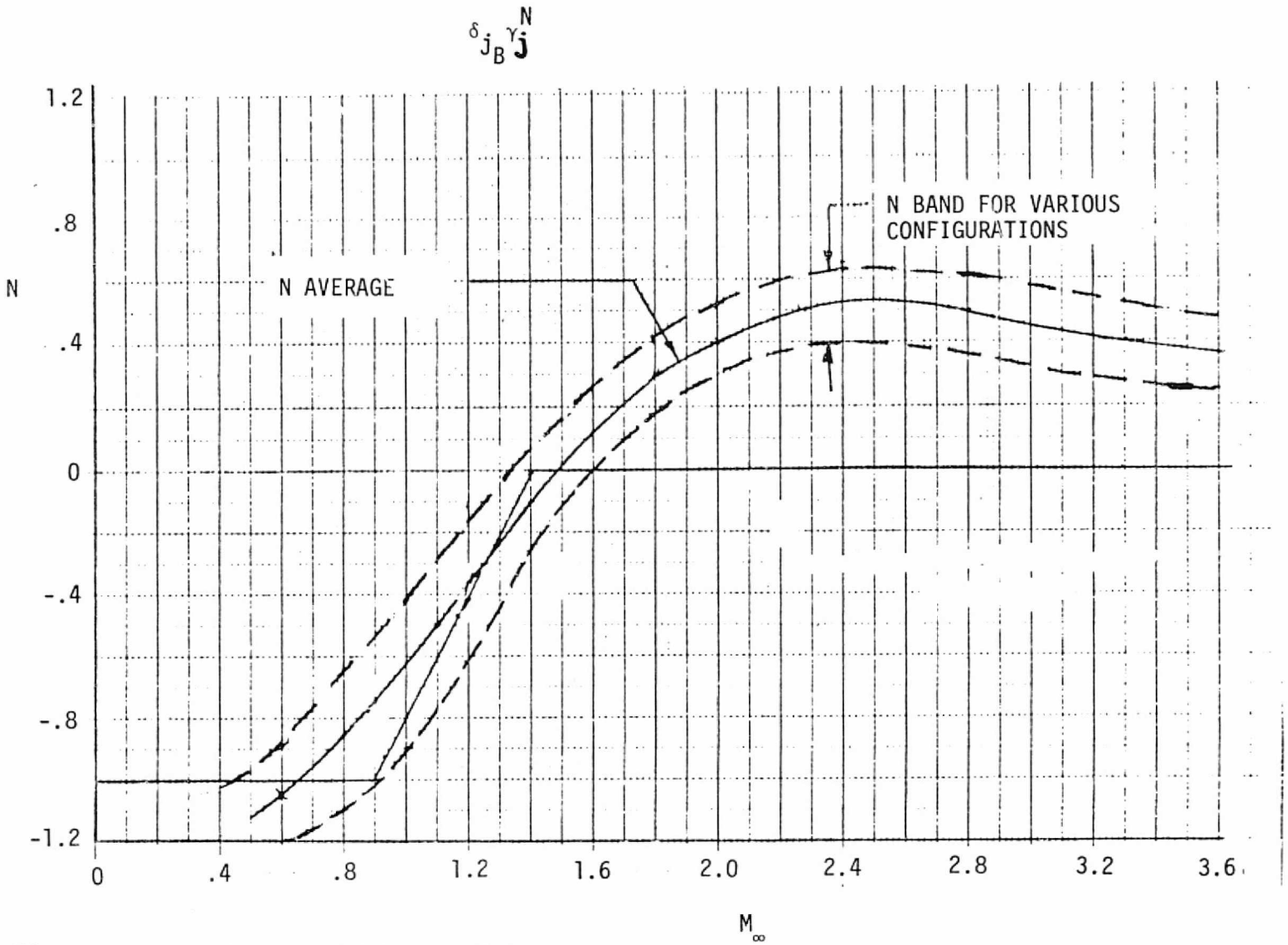

Figure 5-2. SIMILARITY PARAMETER EXPONENT

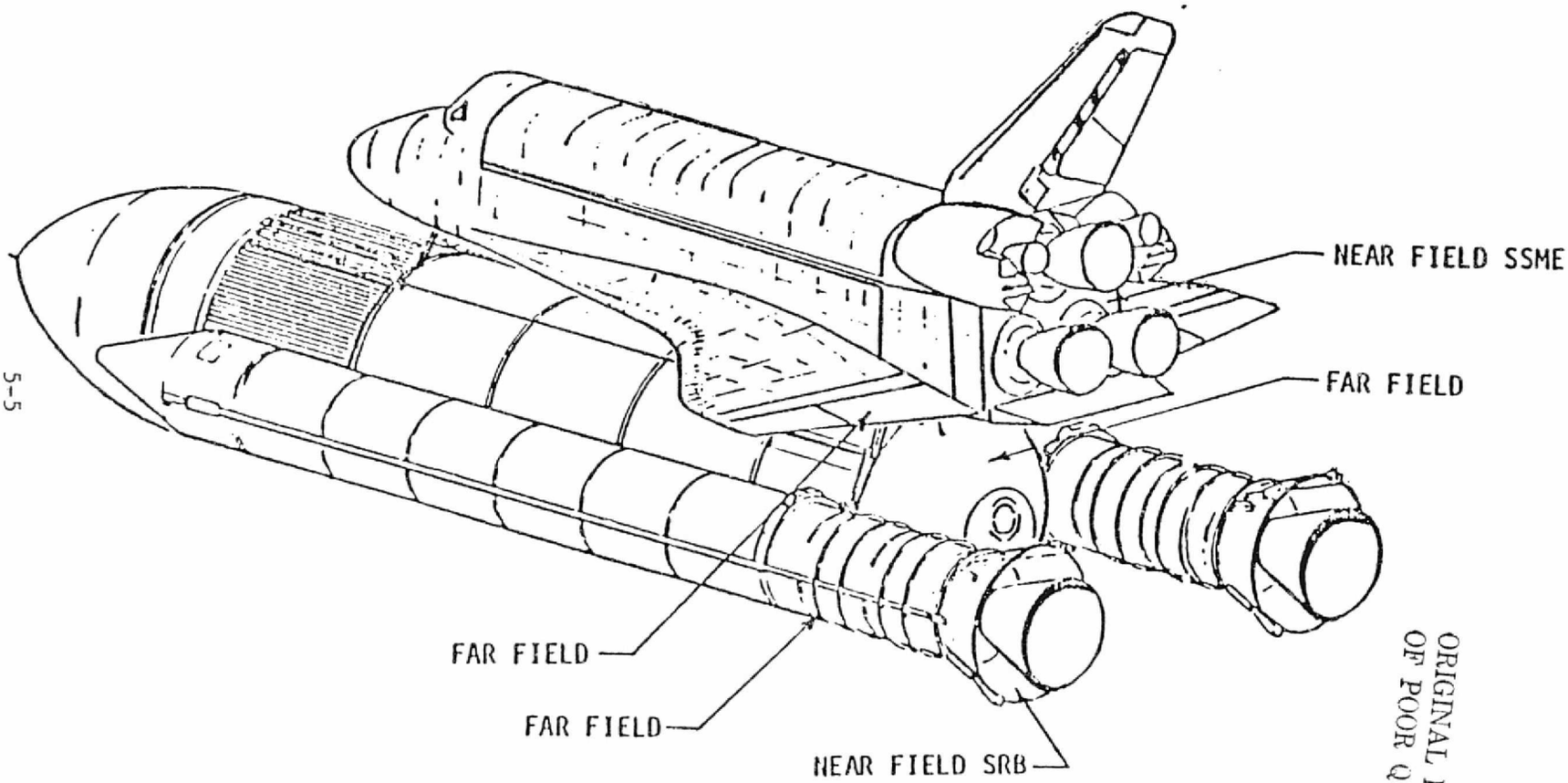

ORIGINAL PAGE IS
OF POOR QUALITY

Figure 5-3. PLUME FLOW FIELD AREAS

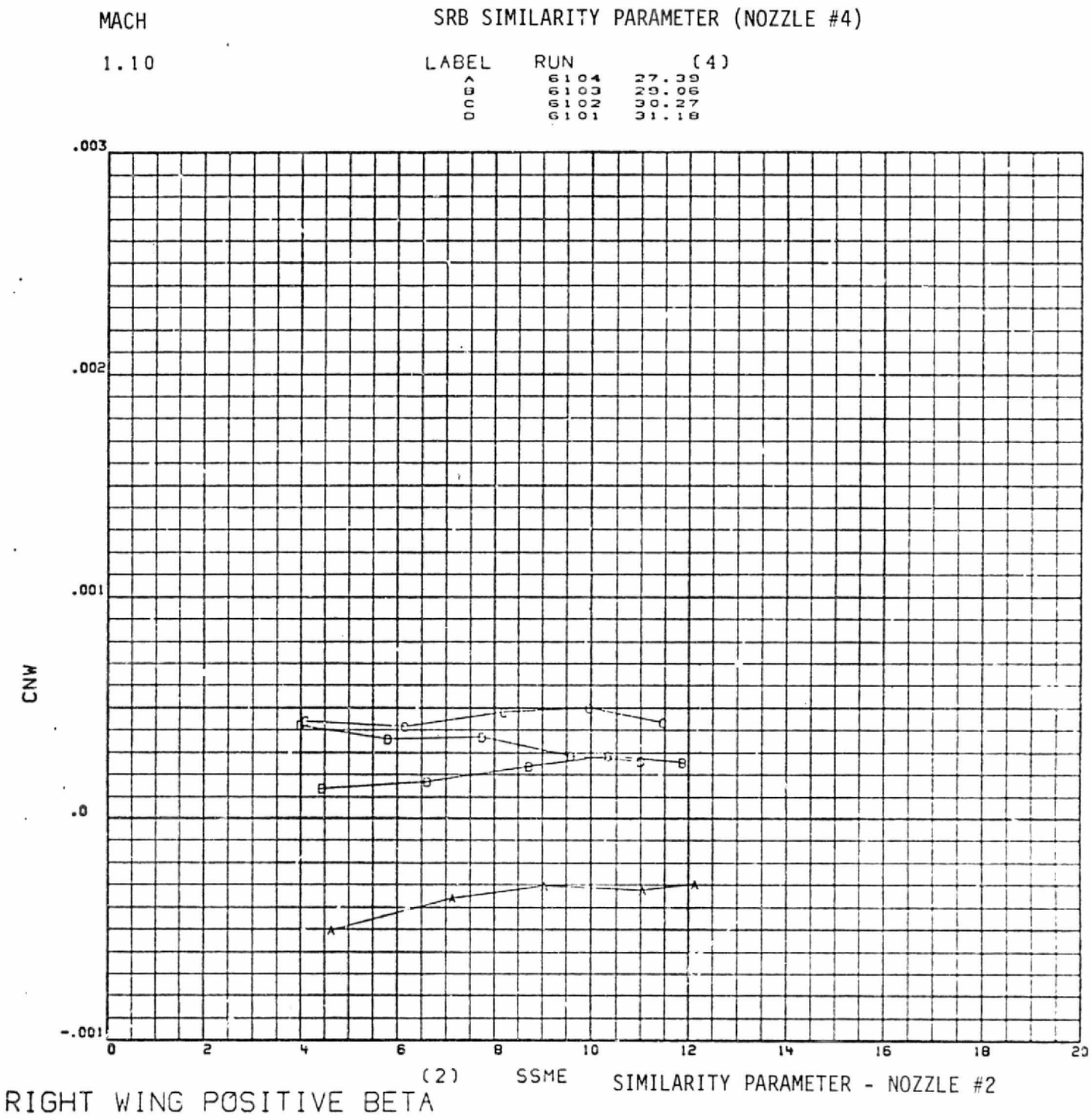

Figure 5-4. FAR FIELD DATA CORRELATION

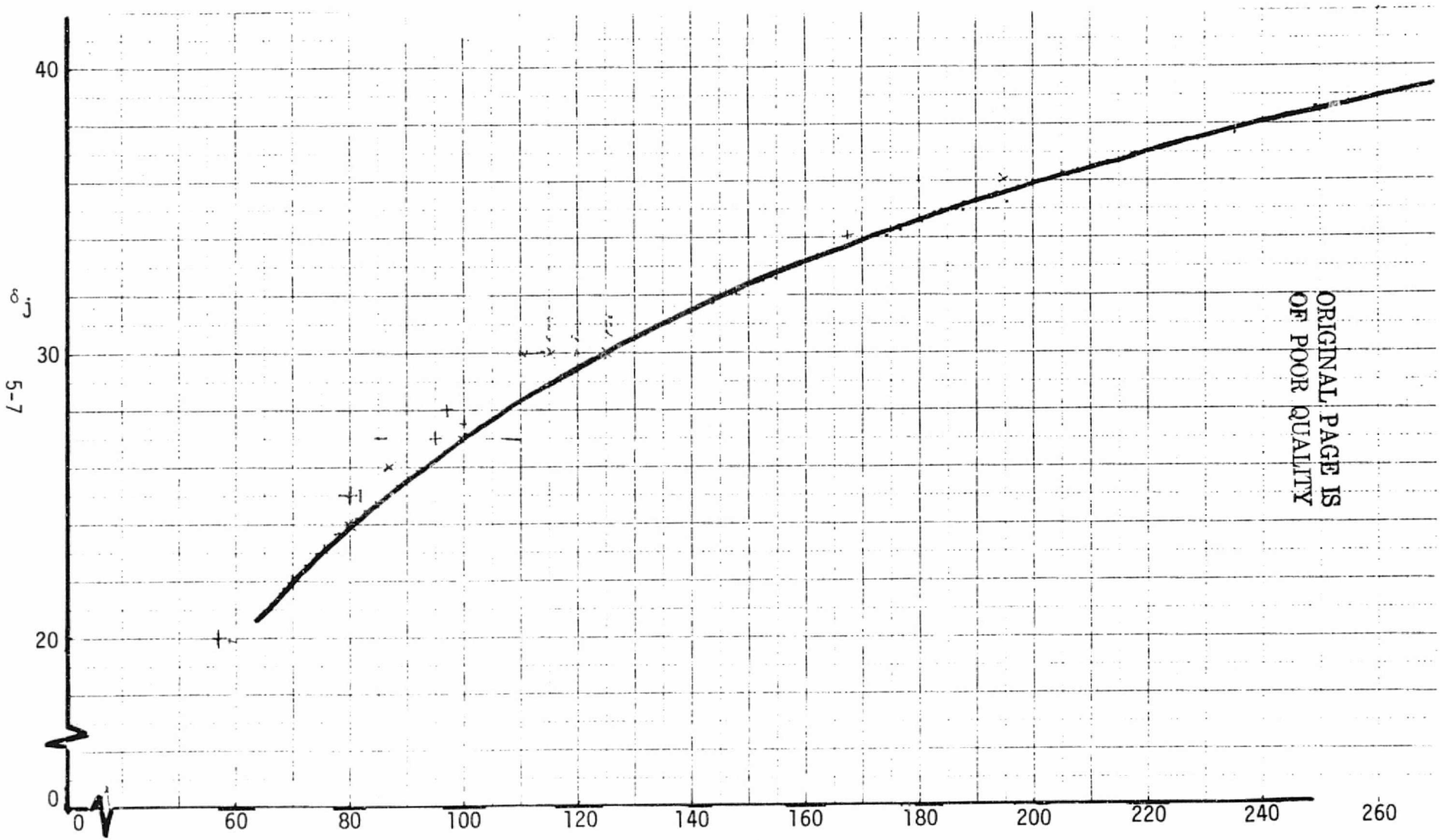

Figure 5-5. SRB PROTOTYPE PLUME ANGLE

ORIGINAL PAGE IS
OF POOR QUALITY

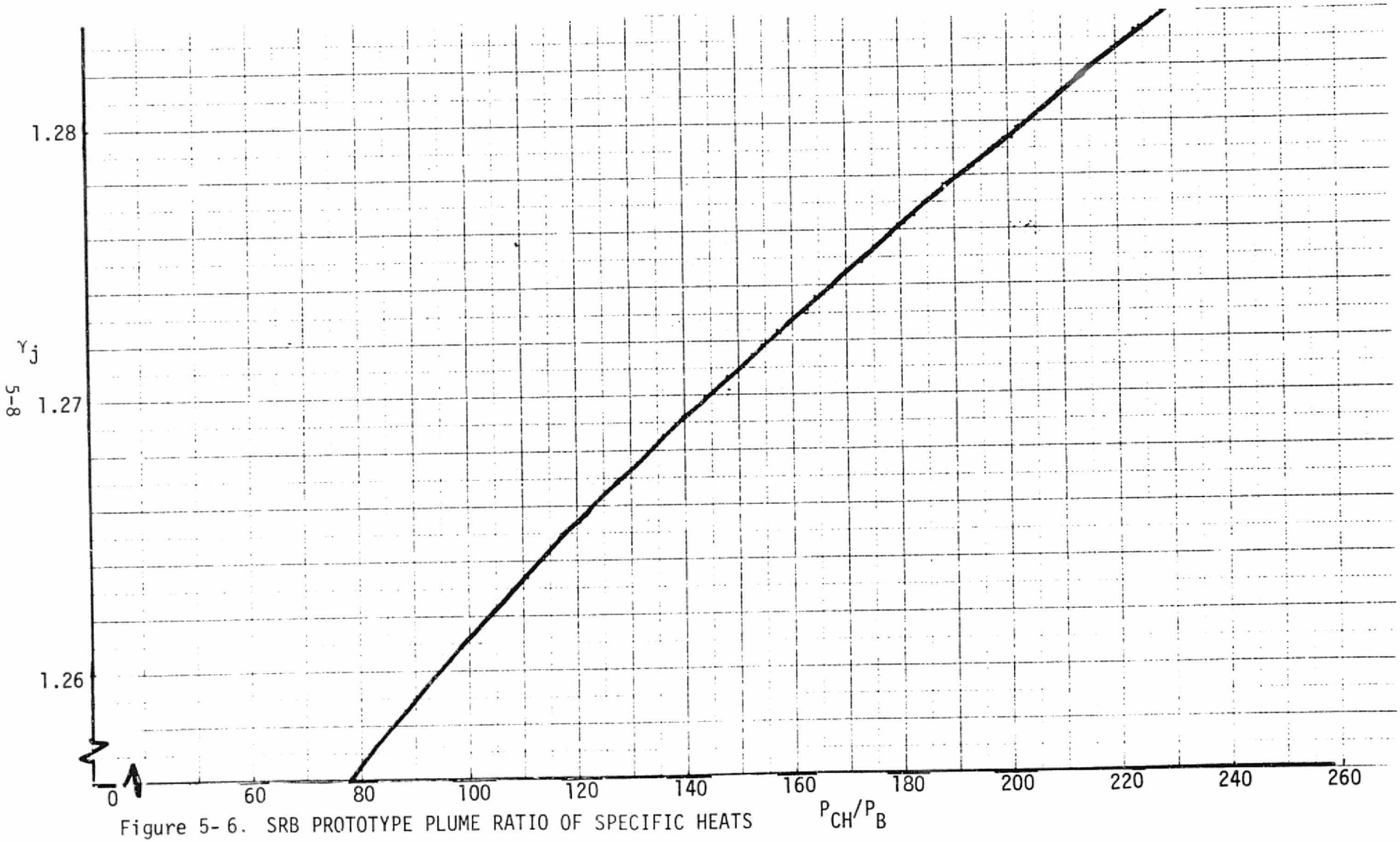

Figure 5-6. SRB PROTOTYPE PLUME RATIO OF SPECIFIC HEATS

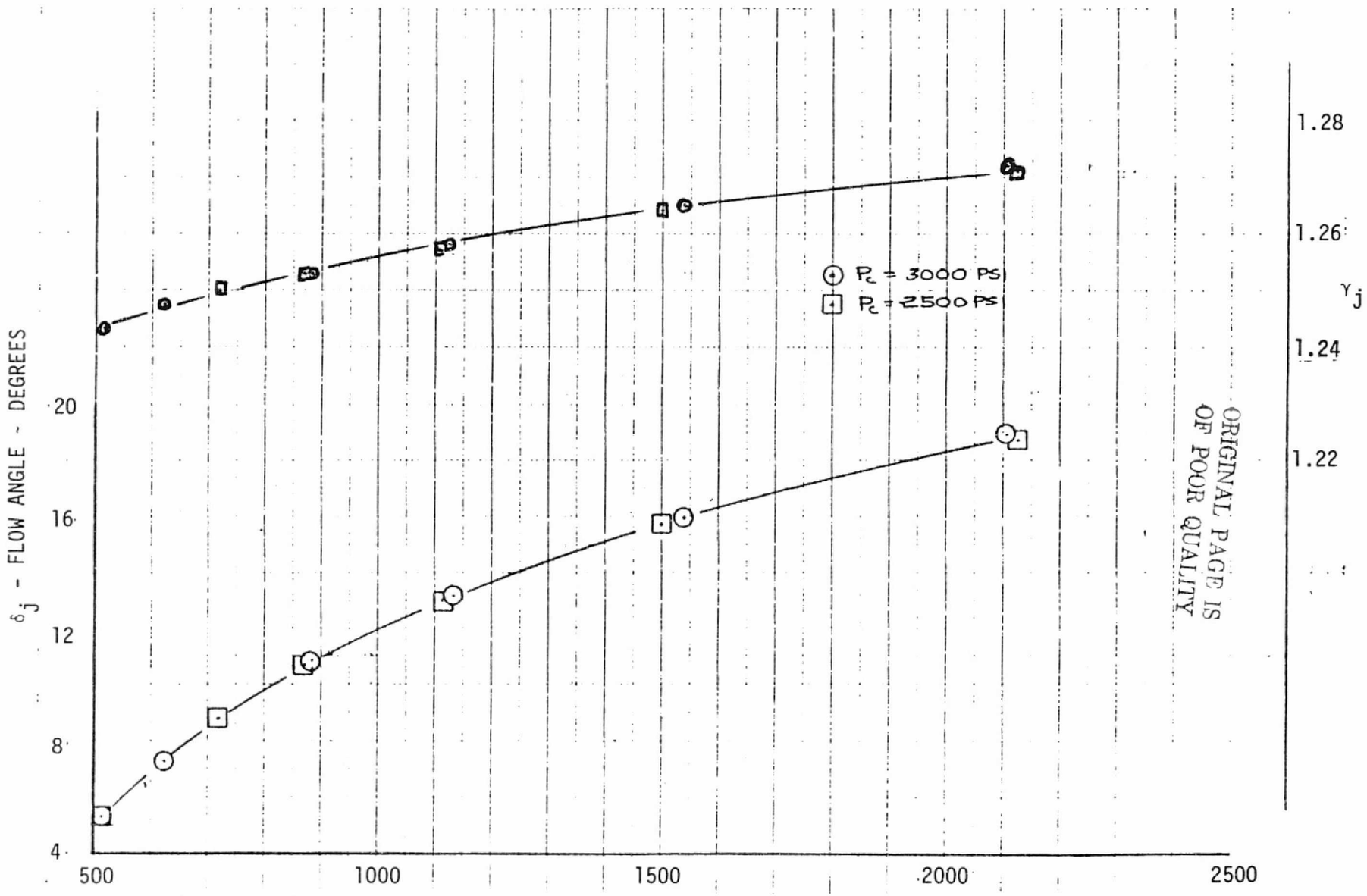

ORIGINAL PAGE IS
OF POOR QUALITY

Figure 5-7. SSME PROTOTYPE δ_j AND RATIO OF SPECIFIC HEATS P_c/P_B - CHAMBER TO BASE PRESSURE RATIO

Table 5-1

ASCENT TRAJECTORY AND SRB — SSME CHAMBER PRESSURE

TIME	MACH NO.	P_∞(PSIA)	q_∞(PSF)	$P_{c_{SRB}}$(PSIA)	SSME PERCENT THROTTLE %
31.0	0.6	10.41	375.5	697	109
40.4	0.8	8.09	526.0	628	88.4
44.8	0.9	7.02	574.2	601	88.4
47.0	0.95	6.51	592.5	592	88.4
51.2	1.05	5.56	617.4	580	88.4
53.2	1.10	5.13	626.4	586	88.4
55.0	1.15	4.76	633.5	584	88.4
58.3	1.25	4.11	642.8	586	88.4
62.9	1.40	3.29	649.5	603	109

Section VI

DATA ANALYSIS

Five computer codes were used to analyze the IA119 data. These programs are: 1. SORT program, 2. Power Delta program, 3. Sigma V Punch, 4. Wind Tunnel Pressure Data Analysis and 5. Plume Integration. A brief discussion of each of these programs is presented below.

SORT PROGRAM

The SORT Program was used to sort the run and sequence data sets into basic groups of four. The four run groups consist of +β power-on, +β power-off, -β power-on and -β power off. The four run data sets were arranged in angle of attack sets of -8, -4, 0, 4. Flags were set to note α, β, Mach, gimbal and configuration incompatibility of the four run sets. (See Tables 1-9 Section III)

The following tolerances were put on the data sets to check compatibility.

VARIABLE	TOLERANCE
MACH	.03
α	.25
β	.25
β	Sign
Gimbal	≠0
CONFIGURATION NO. DO NOT AGREE	
RUN NUMBER/SEQUENCE OUT OF PLACE	
δ_{INB}	±.25
δ_{OUT}	±.25

The SORT program proved very useful in identifying errors in the post test run schedule and differences between the power-on and power-off model attitude.

POWER DELTA PROGRAM

The Power Delta program was used to evaluate the change in the pressure data due to power. The program lists all data from the power on run and all data from the power off run and then subtracts the two data sets and lists the power delta's. This allows a rapid survey of the power delta's for abnormal numbers and a reference to the power on run and power off run to determine the error source.

SIGMA V PUNCH

The Sigma V Punch program was used in conjunction with the Power Delta program to sort the forebody power delta data into various elements and components and punch cards of the power delta in a format compatible with the "Wind Tunnel Pressure Data Analysis Program - WTPDA". WTPDA is an interactive graphic pressure data integration computer program which operates on the Sigma V Graphics System.

WIND TUNNEL PRESSURE DATA ANALYSIS (WTPDA)

. PROGRAM DESCRIPTION

WTPDA is an interactive computer graphics program which allows an engineer to apply his judgement to the smoothing of wind tunnel pressure data in a real time environment. The purpose of the program is to produce airloads which are compatible with vehicle stability data and which reflect engineering judgement. WTPDA employs interactive computer techniques so that an engineer can develop balanced airloads in a timely manner.

WTPDA can integrate pressure data on wings, vertical stabilizers, fins, cylinders, and arbitrary cross-section fuselages. Although WTPDA was developed specifically to handle the Space Shuttle launch vehicle, it is capable of handling almost any arbitrary cross-section body.

The WTPDA program was used to plot and smooth the power delta CP's on the forebody. Only limited integration of pressures were performed to check the main pressure integration computer program which is discussed below.

PLUME INDUCED PRESSURE INTEGRATION

The Plume Integration computer program was the main tool used to analyze the IA119 pressure data. This computer program was developed specifically to analyze the IA119 pressure data and was used to integrate the pressure data to obtain base and forebody plume induced aerodynamic loads and moments. The computer program was developed to analyze four run sequences of positive and negative β sets. This operation is required since portions of the model have pressure data on only one side. Thus, to analyze the effects of sideslip required the evaluation of + and - β runs. An example of a four run data set used for analysis at Mach 0.6 would be run sets 153, 158, 155 and 156. These four sets are shown at the top of Table 3-1 as positive and negative sideslip data sets for elevon deflections of 10/9 and nominal nozzle gimbal angles. Both power-on and power-off data sets are required since a portion of the plume induced data uses power on pressure coefficients while other portions require only the change in pressure coefficient due to power.

The analysis of the plume induced aerodynamic characteristics was performed using different pressure data over different portions of the vehicle. This type of analysis was required because of the unique configuration of the Space Shuttle and the model configurations used to obtain the forebody aerodynamic characteristics. The two types of pressure data used for analysis are: 1) The power on C_p's for nominal SSME and SRB model power settings; and 2) The power delta C_p's where $\Delta_{C_{p_{Power}}} = C_{p_{Power\ on}} - C_{p_{Power\ off}}$.

The power on C_p's were used to evaluate the power-on base forces and moments. The power delta C_p's were used to evaluate the change in forebody aerodynamic characteristics. The location on the Space Shuttle vehicle where the different types of pressure data were used is shown in Figure 6-1. Following is a brief discussion of the analysis technique used to evaluate the plume induced aerodynamic characteristics.

ORBITER ANALYSIS

BASE

A photograph of the IA119 model orbiter base is shown in Figure 6-2. The orbiter base includes the base plate, upper body flap areas, and SSME nozzle bells. The base, nozzle bells, and lower portions of the OMS pods are also included in the orbiter base.

A complex base pressure integration procedure was used to develop base force and moment coefficients. The base pressure coefficients were integrated over the base areas and nozzles to determine base axial force coefficients. The nozzle configuration used corresponded to the prototype external nozzle contour, not the model external contour. The rational used was that the external model contour was sufficiently scaled to develop the base pressure environment, but not of the correct shape for the integration of the pressures to determine nozzle axial forces. A schematic of the SSME model and prototype nozzle configurations is shown in Figure 6-3.

A different technique was used for the determination of nozzle normal forces and pitching moments. The Space Shuttle forebody aerodynamic characteristics include power off nozzle forces and moments. Thus, only the power delta forces and moment on the nozzles are included. The model nozzle configuration was used to develop the nozzle forces and moments since the normal forces and moments are developed near the exit plane where model nozzle geometric similitude is the best. The SSME nozzle hinge moments were determined using the nominal power-on pressure coefficients and the SSME model geometry.

The SSME instrumentation layout is shown in Figure 6-4. The SSME tap-line-item and effective axial nozzle area is presented in Tables 6-1 through 6-3.

The SSME nozzle hinge moments were evaluated using the reference dimensions and sign convention shown in Figures 6-5 and 6-6.

The orbiter base plate pressure instrumentation locations are shown in Figure 6-7. The base plate orifice, tap line item numbers, vertical locations and areas used to analyze the base plate are presented in Table 6-4. A schematic showing the relative area size assigned to each pressure is shown in Figure 6-8. The base plate total area was checked from several drawings as noted at the bottom of the tables.

OMS PODS

The OMS pods were analyzed using the effective areas and orientation as shown in Figure 6-9. Since only one OMS pod was instrumented, the effective area is for both pods. The base pressures were averaged at + and - β angle for a β run. Close proximity orbiter base plate pressures were used for the pod overhang areas.

BODY FLAP

The orbiter body flap instrumentation is shown in Figure 6-10. The effective areas are presented in Table 6-5. Only the upper portion of the body flap is included as part of the orbiter base.

ORBITER FOREBODY

The orbiter forebody pressure instrumentation layout is shown in Figure 6-11. The forebody plume induced aerodynamic characteristics were evaluated using the power delta C_p's. An evaluation of the power delta C_p's at the highest power setting showed that the forebody power effects are confined to stations aft of 1375.0, thus only data in this area was considered. Radial ring locations are presented in Table 6-6. A major problem existed with the orbiter forebody in that no pressure instrumentation was located on the bottom aft portion of the orbiter forward of the body flap. The closest wing pressures were used to determine the plume induced pressure environment in this area as shown in Figure 6-11.

WING AND ELEVONS

The wing pressure instrumentation layout is presented in Figure 6-12. The wing power-delta pressures were evaluated at high power levels to determine

the wing spacial content of the plume induced effects. The limits of the plume induced effects were found to be limited to the area shown in Figure 6-13. The pressure instrumentation used to evaluate the wing plume induced aerodynamics was thus limited to that shown in the figure. The net wing instrumentation used is presented in Tables 6-7 through 6-9. The resultant power induced wing loads from the pressure integration were different from the gauge data. The differences are shown in Figures 6-14 through 6-18. The wing power delta torsion moment from pressure integration had a different sign than the gauge data as shown in Figure 6-15. The gauge data indicates that the X_{CP} was forward of the elevon hinge line. The pressure data gave power induced load centers aft of the MRP which is believed to be more correct. The sign convention used for the wing plume induced aerodynamic characteristics is presented in Figure 6-19.

VERTICAL TAIL

The vertical tail instrumentation location is shown in Figures 6-20 and 6-21. The sign convention used for the vertical tail forces and moments is shown in Figure 6-22. The effective areas are presented in Table 6-10.

SRB BASE

The SRB nozzle instrumentation layout is shown in Figure 6-23. The prototype nozzle configuration was used to determine external aerodynamic loads. The nozzle configuration used is shown in Figure 6-24. The nozzle pressure integration was terminated at the compliance ring shown in Figure 6-25. The nozzle axial areas assigned to each pressure location is presented in Table 6-11. The SRB nozzle hinge moment sign convention is the same as that used for the SSME as shown in Figure 6-26.

SRB FOREBODY

The SRB forebody instrumentation layout is shown in Figure 6-27 and the pressure integration area layout in Table 6-12. No consistent trend in power-delta pressure could be determined except on the skirt. Thus only the skirt area was used to determine power-induced forebody aerodynamic characteristics.

ET BASE

The ET base instrumentation layout is shown in Figure 6-28. The area assignment is presented in Table 6-13. The area assignments were determined by plotting the ET base pressures and determining pressure contours for selected Mach numbers. The areas were then evaluated using the base pressure contours.

ET FOREBODY

The ET forebody power delta pressures were evaluated at the highest power levels and no forebody pressure delta could be determined. Thus no ET forebody was modeled.

Reference areas, lengths, and moment reference locations used for all aerodynamic characteristics are presented in Table 6-14.

The results of integration of the base pressure and the forebody power delta pressures have been listed in a special format which is discussed in Section VII.

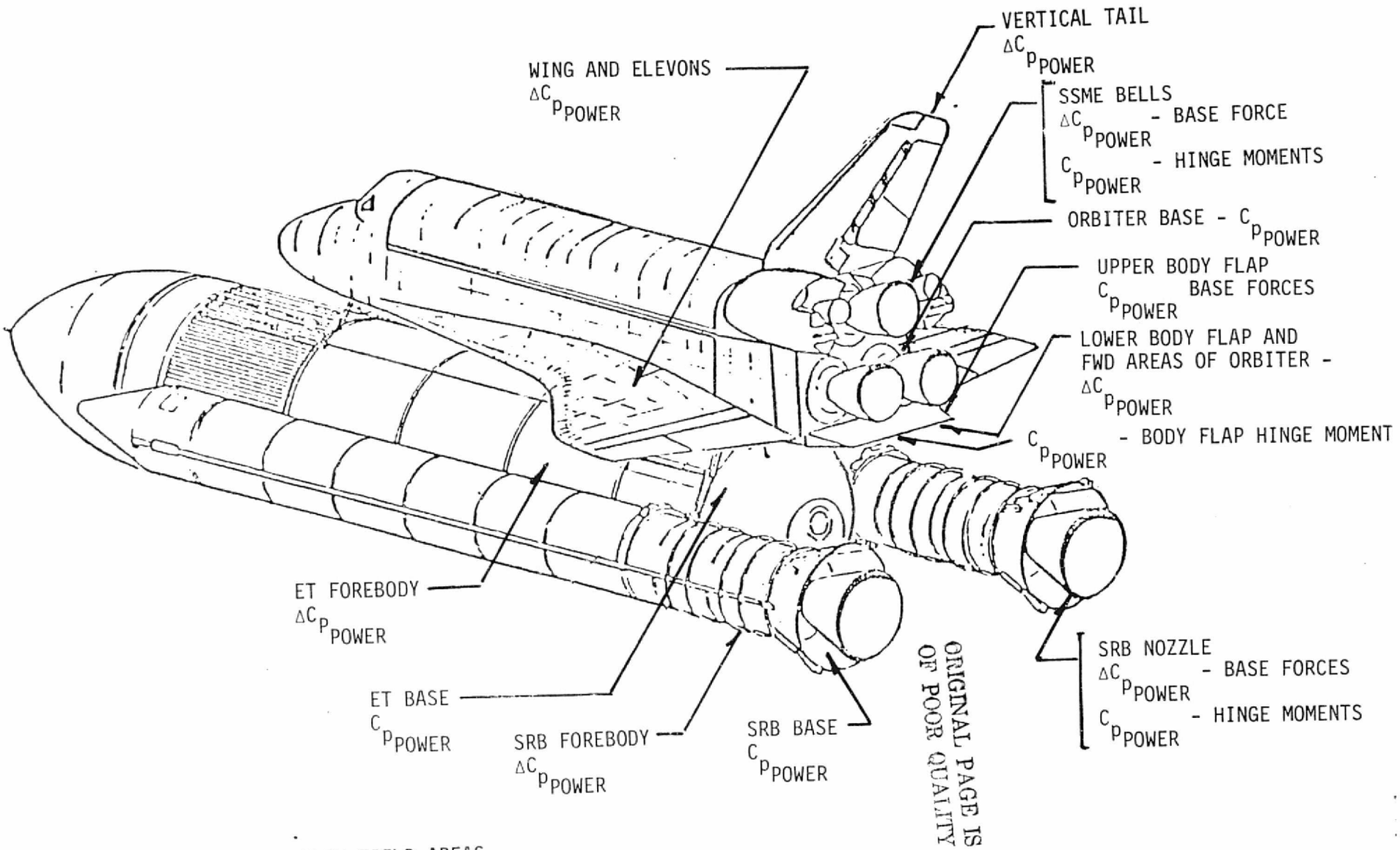

ORIGINAL PAGE IS
OF POOR QUALITY

Figure 6-1. PLUME FLOW FIELD AREAS

ORIGINAL PAGE IS
OF POOR QUALITY

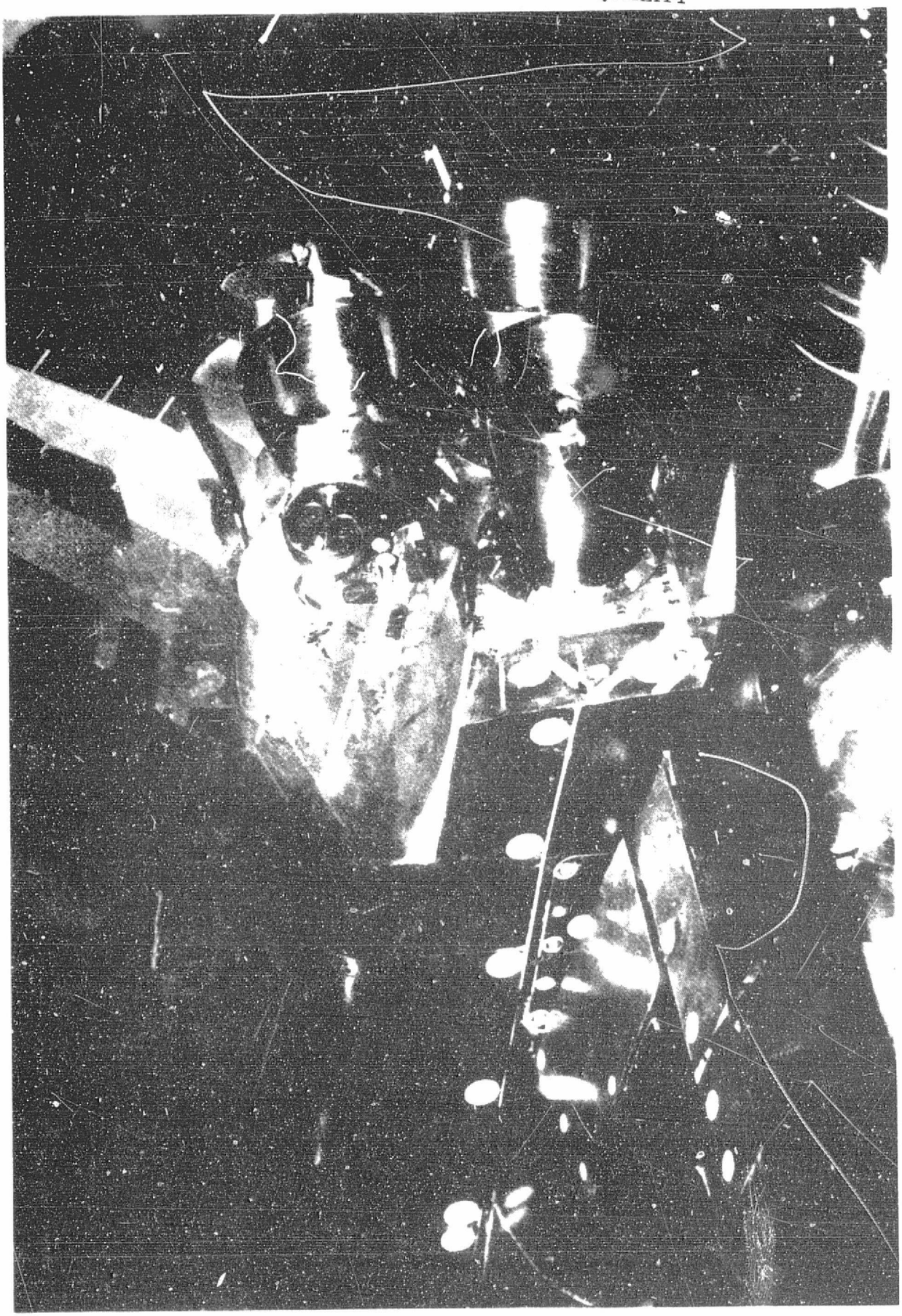

Figure 6-2. IA119 MODEL ORBITER BASE CONFIGURATION

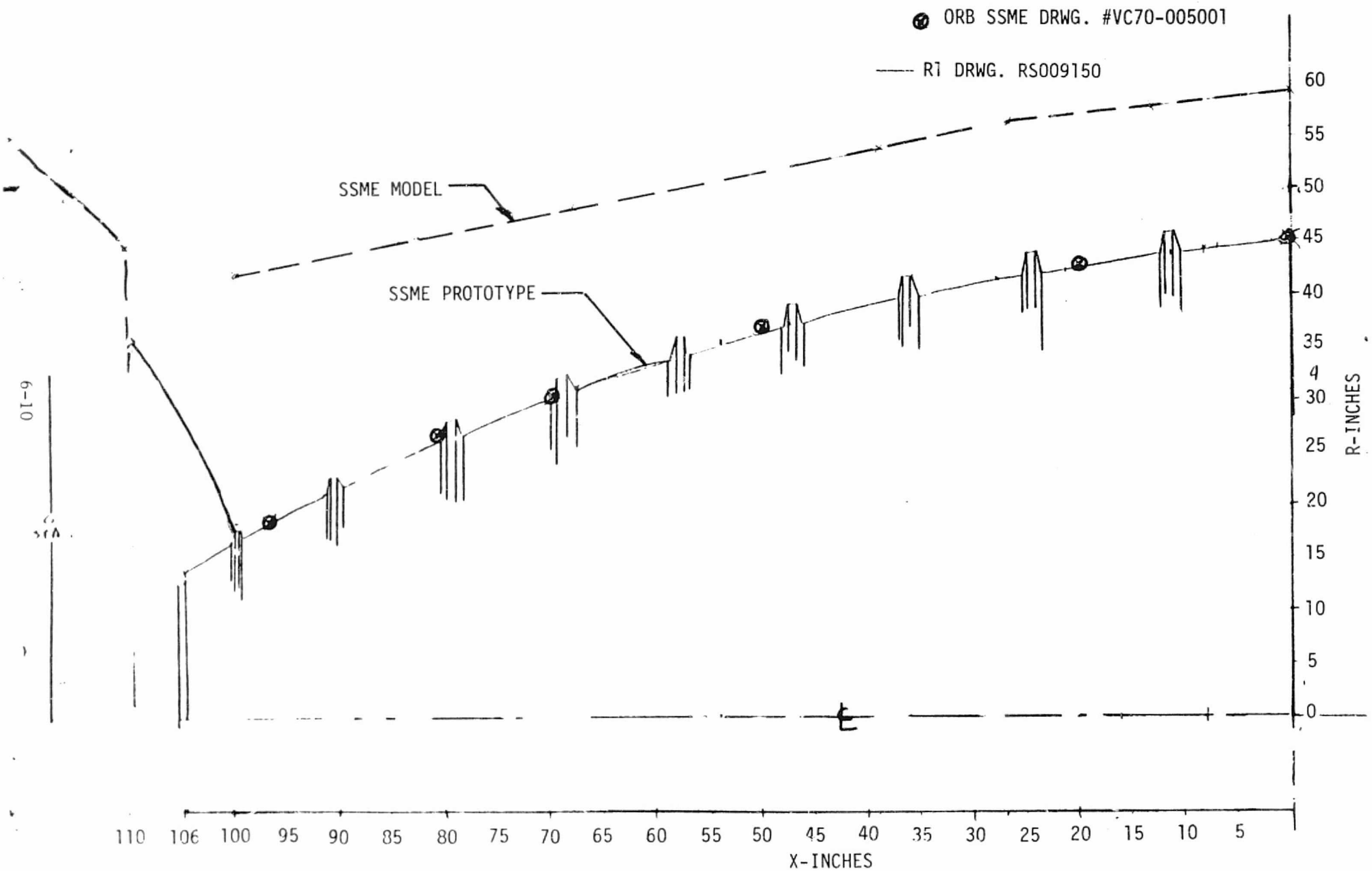

Figure 6-3. MODEL AND PROTOTYPE SSME EXTERNAL CONTOUR

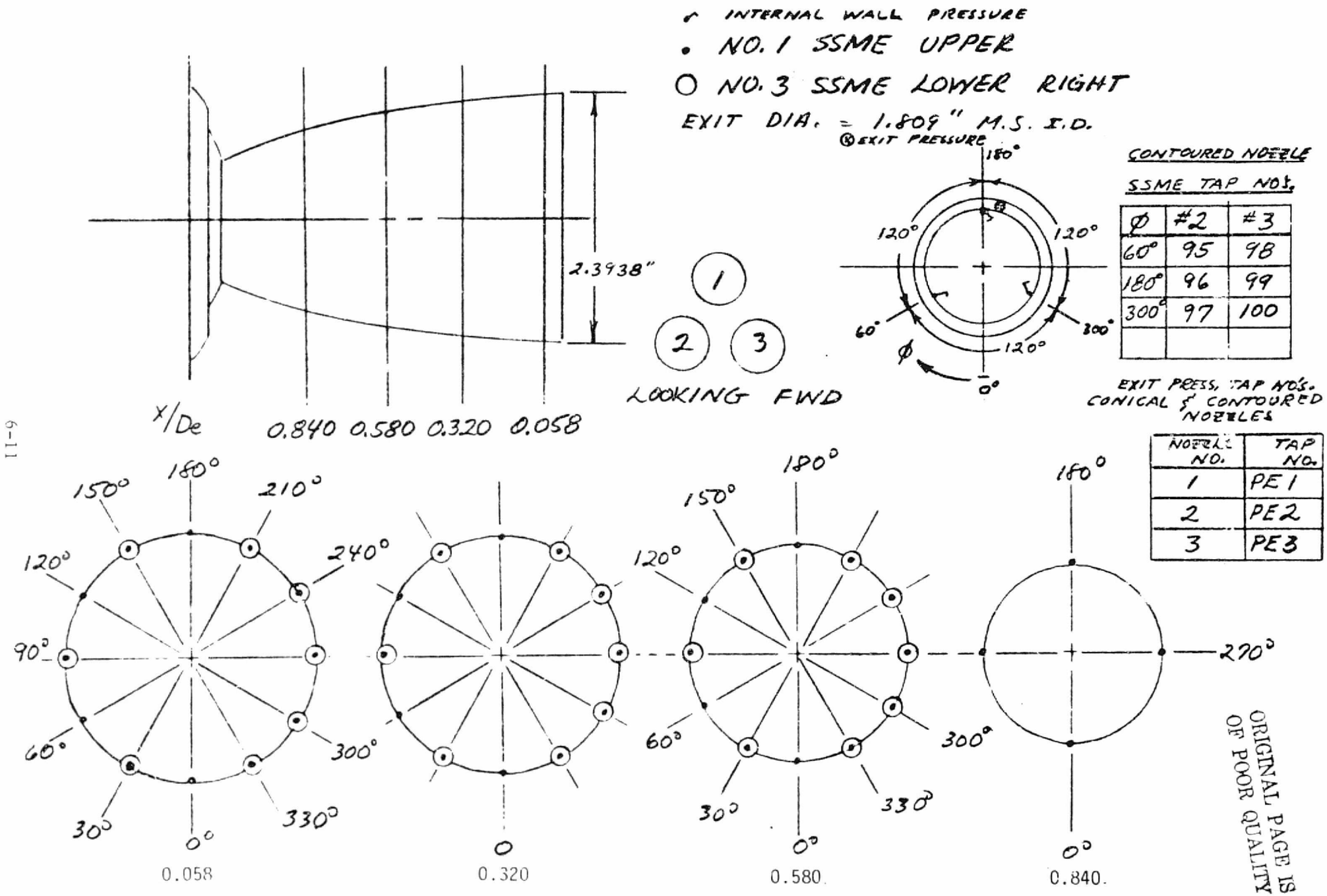

φ	#2	#3
60°	95	98
180°	96	99
300°	97	100

NOZZLE NO.	TAP NO.
1	PE1
2	PE2
3	PE3

Figure 6-4. ORBITER SSME NOZZLE PRESSURE INSTRUMENTATION

ORIGINAL PAGE IS OF POOR QUALITY

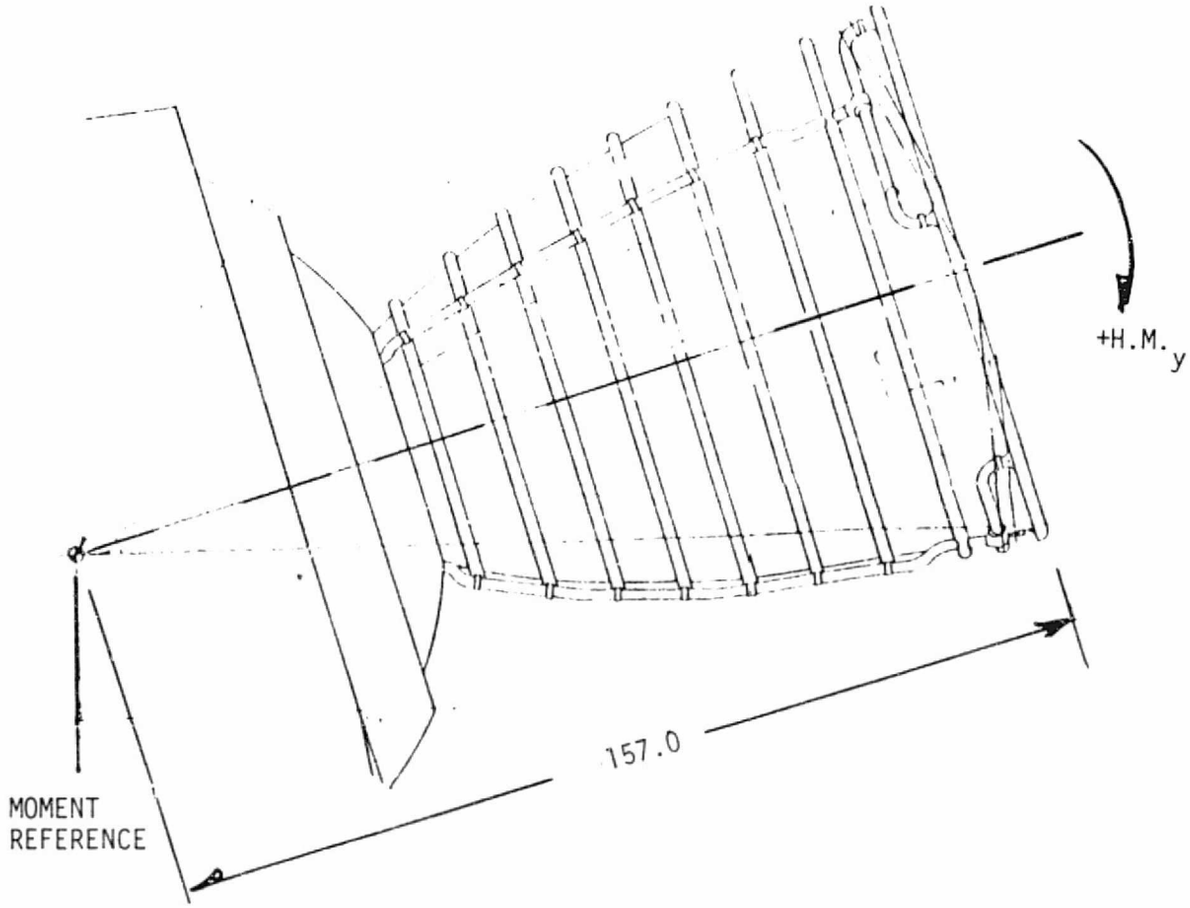

$$CH = \frac{H.M.}{44.9 \times 157}$$

Figure 6-5. SSME NOZZLE HINGE MOMENT DEFINITION

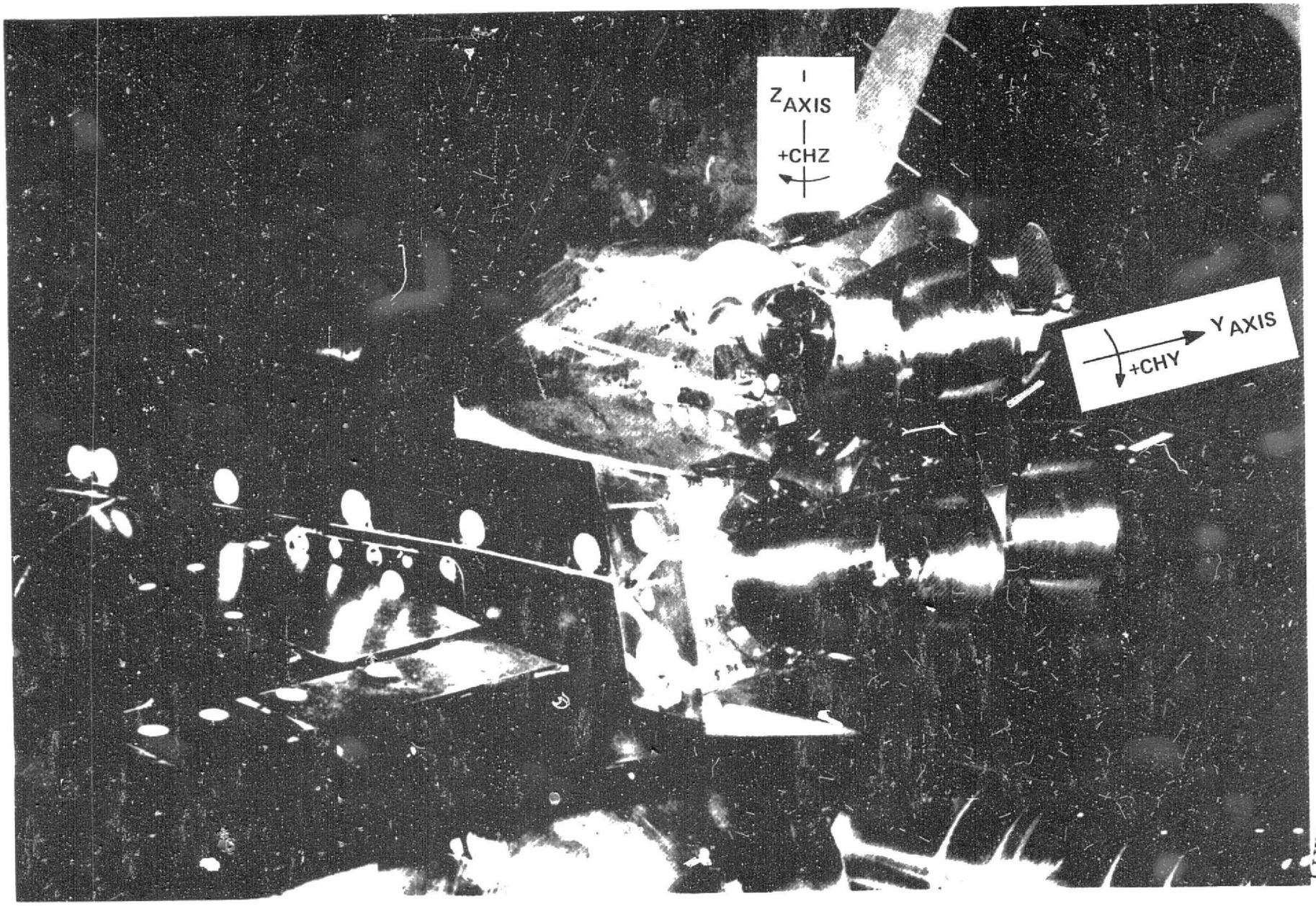

Figure 6-6. SSME NOZZLE HINGE MOMENT NOMENCLATURE

ORIGINAL PAGE IS
OF POOR QUALITY

IA119

ORBITER BASE PRESSURE INSTRUMENTATION LOCATION																				
W.L	B.L											℄	B.L							
Z_0	2.60	2.16	2.14	2.06	1.76	1.56	1.26	1.16	1.08	.76	.56	0	.56	.76	1.16	1.26	1.56	1.76	2.06	2.16
6.040				318	331						325	307	335					342	343	
6.800		334										306								346
7.620		316										305								344
8.000												304								
8.100										326				336						
8.200						313											340			
8.300				315															345	
8.440								329							338					
8.780			323			312											341			
9.260							330									339				
9.300	324																			
9.400					332															
9.760										327				337						
10.100												302								
10.280									328											
10.440					333															
10.640												301								

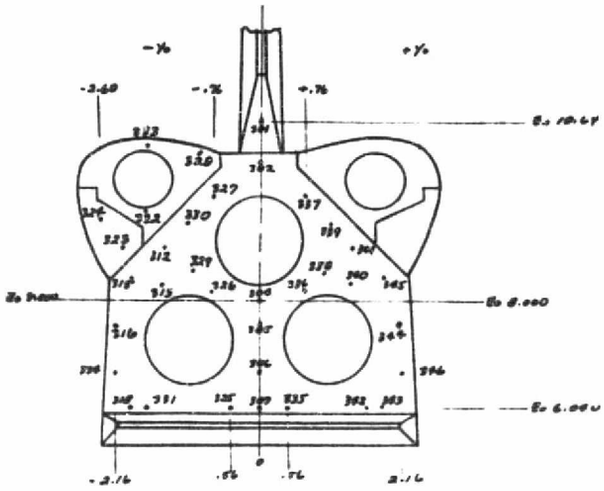

Figure 6-7. ORBITER BASE PRESSURE INSTRUMENTATION

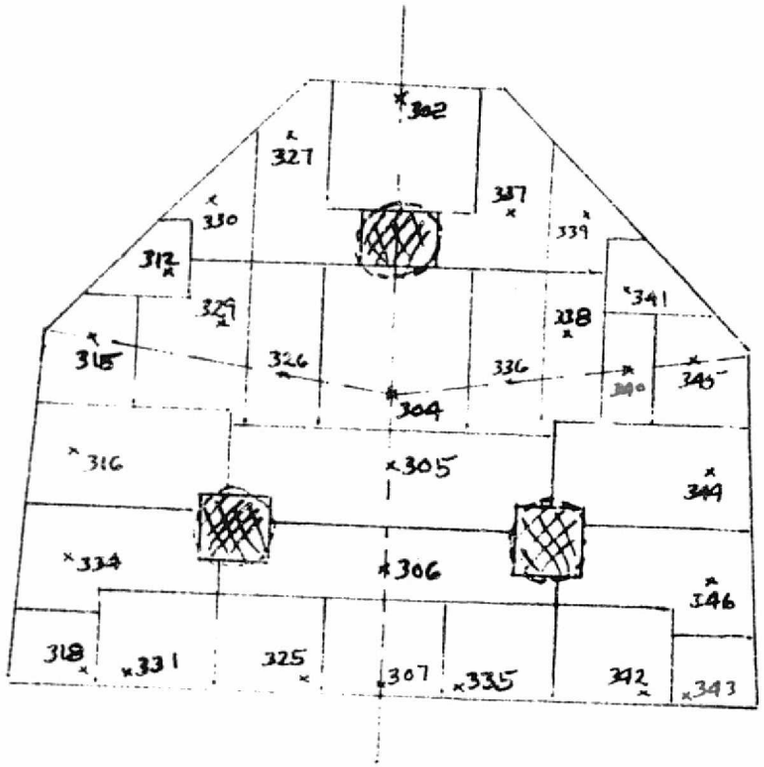

Figure 6-8. ORBITER BASE PLATE RELATIVE AREAS

ORIGINAL PAGE IS
OF POOR QUALITY

ORIFICE	LINE	ITEM	Z	A	X	θ
323	17	1	436.0	18.35	0.0	0.0
324	17	2	465.0	18.35	0.0	0.0
325	17	6	514.0	26.85	0.0	0.0
332	17	10	470.0	26.85	0.0	0.0
333	17	11	522.0	26.85	0.0	0.0
312	16	13	0.0	12.175	1260.5	1.57
327	17	5	0.0	12.175	1260.5	1.57
337	18	12	0.0	12.175	1260.5	1.57
341	18	2	0.0	12.175	1260.5	1.57

$\Sigma Ax = 117.25$
$\Sigma Az = 48.7$

Figure 6-9. OMS POD AREAS

η	X_o / C_{BF} -.10	.20	.22	.47	.60	.95	
.10	405 401	406 402	-	-	407 403	408 404	TOP BOT
.15	-	-	-		-	-	BOT
.20	-	-	-	-	-	-	
.35	-	-	-	-	-	-	
.50	413 409	414 410			415 411	416 412	TOP BOT
.65	-	422 418	-	-	-	424 420	TOP BOT
.80	-	430 426	-	-	-	432 428	TOP BOT
.90	437 433	438 434	-	-	439 435	440 436	TOP BOT

• PRESS TAP

C_{BF} = 81" F.S.

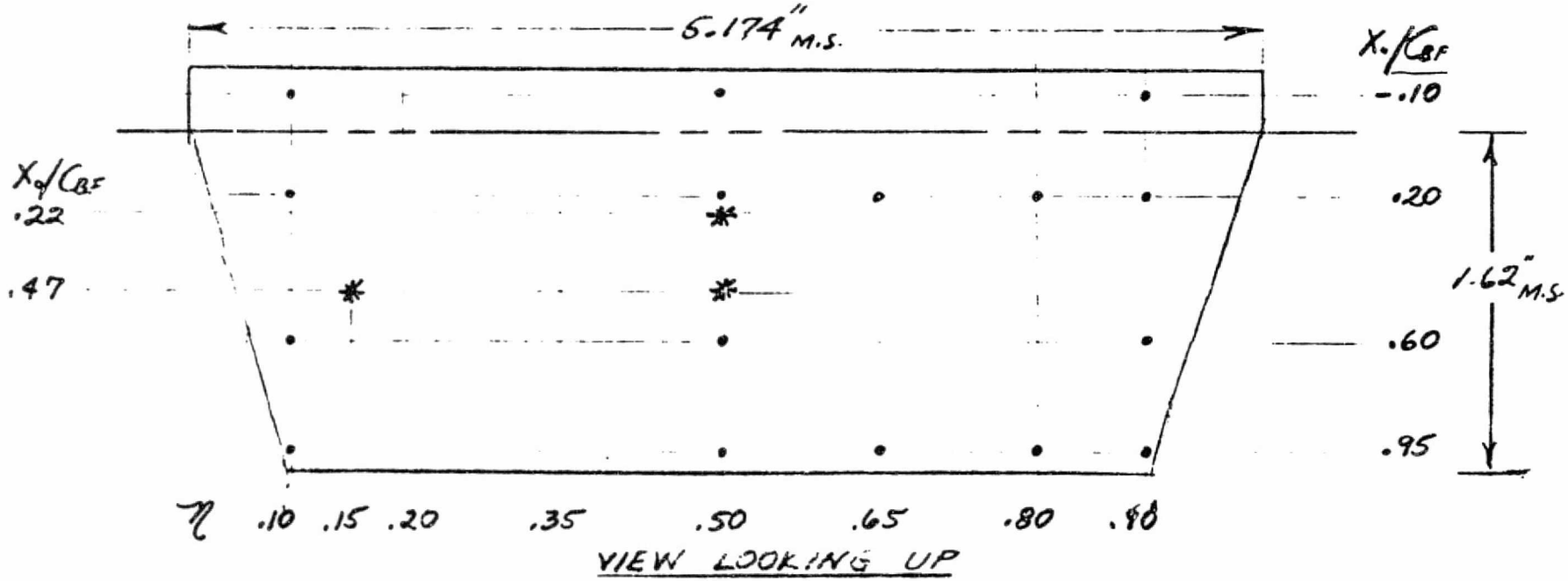

Figure 6-10. ORBITER BODY FLAP PRESSURE INSTRUMENTATION

ORIGINAL PAGE IS OF POOR QUALITY

ORIGINAL PAGE IS
OF POOR QUALITY

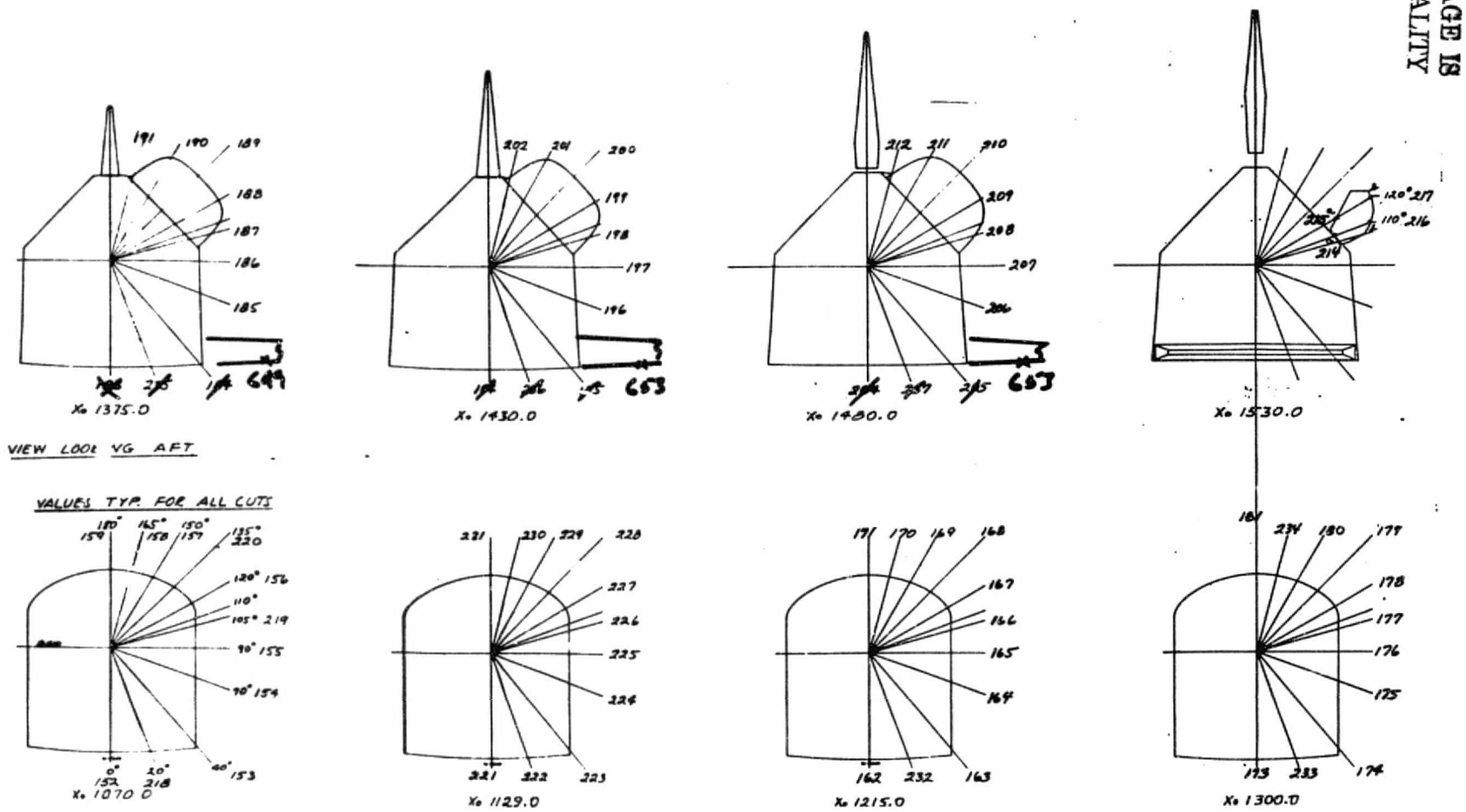

Figure 6-11. ORBITER FUSELAGE PRESSURE INSTRUMENTATION

IA119 ORBITER WING PRESSURE INSTRUMENTATION

	η	Y_o	X_w/C_w										X_o	X_{EL}/C_{EL}							Σ
		L.E	0	.02	.08	.15	.25	.40	.55	.625	.70	.75	1360	-.10	0	.20	.40	.60	.80	1.0	
TOP	.235	110													HL						
BOT																					
TOP	.299	140							630	914	631	915	632	633	-	635	636	637	638	639	21
BOT									647	916	648	917	649	650	-	652	653	654	655		
TOP	.392	160							664	918	665	919	666	667	-	669	670	671	672	673	21
BOT									681	920	682	921	683	684	-	686	687	688	689		
TOP	.427	200	690				696	697	698	922			699	700	-	702	703	704	705	706	22
BOT							712	713	714	923			715	716	-	718	719	720	721		
TOP	.534	250	722			727	728	729	730				731	732	-	734	735	736	737	738	22
BOT						743	744	745	746				747	748	-	750	751	752	753		
TOP	.619	290	754			759	760	761	762				763	764	-	766	767	768	769	770	22
BOT						775	776	777	778				779	780	-	782	783	784	785		
TOP	.726	340	786			791	792	793					795	796	-	798	799	800	801	802	20
BOT						807	808	809					811	812	-	814	815	816	817		
TOP	.811	380	818			823	824	825					826	827	-	829	830	831	832	833	20
BOT						838	839	840					841	842	-	844	845	846	847		
TOP	.897	420	849			853	854	855					856	857	-	859	860	861	862	863	20
BOT						868	869	870					871	872	-	874	875	876	877		
TOP	.961	450	878			883							885	886	-	888	889	890	891	892	16
BOT						897							899	900	-	902	903	904	905		
	1.00	TIP				906		913					908	909	-		910		911		6
																				TOTAL	190

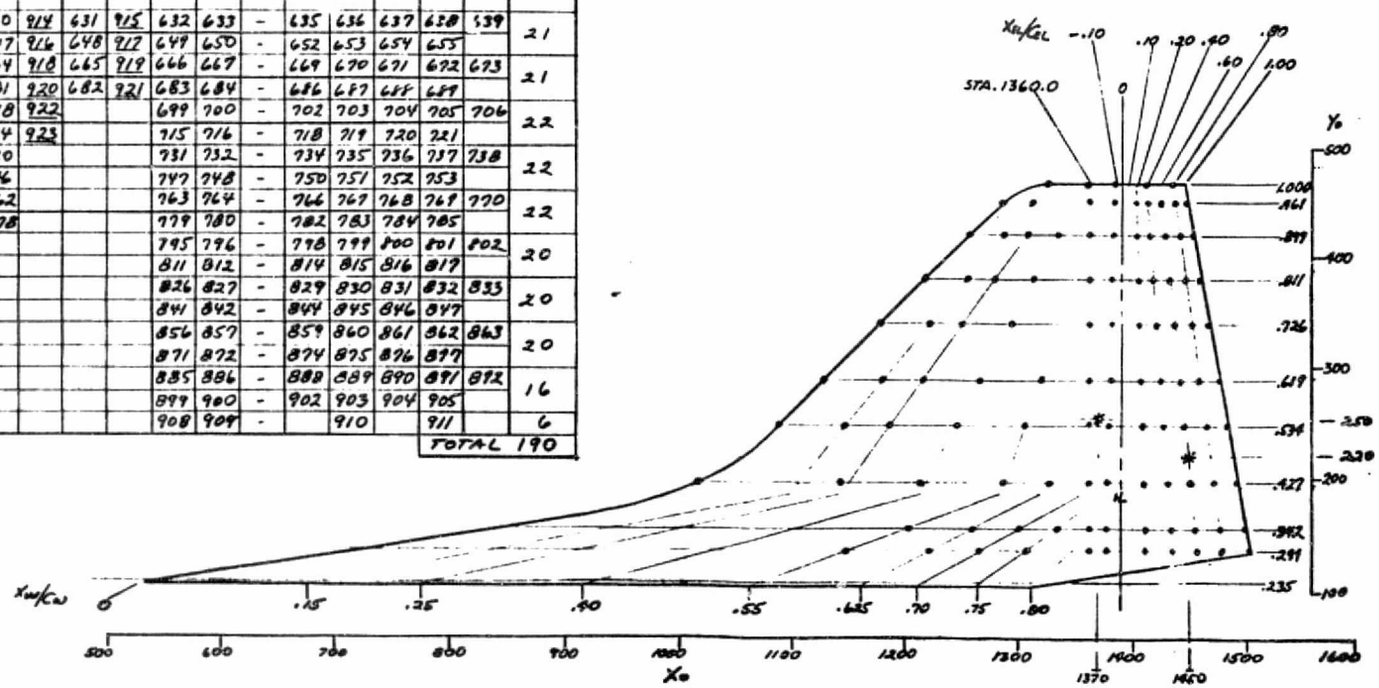

Figure 6-12. ORBITER WING PRESSURE INSTRUMENTATION

ORIGINAL PAGE IS
OF POOR QUALITY

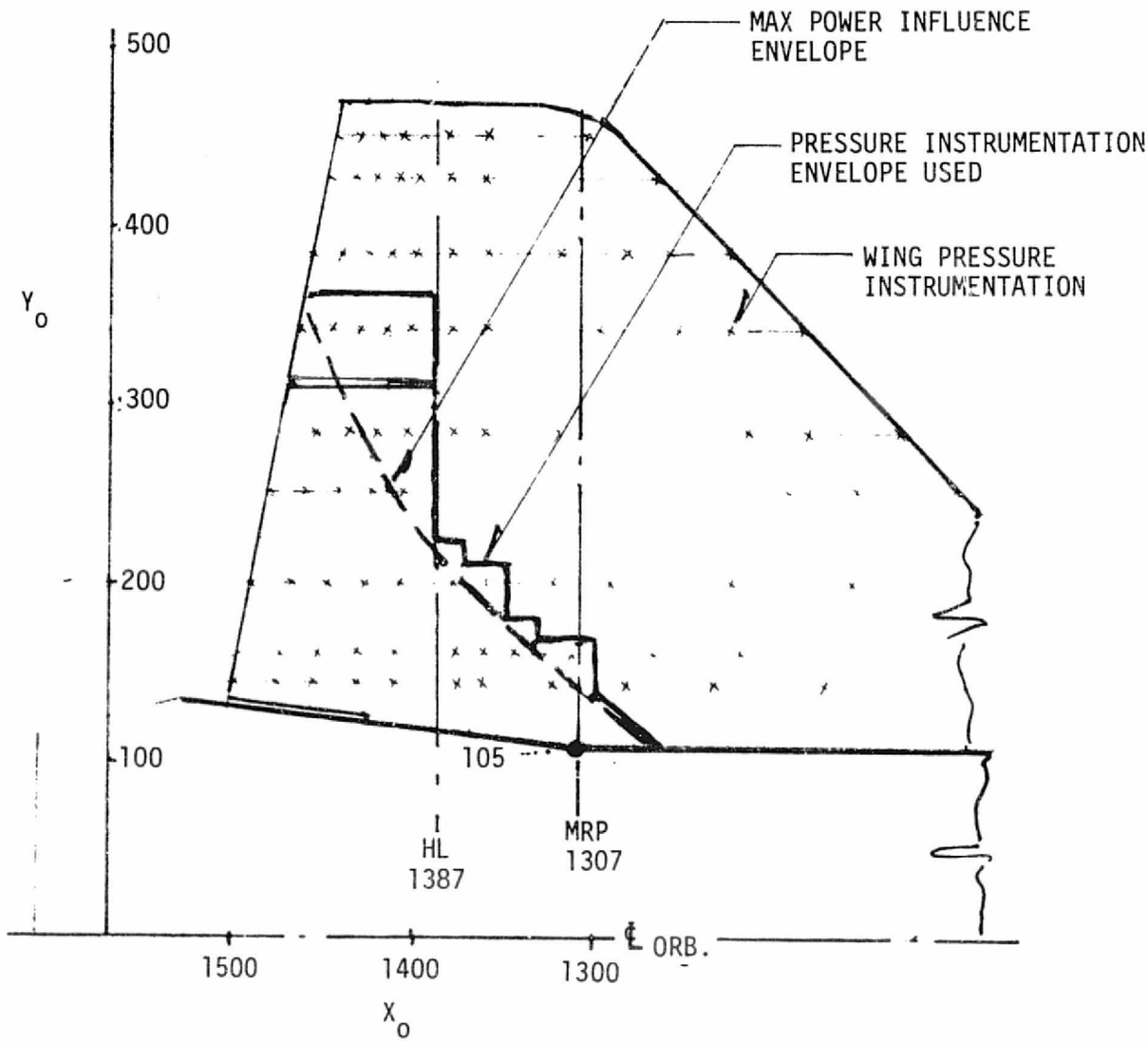

Figure 6-13. ORBITER WING PRESSURE INSTRUMENTATION FOR WING POWER DELTAS

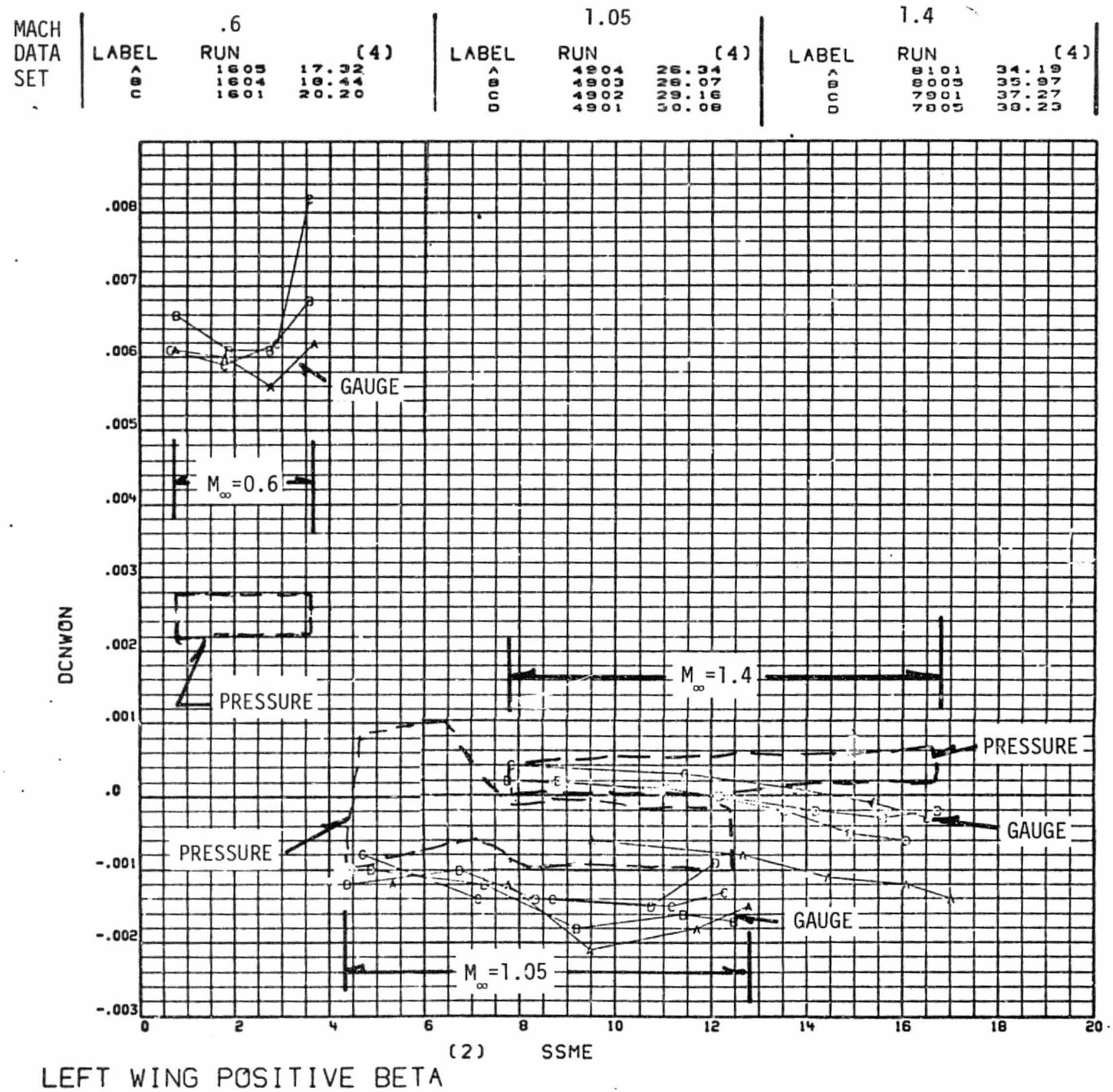

LEFT WING POSITIVE BETA

Figure 6-14. COMPARISON OF GAUGE AND PRESSURE DATA — WING NORMAL FORCE

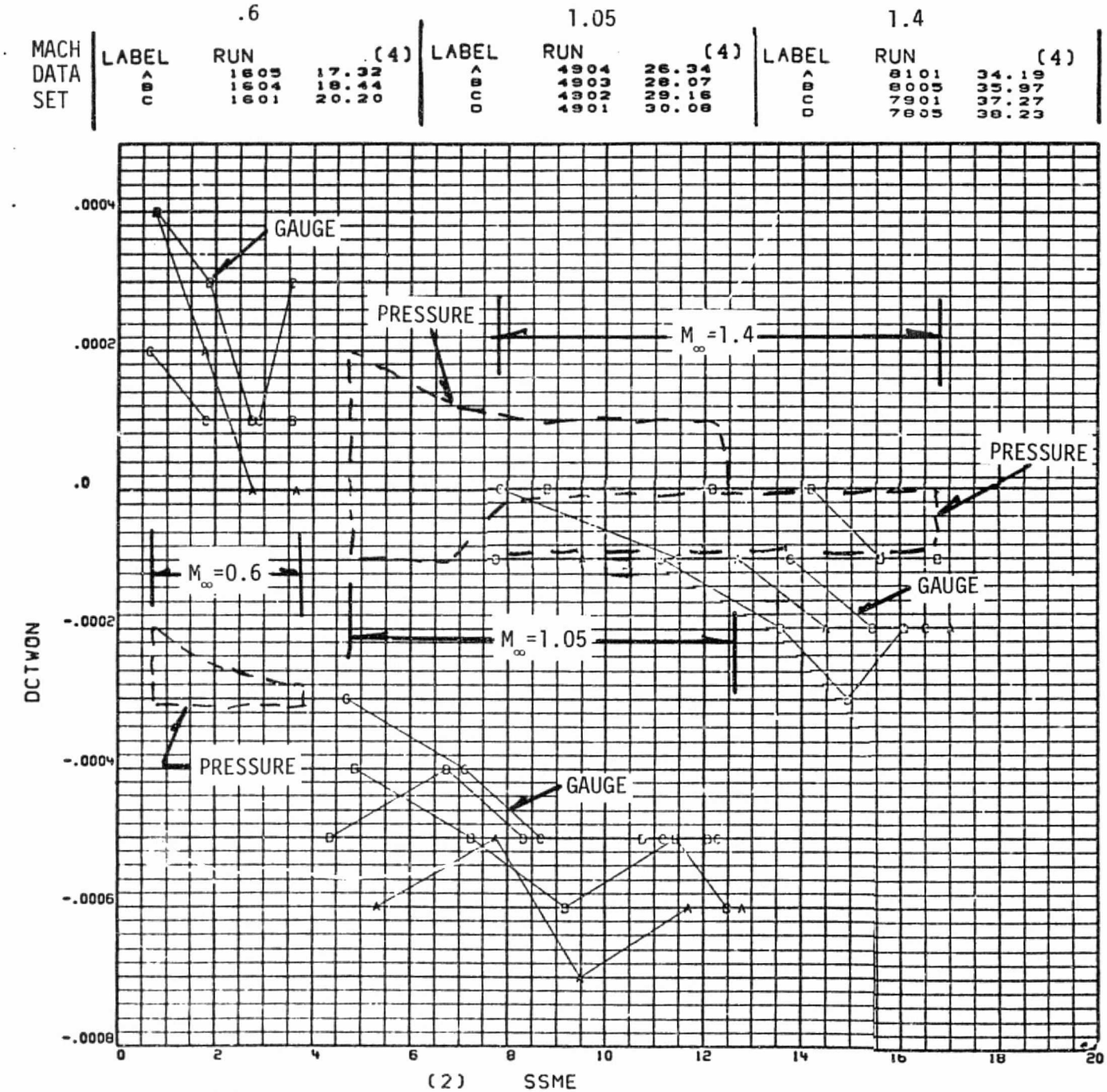

LEFT WING POSITIVE BETA

Figure 6-15. COMPARISON OF GAUGE AND PRESSURE DATA — WING TORSION MOMENT

ORIGINAL PAGE IS OF POOR QUALITY

MACH DATA SET	.6 LABEL	RUN	(4)	1.05 LABEL	RUN	(4)	1.4 LABEL	RUN	(4)
	A	1605	17.32	A	4904	26.34	A	8101	34.19
	B	1604	18.44	B	4903	28.07	B	8005	35.97
	C	1601	20.20	C	4902	29.16	C	7901	37.27
				D	4901	30.08	D	7805	38.23

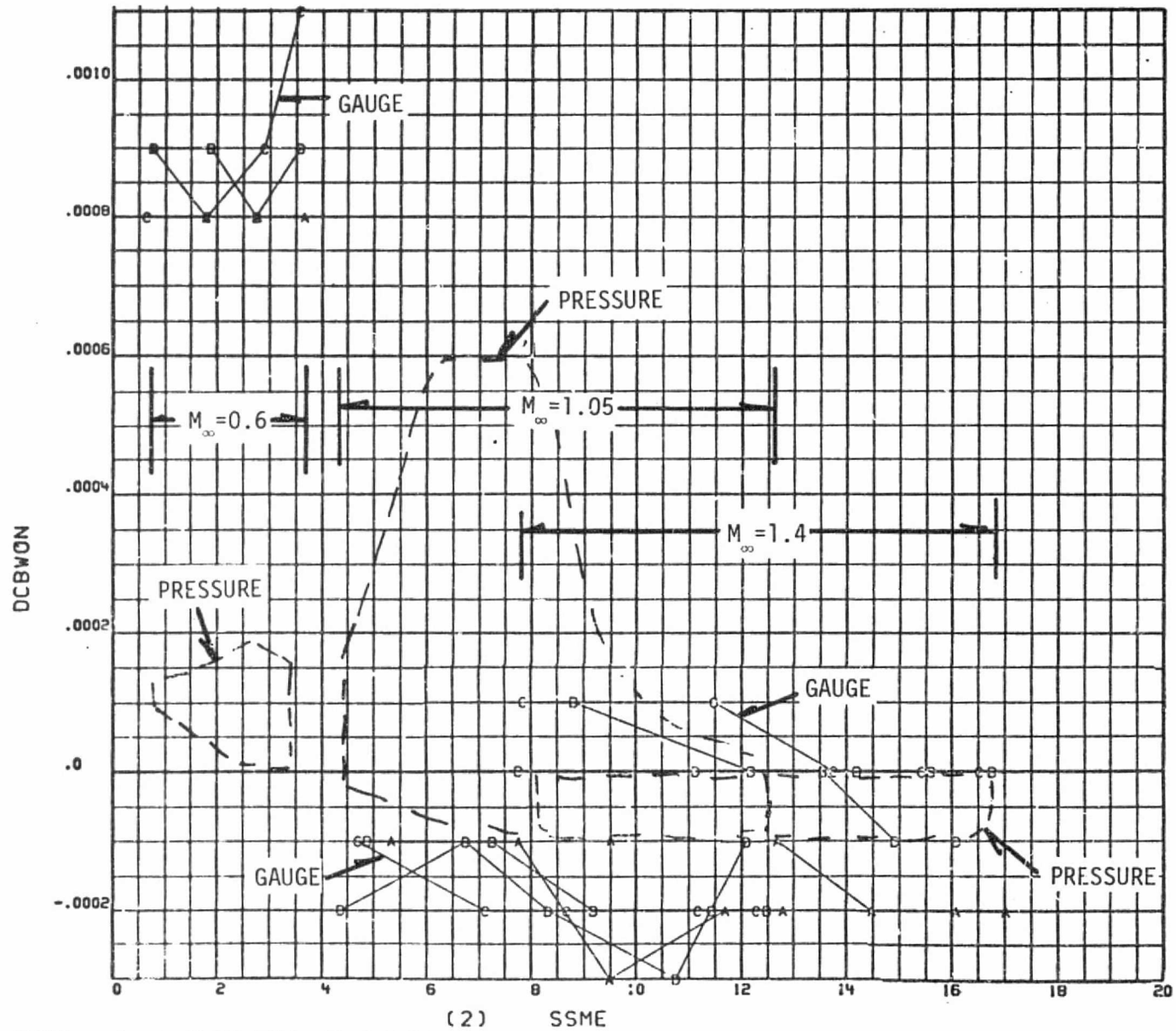

LEFT WING POSITIVE BETA

Figure 6-16. COMPARISON OF GAUGE AND PRESSURE DATA — WING BENDING MOMENT

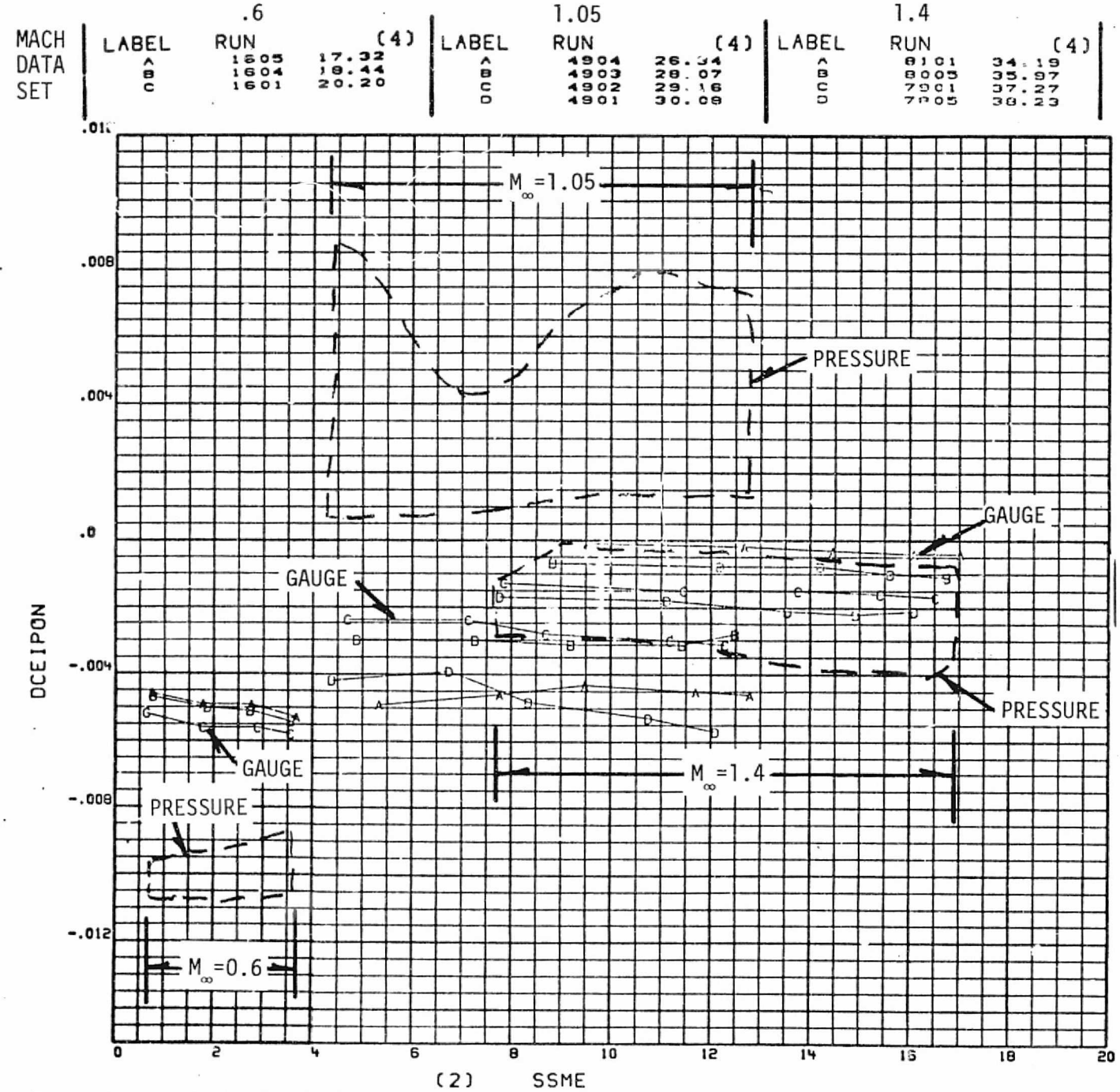

LEFT WING POSITIVE BETA

Figure 6-17. COMPARISON OF GAUGE AND PRESSURE DATA — INBOARD ELEVON HINGE MOMENT

ORIGINAL PAGE IS
OF POOR QUALITY

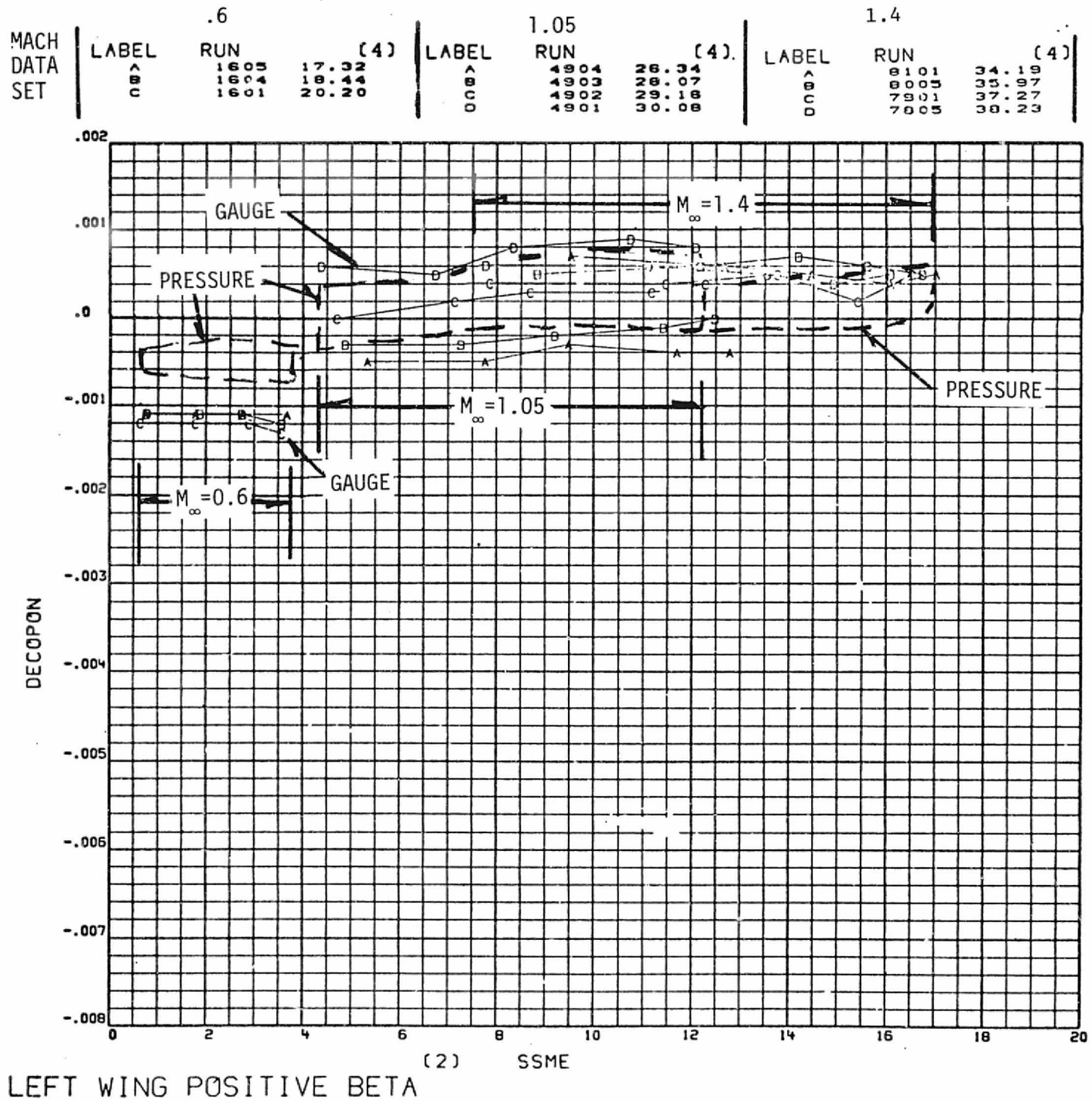

LEFT WING POSITIVE BETA

Figure 6-18. COMPARISON OF GAUGE AND PRESSURE DATA — OUTBOARD ELEVON HINGE MOMENT

ORIGINAL PAGE IS OF POOR QUALITY

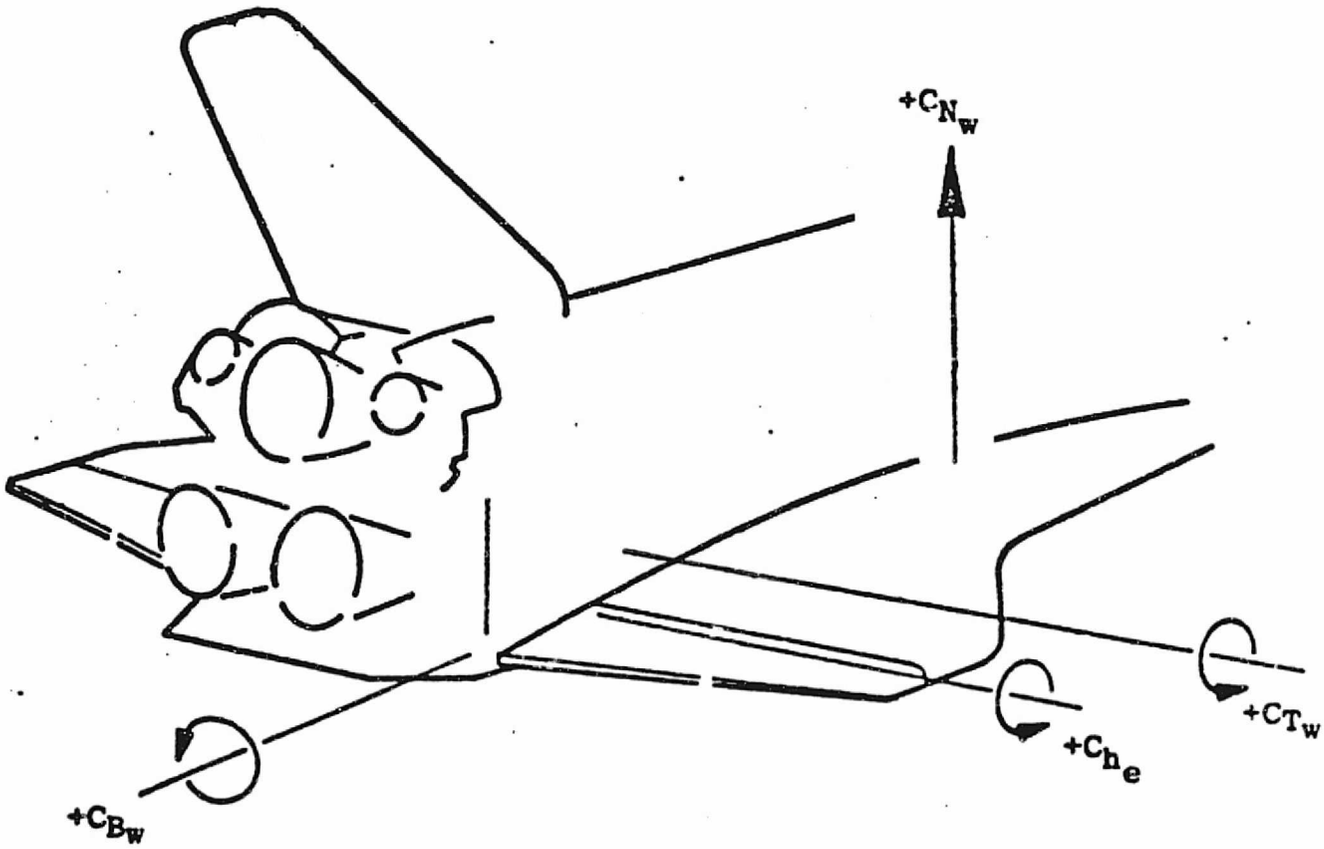

Figure 6-19. WING AND ELEVON FORCE AND MOMENT SIGN CONVENTION

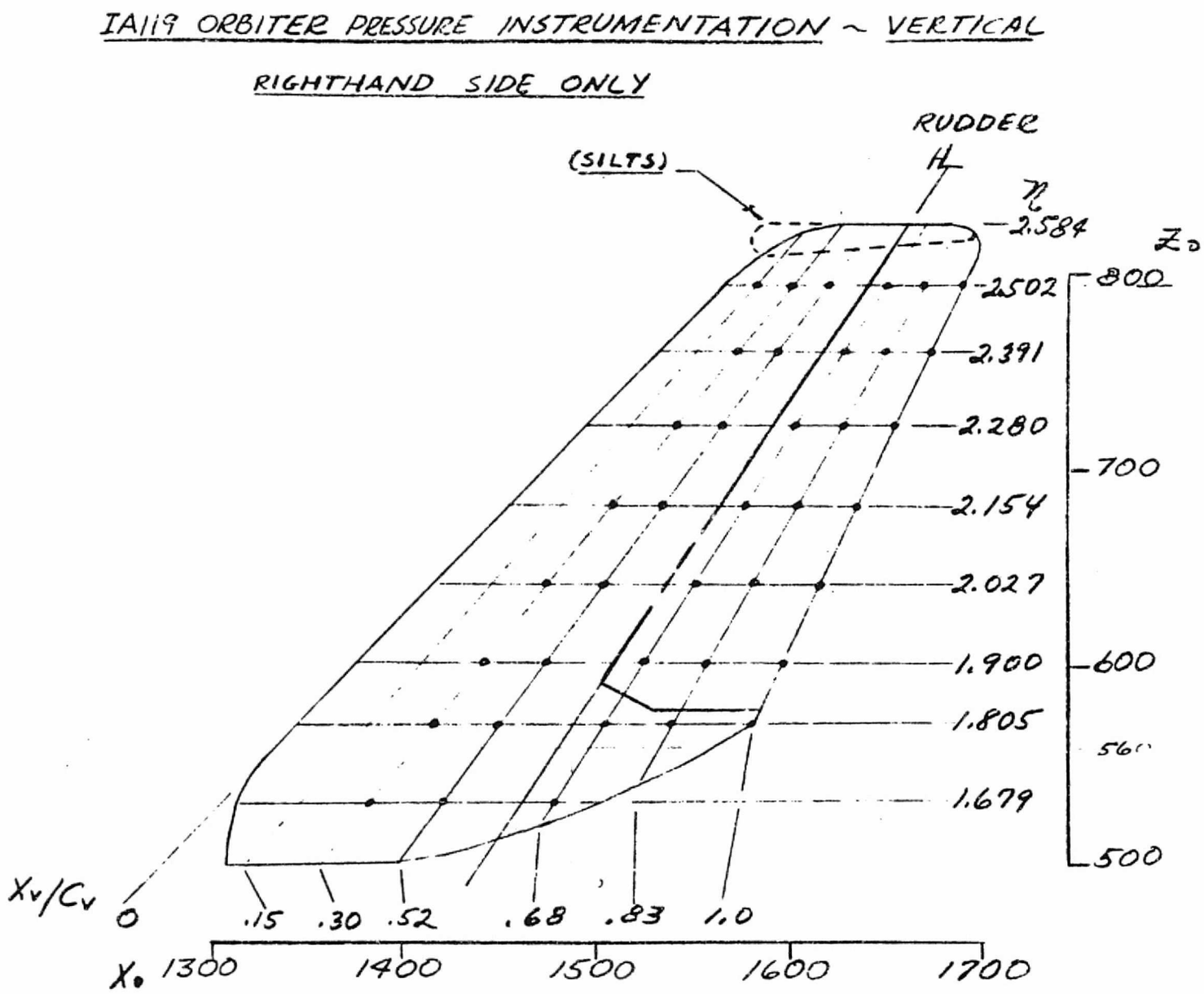

Figure 6-20. VERTICAL TAIL INSTRUMENTATION LOCATION

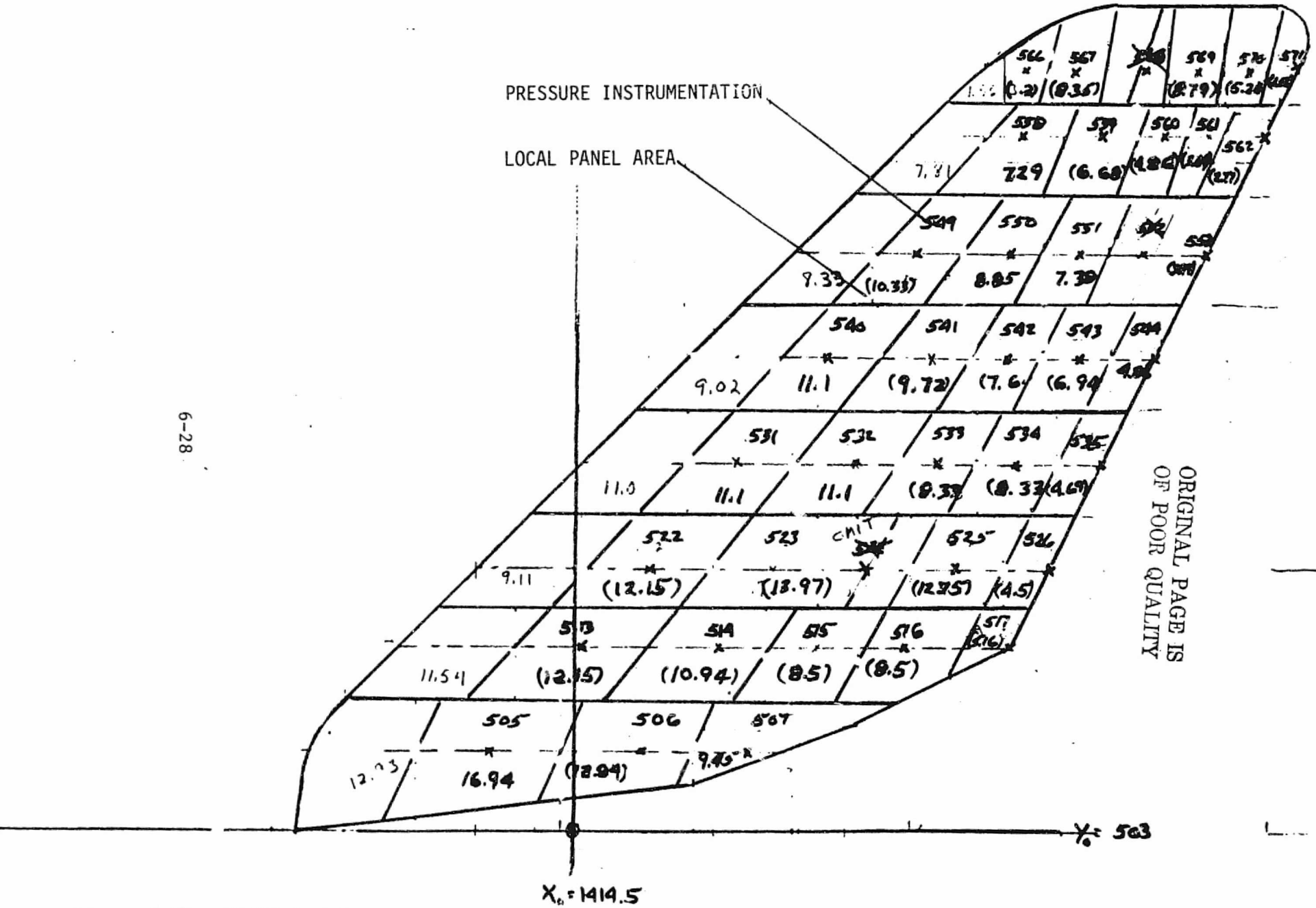

Figure 6-21. VERTICAL TAIL AREAS

ORIGINAL PAGE IS
OF POOR QUALITY

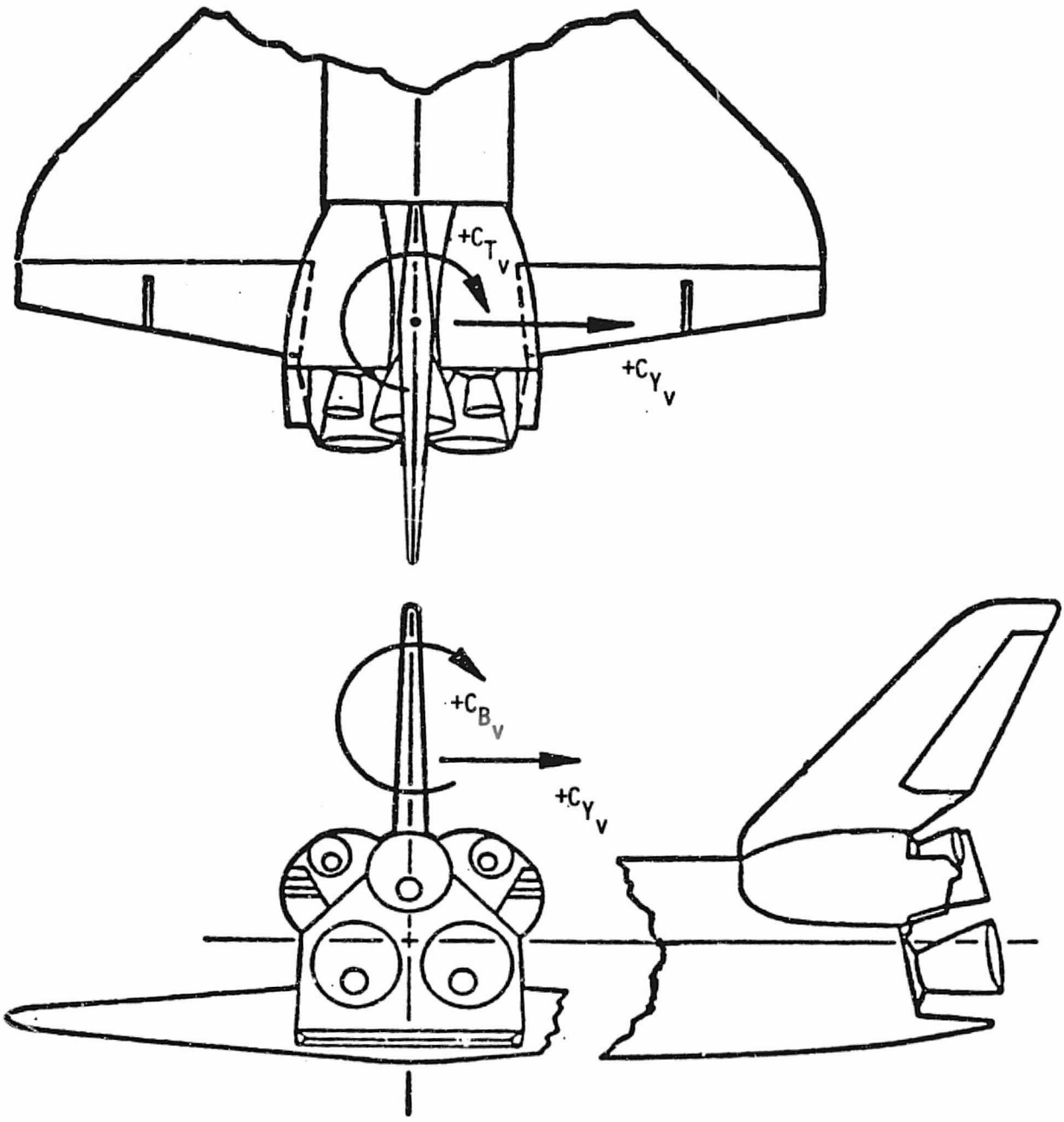

Figure 6-22. VERTICAL STABILIZER FORCE AND MOMENT SIGN CONVENTION

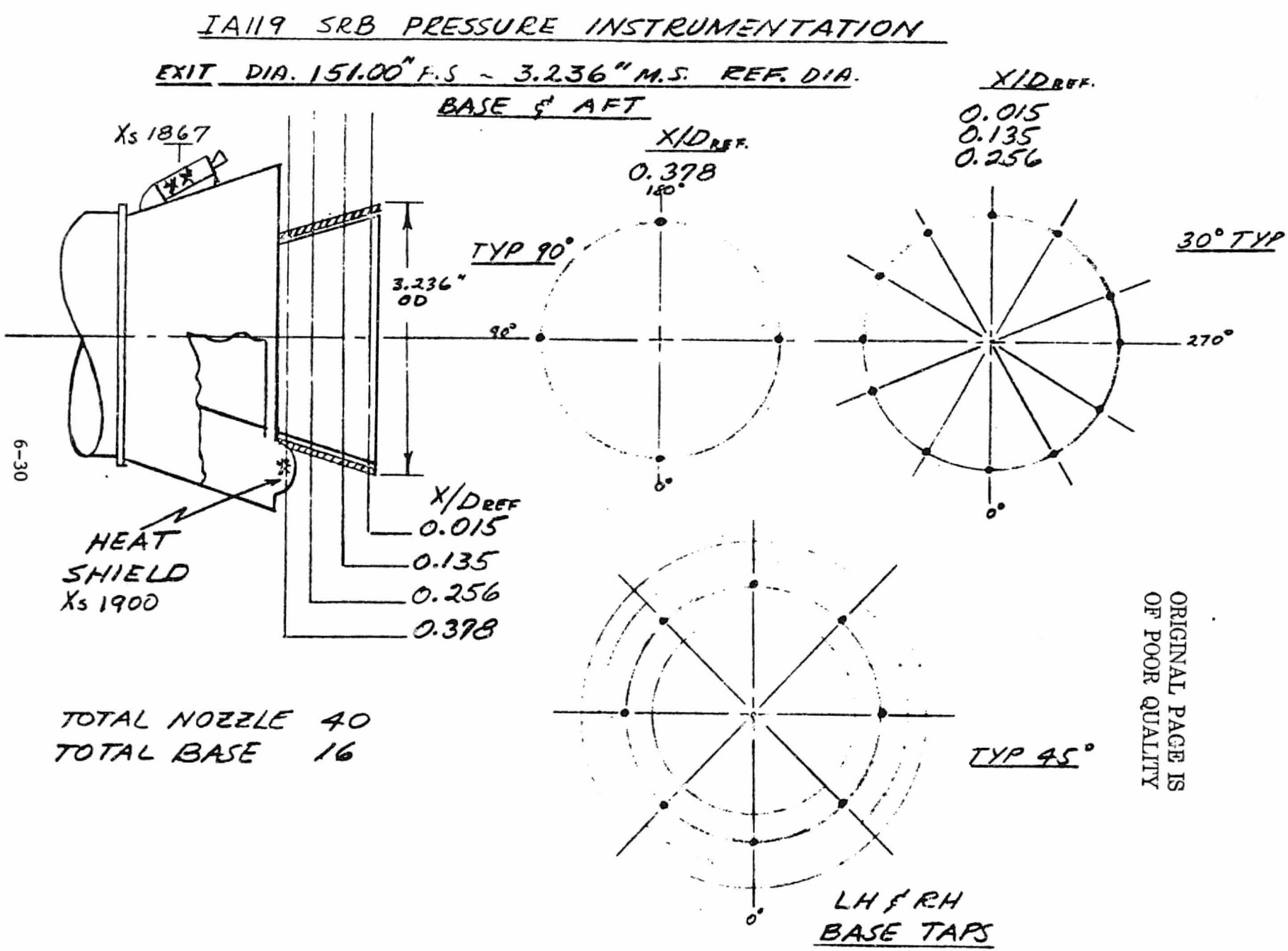

Figure 6-23. SRB BASE INSTRUMENTATION

ORIGINAL PAGE IS OF POOR QUALITY

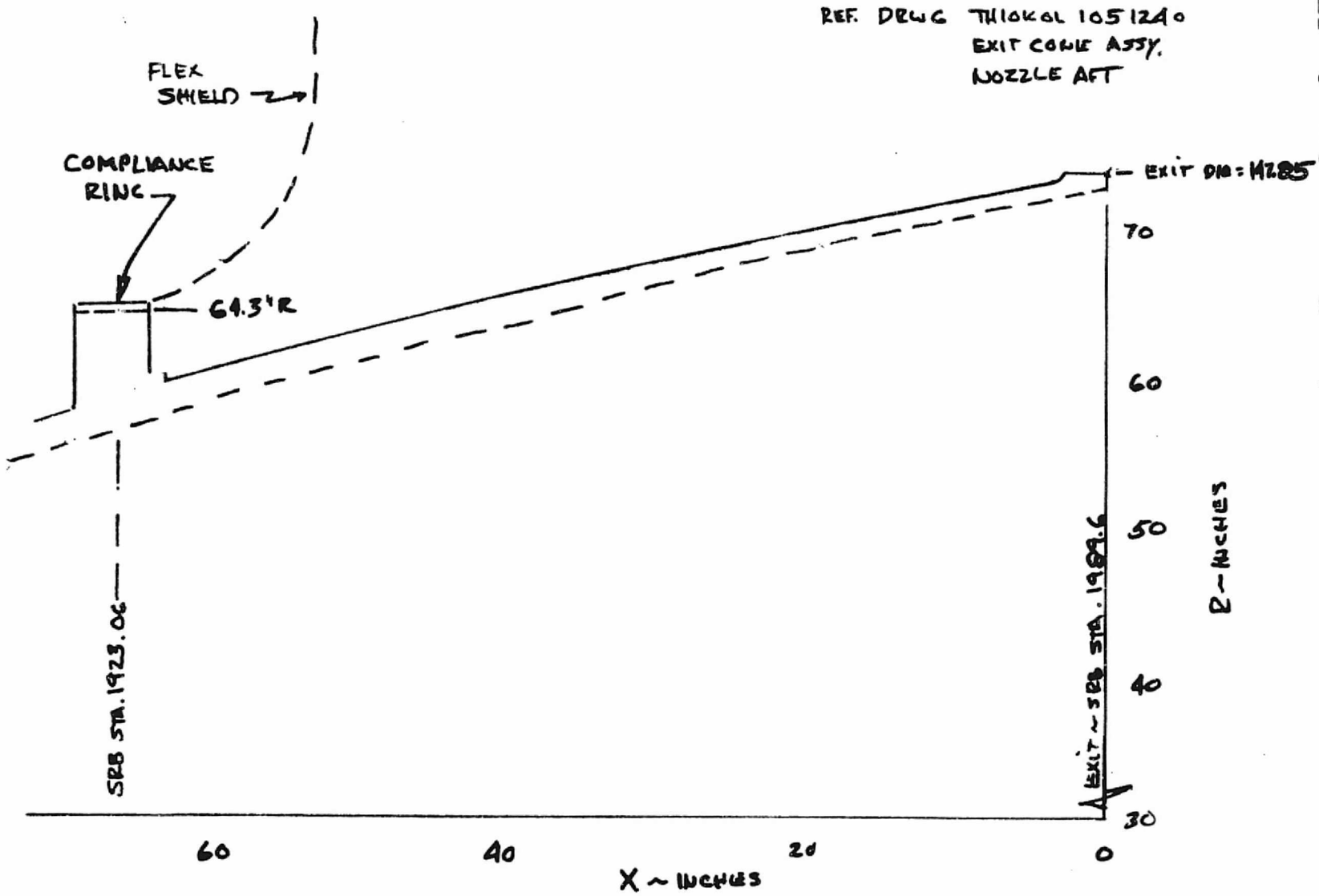

Figure 6-24. SRB NOZZLE CONFIGURATION

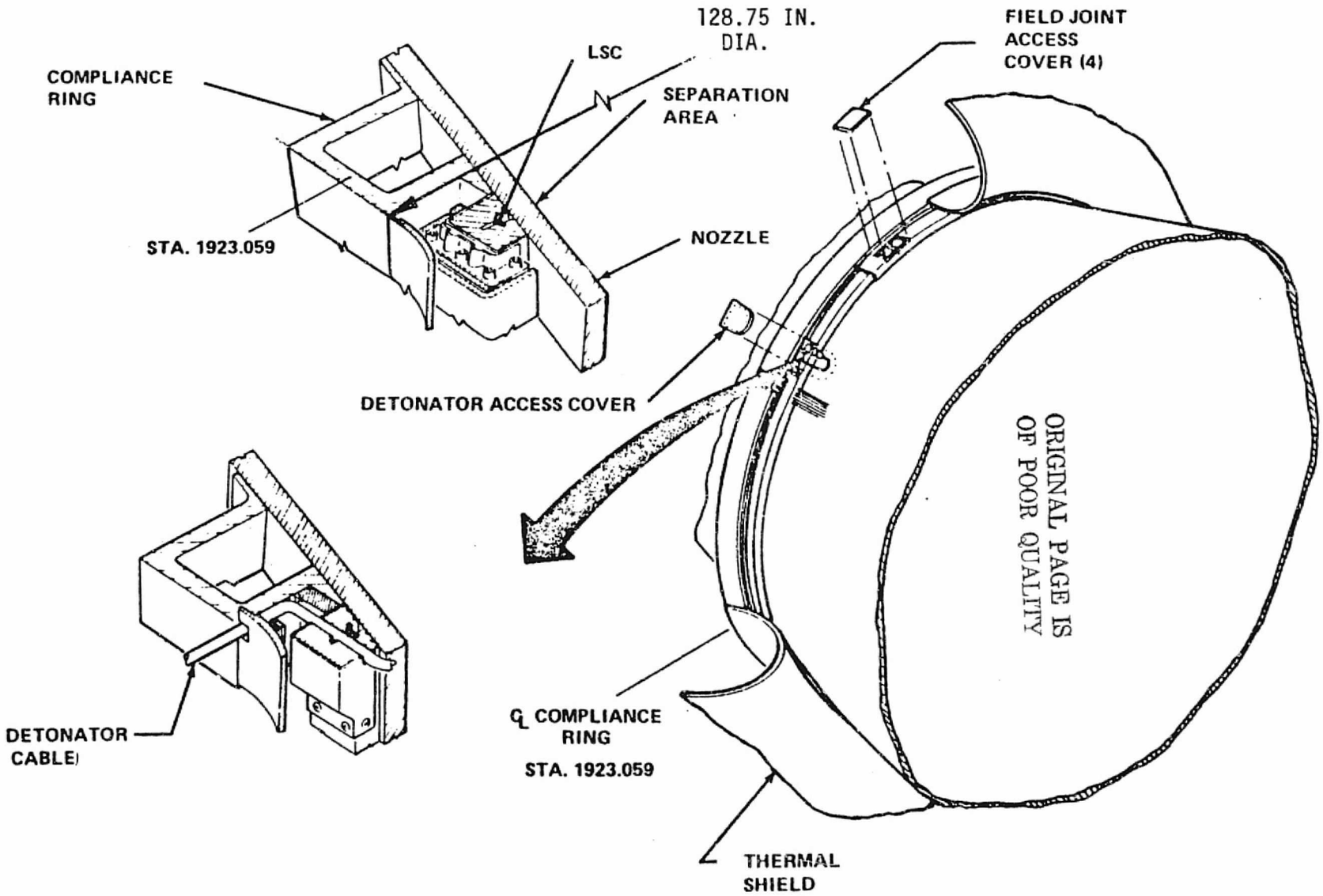

ORIGINAL PAGE IS
OF POOR QUALITY

Figure 6-25. SRB NOZZLE HEAT SHIELD AND COMPLIANCE RING

ORIGINAL PAGE IS
OF POOR QUALITY

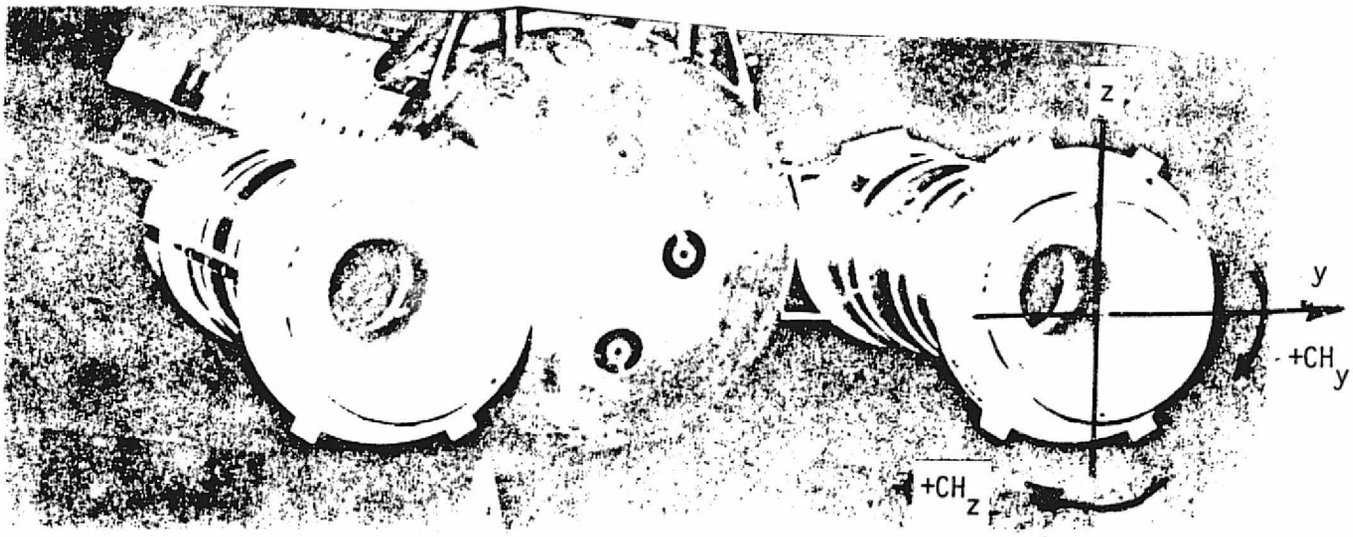

$$CH = \frac{H.M.}{q_\infty (115.7\ FT.^{2'})(126.1'')}$$

Figure 6-26. SRB NOZZLE HINGE MOMENT NOMENCLATURE

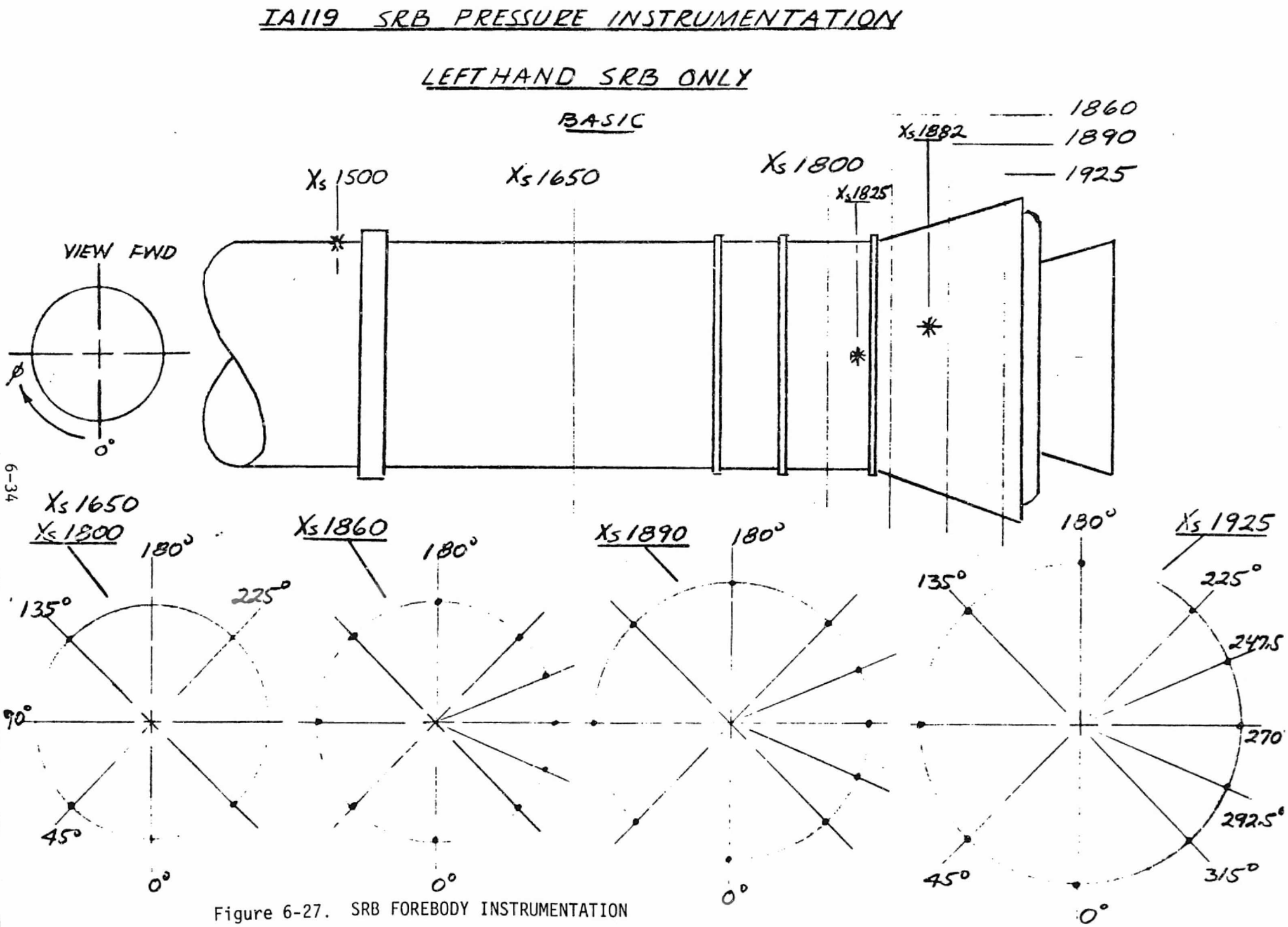

Figure 6-27. SRB FOREBODY INSTRUMENTATION

ORIGINAL PAGE IS
OF POOR QUALITY

IA119 EXTERNAL TANK PRESSURE INSTRUMENTATION

RADIAL LOCATION Ø - DEG.	RAD.-IN.	X_T 3.310	R_1 3.1312	R_2 2.9624	R_3 2.7804	R_4 2.1018	R_5 1.5496	BASE 0
	X_T - STA. M.S.	40.978	41.7827	42.085	42.3247	42.8954	43.1712	43.4600
0			1502	1516	1530	1546		
15					1531			
30			1503	1517				
45			1501		1533			
60			1504	1518	1534			
62.5			1516	1526	1539			
90			1505	1519	1535	1549	1563	
112.5			1506	1520	1536			
135.0			1507	1521	1537	1551		
157.5			1508	1522				
180.0			1509	1523	1539	1553		
202.5			1510	1524				
225.0			1511	1525	1541	1555		
247.5			1512	1526				
270.0			1513	1527	1543	1557	1571	
300.0			1514	1528	1544			
ET ℄								1574

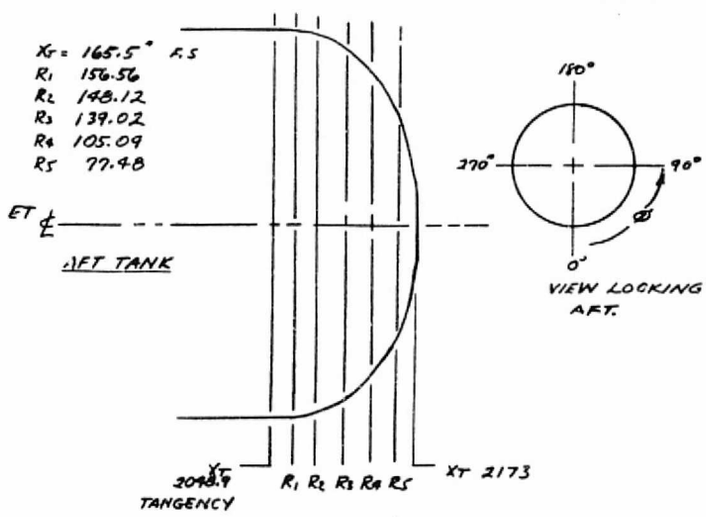

Figure 6-28. EXTERNAL TANK BASE PRESSURE INSTRUMENTATION LOCATION

Table 6-1. SSME #1 PRESSURE INSTRUMENTATION LOCATION AND AREAS

SSME #1

X/D	ORIFICE	θ	TAPLINE		ITEM	NOZZLE AXIAL AREA ~ FT^2
	31	0	1	16	14	.287
	32	30	1	8	2	.287
	33	60	1	8	3	.287
	34	90	1	8	4	.287
	35	120	1	8	5	.287
	36	150	1	8	6	.287
.058	37	180	1	8	7	.287
	38	210	1	8	8	.287
	39	240	1	8	9	.287
	40	270	1	8	10	.287
	41	300	1	8	11	.287
	42	330	1	8	12	.287
	43	0	1	8	13	1.11
	44	30	1	8	14	1.11
	45	60	1	8	15	1.11
	46	90	1	8	16	1.11
	47	120	1	8	17	1.11
.32	48	150	1	9	1	1.11
	49	180	1	9	2	1.11
	50	210	1	9	3	1.11
	51	240	1	9	4	1.11
	52	270	1	9	5	1.11
	53	300	1	10	6	1.11
	54	330	1	9	7	1.11
	55	0	1	9	8	1.28
	56	30	1	9	9	1.28
	57	60	1	9	10	1.28
	58	90	1	9	11	1.28
	59	120	1	9	12	1.28
	60	150	1	9	13	1.28
.58	61	180	1	9	14	1.28
	62	210	1	9	15	1.28
	63	240	1	9	16	1.28
	64	270	1	9	17	1.28
	65	300	1	10	1	1.28
	66	330	1	10	2	1.28
	67	0	1	10	3	2.548
.84	68	90	1	10	4	2.548
	69	180	1	10	5	2.548
	70	270	1	10	6	2.548
					TOT	42.316

Table 6-2. SSME #2 PRESSURE INSTRUMENTATION LOCATION AND AREAS

SSME #2

X/D	ORIFICE	θ	TAP LINE ITEM			NOZZLE AXIAL AREA - FT^2
.058	71	30	2	10	7	.574
	72	90	2	10	8	.574
	73	150	2	10	9	.574
	74	210	2	10	10	.431
	75	240	2	10	11	.287
	76	270	2	17	15	.287
	77	300	2	10	13	.287
	78	330	2	10	14	.431
.32	79	30	2	10	15	2.22
	80	90	2	10	16	2.22
	81	150	2	10	17	2.22
	82	210	2	11	1	1.66
	83	240	2	11	2	1.11
	84	270	2	11	3	1.11
	85	300	2	11	4	1.11
	86	330	2	11	5	1.66
.58	87	30	2	11	6	4.266
	88	90	2	11	7	4.266
	89	150	2	11	8	4.266
	90	210	2	11	9	3.2
	91	240	2	11	10	2.133
	92	270	2	11	11	2.133
	93	300	2	11	12	2.133
	94	330	2	11	13	3.2
					TOT	42.352

Table 6-3. SSME #3 PRESSURE INSTRUMENTATION LOCATION AND AREAS

SSME #3

X/D	ORIFICE	θ	TAP	LINE	ITEM	NOZZLE AXIAL AREA ~ FT^2
.058	71	30	3	10	7	.574
	72	90	3	10	8	.574
	73	150	3	10	9	.574
	74	210	3	10	10	.431
	75	240	3	10	11	.287
	76	270	3	17	15	.287
	77	300	3	10	13	.287
	78	330	3	10	14	.431
.32	79	30	3	10	15	2.22
	80	90	3	10	16	2.22
	81	150	3	10	17	2.22
	82	210	3	11	1	1.66
	83	240	3	11	2	1.11
	84	270	3	11	3	1.11
	85	300	3	11	4	1.11
	86	330	3	11	5	1.66
.58	87	30	3	11	6	4.266
	88	90	3	11	7	4.266
	89	150	3	11	8	4.266
	90	210	3	11	9	3.2
	91	240	3	11	10	2.133
	92	270	3	11	11	2.133
	93	300	3	11	12	2.133
	94	330	3	11	13	3.2
					TOT	42.302

Table 6-4. ORBITER BASE PLATE PRESSURE INSTRUMENTATION LOCATION AND AREAS

ORIFICE	LINE	ITEM	Z	AREA	AREA N BASE
301	16	7	532.	6.5	4.596
302	16	8	502.	16.22	15.59
304	16	9	400.	19.29	18.79
305	16	10	376.	24.77	24.39
306	16	11	340.	17.56	17.29
307	16	12	302.	9.54	9.395
312	16	13	439.	6.05	5.815
315	16	15	15.	7.58	7.286
316	16	16	376.	15.23	14.99
318	16	17	302.	5.28	5.199
325	17	3	302.	8.53	8.400
326	17	4	405.	8.6	8.266
327	17	5	488.	8.6	8.266
329	47	13	422.	10.82	10.40
330	17	8	463.	6.31	6.065
331	17	9	302.	9.84	9.690
334	17	12	340.	13.50	13.29
335	17	13	302.	8.53	8.400
336	17	14	405.	8.6	8.266
337	10	12	488.	8.6	8.266
338	17	16	422.	8.6	8.266
339	17	17	463.	10.82	10.40
340	19	1	410.	5.78	5.556
341	18	2	439.	6.05	5.815
342	18	3	302.	9.84	9.690
343	18	4	302.	5.28	5.199
344	18	5	376.	15.23	14.99
345	18	6	415.	7.59	7.295
346	18	7	340.	13.50	13.29
			TOT	302.64	293.15
			AREA COMPARISON MINUS A_{301}	-6.50	-4.60
				296.14	288.55
			PLUS NOZZLE BASE PLATE PENETRATION	+11.5	+11.2
			TOTAL	307.64	300.35
			ORBITER BASE DRWG (RI RS009150)	308.3	301.0
			IA119 MODEL DRWG(SSA01261)	306.3	299.014

Table 6-5. ORBITER UPPER BODY FLAP PRESSURE INSTRUMENTATION LOCATION AND AREAS

ORIFICE	LINE	ITEM	X	A
405	19	10	1288.0	3.0
406	19	11	1312.3	26.0
407	19	12	1344.7	21.0
408	19	13	1373.0	5.0
413	19	14	1288.0	5.5
414	19	15	1213.3	10.0
415	19	16	1344.7	16.0
416	19	17	1373.0	8.0
422	20	1	1312.3	8.0
424	20	2	1373.0	12.0
430	20	3	1312.3	5.0
432	20	4	1373.0	4.0
437	20	5	1288.0	3.0
438	20	6	1312.3	7.0
439	20	7	1344.7	9.0
440	20	8	1373.0	4.0

$\Sigma A = 146.5$

Table 6-6. ORBITER FOREBODY AND OMS POD INSTRUMENTATION LOCATION

ORIFICE	LINE	ITEM	AREA	X	Y	θ
649						
185	23	12	16.40	1139.0	201.5	0.0
186	14	10	13.89	1139.0	296.5	90.0
187	14	11	1.10	1139.0	336.5	90.0
188	14	12	13.89	1139.0	371.5	45.0
189	14	13	11.10	1139.0	411.5	135.0
190	14	14	11.10	1139.0	411.5	135.0
191	14	15	5.55	1139.0	461.5	180.0
653	14	16	8.33	1139.0	441.5	195.0
196	23	15	16.94	1194.0	206.5	0.0
197	15	3	13.89	1194.0	296.5	90.0
195	15	4	11.10	1194.0	336.5	90.0
199	15	5	13.89	1194.0	371.5	45.0
200	15	6	8.33	1194.0	416.5	135.0
201	15	7	11.10	1194.0	446.5	135.0
202	15	8	9.70	1194.0	471.5	180.0
653	15	9	11.10	1194.0	446.5	225.0
206	23	15	24.1	1244.0	213.5	0.0
207	15	13	15.56	1244.0	296.5	90.0
208	15	14	15.56	1244.0	336.5	90.0
209	15	15	15.56	1244.0	371.5	45.0
210	15	16	11.66	1244.0	416.5	135.0
211	15	17	15.56	1244.0	451.5	135.0
212	16	1	7.77	1244.0	471.5	180.0
214	16	2	15.56	1244.0	451.5	225.0
215	16	3	6.25	1294.0	386.5	45.0
216	16	4	6.25	1294.0	418.5	110.0
217	16	5	15.62	1294.0	396.5	225.0
409	16	6	6.25	1294.0	371.5	290.0
433	18	15	8.5	1288.0	0.0	0.0
410	19	6	9.0	1288.0	88.0	0.0
418	18	16	5.0	1313.2	0.0	0.0
426	19	2	8.0	1313.2	33.0	0.0
434	19	4	5.0	1313.2	66.0	0.0
411	19	7	7.0	1313.2	88.0	0.0
435	18	17	8.0	1345.6	0.0	0.0
412	19	8	9.0	1345.6	88.0	0.0
420	19	1	4.0	1373.95	0.0	0.0
428	19	3	12.0	1373.95	33.0	0.0
436	19	5	4.0	1373.95	66.0	0.0
	19	9	4.0	1373.95	88.0	0.0

Table 6-7. RIGHT WING PRESSURE INSTRUMENTATION LOCATION AND AREAS

RIGHT WING

ORIFICE	LINE	ITEM	AREA	X	Y	UPPER SURFACE
633	23	2	5.38	-68.5	35.0	3.14
632	23	1	4.63	-53.0	35.0	3.14
915	22	17	13.19	-11.0	35.0	3.14
667	24	6	4.58	-67.5	55.0	3.14
666	24	5	3.75	-53.0	55.0	3.14
919	24	4	4.16	-11.0	55.0	3.14
700	25	11	8.04	-68.5	95.	3.14

ORIFICE	LINE	ITEM	AREA	X	Y	LOWER SURFACE
650	23	13	5.38	-68.5	35.0	0.04
649	23	12	4.63	-53.0	35.0	0.04
917	23	11	13.19	-11.0	35.0	0.04
684	24	17	4.58	-69.2	55.00	0.04
683	24	16	3.75	-53.0	55.00	0.04
921	24	15	4.16	-33.0	55.00	0.04
716	26	5	5.70	-69.0	95.00	0.04
715	26	4	2.35	-53.0	95.00	0.04

Table 6-8. RIGHT ELEVON INBOARD PRESSURE INSTRUMENTATION LOCATION AND AREAS

ORIFICE	LINE	ITEM	AREA	X	Y	UPPER SURFACE
639	23	7	1.86	-189.0	35.0	3.14
638	23	6	3.99	-172.0	35.0	3.14
637	23	5	4.34	-149.0	35.0	3.14
636	23	4	4.27	-123.0	35.0	3.14
635	23	3	6.46	-103.0	35.0	3.14
6 3	24	11	2.71	-185.5	55.0	3.14
672	24	10	4.58	-169.6	55.0	3.14
671	24	9	4.79	-147.2	55.0	3.14
670	24	8	4.38	-124.8	55.0	3.14
669	24	7	6.66	-102.4	55.0	3.14
706	25	16	3.7	-178.5	95.	3.14
705	25	15	6.0	-162.0	95.	3.14
704	25	14	6.55	-143.0	95.	3.14
703	25	13	5.42	-122.0	95.	3.14
702	25	12	8.56	-101.0	95.	3.14
738	27	4	3.44	-169.5	145.0	3.14
737	27	3	6.56	-156.0	145.0	3.14
736	27	2	5.94	-137.0	145.0	3.14
735	27	1	5.63	-118.0	145.0	3.14
734	26	17	8.44	-99.0	145.0	3.14
770	28	9	2.5	-164.5	185.0	3.14
769	28	8	5.27	-148.2	185.0	3.14
768	28	7	5.27	-133.4	185.0	3.14
767	28	6	5.27	-115.6	185.0	3.14
766	28	5	6.66	-97.8	185.0	3.14

$\Sigma A_{UPPER} = 129.25$

ORIFICE	LINE	ITEM	AREA	X	Y	LOWER SURFACE
655	24	1	7.66	-165.0	35.0	0.04
653	23	15	6.8	-135.0	35.0	0.04
652	23	14	6.46	-103.0	35.0	0.04
689	25	5	7.29	-167.6	55.00	0.04
688	25	3	4.79	-147.2	55.00	0.04
687	25	2	4.38	-124.8	55.00	0.04
686	25	1	6.66	-102.4	55.00	0.04
721	26	9	9.70	-162.0	95.00	0.04
720	26	8	6.55	-143.0	95.00	0.04
719	26	7	5.42	-122.0	95.00	0.04
718	26	6	8.56	-101.0	95.00	0.04
753	27	14	10.0	-156.0	145.0	0.04
752	27	13	5.94	-137.0	145.0	0.04
751	27	12	5.63	-118.0	145.0	0.04
750	27	11	8.44	-99.0	145.0	0.04
785	29	2	7.77	-151.2	815.0	0.04
784	29	1	5.27	-133.4	815.0	0.04
783	28	17	5.27	-115.6	815.0	0.04
782	28	16	6.66	-97.8	815.0	0.04

$\Sigma A_{LOWER} = 129.25$

Table 6-9. RIGHT ELEVON OUTBOARD PRESSURE INSTRUMENTATION LOCATION AND AREAS

ORIFICE	LINE	ITEM	AREA	X	Y	UPPER SURFACE
802	29	13	2.77	-152.5	235.0	3.14
801	29	12	9.03	-135.8	235.0	3.14
799	29	10	7.29	-110.4	235.0	3.14
796	29	9	7.29	-95.2	235.0	3.14

ORIFICE	LINE	ITEM	AREA	X	Y	LOWER SURFACE
817	30	5	8.33	-140.0	235.0	0.04
816	30	4	8.33	-118.0	235.0	0.04
814	30	2	9.72	-102.0	235.0	0.04

Table 6-10. VERTICAL TAIL PRESSURE INSTRUMENTATION LOCATION AND AREAS

ORIFICE	LINE	ITEM	A	X	Z
505	20	9	16.94	-32.0	27.0
506	20	10	12.84	25.5	27.0
507	20	11	9.45	67.0	27.0
513	20	12	12.15	3.0	67.0
514	20	13	10.94	+53.0	67.0
515	20	14	8.5	92.0	67.0
516	20	15	8.5	126.0	67.0
517	20	16	5.16	165.0	67.0
522	20	17	12.15	31.0	97.0
523	21	1	13.97	75.5	97.0
525	21	3	12.75	145.0	97.0
526	21	4	4.5	180.0	97.0
531	21	5	11.1	61.0	137.0
532	21	6	11.1	106.0	137.0
533	21	7	8.33	139.0	137.0
534	21	8	8.33	167.0	137.0
535	21	9	4.69	199.0	137.0
540	21	10	11.1	96.0	177.0
541	21	11	9.72	136.0	177.0
542	21	12	7.64	165.0	177.0
543	21	13	6.94	196.0	177.0
544	21	14	4.86	220.5	177.0
549	21	15	10.33	130.5	217.0
550	21	16	8.85	166.0	217.0
551	21	17	7.38	191.0	217.0
553	22	2	3.99	240.0	217.0
558	22	3	7.29	170.0	252.0
559	22	4	6.68	201.0	252.0
560	22	5	4.86	225.0	252.0
561	22	6	3.64	240.0	252.0
562	22	7	2.77	260.0	252.0
566	22	8	3.2	173.0	287.0
567	22	9	8.35	191.0	287.0
569	22	11	8.79	238.0	287.0
570	22	12	5.21	256.0	287.0
571	22	13	1.56	275.0	287.0
			$\Sigma A = 294.56$		

Table 6-11. RIGHT SRB NOZZLE PRESSURE INSTRUMENTATION LOCATION AND AREAS

X/D	ORIFICE	θ	TAP	LINE	ITEM	NOZZLE AXIAL AREA- FT^2
.256	2405	0	9	47	17	.767
	2406	30	9	48	1	.767
	2407	60	9	48	2	.767
	2408	90	9	48	3	.767
	2409	120	9	48	4	.767
	2410	150	9	48	5	.767
	2411	180	9	48	6	.767
	2412	210	9	48	7	.767
	2413	240	9	48	8	.767
	2414	270	9	48	9	.767
	2415	300	9	48	10	.767
	2416	330	9	48	11	.767
.135	2417	0	9	48	12	1.01
	2418	30	9	48	13	1.52
	2420	90	9	48	15	1.52
	2421	120	9	48	16	1.01
	2422	150	9	48	17	1.01
	2423	180	9	47	14	1.01
	2424	210	9	49	2	1.01
	2425	240	9	49	3	1.01
	2426	270	9	49	4	1.01
	2427	300	9	49	5	1.01
	2428	330	9	49	6	1.01
.015	2429	0	9	49	7	.582
	2430	30	9	49	8	.582
	2431	60	9	49	9	.582
	2432	90	9	49	10	.582
	2433	120	9	49	11	.582
	2434	150	9	49	12	.582
	2435	180	9	49	13	.582
	2436	210	9	49	14	.582
	2437	240	9	49	15	.8733
	2439	300	9	49	17	.8733
	2440	330	9	50	1	.582
						TOT 28.32

Table 6-12. LEFT SRB FOREBODY PRESSURE INSTRUMENTATION LOCATION

ORIFICE	LINE	ITEM	X_1	X_2	θ_1	θ_2
2150	43	4	1397.6	1432.3	5.8875	.3925
2151	43	5	1397.6	1432.2	.3925	1.1775
2152	43	6	1397.6	1432.2	1.1775	1.9625
2153	43	7	1397.6	1432.2	1.9625	2.74
2154	43	8	1397.6	1432.2	2.74	3.532
2155	43	9	1397.6	1432.3	3.532	4.1215
2156	43	10	1397.6	1432.3	4.1205	4.513
2157	43	11	1397.6	1432.3	4.513	4.906
2158	43	12	1397.6	1432.3	4.906	5.303
2159	43	13	1397.6	1432.3	5.303	5.8875
2160	43	14	1432.3	1467.3	5.8875	.3925
2161	43	15	1432.3	1467.3	.3925	1.1775
2162	43	16	1432.3	1467.3	1.1775	1.9625
2163	43	17	1432.3	1467.3	1.9625	2.74
2164	44	1	1432.3	1467.3	2.74	3.532
2165	44	2	1432.3	1467.3	3.532	4.1215
2166	44	3	1432.3	1467.3	4.1205	4.513
2167	44	4	1432.3	1467.3	4.513	4.906
2168	44	5	1432.3	1467.3	4.906	5.303
2169	44	6	1432.3	1467.3	5.303	5.8875
2170	44	7	1467.3	1487.9	5.8875	.3925
2171	44	8	1467.3	1487.9	.3925	1.1775
2172	44	9	1467.3	1487.9	1.1775	1.9625
2173	44	10	1467.3	1487.9	1.9625	2.74
2174	44	11	1467.3	1487.9	2.74	3.532
2175	44	12	1467.3	1487.9	3.532	4.1215
2176	44	13	1467.3	1487.9	4.1205	4.513
2177	44	14	1467.3	1487.9	4.513	4.906
2178	44	15	1467.3	1487.9	4.906	5.303
2179	44	16	1467.3	1487.9	5.303	5.8875

Table 6-13. EXTERNAL TANK BASE PRESSURE INSTRUMENTATION

ORIFICE	LINE	ITEM		
1501	39	16	.0065	3.882
1502	39	14	.0195	11.64
1503	39	15	.0095	5.674
1504	39	17	.0043	2.568
1505	40	2	.0095	5.674
1506	40	3	.0108	6.450
1507	40	4	.0086	5.136
1508	40	5	.0095	5.674
1509	40	6	.0095	5.674
1510	40	7	.0108	6.450
1511	40	8	.0095	5.674
1512	40	9	.0108	6.450
1513	40	10	.0108	6.450
1514	40	11	.0195	11.64
1516	40	12	.0108	6.450
1517	40	13	.0072	4.300
1518	40	14	.0048	2.867
1519	40	16	.0053	3.165
1520	40	17	.0060	3.583
1521	41	1	.0048	2.867
1522	41	2	.0054	3.225
1523	41	3	.0053	3.165
1524	41	4	.0055	3.285
1525	41	5	.0053	3.165
1526	41	6	.0055	3.285

ORIFICE	LINE	ITEM		
1527	41	7	.0060	3.583
1528	41	8	.0108	6.450
1530	41	9	.0220	13.14
1531	41	10	.0130	7.764
1533	41	11	.0130	7.764
1534	41	12	.0060	3.583
1535	41	14	.0130	7.764
1536	41	15	.0148	8.840
1537	41	16	.0190	11.34
1539	41	17	.0270	16.12
1541	42	1	.0270	16.12
1543	42	2	.0240	14.33
1544	42	3	.0270	16.12
1546	42	4	.1130	67.49
1549	42	5	.0482	28.79
1551	42	6	.0334	19.94
1553	42	7	.0565	33.74
1555	42	8	.0334	19.94
1557	42	9	.0520	31.05
1563	42	10	.0576	34.40
1571	42	11	.0580	34.64
1574	42	12	.0912	54.47
1575	40	1	.0065	3.882
1576	40	15	.0036	2.150
1577	41	15	.0090	5.375

$\Sigma A = 597.3$

Table 6-14. **REFERENCE DIMENSIONS**

TOTAL VEHICLE	FULL SCALE REFERENCE DIMENSIONS
S_{REF}	2690 ft^2
ℓ_{REF}	1290.3 in.
Wing	
Planform area, S_{REF}	2690 ft^2
MAC, $\bar{c}$	474.81 in.
Span, b	936.68 in.
Elevons	
S_{REF}	210 ft^2
ℓ_{REF}	90.7 in.
Vertical Stabilizer	
S_{REF}	413.25 ft^2
ℓ_{REF}	199.8 in.

The moment reference locations

Total vehicle:	X_T 976, Y_T0, Z_T 400
ORB, ET, SRB:	X_T 976, Y_T0, Z_T 400

COMPONENTS

Wing:	X_o1307, Y_o105, Z_o288
Elevons:	Hingeline at X_o1387
Vertical Tail:	X_o1414.3, Y_o0, Z_o503

Section VII

TEST RESULTS

The results of the integration of the base pressure and forebody power delta's are presented in table form in the Appendix. The output of the Plume Integration computer program contains all the results of the pressure integration including base coefficients, forces and moments and forebody coefficient data from pressure integration along with the gauge data.

An example of the printout from a data set is presented below. The data are arranged in 9 sections. Section 1 presents the run numbers, Mach number vehicle configuration and attitude. Section 2 presents the nozzle gas dynamic properties. Section 3 presents the nozzle gas dynamic similarity parameter. Section 4 presents the results of the pressure integration over the base elements and components. Section 5 presents the average base pressure coefficient for each element. Section 6 presents the nozzle average base pressure coefficients. Section 7 presents the nozzle hinge moment data. Section 8 presents the forebody data from the gauges. Section 9 presents the forebody data from pressure integration.

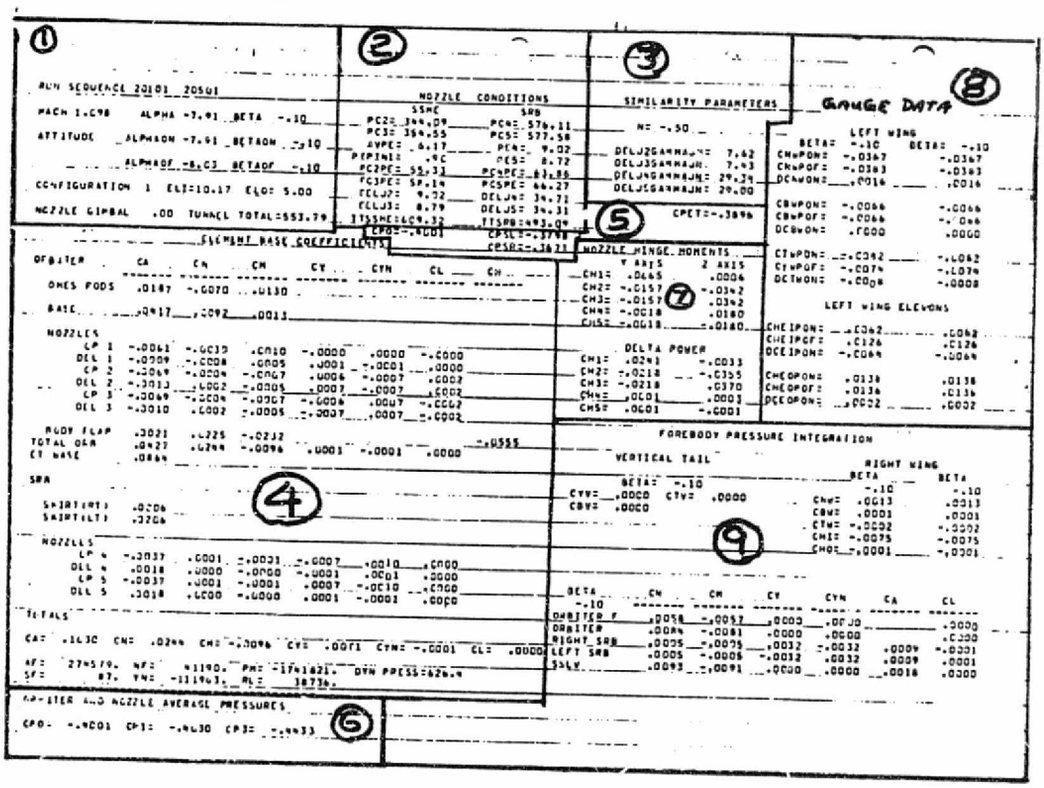

ORIGINAL PAGE IS
OF POOR QUALITY

Printouts of each run sequence set is presented in the Appendix. The data sets are grouped for a constant Mach number. The first data set within a Mach group is the power off runs. The second group contains the variable power runs. The third group are the various elevon deflections. The fourth group contains the various gimbal angle runs and the fifth group is a 90° roll run sets.

Section VIII

BASE MATH MODEL

A math model of the plume induced aerodynamic characteristics has been developed which can be used in conjunction with the forebody aerodynamic characteristics to evaluate the aerodynamic characteristics of the total space shuttle launch vehicle and each element. Three types of base aerodynamic characteristics have been developed. These include 1. SSLV and element base aerodynamic coefficients for Mach numbers of 0.6, 1.05, 1.1, 1.25 and 1.4, 2. SSLV base forces and moments versus altitude up to 160,000 ft. and 3. SSLV and element base coefficient tolerances for Mach numbers from 0.6 to 1.4. The math model consists of a description of the base aerodynamic coefficients at a given Mach number and elevon deflection for various α, β values. Gradients are provided giving the change in the aerodynamic characteristics with the two primary variables that influence the base flow (inboard elevon deflection and SSME power level).

The base aerodynamic math model is limited to base axial force, normal forces and pitching moments. Lateral-directional forces and moments exist on some base components, but no consistent trend could be identified and thus they are included in the base tolerance model. Base coefficients and tolerances for each element are provided for Mach numbers of 0.6, 1.05, 1.1, 1.25 and 1.40. These Mach numbers are compatible with the forebody aerodynamic data base developed in reference 10 except for Mach 1.4. The forebody aerodynamic data is at Mach 1.55. The highest Mach number for which data is available from the IA119 test is 1.4, thus data at Mach 1.4 is provided. The base aerodynamic coefficient math model is described by the following equation,

$$C_{x_i} = [C_{x_i}]_{\alpha,\beta} + [\partial C_{x_i}/\partial \delta_{EI}] \times \Delta\delta_{EI} + [\partial C_{x_i}/\partial \%\ \text{SSME POWER}] \times (\Delta\%\ \text{SSME POWER})$$

where $[C_{x_i}]_{\alpha,\beta}$ is a 4x7 matrix for $\alpha = +4,0,-4,-8$
$\beta = -6,-4,-2,0,2,4,6$

elevon deflection corresponds to close schedule 6 (Table 9-1)

i = SSLV, ORBITER, ET, LEFT SRB, RIGHT SRB

$\partial C_{x_i}/\partial\delta_{EI}$ Gradient for inboard elevon deflection - function of Mach number only

i = SSLV, ORBITER, ET

$\partial C_{x_i}/\partial$ %SSME POWER Gradient for percent change in SSME power level - function of Mach number only

i = SSLV,ORBITER

$\Delta\delta_{EI}$ - Change in inboard elevon deflection from math model value to inboard elevon deflection of interest.

Δ%SSME POWER LEVEL - Change in percent SSME power level from math model value to SSME power level of interest

Values of the coefficient $[C_{x_i}]_{\alpha,\beta}$ are presented in Tables 8-1 through 8-15 for each element and the total SSLV vehicle. Values of the coefficient gradients are presented in Table 8-16.

Base forces and moments have been determined versus altitude using the base coefficient math model. The base force math model is for the total vehicle and uses the following model,

$$\left.\begin{matrix}F\\M\end{matrix}\right|_{ALT} = \left.\begin{matrix}F\\M\end{matrix}\right|_{\alpha=0} + \left[\frac{\partial F}{\partial \alpha}\right] \times \alpha + \left[\frac{\partial F_X}{\partial \delta_{EI}}\right] \Delta\delta_{EI} + \frac{\partial F}{\partial \%\ \text{SSME POWER}} \times (\Delta\%\ \text{SSME POWER})$$

where:

$\left.\begin{matrix}F\\M\end{matrix}\right|_{\alpha=0}$ SSLV base force or moment - function of altitude only

$[\partial F/\partial \alpha]$	Gradient for angle of attack - function of only altitude
$[\partial F/\partial \delta_{EI}]$	Gradient for inboard elevon deflection - function of altitude only
[∂F/∂%SSME POWER]	Gradient for percent change in SSME power level
α	angle of attack
$\Delta\delta_{EI}$	Change in inboard elevon deflection from math model value to inboard elevon deflection of interest
Δ%SSME POWER level	Change in percent SSME power level from math model value to SSME power level of interest.

Values of the base axial force, normal force and pitching moment are presented in Tables 8-17 through 8-19. The base force partials are presented in Tables 8-20 through 8-22.

It is noted that the base axial force coefficient peaks to values higher than the Space Shuttle Aerodynamic Data Book (ref. 11). An evaluation of the element axial force contributions has shown that the main difference was due to the ET axial force which is presented in Figure 8-1.

An evaluation of the ET power-on and power-off base pressures was made and the results are shown in Figure 8-2. The figure shows that the power off ET base pressure compares very well with the ET base pressure from other tests. The figure also shows that during power-on conditions the ET base is slightly asperated for Mach numbers less than 1.0 and has base pressures showing recirculation conditions for Mach numbers greater than 1.0. The present DATA BOOK average ET base pressure coefficients show slight asperation conditions for Mach numbers less than .9 but a large recirculation condition between .9 and 1.1, and then a reduction in recirculation from Mach 1.0 to Mach 1.1. This trend appears questionable and it is believed that the trends shown by the IA119 data are more accurate.

The IA156 test noted on Figure 8-2 was conducted using a .02 scale model of the Space Shuttle Launch vehicle. The model was supported by a sting attached to the base of the orbiter. The ET base pressure should have a minimum of support sting interference. Details of the test program and model configuration can be obtained from reference 12. The IA105 test noted on Figure 8-2 was conducted using a .03 scale model of the Space Shuttle Launch vehicle. The model was supported by a forked sting which was attached to the SRB's. The base pressure on the ET measured during the IA105 test was very near the base pressure from the IA156 test. Details of the IA105 test program and model configuration can be obtained from reference 13.

BASE COEFFICIENT TOLERANCES

The base coefficient tolerances are presented in Tables 8-23 and 8-24. The coefficient tolerances cover all altitudes and configurations from the base coefficients presented in the math model to flight data and are to a $\pm 3\sigma$ level. The moment tolerances are considered to be only due to force tolerances. The moment tolerance due to the aerodynamic center location uncertainty being a smaller order of magnitude. The base moment coefficient increment equations are presented in Table 8-24.

Approximately 60 percent of the orbiter normal force is due to the orbiter axial force. The orbiter normal force tolerance presented in Table 8-23 was therefore calculated using the orbiter axial force tolerance. The equation used to determine the normal force tolerance is presented at the bottom of Table 8-23. The side force coefficient tolerances are due to side forces that exist on the SSME nozzle bells. Side forces will exist on the nozzle bells during various gimbal patterns and under angle of sideslip conditions. These side forces also produce yawing moments and rolling moments. The majority of the lateral-directional tolerances are due to the orbiter.

The base tolerances include contributions due to 1. test instrumentation uncertainty, 2. simulation parameter uncertainty, 3. Reynolds number characteristics, 4. Model-tunnel testing uncertainties, 5. Pressure integration uncertainties and 6. Math model uncertainties. Each tolerance contribution is assumed independent and therefore the contributions are combined using

the RSS technique. The tolerances thus cover the uncertainty from the math model to flight data and are to a $\pm 3\sigma$ level with a Gaussian distribution.

The model instrumentation contribution includes the accuracy of the Scanivalve[R] calculations. The general accuracy is estimated to be $C_p = \pm .013$ for values of C_p in the range of $\pm .5$. The general uncertainty of the measured pressure coefficients was assumed to be 3%.

The simulation parameter uncertainty was assumed to be due to an uncertainty in the exponent. The estimated uncertainty in the exponent is shown in Figure 5-2. The exponent uncertainty was converted to an error in simulation that generally represented a 10 percent uncertainty in base force coefficients. The Reynolds number-scale uncertainty was obtained using past flight test to wind-tunnel test results. This factor is a judgement factor and includes the differences between the Saturn V and Titan 3C flight and wind tunnel data, reduced to account for the plume technology program learning curve. This factor also includes a hot flow simulation uncertainty factor. The Reynolds number-scale uncertainty was generally 10% of the nominal base coefficient.

Model configuration uncertainties includes the effect of the support stings that will influence the flow field at angles of sideslip along with uncertainties due to other model configuration inaccuracies that potentially influence the local flow fields. Uncertainties due to model configuration similitude were approximately 7% of the nominal force coefficients.

Integration uncertainties include the potential error involved in the integration technique and represent approximately 3 percent of the nominal force coefficients.

The math model uncertainty includes the errors of independent variables in the math model of the base forces and moments. Independent variables not included in the math model of the base forces and moments include nozzle gimbal angle and outboard elevon position.

An evaluation of the base coefficients was made to determine the technique for combining the element tolerances to obtain the SSLV tolerances. The different base flow conditions can be compared by considering the variation of the element axial force coefficients versus the similarity parameter. Presented in Figures 8-3 and 8-4 are the base axial force coefficients for each element versus the similarity parameter. Figure 8-3 shows that the orbiter base axial force coefficient increases with SSME nozzle similarity parameter and decreases with SRB similarity parameter. Figure 8-4 shows that the ET and SRB base axial force coefficient decreases with both the SRB similarity parameter and the SSME similarity parameter. Thus an error that would cause the nominal value of similarity parameter to increase or decrease would result in a correlated increase or decrease in the base axial force of both the ET and the SRB's, but not the orbiter. The total vehicle base axial force increases with SSME similarity parameter and decreases with SRB similarity parameter as shown in Figure 8-5. This trend is similar for the majority of the Mach numbers.

The technique that was used to develop the SSLV base tolerances was to correlate the SRB and ET base tolerances and RSS those to the orbiter base coefficient tolerance. This procedure was used for the base axial force and normal force coefficients. The SSLV base side force coefficient was obtained by using the RSS technique for each element.

The forebody plume induced aerodynamic characteristics have been developed in conjunction with the base plume induced aerodynamic characteristics to allow a complete description of the plume induced characteristics of the Space Shuttle Launch Vehicle. The forebody plume induced aerodynamic characteristics are presented in Section IX.

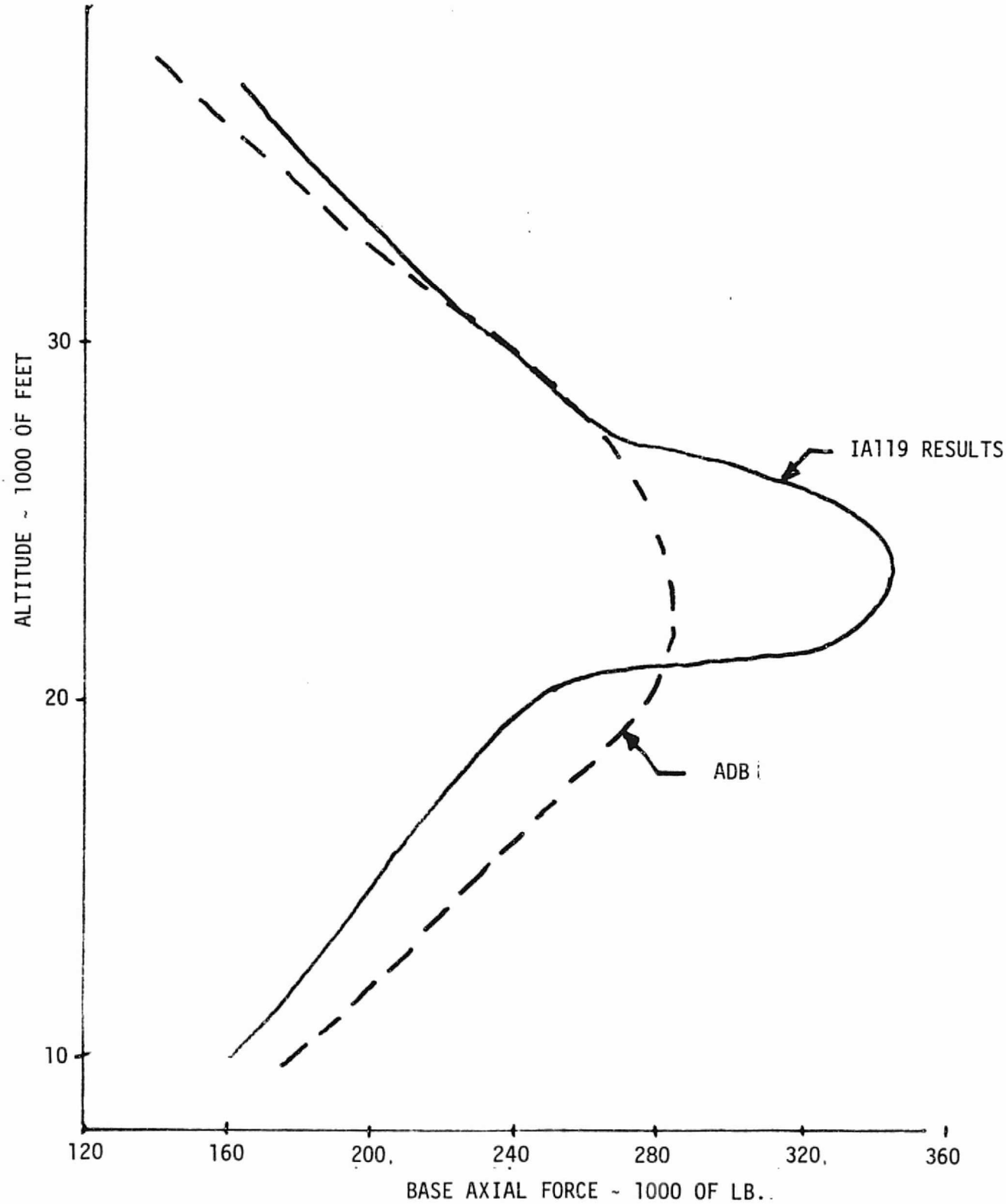

Figure 8-1. ET BASE AXIAL FORCE

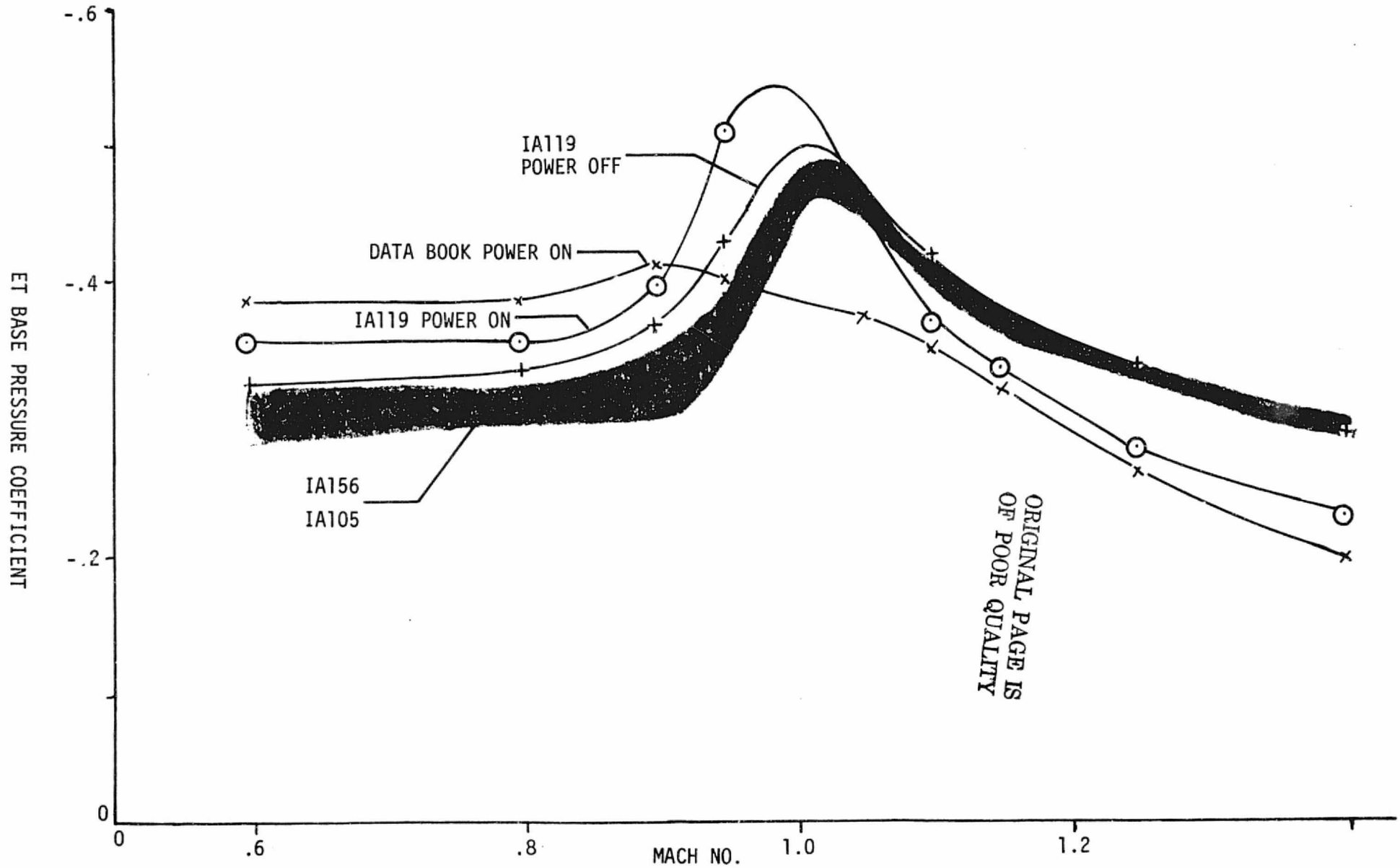

ORIGINAL PAGE IS
OF POOR QUALITY

Figure 8-2. ET BASE PRESSURE COEFFICIENTS

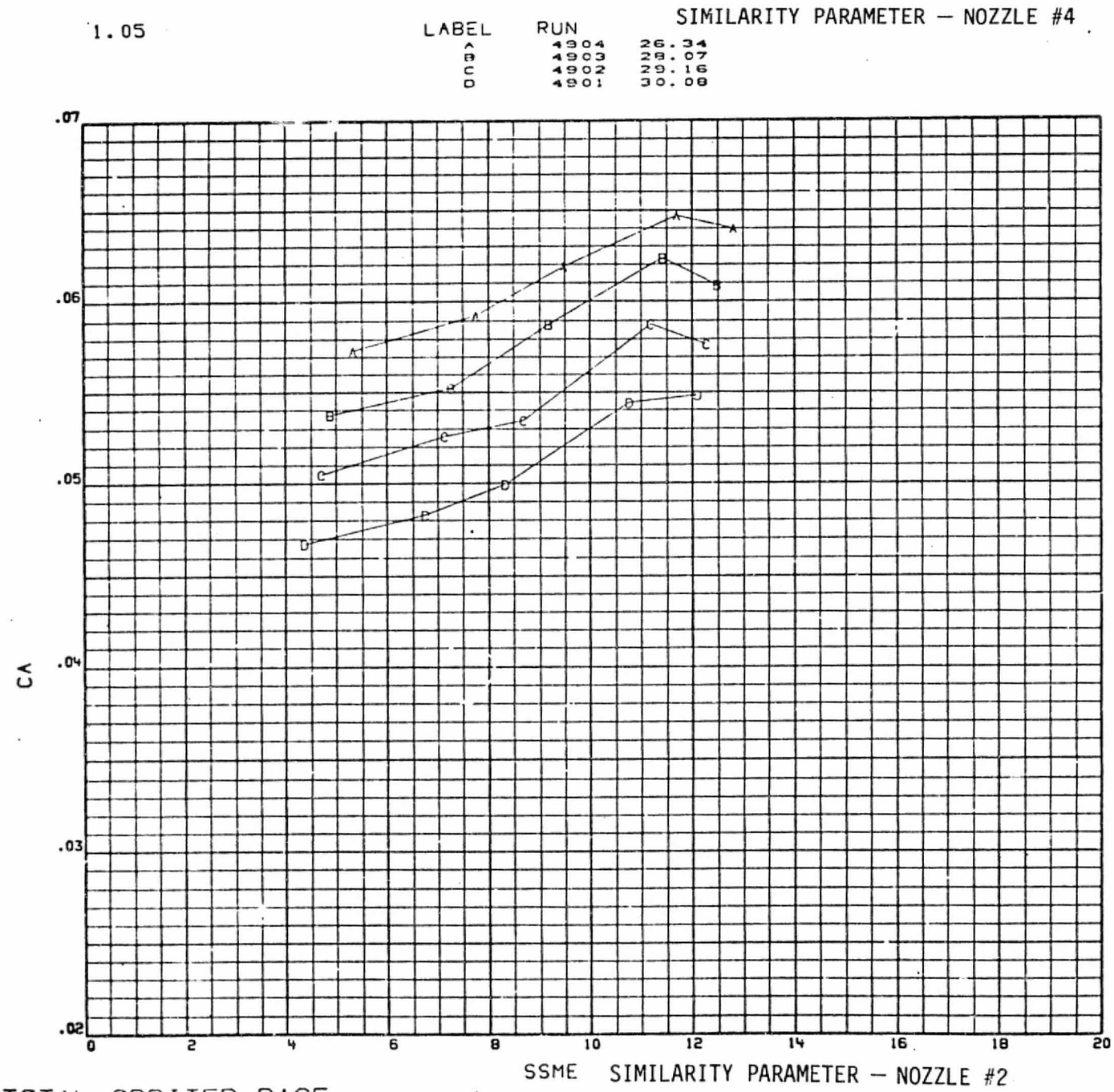

Figure 8-3. TOTAL ORBITER BASE

ORIGINAL PAGE IS
OF POOR QUALITY

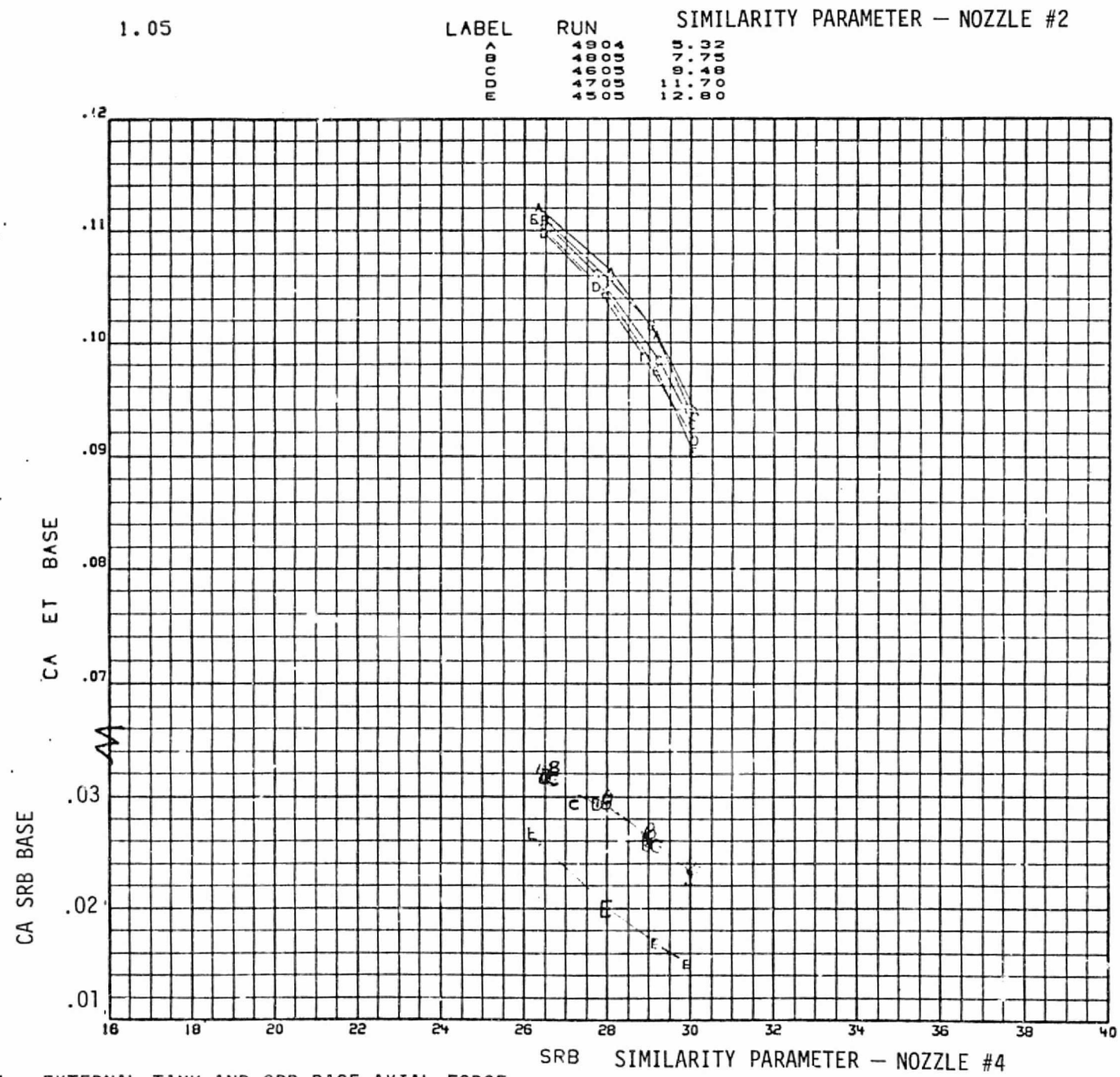

Figure 8-4. EXTERNAL TANK AND SRB BASE AXIAL FORCE

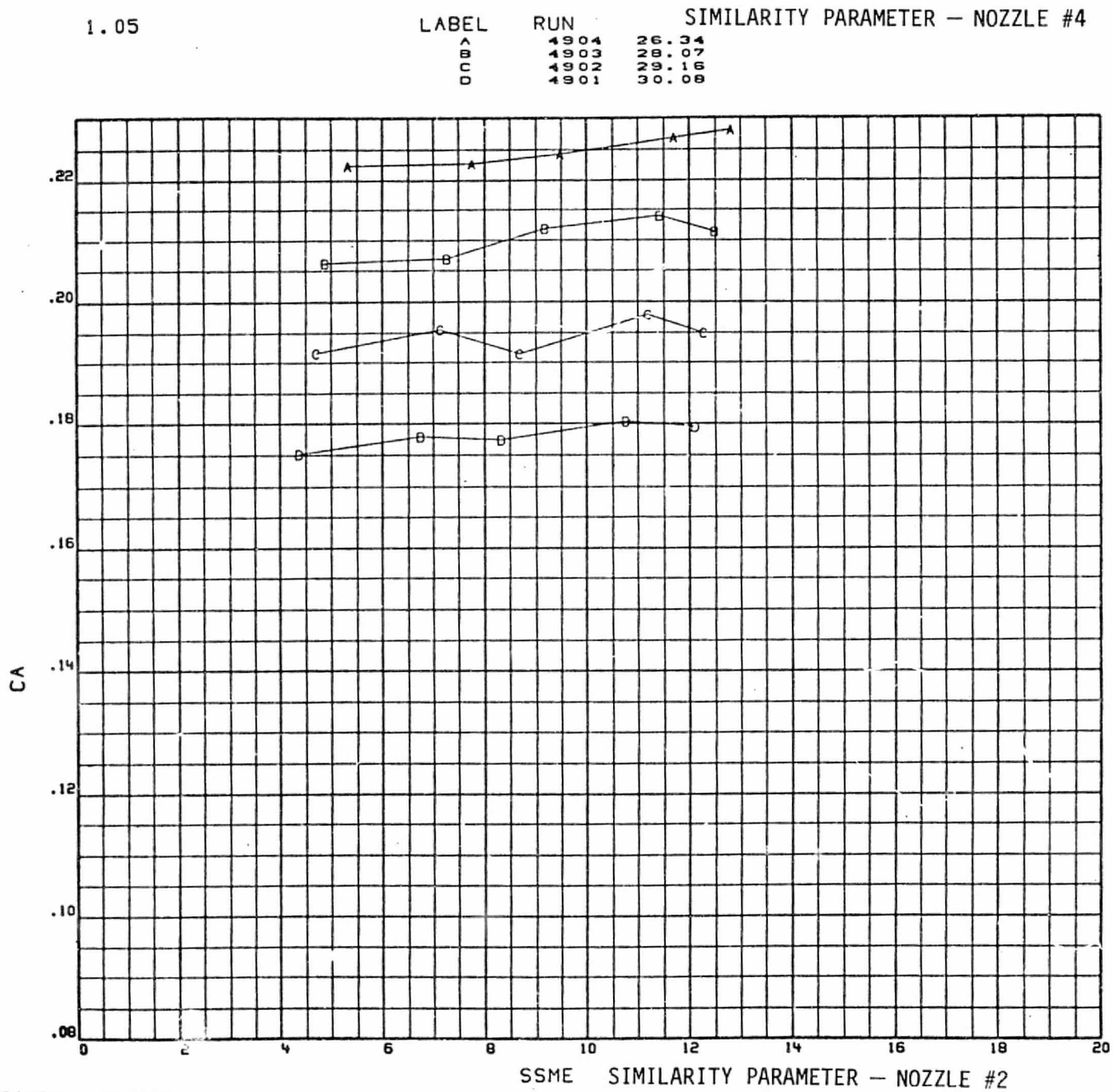

Figure 8-5. TOTAL BASE

ORIGINAL PAGE IS
OF POOR QUALITY

Table 8-1.

BASE AXIAL FORCE COEFFICIENT $M_\infty = 0.6$ $\delta_{e_{IO}} = 10/9$

% SSME POWER = 109%

ELEMENT			α	β: -6	-4	-2	0	2	4	6
TOTAL	ΔCAF	600	-8.	.1684	.1688	.1694	.1694	.1694	.1688	.1684
TOTAL	ΔCAF	600	-4.	.1632	.1629	.1628	.1628	.1628	.1629	.1632
TOTAL	ΔCAF	600	0.	.1579	.1575	.1573	.1573	.1573	.1575	.1579
TOTAL	ΔCAF	600	4.	.1586	.1562	.1536	.1536	.1536	.1562	.1586
ORB	ΔCAF	600	-8.	.0429	.0419	.0410	.0410	.0410	.0419	.0429
ORB	ΔCAF	600	-4.	.0423	.0414	.0404	.0404	.0404	.0414	.0423
ORB	ΔCAF	600	0.	.0425	.0408	.0391	.0391	.0391	.0408	.0425
ORB	ΔCAF	600	4.	.0429	.0406	.0382	.0382	.0362	.0406	.0429
ET	ΔCAF	600	-8.	.0820	.0847	.0874	.0874	.0874	.0847	.0820
ET	ΔCAF	600	-4.	.0768	.0785	.0803	.0803	.0803	.0785	.0768
ET	ΔCAF	600	0.	.0726	.0749	.0772	.0772	.0772	.0749	.0726
ET	ΔCAF	600	4.	.0732	.0743	.0753	.0753	.0753	.0743	.0732
R-SRB	ΔCAF	600	-8.	.0215	.0210	.0205	.0205	.0205	.0212	.0220
R-SRB	ΔCAF	600	-4.	.0217	.0213	.0210	.0210	.0210	.0217	.0224
R-SRB	ΔCAF	600	0.	.0210	.0207	.0205	.0205	.0205	.0211	.0217
R-SRB	ΔCAF	600	4.	.0209	.0205	.0202	.0202	.0202	.0208	.0214
L-SRB	ΔCAF	600	-8.	.0220	.0212	.0205	.0205	.0205	.0210	.0215
L-SRB	ΔCAF	600	-4.	.0224	.0217	.0210	.0210	.0210	.0213	.0217
L-SRB	ΔCAF	600	0.	.0217	.0211	.0205	.0205	.0205	.0207	.0210
L-SRB	ΔCAF	600	4.	.0214	.0208	.0202	.0202	.0202	.0205	.0209

Table 8-2

BASE NORMAL FORCE COEFFICIENT $M_\infty = 0.6$ $\delta_{e_{IO}} = 10/9$

% SSME POWER = 109%

ELEMENT			α	β = -6	-4	-2	0	2	4	6
TOTAL	ΔCN	600	-8.	.0252	.0257	.0261	.0261	.0261	.0257	.0252
TOTAL	ΔCN	600	-4.	.0253	.0252	.0251	.0251	.0251	.0252	.0253
TOTAL	ΔCN	600	0.	.0253	.0246	.0240	.0240	.0240	.0246	.0253
TOTAL	ΔCN	600	4.	.0254	.0241	.0230	.0230	.0230	.0241	.0254
ORB	ΔCN	600	-8.	.0262	.0264	.0265	.0257	.0265	.0264	.0262
ORB	ΔCN	600	-4.	.0260	.0257	.0255	.0255	.0255	.0257	.0260
ORB	ΔCN	600	0.	.0265	.0254	.0244	.0244	.0244	.0254	.0265
ORB	ΔCN	600	4.	.0266	.0249	.0234	.0234	.0234	.0249	.0266
ET	ΔCN	600	-8.	.0	.0	.0	.0	.0	.0	.0
ET	ΔCN	600	-4.	.0	.0	.0	.0	.0	.0	.0
ET	ΔCN	600	0.	.0	.0	.0	.0	.0	.0	.0
ET	ΔCN	600	4.	.0	.0	.0	.0	.0	.0	.0
R-SRB	ΔCN	600	-8.	-.0006	-.0004	-.0002	.0002	-.0002	-.0003	-.0004
R-SRB	ΔCN	600	-4.	-.0004	-.0003	-.0002	-.0002	-.0002	-.0002	-.0003
R-SRB	ΔCN	600	0.	-.0008	-.0005	-.0002	-.0002	-.0002	-.0003	-.0004
R-SRB	ΔCN	600	4.	-.0008	-.0005	-.0002	-.0002	-.0002	-.0003	-.0004
L-SRB	ΔCN	600	-8.	-.0004	-.0003	-.0002	.0002	-.0002	-.0004	-.0006
L-SRB	ΔCN	600	-4.	-.0003	-.0002	-.0002	-.0002	-.0002	-.0003	-.0004
L-SRB	ΔCN	600	0.	-.0004	-.0003	-.0002	-.0002	-.0002	-.0005	-.0008
L-SRB	ΔCN	600	4.	-.0004	-.0003	-.0002	-.0002	-.0002	-.0005	-.0008

Table 8-3

BASE PITCHING MOMENT COEFFICIENT $M_\infty = 0.6$ $\delta_{e_{IO}} = 10/9$

% SSME POWER = 109%

ELEMENT			α	β = -6	-4	-2	0	2	4	6
TOTAL	ΔCM	600	-8.	-.0113	-.0122	-.0131	-.0131	-.0131	-.0122	-.0113
TOTAL	ΔCM	600	-4.	-.0116	-.0123	-.0123	-.0123	-.0123	-.0123	-.0116
TOTAL	ΔCM	600	0.	-.0115	-.0116	-.0116	-.0116	-.0116	-.0116	-.0115
TOTAL	ΔCM	600	4.	-.0114	-.0109	-.0109	-.0109	-.0109	-.0109	-.0114
ORB	ΔCM	600	-8.	-.0125	-.0126	-.0127	-.0127	-.0127	-.0126	-.0125
ORB	ΔCM	600	-4.	-.0123	-.0129	-.0129	-.0129	-.0129	-.0129	-.0123
ORB	ΔCM	600	0.	-.0128	-.0122	-.0122	-.0122	-.0122	-.0122	-.0128
ORB	ΔCM	600	4.	-.0128	-.0115	-.0115	-.0115	-.0115	-.0115	-.0128
ET	ΔCM	600	-8.	.0	.0	.0	.0	.0	.0	.0
ET	ΔCM	600	-4.	.0	.0	.0	.0	.0	.0	.0
ET	ΔCM	600	0.	.0	.0	.0	.0	.0	.0	.0
ET	ΔCM	600	4.	.0	.0	.0	.0	.0	.0	.0
R-SRB	ΔCM	600	-8.	.0007	.0002	-.0002	-.0002	-.0002	.0002	.0005
R-SRB	ΔCM	600	-4.	.0004	.0003	.0003	.0003	.0003	.0003	.0003
R-SRB	ΔCM	600	0.	.0009	.0003	.0003	.0003	.0003	.0003	.0004
R-SRB	ΔCM	600	4.	.0009	.0003	.0003	.0003	.0003	.0003	.0005
L-SRB	ΔCM	600	-8.	.0005	.0002	-.0002	-.0002	-.0002	.0002	.0007
L-SRB	ΔCM	600	-4.	.0003	.0003	.0003	.0003	.0003	.0003	.0004
L-SRB	ΔCM	600	0.	.0004	.0003	.0003	.0003	.0003	.0003	.0009
L-SRB	ΔCM	600	4.	.0005	.0003	.0003	.0003	.0003	.0003	.0009

ORIGINAL PAGE IS
OF POOR QUALITY

Table 8-4

BASE AXIAL FORCE COEFFICIENT

$M_\infty = 1.05$ $\delta_{e_{IO}} = 10/9$

% SSME POWER = 88.4%

ELEMENT			α	β -6	-4	-2	0	2	4	6
TOTAL	ΔCA	1050	-8.	.1907	.1892	.1892	.1892	.1892	.1892	.1907
TOTAL	ΔCA	1050	-4.	.1914	.1895	.1895	.1895	.1895	.1895	.1914
TOTAL	ΔCA	1050	0.	.1971	.1970	.1970	.1970	.1970	.1970	.1971
TOTAL	ΔCA	1050	4.	.2031	.2047	.2047	.2047	.2047	.2047	.2031
ORB	ΔCA	1050	-8.	.0550	.0486	.0486	.0486	.0486	.0486	.0550
ORB	ΔCA	1050	-4.	.0557	.0496	.0496	.0496	.0496	.0496	.0557
ORB	ΔCA	1050	0.	.0594	.0534	.0534	.0534	.0534	.0534	.0594
ORB	ΔCA	1050	4.	.0610	.0561	.0561	.0561	.0561	.0561	.0610
ET	ΔCA	1050	-8.	.0947	.1004	.1004	.1004	.1004	.1004	.0947
ET	ΔCA	1050	-4.	.0926	.0983	.0983	.0983	.0983	.0983	.0926
ET	ΔCA	1050	0.	.0942	.1012	.1012	.1012	.1012	.1012	.0942
ET	ΔCA	1050	4.	.0969	.1050	.1050	.1050	.1050	.1050	.0969
R-SRB	ΔCA	1050	-8.	.0212	.0201	.0201	.0201	.0201	.0201	.0205
R-SRB	ΔCA	1050	-4.	.0220	.0208	.0208	.0208	.0208	.0208	.0211
R-SRB	ΔCA	1050	0.	.0222	.0212	.0212	.0212	.0212	.0212	.0213
R-SRB	ΔCA	1050	4.	.0225	.0218	.0218	.0218	.0218	.0218	.0227
L-SRB	ΔCA	1050	-8.	.0205	.0201	.0201	.0201	.0201	.0201	.0212
L-SRB	ΔCA	1050	-4.	.0211	.0208	.0208	.0208	.0208	.0208	.0220
L-SRB	ΔCA	1050	0.	.0213	.0212	.0212	.0212	.0212	.0212	.0222
L-SRB	ΔCA	1050	4.	.0227	.0218	.0218	.0218	.0218	.0218	.0225

ORIGINAL PAGE IS
OF POOR QUALITY

Table 8-5

BASE NORMAL FORCE COEFFICIENT $M_\infty = 1.05$ $\delta_{e_{IO}} = 10/9$

% SSME POWER = 88.4%

ELEMENT			α	β -6	-4	-2	0	2	4	6
TOTAL	ΔCN	1050	-8.	.0300	.0285	.0269	.0269	.0269	.0285	.0300
TOTAL	ΔCN	1050	-4.	.0316	.0297	.0275	.0275	.0275	.0295	.0316
TOTAL	ΔCN	1050	0.	.0341	.0316	.0296	.0296	.0296	.0316	.0341
TOTAL	ΔCN	1050	4.	.0357	.0337	.0317	.0317	.0317	.0337	.0357
ORB	ΔCN	1050	-8.	.0303	.0285	.0269	.0269	.0269	.0285	.0303
ORB	ΔCN	1050	-4.	.0317	.0293	.0273	.0273	.0273	.0293	.0317
ORB	ΔCN	1050	0.	.0340	.0316	.0296	.0296	.0296	.0316	.0340
ORB	ΔCN	1050	4.	.0354	.0333	.0313	.0313	.0313	.0333	.0354
ET	ΔCN	1050	-8.	.0	.0	.0	.0	.0	.0	.0
ET	ΔCN	1050	-4.	.0	.0	.0	.0	.0	.0	.0
ET	ΔCN	1050	0.	.0	.0	.0	.0	.0	.0	.0
ET	ΔCN	1050	4.	.0	.0	.0	.0	.0	.0	.0
R-SRB	ΔCN	1050	-8.	-.0001	.0000	.0000	.0000	.0000	.0000	-.0002
R-SRB	ΔCN	1050	-4.	.0000	.0001	.0001	.0001	.0001	.0001	-.0001
R-SRB	ΔCN	1050	0.	.0001	.0000	.0000	.0000	.0000	.0000	.0000
R-SRB	ΔCN	1050	4.	.0003	.0002	.0002	.0002	.0002	.0002	.0000
L-SRB	ΔCN	1050	-8.	-.0002	.0000	.0000	.0000	.0000	.0000	-.0001
L-SRB	ΔCN	1050	-4.	-.0001	.0001	.0001	.0001	.0001	.0001	.0000
L-SRB	ΔCN	1050	0.	.0000	.0000	.0000	.0000	.0000	.0000	.0001
L-SRB	ΔCN	1050	4.	.0000	.0002	.0002	.0002	.0002	.0002	.0003

Table 8-6

BASE PITCHING MOMENT COEFFICIENT $M_\infty = 1.05$ $\delta_{e_{IO}} = 10/9$

% SSME POWER = 88.4%

ELEMENT			α	β -6	-4	-2	0	2	4	6
TOTAL	ΔCM	1050	-8.	-.0114	-.0108	-.0102	-.0102	-.0102	-.0108	-.0114
TOTAL	ΔCM	1050	-4.	-.0126	-.0116	-.0106	-.0106	-.0106	-.0116	-.0126
TOTAL	ΔCM	1050	0.	-.0140	-.0128	-.0116	-.0116	-.0116	-.0128	-.0140
TOTAL	ΔCM	1050	4.	-.0149	-.0140	-.0130	-.0130	-.0130	-.0140	-.0149
ORB	ΔCM	1050	-8.	-.0118	-.0109	-.0102	-.0102	-.0102	-.0109	-.0118
ORB	ΔCM	1050	-4.	-.0127	-.0115	-.0104	-.0104	-.0104	-.0115	-.0127
ORB	ΔCM	1050	0.	-.0139	-.0128	-.0116	-.0116	-.0116	-.0128	-.0139
ORB	ΔCM	1050	4.	-.0145	-.0136	-.0126	-.0126	-.0126	-.0136	-.0145
ET	ΔCM	1050	-8.	.0	.0	.0	.0	.0	.0	.0
ET	ΔCM	1050	-4.	.0	.0	.0	.0	.0	.0	.0
ET	ΔCM	1050	0.	.0	.0	.0	.0	.0	.0	.0
ET	ΔCM	1050	4.	.0	.0	.0	.0	.0	.0	.0
R-SRB	ΔCM	1050	-8.	.0001	.0000	.0000	.0000	.0000	.0001	.0003
R-SRB	ΔCM	1050	-4.	.0000	-.0001	-.0001	-.0001	-.0001	.0000	.0001
R-SRB	ΔCM	1050	0.	-.0001	.0000	.0000	.0000	.0000	.0000	.0000
R-SRB	ΔCM	1050	4.	-.0004	-.0003	-.0002	-.0002	-.0002	-.0001	.0000
L-SRB	ΔCM	1050	-8.	.0003	.0001	.0000	.0000	.0000	.0000	.0001
L-SRB	ΔCM	1050	-4.	.0001	.0000	-.0001	-.0001	-.0001	-.0001	.0000
L-SRB	ΔCM	1050	0.	.0000	.0000	.0000	.0000	.0000	.0000	-.0001
L-SRB	ΔCM	1050	4.	.0000	-.0001	-.0002	-.0002	-.0002	-.0003	-.0004

ORIGINAL PAGE IS OF POOR QUALITY

Table 8-7

BASE AXIAL FORCE COEFFICIENT

$M_\infty = 1.10$ $\delta_{e_{IO}} = 10/9$

% SSME POWER = 88.4%

ELEMENT			α	β -6	-4	-2	0	2	4	6
TOTAL	ΔCA	1100	-8.	.1663	.1625	.1591	.1591	.1591	.1625	.1663
TOTAL	ΔCA	1100	-4.	.1637	.1599	.1569	.1569	.1569	.1599	.1637
TOTAL	ΔCA	1100	0.	.1671	.1629	.1589	.1589	.1589	.1629	.1671
TOTAL	ΔCA	1100	4.	.1720	.1694	.1664	.1664	.1664	.1694	.1720
ORB	ΔCA	1100	-8.	.0475	.0435	.0415	.0415	.0415	.0435	.0475
ORB	ΔCA	1100	-4.	.0492	.0454	.0419	.0419	.0419	.0454	.0492
ORB	ΔCA	1100	0.	.0519	.0478	.0438	.0438	.0438	.0478	.0519
ORB	ΔCA	1100	4.	.0535	.0497	.0467	.0467	.0467	.0497	.0535
ET	ΔCA	1100	-8.	.0826	.0836	.0846	.0846	.0846	.0836	.0826
ET	ΔCA	1100	-4.	.0786	.0800	.0814	.0814	.0814	.0800	.0786
ET	ΔCA	1100	0.	.0789	.0802	.0813	.0813	.0813	.0802	.0789
ET	ΔCA	1100	4.	.0814	.0830	.0845	.0845	.0845	.0830	.0814
R-SRB	ΔCA	1100	-8.	.0185	.0175	.0165	.0165	.0165	.0170	.0177
R-SRB	ΔCA	1100	-4.	.0184	.0176	.0168	.0168	.0168	.0171	.0175
R-SRB	ΔCA	1100	0.	.0186	.0177	.0169	.0169	.0169	.0173	.0177
R-SRB	ΔCA	1100	4.	.0190	.0183	.0176	.0176	.0176	.0178	.0181
L-SRB	ΔCA	1100	-8.	.0177	.0170	.0165	.0165	.0165	.0175	.0185
L-SRB	ΔCA	1100	-4.	.0175	.0171	.0168	.0168	.0168	.0176	.0184
L-SRB	ΔCA	1100	0.	.0177	.0173	.0169	.0169	.0169	.0177	.0186
L-SRB	ΔCA	1100	4.	.0181	.0178	.0176	.0176	.0176	.0183	.0190

ORIGINAL PAGE IS
OF POOR QUALITY

Table 8-8

BASE NORMAL FORCE COEFFICIENT

$M_\infty = 1.10$ $\delta_{e_{IO}} = 10/9$

% SSME POWER = 88.4%

ELEMENT			α	β -6	-4	-2	0	2	4	6
TOTAL	ΔCN	1100	-8.	.0269	.0255	.0240	.0240	.0240	.0255	.0269
TOTAL	ΔCN	1100	-4.	.0287	.0264	.0242	.0242	.0242	.0264	.0287
TOTAL	ΔCN	1100	0.	.0309	.0278	.0253	.0253	.0253	.0278	.0309
TOTAL	ΔCN	1100	4.	.0320	.0299	.0274	.0274	.0274	.0299	.0320
ORB	ΔCN	1100	-8.	.0271	.0255	.0240	.0240	.0240	.0255	.0271
ORB	ΔCN	1100	-4.	.0286	.0262	.0240	.0240	.0240	.0262	.0286
ORB	ΔCN	1100	0.	.0307	.0278	.0253	.0253	.0253	.0278	.0307
ORB	ΔCN	1100	4.	.0316	.0286	.0272	.0272	.0272	.0296	.0316
ET	ΔCN	1100	-8.	.0	.0	.0	.0	.0	.0	.0
ET	ΔCN	1100	-4.	.0	.0	.0	.0	.0	.0	.0
ET	ΔCN	1100	0.	.0	.0	.0	.0	.0	.0	.0
ET	ΔCN	1100	4.	.0	.0	.0	.0	.0	.0	.0
R-SRB	ΔCN	1100	-8.	-.0001	.0000	.0000	.0000	.0000	.0000	-.0001
R-SRB	ΔCN	1100	-4.	.0000	.0001	.0001	.0001	.0001	.0001	.0001
R-SRB	ΔCN	1100	0.	.0001	.0000	.0000	.0000	.0000	.0000	.0001
R-SRB	ΔCN	1100	4.	.0004	.0002	.0001	.0001	.0001	.0001	.0000
L-SRB	ΔCN	1100	-8.	-.0001	.0000	.0000	.0000	.0000	.0000	-.0001
L-SRB	ΔCN	1100	-4.	.0001	.0001	.0001	.0001	.0001	.0001	.0000
L-SRB	ΔCN	1100	0.	.0001	.0000	.0000	.0000	.0000	.0000	.0001
L-SRB	ΔCN	1100	4.	.0000	.0001	.0001	.0001	.0001	.0002	.0004

Table 8-9

BASE PITCHING MOMENT COEFFICIENT

$M_\infty = 1.10$ $\delta_{e_{IO}} = 10/9$

% SSME POWER = 88.4%

ELEMENT			α	β: -6	-4	-2	0	2	4	6
TOTAL	ΔCM	1100	-8.	-.0104	-.0100	-.0095	-.0095	-.0095	-.0100	-.0104
TOTAL	ΔCM	1100	-4.	-.0116	-.0106	-.0096	-.0096	-.0096	-.0106	-.0116
TOTAL	ΔCM	1100	0.	-.0130	-.0116	-.0101	-.0101	-.0101	-.0116	-.0130
TOTAL	ΔCM	1100	4.	-.0136	-.0124	-.0112	-.0112	-.0112	-.0124	-.0136
ORB	ΔCM	1100	-8.	-.0106	-.0100	-.0095	-.0095	-.0095	-.0100	-.0106
ORB	ΔCM	1100	-4.	-.0116	-.0104	-.0094	-.0094	-.0094	-.0104	-.0116
ORB	ΔCM	1100	0.	-.0128	-.0116	-.0101	-.0101	-.0101	-.0116	-.0128
ORB	ΔCM	1100	4.	-.0132	-.0120	-.0110	-.0110	-.0110	-.0120	-.0132
ET	ΔCM	1100	-8.	.0	.0	.0	.0	.0	.0	.0
ET	ΔCM	1100	-4.	.0	.0	.0	.0	.0	.0	.0
ET	ΔCM	1100	0.	.0	.0	.0	.0	.0	.0	.0
ET	ΔCM	1100	4.	.0	.0	.0	.0	.0	.0	.0
R-SRB	ΔCM	1100	-8.	.0001	.0000	.0000	.0000	.0000	.0000	.0001
R-SRB	ΔCM	1100	-4.	.0000	-.0001	-.0001	-.0001	-.0001	-.0001	.0000
R-SRB	ΔCM	1100	0.	-.0001	.0000	.0000	.0000	.0000	.0000	-.0001
R-SRB	ΔCM	1100	4.	-.0004	-.0002	-.0001	-.0001	-.0001	-.0001	.0000
L-SRB	ΔCM	1100	-8.	.0001	.0000	.0000	.0000	.0000	.0000	.0001
L-SRB	ΔCM	1100	-4.	.0000	-.0001	-.0001	-.0001	-.0001	-.0001	.0000
L-SRB	ΔCM	1100	0.	-.0001	.0000	.0000	.0000	.0000	.0000	-.0001
L-SRB	ΔCM	1100	4.	.0000	-.0001	-.0001	-.0001	-.0001	-.0002	-.0004

ORIGINAL PAGE IS OF POOR QUALITY

Table 8-10

BASE AXIAL FORCE COEFFICIENT

$M_\infty = 1.25$ $\delta_{e_{IO}} = 10/-2$

% SSME POWER = 88.4%

ELEMENT			α	β -6	-4	-2	0	2	4	6
TOTAL	ΔCA	1250	-8.	.1420	.1363	.1300	.1300	.1300	.1363	.1420
TOTAL	ΔCA	1250	-4.	.1356	.1296	.1245	.1245	.1245	.1296	.1356
TOTAL	ΔCA	1250	0.	.1336	.1276	.1214	.1214	.1214	.1276	.1336
TOTAL	ΔCA	1250	4.	.1350	.1290	.1233	.1233	.1233	.1290	.1350
ORB	ΔCA	1250	-8.	.0390	.0384	.0375	.0375	.0375	.0384	.0390
ORB	ΔCA	1250	-4.	.0392	.0376	.0374	.0374	.0374	.0376	.0392
ORB	ΔCA	1250	0.	.0402	.0386	.0372	.0372	.0372	.0386	.0402
ORB	ΔCA	1250	4.	.0419	.0397	.0383	.0383	.0383	.0397	.0419
ET	ΔCA	1250	-8.	.0761	.0731	.0703	.0703	.0703	.0731	.0761
ET	ΔCA	1250	-4.	.0672	.0662	.0653	.0653	.0653	.0662	.0672
ET	ΔCA	1250	0.	.0656	.0636	.0610	.0610	.0610	.0636	.0656
ET	ΔCA	1250	4.	.0652	.0630	.0604	.0604	.0604	.0630	.0652
R-SRB	ΔCA	1250	-8.	.0135	.0124	.0111	.0111	.0111	.0124	.0134
R-SRB	ΔCA	1250	-4.	.0151	.0132	.0109	.0109	.0109	.0126	.0141
R-SRB	ΔCA	1250	0.	.0146	.0130	.0116	.0116	.0116	.0124	.0132
R-SRB	ΔCA	1250	4.	.0144	.0134	.0123	.0123	.0123	.0129	.0135
L-SRB	ΔCA	1250	-8.	.0134	.0124	.0111	.0111	.0111	.0124	.0135
L-SRB	ΔCA	1250	-4.	.0141	.0126	.0109	.0109	.0109	.0132	.0151
L-SRB	ΔCA	1250	0.	.0132	.0124	.0116	.0116	.0116	.0130	.0146
L-SRB	ΔCA	1250	4.	.0135	.0129	.0123	.0123	.0123	.0134	.0144

Table 8-11

BASE NORMAL FORCE COEFFICIENT

$M_\infty = 1.25$ $\delta_{e_{IO}} = 10/-2$

% SSME POWER = 88.4%

ELEMENT			α	β -6	-4	-2	0	2	4	6
TOTAL	ΔCN	1250	-8.	.0215	.0215	.0214	.0214	.0214	.0215	.0215
TOTAL	ΔCN	1250	-4.	.0214	.0214	.0215	.0215	.0215	.0214	.0214
TOTAL	ΔCN	1250	0.	.0236	.0229	.0222	.0217	.0222	.0229	.0236
TOTAL	ΔCN	1250	4.	.0247	.0239	.0231	.0223	.0231	.0239	.0247
ORB	ΔCN	1250	-8.	.0212	.0212	.0213	.0214	.0213	.0212	.0212
ORB	ΔCN	1250	-4.	.0215	.0215	.0215	.0215	.0215	.0215	.0215
ORB	ΔCN	1250	0.	.0234	.0227	.0220	.0215	.0220	.0227	.0234
ORB	ΔCN	1250	4.	.0248	.0240	.0233	.0225	.0233	.0240	.0248
ET	ΔCN	1250	-8.	.0	.0	.0	.0	.0	.0	.0
ET	ΔCN	1250	-4.	.0	.0	.0	.0	.0	.0	.0
ET	ΔCN	1250	0.	.0	.0	.0	.0	.0	.0	.0
ET	ΔCN	1250	4.	.0	.0	.0	.0	.0	.0	.0
R-SRB	ΔCN	1250	-8.	.0001	.0001	.0000	.0000	.0001	.0002	.0002
R-SRB	ΔCN	1250	-4.	-.0001	-.0001	.0000	.0000	.0000	.0000	.0000
R-SRB	ΔCN	1250	0.	.0000	.0000	.0001	.0001	.0001	.0002	.0002
R-SRB	ΔCN	1250	4.	-.0001	-.0001	-.0001	-.0001	-.0001	.0000	.0000
L-SRB	ΔCN	1250	-8.	.0002	.0002	.0001	.0000	.0000	.0001	.0001
L-SRB	ΔCN	1250	-4.	.0000	.0000	.0000	.0000	.0000	-.0001	-.0001
L-SRB	ΔCN	1250	0.	.0002	.0002	.0001	.0001	.0001	.0000	.0000
L-SRB	ΔCN	1250	4.	.0000	.0000	-.0001	-.0001	-.0001	-.0001	-.0001

ORIGINAL PAGE IS
OF POOR QUALITY

Table 8-12

BASE PITCHING MOMENT COEFFICIENT

$M_\infty = 1.25$ $\delta_{\epsilon_{IO}} = 10/-2$

% SSME POWER = 88.4%

ELEMENT			α	β -6	-4	-2	0	2	4	6
TOTAL	ΔCM	1250	-8.	-.0082	-.0082	-.0082	-.0082	-.0082	-.0082	-.0082
TOTAL	ΔCM	1250	-4.	-.0082	-.0082	-.0085	-.0085	-.0085	-.0082	-.0082
TOTAL	ΔCM	1250	0.	-.0097	-.0094	-.0090	-.0087	-.0090	-.0094	-.0097
TOTAL	ΔCM	1250	4.	-.0103	-.0098	-.0093	-.0088	-.0093	-.0098	-.0103
ORB	ΔCM	1250	-8.	-.0078	-.0078	-.0080	-.0082	-.0080	-.0078	-.0078
ORB	ΔCM	1250	-4.	-.0083	-.0083	-.0085	-.0085	-.0085	-.0083	-.0083
ORB	ΔCM	1250	0.	-.0094	-.0091	-.0088	-.0085	-.0088	-.0091	-.0094
ORB	ΔCM	1250	4.	-.0104	-.0099	-.0095	-.0090	-.0095	-.0099	-.0104
ET	ΔCM	1250	-8.	.0	.0	.0	.0	.0	.0	.0
ET	ΔCM	1250	-4.	.0	.0	.0	.0	.0	.0	.0
ET	ΔCM	1250	0.	.0	.0	.0	.0	.0	.0	.0
ET	ΔCM	1250	4.	.0	.0	.0	.0	.0	.0	.0
R-SRB	ΔCM	1250	-8.	-.0001	-.0001	.0000	.0000	-.0002	-.0003	-.0003
R-SRB	ΔCM	1250	-4.	.0001	.0001	.0000	.0000	.0000	.0000	.0000
R-SRB	ΔCM	1250	0.	.0000	.0000	-.0001	-.0001	-.0001	-.0003	-.0003
R-SRB	ΔCM	1250	4.	.0001	.0001	.0001	.0001	.0001	.0000	.0000
L-SRB	ΔCM	1250	-8.	-.0003	-.0003	-.0002	.0000	.0000	-.0001	-.0001
L-SRB	ΔCM	1250	-4.	.0000	.0000	.0000	.0000	.0000	.0001	.0001
L-SRB	ΔCM	1250	0.	-.0003	-.0003	-.0001	-.0001	-.0001	.0000	.0000
L-SRB	ΔCM	1250	4.	.0000	.0000	.0001	.0001	.0001	.0001	.0001

Table 8-13

BASE AXIAL FORCE COEFFICIENT

$M_\infty = 1.40$ $\delta_{e_{IO}} = 10/-2$

% SSME POWER = 97%

ELEMENT			α	β -6	-4	-2	0	2	4	6
TOTAL	ΔCA	1400	-8.	.1082	.1082	.1042	.1006	.1042	.1082	.1082
TOTAL	ΔCA	1400	-4.	.0999	.0999	.0978	.0963	.0978	.0999	.0999
TOTAL	ΔCA	1400	0.	.0993	.0993	.0962	.0932	.0962	.0993	.0993
TOTAL	ΔCA	1400	4.	.0969	.0961	.0939	.0919	.0939	.0961	.0969
ORB	ΔCA	1400	-8.	.0295	.0295	.0287	.0285	.0289	.0295	.0295
ORB	ΔCA	1400	-4.	.0297	.0297	.0292	.0292	.0292	.0297	.0297
ORB	ΔCA	1400	0.	.0309	.0309	.0303	.0297	.0303	.0309	.0309
ORB	ΔCA	1400	4.	.0314	.0306	.0303	.0301	.0303	.0306	.0314
ET	ΔCA	1400	-8.	.0602	.0602	.0583	.0563	.0583	.0602	.0602
ET	ΔCA	1400	-4.	.0525	.0525	.0525	.0525	.0525	.0525	.0525
ET	ΔCA	1400	0.	.0505	.0505	.0500	.0495	.0500	.0505	.0505
ET	ΔCA	1400	4.	.0482	.0482	.0477	.0472	.0477	.0482	.0482
R-SRB	ΔCA	1400	-8.	.0095	.0095	.0086	.0079	.0084	.0090	.0090
R-SRB	ΔCA	1400	-4.	.0091	.0091	.0083	.0073	.0078	.0086	.0086
R-SRB	ΔCA	1400	0.	.0094	.0094	.0082	.0070	.0077	.0085	.0085
R-SRB	ΔCA	1400	4.	.0090	.0090	.0081	.0073	.0078	.0083	.0083
L-SRB	ΔCA	1400	-8.	.0090	.0090	.0084	.0079	.0086	.0095	.0095
L-SRB	ΔCA	1400	-4.	.0086	.0086	.0078	.0073	.0083	.0091	.0091
L-SRB	ΔCA	1400	0.	.0085	.0085	.0077	.0070	.0082	.0094	.0094
L-SRB	ΔCA	1400	4.	.0083	.0083	.0078	.0073	.0081	.0090	.0090

ORIGINAL PAGE IS
OF POOR QUALITY

Table 8-14

BASE NORMAL FORCE COEFFICIENT $M_\infty = 1.40$ $\delta_{e_{IO}} = 10/-2$

% SSME POWER = 97%

ELEMENT			α	β -6	-4	-2	0	2	4	6
TOTAL	ΔCN	1400	-8.	.0171	.0171	.0169	.0168	.0169	.0171	.0171
TOTAL	ΔCN	1400	-4.	.0168	.0168	.0167	.0167	.0167	.0168	.0168
TOTAL	ΔCN	1400	0.	.0185	.0185	.0179	.0174	.0179	.0185	.0185
TOTAL	ΔCN	1400	4.	.0187	.0187	.0180	.0173	.0180	.0187	.0187
ORB	ΔCN	1400	-8.	.0169	.0169	.0168	.0168	.0168	.0169	.0169
ORB	ΔCN	1400	-4.	.0172	.0172	.0170	.0169	.0170	.0172	.0172
ORB	ΔCN	1400	0.	.0184	.0184	.0179	.0176	.0179	.0184	.0184
ORB	ΔCN	1400	4.	.0192	.0192	.0187	.0181	.0187	.0192	.0192
ET	ΔCN	1400	-8.	.0	.0	.0	.0	.0	.0	.0
ET	ΔCN	1400	-4.	.0	.0	.0	.0	.0	.0	.0
ET	ΔCN	1400	0.	.0	.0	.0	.0	.0	.0	.0
ET	ΔCN	1400	4.	.0	.0	.0	.0	.0	.0	.0
R-SRB	ΔCN	1400	-8.	.0000	.0000	.0000	.0000	.0001	.0002	.0002
R-SRB	ΔCN	1400	-4.	-.0004	-.0004	-.0002	-.0001	-.0001	.0000	.0000
R-SRB	ΔCN	1400	0.	-.0001	-.0001	-.0001	-.0001	.0001	.0002	.0002
R-SRB	ΔCN	1400	4.	-.0003	-.0003	-.0004	-.0004	-.0003	-.0002	-.0002
L-SRB	ΔCN	1400	-8.	.0002	.0002	.0001	.0000	.0000	.0000	.0000
L-SRB	ΔCN	1400	-4.	.0000	.0000	-.0001	-.0001	-.0002	-.0004	-.0004
L-SRB	ΔCN	1400	0.	.0002	.0002	.0001	-.0001	-.0001	-.0001	-.0001
L-SRB	ΔCN	1400	4.	-.0002	-.0002	-.0003	-.0004	-.0004	-.0003	-.0003

Table 8-15

BASE PITCHING MOMENT COEFFICIENT

$M_\infty = 1.40$ $\delta_{e_{IO}} = 10/-2$

% SSME POWER = 97%

ELEMENT			α	β -6	-4	-2	0	2	4	6
TOTAL	ΔCM	1400	-8.	-.0063	-.0063	-.0064	-.0065	-.0064	-.0063	-.0063
TOTAL	ΔCM	1400	-4.	-.0060	-.0060	-.0062	-.0062	-.0062	-.0060	-.0060
TOTAL	ΔCM	1400	0.	-.0074	-.0074	-.0071	-.0068	-.0071	-.0074	-.0074
TOTAL	ΔCM	1400	4.	-.0076	-.0076	-.0070	-.0064	-.0070	-.0076	-.0076
ORB	ΔCM	1400	-8.	-.0060	-.0060	-.0063	-.0065	-.0063	-.0060	-.0060
ORB	ΔCM	1400	-4.	-.0064	-.0064	-.0066	-.0066	-.0066	-.0064	-.0064
ORB	ΔCM	1400	0.	-.0074	-.0074	-.0073	-.0070	-.0073	-.0074	-.0074
ORB	ΔCM	1400	4.	-.0081	-.0081	-.0077	-.0074	-.0077	-.0081	-.0081
ET	ΔCM	1400	-8.	.0	.0	.0	.0	.0	.0	.0
ET	ΔCM	1400	-4.	.0	.0	.0	.0	.0	.0	.0
ET	ΔCM	1400	0.	.0	.0	.0	.0	.0	.0	.0
ET	ΔCM	1400	4.	.0	.0	.0	.0	.0	.0	.0
R-SRB	ΔCM	1400	-8.	.0000	.0000	.0000	.0000	-.0001	-.0003	-.0003
R-SRB	ΔCM	1400	-4.	.0004	.0004	.0003	.0002	.0001	.0000	.0000
R-SRB	ΔCM	1400	0.	.0002	.0002	.0001	.0001	.0001	-.0002	-.0002
R-SRB	ΔCM	1400	4.	.0003	.0003	.0004	.0005	.0003	.0002	.0002
L-SRB	ΔCM	1400	-8.	-.0003	-.0003	-.0001	.0000	.0000	.0000	.0000
L-SRB	ΔCM	1400	-4.	.0000	.0000	.0001	.0002	.0003	.0004	.0004
L-SRB	ΔCM	1400	0.	-.0002	-.0002	.0001	.0001	.0001	.0002	.0002
L-SRB	ΔCM	1400	4.	.0002	.0002	.0003	.0005	.0004	.0003	.0003

NORTHROP SERVICES, INC.

Table 8-16

BASE COEFFICIENT PARTIALS

	$\partial C_{x_i}/\partial \delta_{EI}$			$[\partial C_{x_i}/\partial \%$ SSME POWER$] \times 10$	
MACH	SSLV	ORBITER	ET	SSLV	ORBITER
CA 800	.0025	-.0003	.0028	.0007	.0007
CA 1050	.0040	.0002	.0038	.0010	.0010
CA 1100	.0018	.0003	.0015	.0008	.0008
CA 1250	.0000	.0001	-.0001	.0010	.0010
CA 1400	.0000	.0000	.0000	-.0006	-.0006
CN 800	.0000	.0000	.0000	.0002	.0002
CN 1050	.0001	.0001	.0000	.0005	.0005
CN 1100	.0001	.0001	.0000	.0004	.0004
CN 1250	.0001	.0001	.0000	.0004	.0004
CN 1400	.0001	.0001	.0000	-.0003	-.0003
CM 800	.0000	.0000	.0000	-.0001	-.0001
CM 1050	-.0001	-.0001	.0000	-.0002	-.0002
CM 1100	-.0001	-.0001	.0000	-.0002	-.0002
CM 1250	-.0001	-.0001	.0000	-.0002	-.0002
CM 1400	-.0001	-.0001	.0000	.0001	.0001

ORIGINAL PAGE IS
OF POOR QUALITY

Table 8-17

BASE AXIAL FORCE (LBS)

ALTITUDE (ft)	TOTAL	NOMINAL % SSME POWER LEVEL	ALTITUDE (ft)	TOTAL	NOMINAL % SSME POWER LEVEL
0	0	109	52500	46240	109
4000	41295	109	55000	33015	
6000	112146	109	57500	27690	
8000	148363	109	60000	19389	
10000	162595	107	62500	12579	
12000	178724	101	65000	7039	
14000	193983	95	67500	2504	
16000	209734	88.4	70000	-2022	
18000	226100		72500	-5026	
19000	240776		75000	-7416	
20000	257649		77500	-9434	
21000	309484		80000	-10837	
22000	341482		85000	-12161	
23000	354185		90000	-12341	
24000	357716		95000	-12191	
25000	338036		100000	-11700	
26000	294479		110000	-10812	
28000	256747		120000	-9258	
30000	230650	88.4	130000	-7641	
34000	193188	93	140000	-7074	
38000	157365	105	145000	-6554	
42000	107143	109	160000	-6334	109
44000	91278				
46000	78961				
48000	67757				
50000	56630	109			

ORIGINAL PAGE IS
OF POOR QUALITY

Table 8-18

BASE NORMAL FORCE (LBS)

ALTITUDE (ft)	TOTAL	NOMINAL % SSME POWER LEVEL	ALTITUDE (ft)	TOTAL	NOMINAL % SSME POWER LEVEL
0	0	109	47500	15315	109
5000	18500	109	50000	12685	
10000	24966	107	52500	10322	
12000	26867	101	55000	8303	
14000	28381	95	57500	6785	
16000	30163	88.4	60000	5476	
18000	32278		62500	4500	
19000	33678		65000	3900	
20000	36009		67500	2700	
21000	41054		70000	2090	
22000	48096		75000	1175	
23000	50853		80000	391	
24000	51688		85000	-193	
25000	50621		90000	-565	
26000	45343		95000	-791	
28000	40842		100000	-1023	
30000	39239	88.4	110000	-1221	
34000	35678	93	120000	-1380	
38000	28850	105	130000	-1384	
40000	25704	109	140000	-1451	
42500	21982	109	150000	-1500	
450000	18546	109	160000	-1400	109

Table 8-19

BASE PITCHING MOMENT

ALTITUDE (ft)	PITCHING MOMENT (ft-lbs)	NOMINAL % SSME POWER LEVEL	ALTITUDE (ft)	PITCHING MOMENT (ft-lbs)	NOMINAL % SSME POWER LEVEL
0	0	109	47500	-995473	109
5000	-1220000	109	50000	-828630	
10000	-1296826	107	52500	-684740	
12000	-1374159	101	55000	-563750	
14000	-1441528	95	57500	-462600	
16000	-1484908	88.4	60000	-385320	
18000	-1535100		62500	-320000	
19000	-1589046		65000	-250000	
20000	-1701877		67500	-200000	
21000	-1937440		70000	-159200	
22000	-2206003		75000	-38110	
23000	-2218121		80000	-39080	
24000	-2187319		85000	-4825	
25000	-2101904		90000	14130	
26000	-1942585		95000	41395	
28000	-1785366		100000	55800	
30000	-1713072	88.4	110000	72303	
34000	-1515453	93	120000	82300	
38000	-1202968	105	130000	84635	
40000	-1750000	109	140000	88920	
42500	-1458720	109	150000	95000	
45000	-1232990	109	160000	95000	109

Table 8-20

BASE AXIAL FORCE PARTIALS

ALTITUDE (ft)	$\partial AF/\partial \alpha$ (LB/DEG)	$\partial AF/\partial \delta_{EI}$ (LB/DEG)	$\partial AF/\partial$% SSME POWER (LB/%)
10000	-1331.0	2623.0	73.0
12000	-1361.0	2959.0	71.0
14000	-1536.0	3255.0	62.0
16000	-1823.0	3665.0	43.0
18000	-2454.0	5653.0	26.0
19000	-2667.0	6400.0	23.0
20000	-2716.0	7761.0	31.0
21000	-2021.0	8842.0	107.0
22000	-705.0	9138.0	138.0
23000	1040.0	9098.0	159.0
24000	2461.0	8533.0	167.0
25000	3148.0	6959.0	169.0
26000	2911.0	4350.0	167.0
28000	1627.0	1864.0	142.0
30000	514.0	171.0	158.0
34000	-583.0	87.0	96.0
38000	-1014.0	21.0	-112.0

Table 8-21

NORMAL FORCE PARTIALS

ALTITUDE (ft)	$\partial NF/\partial \alpha$ (LB/DEG)	$\partial NF/\partial \delta_{EI}$ (LB/DEG)	$\partial NF/\partial$% SSME POWER (LB/%)
10000	-270.0	0.0	20.0
12000	-307.0	0.0	18.0
14000	-318.0	13.0	13.0
16000	-318.0	35.0	9.6
18000	-337.0	176.0	15.0
19000	-381.0	213.0	18.0
20000	-403.0	264.0	39.0
21000	-410.0	276.0	83.0
22000	-352.0	280.0	90.0
23000	0.0	244.0	91.0
24000	328.0	213.0	87.0
25000	845.0	166.0	83.0
26000	886.0	167.0	80.0
28000	551.0	169.0	68.0
30000	282.0	171.0	73.0
34000	139.0	174.0	45.0
38000	131.0	175.0	-47.0

Table 8-22

PITCHING MOMENT PARTIALS

ALTITUDE (ft)	$\partial PM/\partial \alpha$ (FT.LB./DEG.)	$\partial PM/\partial \delta_{EI}$ (FT. LB/DEG)	$\partial PM/\partial$% SSME POWER (FT.LB./%)
10000	14019.0	0.0	-1070.0
12000	15742.0	0.0	-943.0
14000	16238.0	-1398.0	-683.0
16000	15725.0	-3763.0	-496.0
18000	16013.0	-18920.0	-755.0
19000	18021.0	-22898.0	-898.0
20000	19062.0	-28380.0	-1916.0
21000	19349.0	-29670.0	-4051.0
22000	16082.0	-30100.0	-4354.0
23000	0.0	-26230.0	-4246.0
24000	-13892.0	-22898.0	-3928.0
25000	-44056.0	-17845.0	-3587.0
26000	-37908.0	-17953.0	-4068.0
28000	-24108.0	-18167.0	-3713.0
30000	-12308.0	-18382.0	-4034.0
34000	-5947.0	-18705.0	-2322.0
38000	-5646.0	-18813.0	1667.0

Table 8-23

IA-119
BASE COEFFICIENT TOLERANCES

MACH NO.	SSLV[1]	ORB	ET	SRB(1)
		$\pm\Delta C_A$		
.6	.0104	.0031	.0065	.0017
.8	.0107	.0031	.0072	.0015
.9	.0156	.0046	.0107	.0021
.95	.0359	.0088	.0270	.0039
1.05	.0239	.0080	.0161	.0032
1.10	.0169	.0057	.0115	.0022
1.15	.0133	.0046	.0091	.0017
1.25	.0086	.0033	.0060	.0010
1.40	.0062	.0024	.0045	.0006
		$\pm\Delta C_N$*		
.6	.0029[1]	.0019[3]	.0010	.0006
.8	.0028	.0019	.0009	.0006
.9	.0037	.0028	.0013	.0006
.95	.0065	.0053	.0025	.0006
1.05	.0058	.0048	.0022	.0005
1.10	.0047	.0034	.0016	.0008
1.15	.0037	.0028	.0013	.0006
1.25	.0032	.0020	.0009	.0008
1.40	.0027	.0014	.0007	.0008
		$\pm\Delta C_Y$		
.6	.0027[2]	.0025	.0005	.0006
.8	.0022	.0020	.0005	.0005
.9	.0017	.0015	.0006	.0004
.95	.0017	.0015	.0007	.0004
1.05	.0018	.0015	.0009	.0004
1.10	.0019	.0015	.0010	.0004
1.15	.0017	.0015	.0007	.0004
1.25	.0017	.0015	.0006	.0004
1.40	.0016	.0014	.0005	.0004

1. $\Delta C_{A_{SSLV}} = \sqrt{(\Delta C_{A_o})^2 + (\Delta C_{A_{ET}} + 2\Delta C_{A_{SRB}})^2}$
2. $\Delta C_{y_{SSLV}} = \sqrt{(\Delta C_{y_o})^2 + (\Delta C_{y_{ET}})^2 + (\Delta C_{A_{SRB}})^2 + (\Delta C_{A_{SRB}})^2}$
3. $\Delta C_{N_o} = 0.6\Delta C_{A_o}$

Table 8-24

BASE MOMENT INCREMENTS

The general equations for the element moment increments are

$$\Delta C_M = \Delta C_N \left(\frac{X_N}{L}\right) + \Delta C_A \left(\frac{Z_A}{L}\right)$$

$$\Delta C_{YN} = \Delta C_Y \left(\frac{X_{YN}}{L}\right) + \Delta C_A \left(\frac{Y_L}{L}\right)$$

$$\Delta C_\ell = \Delta C_Y \left(\frac{Z_L}{L}\right) - \Delta C_N \left(\frac{Y_L}{L}\right)$$

The SSLV moment increment is determined by the following equations

$$\Delta C_{M_{SSLV}} = \sqrt{(\Delta C_{M_O})^2 + (\Delta C_{M_{ET}} + \Delta C_{M_{RSRB}} + \Delta C_{M_{LSRB}})^2}$$

$$\Delta C_{\ell_{YN_{SSLV}}} = \sqrt{(\Delta C_{\ell_{YN_O}})^2 + (\Delta C_{\ell_{YN_{ET}}})^2 + (\Delta C_{\ell_{YN_{RSRB}}})^2 + (\Delta C_{\ell_{YN_{LSRB}}})^2}$$

	ORBITER	ET	SRB RIGHT LEFT
$\frac{X_N}{L}$ =	-.99	-.87	-1.18
$\frac{Z_A}{L}$ =	.31	0.0	0.0
$\frac{X_{YN}}{L}$ =	-1.08	-0.87	1.18
$\frac{Y_L}{L}$ =	0.0	0.0	±0.195
$\frac{Z_L}{L}$ =	.27	0.03	0.0

NOTE; L = 1290 INCHES

Section IX

FOREBODY PLUME INDUCED MATH MODEL

The nominal forebody plume induced aerodynamic characteristics were small except on the Orbiter fuselage, inboard elevon and the vertical tail. Math models have thus been developed for the SSLV, Orbiter, the inboard elevon hinge moment and the vertical tail. The SSLV and Orbiter normal force, pitching moment and inboard elevon hinge moment has the following type of math model.

$$\begin{matrix} C_N = \\ C_M = \\ C_{H_{e_I}} = \end{matrix} \quad C_{N\,\alpha-\beta_{MATRIX}} + \left[\partial C_N/\partial\delta_{EI}\,{}^{>}_{<}\,{}_{\alpha-\beta\ MATRIX}\right] \times \Delta\delta_{EI} + \left[\partial C_N/\partial\delta_{EO}\,{}^{>}_{<}\right] \times \Delta\delta_{EO}\,{}_{\alpha-\beta\ MATRIX}$$

where C_N is a 4x7 matrix for $\alpha = +4,0,-4,-8$
$\beta = -6,-4,-2,0,2,4,6$

elevon deflection corresponds to close schedule 6 (Table 9-1, -6,-11)

$\partial C_N/\partial\delta_{EI}\,{}^{>}_{<}$ is a 4x7 matrix for $\alpha = +4,0,-4,-8$
$\beta = -6,-4,-2,0,2,4,6$

> gradient for inboard elevon deflections > nominal (Table 9-2, -7,-12)
< gradient for inboard elevon deflections < nominal (Table 9-3, -8,-13)

$\partial C_N/\partial\delta_{EO}\,{}^{>}_{<}$ is a 4x7 matrix for $\alpha = +4,0,-4,-8$
$\beta = -6,-4,-2,0,2,4,6$

> gradient for outboard elevon deflections > nominal (Table 9-4, -9,-14)
< gradient for outboard elevon deflections < nominal (Table 9-5, -10,-15)

$\Delta\delta_{EI}$ - change in inboard elevon deflection from nominal value specified in Table 9-1 to inboard elevon deflection of interest.

$\Delta\delta_{EO}$ - change in outboard elevon deflection from nominal value specified in Table 9-1 to outboard elevon deflection of interest.

The orbiter normal force and pitching moment math models were derived from the results of the pressure integration of the power-delta pressure coefficients. The orbiter data used to derive the math model is presented in the tabulated data in the Appendix - Section 9 (Forebody Pressure Integration) of the printout sheet (see Section VII). The SSLV and Orbiter math models are identical since only the orbiter plume effects are included in the math model.

The hinge moment math model was derived from the left wing gauge data, although the data is presented for the right wing. A comparison of the left wing gauge data and the right wing pressure integration data was made to evaluate the best data to use and the gauge data had the most consistent trend with changes in attitude and configuration. The left wing gauge data used to develop the hinge moment math model is presented in the tabulated data in the appendix in Section 8 (GAUGE DATA) of the printout sheet (see Section VII).

The vertical tail shear force, bending moment and torsion moment coefficient have been formulated into the following math model

$$C_v = [C_{v_{\alpha-\beta_{Matrix}}}]$$

where

$[C_{v_{\alpha-\beta_{Matrix}}}]$ is a 4 x 7 matrix for $\alpha = +4,0,-4,-8$
$\beta = -6,-4,-2,0,2,4,6$

for elevon deflections noted on the table.

C_{Yv}, vertical tail power delta shear force coefficient is presented in Table 9-16

C_{Bv}, vertical tail power delta bending moment coefficient is presented in Table 9-17

C_{Tv}, vertical tail power delta torsion moment coefficient is presented in Table 9-18

The vertical tail shear force math model includes only the α-β matrix at the nominal elevon deflection. No influence of elevon deflections are included. The vertical tail power induced shear force, bending moment, and torsion moment coefficients are presented in Tables 9-16 through 9-18.

The vertical tail math model was derived from the integration of the vertical tail pressure data presented in the tabulated data in the appendix in Section 9 (Forebody Pressure Integration) of the printout sheet (see Section VII).

FOREBODY COEFFICIENT TOLERANCES

Forebody tolerances have been developed for all forebody elements and components. As mentioned above, only the Orbiter, inboard elevon hinge moment and the vertical tail had measurable plume induced aerodynamic changes that could be effectively modeled. The other elements and components have zero nominal math model plume induced aerodynamic characteristics. Tolerances have been developed for all element and components, however, to account for all possible variations in plume induced aerodynamic characteristics. The forebody element and component force coefficient tolerances are presented as tabled values that are the $\pm 3\sigma$ variation of the nominal coefficient. The $\pm 3\sigma$ variation covers the potential variation of the coefficient from the math model results to expected flight data values.

The SSLV and element force coefficient tolerances are presented in Table 9-19. The moment increment equations are presented in Table 9-20. The component force coefficient tolerances and moment equations are presented in Tables 9-21 and 9-22. The moment tolerances require using equations that include the force coefficient tolerances along with the nominal aerodynamic center in conjunction with the nominal forebody power delta (when $\neq 0$) times the aerodynamic center tolerance.

The forebody tolerances include contributions due to 1. test instrumentation uncertainty, 2. simulation parameter uncertainty, 3. Reynolds number characteristics, 4. Model-tunnel testing uncertainties, 5. Pressure integration uncertainties and 6. Math model uncertainties. Each tolerance contribution is assumed independent and therefore the contributions are combined using the RSS technique. The tolerances thus cover the uncertainty from the math model to flight data and are to a $\pm 3\sigma$ level with a Gussian distribution.

The forebody coefficients are determined using power delta's. Thus the instrumentation accuracy includes two independent measurements that are combined

by the RSS techniques. The instrumentation accuracy for a single measurement is estimated to be 3 percent. Thus two measurements would be 4.3 percent. The general uncertainty in the nominal forebody force coefficient due to instrumentation uncertainty was estimated at 50 percent of the calculated nominal forebody coefficient. The similarity parameter uncertainty was estimated to be 30 percent of the nominal, Reynolds number and scale effect was estimated to be 100 percent of the nominal, model uncertainties were estimated to be 30 percent of the nominal, integration uncertainties at 30 percent of the nominal and math model uncertainties were estimated at 20 percent of the nominal value. The net RSS tolerance value for the forebody coefficients are large compared to the nominal math model values. This is because the nominal math model force coefficients are small. If the math model is not used the tolerance would be approximately double the values presented and it was determined that forebody tolerances approaching double the values presented in Table 9-19 would be excessive.

Portions of the forebody have zero nominal plume induced aerodynamic force coefficients in the math model although specific computed values have been determined and are listed in the tabulated data in the appendix (see Section VII). The tolerance analysis discussed above considered the nominal values calculated although the math model nominal force coefficients are zero.

The analysis of the forebody plume induced aerodynamic characteristics and tolerances was a difficult task. The majority of the plume induced loads occurred on the aft portion of the orbiter, where there is little pressure instrumentation, and on the inboard elevon. The pressure data on the inboard elevon was generally sufficient to determine loads, but was not sufficiently accurate to determine hinge moments. The gauge data was more consistent, although the gauge hinge moment data does not agree with the hinge moment from more recent power off tests (refs. 12 and 13). One possible reason for this disagreement is due to the IA119 model having an old wing configuration. Attempts have been made to account for those problems in the tolerance values presented. Difficulties were also experienced with the vertical tail pressure data in that certain pressure data had to be discarded.

Table 9-1a. SSLV AND ORBITER POWER DELTA - NORMAL FORCE COEFFICIENT - FOREBODY

MACH	$\delta_{e_{IO}}$	α	β -6	-4	-2	0	+2	+4	+6
.6	10/9	4	+.0060	+.0059	+.0058	+.0057	+.0058	+.0059	+.0060
		0	+.0062	+.0062	+.0063	+.0064	+.0063	+.0062	+.0062
		-4	+.0069	+.0069	+.0070	+.0070	+.0070	+.0069	+.0069
		-8	+.0066	+.0067	+.0070	+.0073	+.0070	+.0067	+.0066
.8	10/9	4	+.0046	+.0045	+.0044	+.0043	+.0044	+.0045	+.0046
		0	+.0045	+.0044	+.0043	+.0041	+.0043	+.0044	+.0045
		-4	+.0042	+.0045	+.0047	+.0050	+.0047	+.0045	+.0042
		-8	+.0037	+.0043	+.0049	+.0055	+.0049	+.0043	+.0037
.90	10/9	4	+.0039	+.0039	+.0039	+.0039	+.0039	+.0039	+.0039
		0	+.0020	+.0016	+.0013	+.0010	+.0013	+.0016	+.0020
		-4	+.0006	+.0012	+.0018	+.0023	+.0018	+.0012	+.0006
		-8	+.0021	+.0023	.0025	+.0026	+.0025	+.0023	+.0021
.95	10/9	4	-.0007	-.0026	-.0045	-.0065	-.0045	-.0026	-.0007
		0	-.0034	-.0041	-.0048	-.0055	-.0048	-.0041	-.0034
		-4	-.0050	-.0046	-.0041	-.0036	-.0041	-.0046	-.0050
		-8	-.0024	-.0030	-.0036	-.0041	-.0036	-.0030	-.0024
1.05	10/9	4	+.0037	+.0026	+.0014	+.0003	+.0014	+.0026	+.0037
		0	+.0039	+.0029	+.0020	+.0010	+.0020	+.0029	+.0039
		-4	+.0052	+.0043	+.0034	+.0024	+.0034	+.0043	+.0052
		-8	+.0063	+.0054	+.0045	+.0036	+.0045	+.0054	+.0063

Table 9-1b. SSLV AND ORBITER POWER DELTA - NORMAL FORCE COEFFICIENT - FOREBODY

MACH	$\delta_{e_{IO}}$	α	β -6	-4	-2	0	+2	+4	+6
1.10	10/9	4	+.0063	+.0061	+.0058	+.0056	+.0058	+.0061	+.0063
		0	+.0085	+.0080	+.0070	+.0053	+.0070	+.0080	+.0085
		-4	+.0090	+.0085	+.0080	+.0075	+.0080	+.0085	+.0090
		-8	+.0096	+.0093	+.0090	+.0088	+.0090	+.0093	+.0096
1.15	10/5	4	+.0080	+.0077	+.0057	+.0053	+.0057	+.0077	+.0080
		0	+.0079	+.0075	+.0057	+.0052	+.0057	+.0075	+.0079
		-4	+.0080	+.0077	+.0072	+.0070	+.0072	+.0077	+.0080
		-8	+.0095	+.0092	+.0081	+.0075	+.0081	+.0092	+.0095
1.25	10/-2	4	+.0043	+.0048	+.0053	+.0058	+.0053	+.0048	+.0043
		0	+.0055	+.0059	+.0063	+.0067	+.0063	+.0059	+.0055
		-4	+.0070	+.0070	+.0071	+.0071	+.0071	+.0070	+.0070
		-8	+.0093	+.0096	+.0099	+.0102	+.0099	+.0096	+.0093
1.40	10/-2	4	+.0060	+.0056	+.0051	+.0047	+.0051	+.0056	0.0060
		0	+.0060	+.0056	+.0051	+.0047	+.0051	+.0056	+.0060
		-4	+.0068	+.0070	+.0073	+.0075	+.0073	+.0070	+.0068
		-8	+.0096	+.0101	+.0105	+.0108	+.0105	+.0101	+.0096

Table 9-2a. SSLV AND ORBITER POWER DELTA - NORMAL FORCE COEFFICIENT - FOREBODY INBOARD ELEVON GRADIENT - δ_{EI} GREATER THAN NOMINAL

MACH	α	β = -6	-4	-2	0	+2	+4	+6
.6	4	+.0005	+.0004	+.0004	+.0003	+.0004	+.0004	+.0005
	0	+.0005	+.0005	+.0004	+.0003	+.0004	+.0005	+.0005
	-4	+.0005	+.0005	+.0004	+.0003	+.0004	+.0005	+.0005
	-8	+.0005	+.0005	+.0003	+.0002	+.0003	+.0005	+.0005
.8	4	+.0009	+.0007	+.0005	+.0003	+.0005	+.0007	+.0009
	0	+.0009	+.0008	+.0008	+.0007	+.0008	+.0008	+.0009
	-4	+.0011	+.0008	+.0005	+.0002	+.0005	+.0008	+.0011
	-8	+.0013	+.0007	+.0001	-.0004	+.0001	+.0007	+.0013
.90	4	+.0004	+.0003	+.0001	-.0001	+.0001	+.0003	+.0004
	0	+.0008	+.0006	+.0005	+.0004	+.0005	+.0006	+.0008
	-4	+.0007	+.0007	+.0008	+.0008	+.0008	+.0007	+.0007
	-8	-.0004	+.0006	+.0004	+.0008	+.0004	+.0000	-.0004
.95	4	+.0003	+.0002	+.0001	+.0000	+.0001	+.0002	+.0003
	0	-.0004	-.0006	-.0008	-.0010	-.0008	-.0006	-.0004
	-4	+.0001	+.0001	+.0000	+.0000	+.0000	+.0001	+.0001
	-8	+.0001	+.0001	+.0001	+.0001	+.0001	+.0001	+.0001
1.05	4	-.0001	+.0000	+.0002	+.0003	+.0002	+.0000	-.0001
	0	+.0001	+.0003	+.0004	+.0006	+.0004	+.0003	+.0001
	-4	-.0013	-.0008	-.0002	+.0004	-.0002	-.0008	-.0013
	-8	-.0008	-.0005	-.0002	+.0002	-.0002	-.0005	-.0008

ORIGINAL PAGE IS
OF POOR QUALITY

Table 9-2b. SSLV AND ORBITER POWER DELTA - NORMAL FORCE COEFFICIENT - FOREBODY
INBOARD ELEVON GRADIENT - δ_{EI} GREATER THAN NOMINAL

MACH	α \ β	-6	-4	-2	0	+2	+4	+6
1.10	4	+.0006	+.0002	-.0003	-.0007	-.0003	+.0002	+.0006
	0	-.0001	-.0005	-.0009	-.0013	-.0009	-.0005	-.0001
	-4	-.0012	-.0010	-.0008	-.0007	-.0008	-.0010	-.0012
	-8	-.0014	-.0008	-.0002	+.0004	-.0002	-.0008	-.0014
1.15	4	-.0011	-.0008	-.0005	-.0002	-.0005	-.0008	-.0011
	0	+.0000	+.0000	+.0000	+.0001	+.0000	+.0000	+.0000
	-4	-.0010	-.0007	-.0004	-.0001	-.0004	-.0007	-.0010
	-8	+.0004	+.0002	-.0002	-.0006	-.0002	+.0002	+.0004
1.25	4	+.0002	-.0001	-.0004	-.0007	-.0004	-.0001	+.0002
	0	-.0001	-.0002	-.0003	-.0004	-.0003	-.0002	-.0001
	-4	-.0003	-.0003	-.0002	-.0002	-.0002	-.0003	-.0003
	-8	-.0002	-.0002	-.0003	-.0003	-.0003	-.0002	-.0002
1.40	4	-.0006	-.0005	-.0004	-.0003	-.0004	-.0005	-.0006
	0	-.0003	-.0003	-.0003	-.0003	-.0003	-.0003	-.0003
	-4	-.0003	-.0002	-.0001	-.0001	-.0001	-.0002	-.0003
	-8	+.0000	+.0000	-.0002	-.0003	-.0002	+.0000	+.0000

Table 9-3a. SSLV AND ORBITER POWER DELTA - NORMAL FORCE COEFFICIENT - FOREBODY INBOARD ELEVON GRADIENT - δ_{E_I} LESS THAN NOMINAL

MACH	α	β = -6	-4	-2	0	+2	+4	+6
.6	4	+.0004	+.0003	+.0003	+.0003	+.0003	+.0003	+.0004
	0	+.0001	+.0001	+.0002	+.0003	+.0002	+.0001	+.0001
	-4	+.0005	+.0005	+.0005	+.0004	+.0005	+.0005	+.0005
	-8	+.0003	+.0004	+.0003	+.0002	+.0003	+.0004	+.0003
.8	4	+.0000	+.0000	+.0001	+.0002	+.0001	+.0000	+.0000
	0	-.0005	-.0003	-.0001	+.0000	-.0001	-.0003	-.0005
	-4	-.0007	-.0003	+.0001	+.0005	+.0001	-.0003	-.0007
	-8	-.0003	-.0001	+.0002	+.0005	+.0002	-.0001	-.0003
.90	4	+.0018	+.0012	+.0005	-.0002	+.0005	+.0012	+.0018
	0	+.0011	+.0007	+.0004	+.0001	+.0004	+.0007	+.0011
	-4	-.0004	+.0004	+.0012	+.0020	+.0012	+.0004	-.0004
	-8	+.0022	+.0020	+.0018	+.0016	+.0018	+.0020	+.0022
.95	4	+.0029	+.0012	-.0005	-.0022	-.0005	+.0012	+.0029
	0	-.0005	-.0011	-.0015	-.0020	-.0015	-.0011	-.0005
	-4	-.0014	-.0022	-.0030	-.0039	-.0030	-.0022	-.0014
	-8	-.0022	-.0029	-.0036	-.0043	-.0036	-.0029	-.0022
1.05	4	-.0001	-.0002	-.0003	-.0004	-.0003	-.0002	-.0001
	0	-.0010	-.0006	-.0002	+.0001	-.0002	-.0006	-.0010
	-4	-.0007	-.0005	-.0002	+.0000	-.0002	-.0005	-.0007
	-8	-.0011	-.0009	-.0007	-.0005	-.0007	-.0009	-.0011

Table 9-3b. SSLV AND ORBITER POWER DELTA - NORMAL FORCE COEFFICIENT - FOREBODY INBOARD ELEVON GRADIENT - δ_{E_I} LESS THAN NOMINAL

MACH	α	β = -6	-4	-2	0	+2	+4	+6
1.10	4	-.0011	-.0006	-.0005	-.0002	-.0005	-.0008	-.0011
	0	-.0002	+.0000	+.0003	+.0005	+.0003	+.0000	-.0002
	-4	-.0005	-.0002	+.0002	+.0005	+.0002	-.0002	-.0005
	-8	-.0006	-.0006	-.0004	-.0002	-.0004	-.0006	-.0008
1.15	4	-.0005	-.0004	-.0003	-.0003	-.0003	-.0004	-.0005
	0	-.0013	-.0011	-.0009	-.0007	-.0009	-.0011	-.0013
	-4	-.0007	-.0007	-.0007	-.0007	-.0007	-.0007	-.0007
	-8	-.0007	-.0004	+.0000	+.0003	+.0000	-.0004	-.0007
1.25	4	+.0008	+.0005	+.0001	-.0002	+.0001	+.0005	+.0008
	0	+.0001	+.0001	+.0000	+.0000	+.0000	+.0001	+.0001
	-4	+.0001	+.0000	-.0002	-.0003	-.0002	+.0000	+.0001
	-8	-.0007	-.0005	-.0002	+.0000	-.0002	-.0005	-.0007
1.40	4	+.0000	+.0000	+.0000	+.0000	+.0000	+.0000	+.0000
	0	+.0000	+.0000	+.0000	+.0000	+.0000	+.0000	+.0000
	-4	+.0000	+.0000	+.0000	+.0000	+.0000	+.0000	+.0000
	-8	+.0000	+.0000	+.0000	+.0000	+.0000	+.0000	+.0000

Table 9-4a. SSLV AND ORBITER POWER DELTA - NORMAL FORCE COEFFICIENT - FOREBODY OUTBOARD ELEVON GRADIENT - δ_{E_0} GREATER THAN NOMINAL

MACH	α	β -6	-4	-2	0	+2	+4	+6
.6	4	+.0001	+.0002	+.0003	+.0004	+.0003	+.0002	+.0001
	0	+.0005	+.0006	+.0006	+.0006	+.0006	+.0006	+.0005
	-4	+.0004	+.0004	+.0005	+.0007	+.0005	+.0004	+.0004
	-8	+.0008	+.0007	+.0005	+.0004	+.0005	+.0007	+.0008
.8	4	+.0007	+.0005	+.0003	+.0001	+.0003	+.0005	+.0007
	0	+.0010	+.0008	+.0006	+.0005	+.0006	+.0008	+.0010
	-4	+.0011	+.0008	+.0005	+.0001	+.0005	+.0008	+.0011
	-8	+.0011	+.0006	+.0001	-.0004	+.0001	+.0006	+.0011
.90	4	-.0004	-.0004	-.0004	-.0004	-.0004	-.0004	-.0004
	0	+.0014	+.0013	+.0012	+.0010	+.0012	+.0013	.0014
	-4	+.0010	+.0009	+.0008	+.0007	+.0008	+.0009	+.0010
	-8	-.0003	+.0001	+.0005	+.0009	+.0005	+.0001	-.0003
.95	4	-.0018	-.0010	-.0002	+.0006	-.0002	-.0010	-.0018
	0	-.0024	-.0019	-.0013	-.0008	-.0013	-.0019	-.0024
	-4	-.0005	-.0006	-.0008	-.0009	-.0008	-.0006	-.0005
	-8	-.0004	-.0004	-.0004	-.0004	-.0004	-.0004	-.0004
1.05	4	-.0013	-.0005	+.0008	+.0020	+.0008	-.0005	-.0013
	0	+.0004	-.0001	-.0005	-.0010	-.0005	-.0001	+.0004
	-4	-.0001	-.0005	-.0008	-.0012	-.0008	-.0005	-.0001
	-8	+.0004	+.0000	-.0004	-.0007	-.0004	+.0000	+.0004

Table 9-4b. SSLV AND ORBITER POWER DELTA - NORMAL FORCE COEFFICIENT - FOREBODY OUTBOARD ELEVON GRADIENT - δ_{E_0} GREATER THAN NOMINAL

MACH	α	β -6	-4	-2	0	+2	+4	+6
1.10	4	+.0010	+.0005	+.0000	-.0004	+.0000	+.0005	+.0010
	0	-.0002	-.0002	-.0002	-.0002	-.0002	-.0002	-.0002
	-4	-.0008	-.0006	-.0004	-.0003	-.0004	-.0006	-.0008
	-8	-.0004	-.0002	-.0001	+.0001	-.0001	-.0002	-.0004
1.15	4	-.0001	-.0001	+.0000	+.0000	+.0000	-.0001	-.0001
	0	-.0001	-.0001	-.0001	-.0001	-.0001	-.0001	-.0001
	-4	+.0001	+.0001	+.0000	-.0001	+.0000	+.0001	+.0001
	-8	+.0000	+.0000	+.0001	+.0002	+.0001	+.0000	+.0000
1.25	4	+.0003	+.0002	+.0001	+.0000	+.0001	+.0002	+.0003
	0	+.0001	+.0001	+.0000	+.0000	+.0000	+.0001	+.0001
	-4	+.0001	+.0001	+.0000	+.0000	+.0000	+.0001	+.0001
	-8	+.0000	+.0000	+.0000	+.0000	+.0000	+.0000	+.0000
1.40	4	-.0001	-.0001	+.0000	+.0001	+.0000	-.0001	-.0001
	0	-.0001	-.0001	+.0000	+.0000	+.0000	-.0001	-.0001
	-4	-.0001	-.0001	+.0000	+.0000	+.0000	-.0001	-.0001
	-8	+.0000	+.0000	+.0000	+.0000	+.0000	+.0000	+.0000

Table 9-5a. SSLV AND ORBITER POWER DELTA - NORMAL FORCE COEFFICIENT - FOREBODY OUTBOARD ELEVON GRADIENT - δ_{E_0} LESS THAN NOMINAL

MACH	α	β -6	-4	-2	0	+2	+4	+6
.6	4	+.0000	+.0000	+.0000	+.0001	+.0000	+.0000	+.0000
	0	+.0000	+.0000	+.0000	-.0001	+.0000	+.0000	+.0000
	-4	+.0001	+.0001	+.0000	-.0001	+.0000	+.0001	+.0001
	-8	+.0003	+.0001	+.0000	-.0001	+.0000	+.0001	+.0003
.8	4	-.0001	+.0000	+.0001	+.0001	+.0001	+.0000	-.0001
	0	+.0001	+.0000	-.0001	-.0001	-.0001	+.0000	+.0001
	-4	+.0000	+.0000	+.0000	+.0000	+.0000	+.0000	+.0000
	-8	+.0000	+.0000	+.0001	+.0001	+.0001	+.0000	+.0000
.90	4	+.0006	+.0008	+.0009	+.0010	+.0009	+.0008	.0006
	0	+.0005	+.0005	+.0004	+.0003	+.0004	+.0005	+.0005
	-4	+.0004	+.0010	+.0020	+.0033	+.0020	+.0010	+.0004
	-8	+.0010	+.0020	+.0030	+.0040	+.0030	+.0020	+.0010
.95	4	+.0000	-.0002	-.0004	-.0005	-.0004	-.0002	+.0000
	0	-.0004	-.0004	-.0004	-.0005	-.0004	-.0004	-.0004
	-4	+.0000	-.0002	-.0004	-.0005	-.0004	-.0002	+.0000
	-8	+.0004	+.0002	+.0001	+.0000	+.0001	+.0002	+.0004
1.05	4	+.0000	+.0000	+.0000	+.0000	+.0000	+.0000	+.0000
	0	-.0001	-.0001	-.0001	-.0001	-.0001	-.0001	-.0001
	-4	+.0000	-.0001	-.0002	-.0002	-.0002	-.0001	+.0000
	-8	+.0000	+.0000	+.0000	+.0000	+.0000	+.0000	+.0000

Table 9-5b. SSLV AND ORBITER POWER DELTA - NORMAL FORCE COEFFICIENT - FOREBODY OUTBOARD ELEVON GRADIENT - δ_{E_0} LESS THAN NOMINAL

MACH	α	β -6	-4	-2	0	+2	+4	+6
1.10	4	+.0001	+.0001	+.0001	+.0001	+.0001	+.0001	+.0001
	0	+.0000	+.0001	+.0001	+.0002	+.0001	+.0001	+.0000
	-4	+.0000	+.0001	+.0001	+.0002	+.0001	+.0001	+.0000
	-8	+.0000	+.0001	+.0001	+.0002	+.0001	+.0001	+.0000
1.15	4	+.0001	+.0001	+.0000	+.0000	+.0000	+.0001	+.0001
	0	-.0001	-.0001	+.0000	+.0000	+.0000	-.0001	-.0001
	-4	+.0001	+.0001	+.0000	+.0000	+.0000	+.0001	+.0001
	-8	+.0000	+.0000	+.0000	+.0000	+.0000	+.0000	+.0000
1.25	4	+.0001	+.0001	+.0000	-.0001	+.0000	+.0001	+.0001
	0	+.0000	+.0000	+.0001	+.0002	+.0001	+.0000	+.0000
	-4	+.0000	+.0000	+.0000	+.0000	+.0000	+.0000	+.0000
	-8	+.0004	+.0003	+.0002	+.0001	+.0002	+.0003	+.0004
1.40	4	+.0005	+.0005	+.0005	+.0005	+.0005	+.0005	+.0005
	0	+.0003	+.0003	+.0003	+.0003	+.0003	+.0003	+.0003
	-4	+.0001	+.0001	+.0001	+.0001	+.0001	+.0001	+.0001
	-8	+.0001	+.0001	+.0002	+.0002	+.0002	+.0001	+.0001

Table 9-6a. SSLV AND ORBITER POWER DELTA - PITCHING MOMENT COEFFICIENT - FOREBODY

MACH	$\delta_{e_{IO}}$	α	β: -6	-4	-2	0	+2	+4	+6
.6	10/9	4	-.0054	-.0054	-.0053	-.0052	-.0053	-.0054	-.0054
		0	-.0056	-.0057	-.0058	-.0059	-.0058	-.0057	-.0056
		-4	-.0063	-.0063	-.0064	-.0064	-.0064	-.0063	-.0063
		-8	-.0060	-.0063	-.0065	-.0068	-.0065	-.0063	-.0060
.8	10/9	4	-.0042	-.0041	-.0040	-.0039	-.0040	-.0041	-.0042
		0	-.0041	-.0040	-.0039	-.0038	-.0039	-.0040	-.0041
		-4	-.0038	-.0040	-.0043	-.0046	-.0043	-.0040	-.0038
		-8	-.0034	-.0041	-.0046	-.0051	-.0046	-.0041	-.0034
.90	10/9	4	-.0036	-.0036	-.0036	-.0036	-.0036	-.0036	-.0036
		0	-.0016	-.0014	-.0012	-.0009	-.0012	-.0014	-.0016
		-4	-.0003	-.0009	-.0016	-.0022	-.0016	-.0009	-.0003
		-8	-.0016	-.0019	-.0021	-.0025	-.0021	-.0019	-.0016
.95	10/9	4	+.0011	+.0028	+.0045	+.0063	+.0045	+.0028	+.0011
		0	+.0036	+.0042	+.0048	+.0055	+.0048	+.0042	+.0036
		-4	+.0052	+.0048	+.0044	+.0039	+.0044	+.0048	+.0052
		-8	+.0027	+.0033	+.0039	+.0044	+.0039	+.0033	+.0027
1.05	10/9	4	-.0035	-.0024	-.0013	-.0002	-.0013	-.0024	-.0035
		0	-.0037	-.0027	-.0018	-.0009	-.0018	-.0027	-.0037
		-4	-.0049	-.0041	-.0032	-.0023	-.0032	-.0041	-.0049
		-8	-.0059	-.0050	-.0042	-.0034	-.0042	-.0050	-.0059

Table 9-6b. SSLV AND ORBITER POWER DELTA - PITCHING MOMENT COEFFICIENT - FOREBODY

MACH	$\delta_{e_{IO}}$	α	β: -6	-4	-2	0	+2	+4	+6
1.10	10/9	4	-.0060	-.0058	-.0056	-.0055	-.0056	-.0058	-.0060
		0	-.0082	-.0072	-.0062	-.0052	-.0062	-.0072	-.0082
		-4	-.0086	-.0082	-.0078	-.0073	-.0078	-.0082	-.0086
		-8	-.0091	-.0089	-.0087	-.0085	-.0087	-.0069	-.0091
1.15	10/5	4	-.0077	-.0069	-.0060	-.0051	-.0060	-.0069	-.0077
		0	-.0076	-.0067	-.0059	-.0051	-.0059	-.0067	-.0076
		-4	-.0077	-.0074	-.0071	-.0068	-.0071	-.0074	-.0077
		-8	-.0091	-.0085	-.0079	-.0073	-.0079	-.0085	-.0091
1.25	10/-2	4	-.0042	-.0047	-.0052	-.0057	-.0052	-.0047	-.0042
		0	-.0053	-.0058	-.0062	-.0067	-.0062	-.0058	-.0053
		-4	-.0068	-.0069	-.0070	-.0070	-.0070	-.0069	-.0068
		-8	-.0091	-.0094	-.0097	-.0100	-.0097	-.0094	-.0091
1.40	10/-2	4	-.0060	-.0056	-.0052	-.0048	-.0052	-.0056	-.0060
		0	-.0060	-.0056	-.0052	-.0048	-.0052	-.0056	-.0060
		-4	-.0068	-.0070	-.0073	-.0075	-.0073	-.0070	-.0068
		-8	-.0098	-.0100	-.0104	-.0107	-.0104	-.0100	-.0098

Table 9-7a. SSLV AND ORBITER POWER DELTA - PITCHING MOMENT COEFFICIENT - FOREBODY - INBOARD ELEVON GRADIENT - δ_{EI} GREATER THAN NOMINAL

MACH	α	β -6	-4	-2	0	+2	+4	+6
.6	4	+.0000	-.0001	-.0002	-.0003	-.0002	-.0001	+.0000
	0	-.0005	-.0005	-.0005	-.0005	-.0005	-.0005	-.0005
	-4	-.0003	-.0003	-.0005	-.0007	-.0005	-.0003	-.0003
	-8	-.0007	-.0006	-.0004	-.0003	-.0004	-.0006	-.0007
.8	4	-.0007	-.0005	-.0003	-.0001	-.0003	-.0005	-.0007
	0	-.0009	-.0007	-.0006	-.0005	-.0006	-.0007	-.0009
	-4	-.0010	-.0008	-.0005	-.0001	-.0005	-.0008	-.0010
	-8	-.0010	-.0005	-.0001	+.0004	-.0001	-.0005	-.0010
.90	4	-.0002	-.0002	+.0004	+.0004	+.0004	-.0002	-.0002
	0	-.0006	-.0006	-.0011	-.0009	-.0011	-.0006	-.0006
	-4	-.0008	-.0007	-.0007	-.0006	-.0007	-.0007	-.0008
	-8	+.0002	-.0001	-.0005	-.0008	-.0005	-.0001	+.0002
.95	4	+.0016	+.0008	+.0001	-.0005	+.0001	+.0008	+.0016
	0	+.0022	+.0017	+.0012	+.0007	+.0012	+.0017	+.0022
	-4	+.0004	+.0004	+.0007	+.0008	+.0007	+.0004	+.0004
	-8	+.0004	+.0004	+.0004	+.0004	+.0004	+.0004	+.0004
1.05	4	+.0011	+.0005	-.0007	-.0017	-.0007	+.0005	+.0011
	0	-.0004	+.0001	+.0004	+.0008	+.0004	+.0001	-.0004
	-4	+.0001	+.0004	+.0007	+.0010	+.0007	+.0004	+.0001
	-8	-.0004	+.0000	+.0003	+.0006	+.0003	+.0000	-.0004

Table 9-7b. SSLV AND ORBITER POWER DELTA - PITCHING MOMENT COEFFICIENT - FOREBODY - INBOARD ELEVON GRADIENT - δ_{EI} GREATER THAN NOMINAL

MACH	α	β -6	-4	-2	0	+2	+4	+6
1.10	4	-.0009	-.0004	+.0000	+.0004	+.0000	-.0004	-.0009
	0	+.0002	+.0002	+.0002	+.0002	+.0002	+.0002	+.0002
	-4	+.0007	+.0006	+.0004	+.0003	+.0004	+.0006	+.0007
	-8	+.0004	+.0002	+.0001	-.0001	+.0001	+.0002	+.0004
1.15	4	+.0001	+.0001	+.0000	+.0000	+.0000	+.0001	+.0001
	0	+.0001	+.0001	+.0001	+.0001	+.0001	+.0001	+.0001
	-4	-.0001	-.0001	+.0000	+.0001	+.0000	-.0001	-.0001
	-8	+.0000	+.0000	-.0001	-.0002	-.0001	+.0000	+.0000
1.25	4	-.0003	-.0002	-.0001	+.0000	-.0001	-.0002	-.0003
	0	-.0001	-.0001	+.0000	+.0000	+.0000	-.0001	-.0001
	-4	-.0001	-.0001	+.0000	+.0000	+.0000	-.0001	-.0001
	-8	+.0000	+.0000	+.0000	+.0000	+.0000	+.0000	+.0000
1.40	4	+.0001	+.0001	+.0000	-.0001	+.0000	+.0001	+.0001
	0	+.0001	+.0001	+.0000	+.0000	+.0000	+.0001	+.0001
	-4	+.0001	+.0001	+.0000	+.0000	+.0000	+.0001	+.0001
	-8	+.0000	+.0000	+.0000	+.0000	+.0000	+.0000	+.0000

Table 9-8a. SSLV AND ORBITER POWER DELTA - PITCHING MOMENT COEFFICIENT - FOREBODY - INBOARD ELEVON GRADIENT - δ_{E_I} LESS THAN NOMINAL

MACH	α	β = -6	-4	-2	0	+2	+4	+6
.6	4	+.0000	+.0000	+.0000	+.0000	+.0000	+.0000	+.0000
	0	+.0000	+.0000	+.0000	+.0001	+.0000	+.0000	+.0000
	-4	+.0001	+.0001	+.0000	+.0001	+.0000	+.0001	+.0001
	-8	+.0003	+.0001	+.0000	+.0001	+.0000	+.0001	+.0003
.8	4	+.0001	+.0000	-.0001	-.0001	-.0001	+.0000	+.0001
	0	-.0001	+.0000	+.0001	+.0001	+.0001	+.0000	-.0001
	-4	+.0000	+.0000	+.0000	+.0000	+.0000	+.0000	+.0000
	-8	+.0000	+.0000	-.0001	-.0001	-.0001	+.0000	+.0000
.90	4	-.0006	-.0008	-.0008	-.0009	-.0008	-.0008	-.0006
	0	-.0005	-.0005	-.0003	-.0003	-.0003	-.0005	-.0005
	-4	-.0004	-.0010	-.0018	-.0030	-.0018	-.0010	-.0004
	-8	-.0010	-.0020	-.0028	-.0038	-.0028	-.0020	-.0010
.95	4	+.0000	+.0002	+.0003	+.0004	+.0003	+.0002	+.0000
	0	+.0004	+.0004	+.0003	+.0004	+.0003	+.0004	+.0004
	-4	+.0000	+.0002	+.0003	+.0004	+.0003	+.0002	+.0000
	-8	+.0004	-.0002	-.0001	+.0000	-.0001	-.0002	+.0004
1.05	4	+.0000	+.0000	+.0000	+.0000	+.0000	+.0000	+.0000
	0	+.0001	+.0001	+.0001	+.0001	+.0001	+.0001	+.0001
	-4	+.0000	+.0001	+.0002	+.0002	+.0002	+.0001	+.0000
	-8	+.0000	+.0000	+.0000	+.0000	+.0000	+.0000	+.0000

Table 9-8b. SSLV AND ORBITER POWER DELTA - PITCHING MOMENT COEFFICIENT - FOREBODY - INBOARD ELEVON GRADIENT - δ_{E_I} LESS THAN NOMINAL

MACH	α	β -6	-4	-2	0	+2	+4	+6
1.10	4	-.0001	-.0001	-.0001	-.0001	-.0001	-.0001	-.0001
	0	+.0000	-.0001	-.0001	-.0002	-.0001	-.0001	+.0000
	-4	+.0000	-.0001	-.0001	-.0002	-.0001	-.0001	+.0000
	-8	+.0000	-.0001	-.0001	-.0002	-.0001	-.0001	+.0000
1.15	4	-.0001	-.0001	+.0000	+.0000	+.0000	-.0001	-.0001
	0	+.0001	+.0001	+.0000	+.0000	+.0000	+.0001	+.0001
	-4	-.0001	-.0001	+.0000	+.0000	+.0000	-.0001	-.0001
	-8	+.0000	+.0000	+.0000	+.0000	+.0000	+.0000	+.0000
1.25	4	-.0001	-.0001	+.0000	+.0000	+.0000	-.0001	-.0001
	0	+.0000	+.0000	-.0001	-.0002	-.0001	+.0000	+.0000
	-4	+.0000	+.0000	+.0000	+.0000	+.0000	+.0000	+.0000
	-8	-.0003	-.0003	-.0002	-.0001	-.0002	-.0003	-.0003
1.40	4	-.0005	-.0005	-.0005	-.0005	-.0005	-.0005	-.0005
	0	-.0003	-.0003	-.0003	-.0003	-.0003	-.0003	-.0003
	-4	-.0001	-.0001	-.0001	-.0001	-.0001	-.0001	-.0001
	-8	-.0001	-.0001	-.0002	-.0002	-.0002	-.0001	-.0001

Table 9-9a. SSLV AND ORBITER POWER DELTA - PITCHING MOMENT COEFFICIENT - FOREBODY - OUTBOARD ELEVON GRADIENT - δ_{E_0} GREATER THAN NOMINAL

MACH	α	β -6	-4	-2	0	+2	+4	+6
.6	4	-.0005	-.0004	-.0004	-.0003	-.0004	-.0004	-.0005
	0	-.0005	-.0004	-.0004	-.0003	-.0004	-.0004	-.0005
	-4	-.0005	-.0005	-.0004	-.0003	-.0004	-.0005	-.0005
	-8	-.0005	-.0003	-.0003	-.0002	-.0003	-.0003	-.0005
.8	4	-.0008	-.0006	-.0004	-.0002	-.0004	-.0006	-.0008
	0	-.0009	-.0008	-.0008	-.0007	-.0008	-.0008	-.0009
	-4	-.0011	-.0008	-.0005	-.0002	-.0005	-.0008	-.0011
	-8	-.0012	-.0006	-.0001	+.0004	-.0001	-.0006	-.0012
.90	4	-.0003	-.0002	-.0001	+.0001	-.0001	-.0002	-.0003
	0	-.0008	-.0006	-.0005	-.0004	-.0005	-.0006	-.0008
	-4	-.0007	-.0007	-.0007	-.0007	-.0007	-.0007	-.0007
	-8	+.0004	+.0000	-.0004	-.0007	-.0004	+.0000	+.0004
.95	4	-.0003	-.0002	-.0001	+.0000	-.0001	-.0002	-.0003
	0	+.0004	+.0005	+.0008	+.0008	+.0008	+.0005	+.0004
	-4	-.0001	-.0001	+.0000	+.0000	+.0000	-.0001	-.0001
	-8	-.0001	-.0001	-.0001	-.0001	-.0001	-.0001	-.0001
1.05	4	+.0001	+.0000	-.0002	-.0003	-.0002	+.0000	+.0001
	0	-.0001	-.0003	-.0004	-.0006	-.0004	-.0003	-.0001
	-4	+.0012	+.0008	+.0002	-.0004	+.0002	+.0008	+.0012
	-8	+.0007	+.0004	+.0002	-.0002	+.0002	+.0004	+.0007

Table 9-9b. SSLV AND ORBITER POWER DELTA - PITCHING MOMENT COEFFICIENT - FOREBODY - OUTBOARD ELEVON GRADIENT - δ_{E_0} GREATER THAN NOMINAL

MACH	α	β -6	-4	-2	0	+2	+4	+6
1.10	4	-.0005	-.0002	+.0003	+.0006	+.0003	-.0002	-.0005
	0	+.0001	+.0005	+.0008	+.0012	+.0008	+.0005	+.0001
	-4	+.0010	+.0010	+.0007	+.0006	+.0007	+.0010	+.0010
	-8	+.0013	+.0007	+.0002	-.0003	+.0002	+.0007	+.0013
1.15	4	+.0008	+.0006	+.0004	+.0002	+.0004	+.0006	+.0008
	0	+.0000	+.0000	+.0000	-.0001	+.0000	+.0000	+.0000
	-4	+.0008	+.0005	+.0004	+.0001	+.0004	+.0005	+.0008
	-8	-.0004	-.0002	+.0002	+.0006	+.0002	-.0002	-.0004
1.25	4	-.0002	+.0001	+.0004	+.0006	+.0004	+.0001	-.0002
	0	+.0001	+.0002	+.0003	+.0004	+.0003	+.0002	+.0001
	-4	+.0003	+.0003	+.0002	+.0002	+.0002	+.0003	+.0003
	-8	+.0002	+.0002	+.0003	+.0003	+.0003	+.0002	+.0002
1.40	4	+.0006	+.0005	+.0004	+.0003	+.0004	+.0005	+.0006
	0	+.0003	+.0003	+.0003	+.0003	+.0003	+.0003	+.0003
	-4	+.0003	+.0002	+.0001	+.0001	+.0001	+.0002	+.0003
	-8	+.0000	+.0000	+.0002	+.0003	+.0002	+.0000	+.0000

Table 9-10a. SSLV AND ORBITER POWER DELTA - PITCHING MOMENT COEFFICIENT - FOREBODY - OUTBOARD ELEVON GRADIENT - δ_{E_0} LESS THAN NOMINAL

MACH	α	β = -6	-4	-2	0	+2	+4	+6
.6	4	-.0004	-.0003	-.0003	-.0003	-.0003	-.0003	-.0004
	0	-.0001	-.0001	-.0002	-.0003	-.0002	-.0001	-.0001
	-4	-.0005	-.0005	-.0005	-.0003	-.0005	-.0005	-.0005
	-8	-.0003	-.0004	-.0003	-.0002	-.0003	-.0004	-.0003
.8	4	+.0000	+.0000	-.0001	-.0001	-.0001	+.0000	+.0000
	0	+.0005	+.0003	+.0001	+.0000	+.0001	+.0003	+.0005
	-4	+.0007	+.0003	-.0001	-.0004	-.0001	+.0003	+.0007
	-8	-.0003	-.0001	-.0002	-.0004	-.0002	-.0001	-.0003
.90	4	-.0016	-.0008	-.0005	+.0002	-.0005	-.0008	-.0016
	0	-.0009	-.0007	-.0004	-.0001	-.0004	-.0007	-.0009
	-4	+.0003	-.0003	-.0011	-.0019	-.0011	-.0003	+.0003
	-8	-.0020	-.0019	-.0017	-.0015	-.0017	-.0019	-.0020
.95	4	-.0027	-.0011	+.0004	+.0020	+.0004	-.0011	-.0027
	0	+.0004	+.0010	+.0013	+.0018	+.0013	+.0010	+.0004
	-4	+.0012	+.0020	+.0027	+.0038	+.0027	+.0020	+.0012
	-8	+.0020	+.0027	+.0034	+.0043	+.0034	+.0027	+.0020
1.05	4	+.0001	+.0002	+.0003	+.0004	+.0003	+.0002	+.0001
	0	+.0008	+.0006	+.0002	-.0001	+.0002	+.0006	+.0008
	-4	+.0005	+.0004	+.0002	+.0000	+.0002	+.0004	+.0005
	-8	+.0009	+.0006	+.0005	+.0005	+.0005	+.0006	+.0009

Table 9-10b. SSLV AND ORBITER POWER DELTA - PITCHING MOMENT COEFFICIENT - FOREBODY - OUTBOARD ELEVON GRADIENT - δ_{E_0} LESS THAN NOMINAL

MACH	α	β -6	-4	-2	0	+2	+4	+6
1.10	4	+.0010	+.0008	+.0005	+.0002	+.0005	+.0008	+.0010
	0	+.0002	+.0000	-.0003	-.0005	-.0003	+.0000	+.0002
	-4	+.0005	+.0002	-.0002	-.0005	-.0002	+.0002	+.0005
	-8	+.0008	+.0006	+.0004	+.0002	+.0004	+.0006	+.0008
1.15	4	+.0004	+.0004	+.0003	+.0003	+.0003	+.0004	+.0004
	0	+.0011	+.0009	+.0008	+.0007	+.0008	+.0009	+.0011
	-4	+.0006	+.0006	+.0006	+.0006	+.0006	+.0006	+.0006
	-8	+.0006	+.0004	+.0000	-.0003	+.0000	+.0004	+.0006
1.25	4	-.0007	-.0005	-.0001	+.0002	-.0001	-.0005	-.0007
	0	-.0001	-.0001	+.0000	+.0000	+.0000	-.0001	-.0001
	-4	-.0001	+.0000	+.0002	-.0003	+.0002	+.0000	-.0001
	-8	+.0007	+.0005	+.0002	+.0000	+.0002	+.0005	+.0007
1.40	4	+.0000	+.0000	+.0000	+.0000	+.0000	+.0000	+.0000
	0	+.0000	+.0000	+.0000	+.0000	+.0000	+.0000	+.0000
	-4	+.0000	+.0000	+.0000	+.0000	+.0000	+.0000	+.0000
	-8	+.0000	+.0000	+.0000	+.0000	+.0000	+.0000	+.0000

Table 9-11a. INBOARD ELEVON - HINGE MOMENT COEFFICIENT

POWER DELTA

MACH	$\delta_{E_{IO}}$	α \ β	-6	-4	-2	0	+2	+4	+6
.6	10/9	4	-.0066	-.0060	-.0054	-.0047	-.0046	-.0047	-.0048
		0	-.0069	-.0062	-.0055	-.0048	-.0046	-.0044	-.0042
		-4	-.0066	-.0061	-.0057	-.0052	-.0049	-.0046	-.0043
		-8	-.0064	-.0060	-.0056	-.0052	-.0049	-.0046	-.0043
.8	10/9	4	-.0065	-.0056	-.0047	-.0038	-.0037	-.0036	-.0035
		0	-.0060	-.0056	-.0042	-.0034	-.0035	-.0036	-.0037
		-4	-.0055	-.0047	-.0041	-.0035	-.0035	-.0035	-.0036
		-8	-.0045	-.0043	-.0042	-.0041	-.0040	-.0038	-.0036
.90	10/9	4	-.0240	-.0200	-.0180	-.0144	-.0130	-.0123	-.0120
		0	-.0155	-.0140	-.0120	-.0080	-.0075	-.0070	-.0063
		-4	-.0130	-.0130	-.0110	-.0090	-.0070	-.0050	-.0035
		-8	-.0075	-.0075	-.0072	-.0070	-.0070	-.0065	-.0058
.95	10/9	4	-.0111	-.0054	+.0005	+.0066	+.0035	+.0005	-.0025
		0	-.0093	-.0033	+.0028	+.0068	+.0066	+.0045	+.0024
		-4	-.0082	-.0035	+.0015	+.0063	+.0054	+.0045	+.0040
		-8	-.0102	-.0005	+.0000	+.0057	+.0065	+.0075	+.0084
1.05	10/9	4	-.0044	-.0036	-.0028	-.0020	-.0028	-.0036	-.0044
		0	-.0070	-.0055	-.0040	-.0025	-.0003	+.0025	+.0043
		-4	-.0072	-.0051	-.0030	-.0009	+.0013	+.0035	+.0059
		-8	-.0059	-.0042	-.0024	-.0006	+.0032	+.0060	+.0108

Table 9-11b. INBOARD ELEVON - HINGE MOMENT COEFFICIENT

POWER DELTA

MACH	$\delta_{E_{IO}}$	α \ β	-6	-4	-2	0	+2	+4	+6
1.10	10/9	4	-.0100	-.0075	-.0049	-.0023	-.0024	-.0025	-.0026
		0	-.0134	-.0094	-.0053	-.0011	-.0014	+.0039	+.0064
		-4	-.0119	-.0082	-.0045	-.0008	+.0026	+.0060	+.0092
		-8	-.0086	-.0079	-.0073	-.0067	-.0048	-.0031	-.0014
1.15	10/5	4	-.0101	-.0065	-.0032	+.0001	-.0002	-.0005	-.0009
		0	-.0100	-.0103	-.0047	+.0009	-.0002	-.0009	-.0012
		-4	-.0135	-.0102	-.0068	-.0035	-.0033	-.0031	-.0029
		-8	-.0118	-.0101	-.0084	-.0068	-.0068	-.0068	-.0068
1.25	10/-2	4	-.0097	-.0062	-.0028	+.0007	+.0006	+.0005	+.0004
		0	-.0103	-.0071	-.0039	-.0007	-.0009	-.0011	-.0013
		-4	-.0085	-.0072	-.0055	-.0039	-.0040	-.0041	-.0042
		-8	-.0102	-.0099	-.0086	-.0073	-.0066	-.0059	-.0052
1.40	10/-2	4	-.0024	-.0021	-.0017	-.0014	-.0007	+.0000	+.0007
		0	-.0039	-.0030	-.0021	-.0013	-.0009	-.0005	-.0001
		-4	-.0067	-.0055	-.0044	-.0032	-.0022	-.0013	-.0003
		-8	-.0099	-.0093	-.0086	-.0080	-.0076	-.0071	-.0066

Table 9-12a. INBOARD ELEVON POWER DELTA - HINGE MOMENT COEFFICIENT
INBOARD ELEVON GRADIENT - δ_{E_I} GREATER THAN NOMINAL

MACH	α	β = -6	-4	-2	0	+2	+4	+6
.6	4	-.0001	-.0002	-.0003	-.0004	-.0005	-.0004	-.0003
	0	+.0002	+.0000	-.0002	-.0004	-.0005	-.0008	-.0009
	-4	-.0002	-.0003	-.0003	-.0003	-.0003	-.0003	-.0003
	-8	-.0002	-.0002	-.0003	-.0004	-.0003	-.0002	-.0001
.8	4	-.0001	-.0002	-.0003	-.0005	-.0004	-.0003	-.0003
	0	-.0003	-.0005	-.0006	-.0007	-.0005	-.0003	-.0002
	-4	-.0001	-.0003	-.0005	-.0007	-.0004	-.0002	+.0001
	-8	+.0000	-.0001	-.0001	-.0002	+.0000	+.0001	+.0003
.90	4	+.0025	+.0023	+.0015	+.0011	+.0010	+.0025	-.0006
	0	-.0010	-.0010	-.0015	-.0026	-.0020	-.0016	-.0025
	-4	-.0003	-.0005	-.0010	-.0018	-.0015	-.0016	-.0015
	-8	-.0003	-.0007	-.0010	-.0016	-.0010	-.0007	-.0007
.95	4	+.0010	+.0001	-.0008	-.0020	-.0030	-.0042	-.0052
	0	+.0003	+.0003	-.0002	-.0007	-.0008	-.0011	-.0011
	-4	+.0012	+.0008	+.0002	-.0002	+.0001	+.0004	+.0005
	-8	+.0007	+.0001	+.0011	-.0005	-.0008	-.0012	-.0016
1.05	4	+.0004	+.0001	-.0002	-.0006	-.0010	-.0016	-.0020
	0	+.0008	+.0004	+.0001	-.0003	-.0016	-.0032	-.0042
	-4	-.0011	-.0003	+.0001	+.0006	-.0009	-.0023	-.0039
	-8	-.0016	-.0010	-.0003	+.0002	-.0017	-.0032	-.0057

Table 9-125. INBOARD ELEVON POWER DELTA - HINGE MOMENT COEFFICIENT
INBOARD ELEVON GRADIENT - δ_{E_I} GREATER THAN NOMINAL

MACH	α	β = -6	-4	-2	0	+2	+4	+6
1.10	4	+.0020	+.0010	+.0000	-.0011	-.0022	-.0033	-.0049
	0	+.0001	-.0001	-.0004	-.0007	-.0003	-.0026	-.0035
	-4	-.0005	-.0004	+.0003	+.0010	+.0000	-.0007	-.0016
	-8	-.0044	-.0021	+.0000	+.0023	+.0042	+.0063	+.0083
1.15	4	-.0003	-.0007	-.0011	-.0016	-.0020	-.0023	-.0028
	0	+.0008	+.0005	+.0000	-.0004	+.0008	+.0020	+.0028
	-4	+.0010	+.0007	+.0013	+.0012	+.0038	+.0027	+.0079
	-8	-.0009	-.0002	+.0004	+.0010	+.0020	+.0031	+.0055
1.25	4	-.0012	-.0008	-.0004	-.0001	+.0002	+.0006	+.0010
	0	-.0010	-.0006	-.0002	+.0001	+.0003	+.0005	+.0008
	-4	+.0002	+.0003	+.0003	+.0004	+.0002	+.0001	-.0001
	-8	+.0000	+.0004	+.0008	+.0002	+.0002	+.0001	+.0001
1.40	4	-.0010	-.0005	+.0001	+.0003	+.0004	+.0006	+.0007
	0	-.0003	-.0002	-.0001	+.0000	+.0003	+.0005	+.0007
	-4	+.0006	+.0004	+.0003	+.0000	+.0003	+.0005	+.0005
	-8	+.0005	+.0005	+.0004	+.0003	+.0005	+.0004	+.0004

Table 9-13a. INBOARD ELEVON POWER DELTA - HINGE MOMENT COEFFICIENT
INBOARD ELEVON GRADIENT - δ_{E_I} LESS THAN NOMINAL

MACH	α	β = -6	-4	-2	0	+2	+4	+6
.6	4	-.0010	-.0009	-.0007	-.0004	-.0003	-.0002	+.0000
	0	-.0011	-.0009	-.0006	-.0003	-.0002	-.0001	+.0001
	-4	-.0011	-.0008	-.0005	-.0003	-.0001	+.0000	+.0001
	-8	-.0006	-.0004	-.0003	-.0001	-.0001	-.0001	+.0000
.8	4	-.0007	-.0006	-.0005	-.0005	-.0005	-.0005	-.0006
	0	-.0003	-.0002	-.0002	-.0003	-.0003	-.0004	-.0004
	-4	-.0002	-.0002	-.0001	+.0001	-.0001	-.0002	-.0004
	-8	-.0001	-.0001	-.0001	-.0001	-.0001	-.0001	-.0001
.90	4	-.0045	-.0038	-.0035	-.0030	-.0040	-.0050	-.0050
	0	-.0025	-.0025	-.0020	-.0011	-.0018	-.0024	-.0025
	-4	-.0040	-.0040	-.0045	-.0043	-.0030	-.0014	-.0008
	-8	-.0039	-.0039	-.0046	-.0049	-.0048	-.0044	-.0039
.95	4	-.0041	-.0045	-.0044	-.0043	-.0048	-.0050	-.0055
	0	-.0030	-.0015	+.0006	+.0026	+.0020	+.0015	+.0009
	-4	-.0050	-.0007	+.0053	+.0116	+.0052	-.0011	-.0074
	-8	-.0105	+.0016	+.0076	+.0194	+.0111	+.0046	-.0028
1.05	4	-.0004	-.0001	-.0008	-.0011	-.0012	-.0013	-.0014
	0	-.0003	-.0004	-.0008	-.0012	+.0006	+.0026	+.0042
	-4	+.0011	+.0003	+.0009	+.0007	+.0020	+.0034	+.0048
	-8	+.0016	-.0010	+.0056	+.0027	+.0041	+.0048	+.0067

Table 9-13b. INBOARD ELEVON POWER DELTA - HINGE MOMENT COEFFICIENT
INBOARD ELEVON GRADIENT - δ_{E_I} LESS THAN NOMINAL

MACH	α \ β	-6	-4	-2	0	+2	+4	+6
1.10	4	-.0008	-.0004	+.0002	+.0007	+.0008	+.0009	+.0010
	0	+.0015	+.0016	+.0018	+.0020	+.0031	+.0071	+.0110
	-4	+.0015	+.0025	+.0035	+.0044	+.0074	+.0104	+.0132
	-8	+.0055	+.0043	+.0042	+.0036	+.0050	+.0064	+.0077
1.15	4	+.0015	+.0016	+.0018	+.0020	+.0015	+.0010	+.0006
	0	+.0008	+.0013	+.0020	+.0025	+.0034	+.0042	+.0053
	-4	+.0008	+.0015	+.0027	+.0030	+.0056	+.0081	+.0105
	-8	+.0026	+.0023	+.0022	+.0020	+.0031	+.0042	+.0052
1.25	4	+.0025	+.0023	+.0023	+.0007	+.0017	+.0014	+.0010
	0	+.0020	+.0019	+.0020	+.0019	+.0027	+.0022	+.0041
	-4	+.0010	+.0016	+.0016	+.0017	+.0019	+.0020	+.0022
	-8	+.0000	+.0004	+.0009	+.0014	+.0014	+.0013	+.0018
1.40	4	+.0000	+.0000	+.0000	+.0000	+.0000	+.0000	+.0000
	0	+.0000	+.0000	+.0000	+.0000	+.0000	+.0000	+.0000
	-4	+.0000	+.0000	+.0000	+.0000	+.0000	+.0000	+.0000
	-8	+.0000	+.0000	+.0000	+.0000	+.0000	+.0000	+.0000

Table 9-14a. INBOARD ELEVON POWER DELTA - HINGE MOMENT COEFFICIENT
OUTBOARD ELEVON GRADIENT - δ_{E_0} GREATER THAN NOMINAL

MACH	α \ β	-6	-4	-2	0	+2	+4	+6
.6	4	+.0002	+.0001	+.0001	-.0001	-.0001	+.0001	+.0002
	0	+.0003	+.0002	+.0001	-.0001	-.0002	-.0003	-.0004
	-4	-.0001	-.0001	-.0001	-.0001	-.0001	-.0001	-.0002
	-8	-.0001	-.0001	-.0002	-.0003	-.0001	+.0001	+.0003
.8	4	-.0002	-.0001	-.0001	-.0001	-.0001	-.0002	-.0002
	0	-.0001	-.0002	-.0002	-.0003	-.0002	-.0001	+.0001
	-4	-.0001	-.0002	-.0002	-.0003	-.0002	-.0002	-.0001
	-8	-.0002	-.0001	+.0000	+.0001	+.0001	+.0001	+.0000
.90	4	+.0025	+.0021	+.0018	+.0016	+.0020	+.0030	+.0030
	0	+.0001	+.0002	-.0005	-.0014	-.0010	-.0007	-.0005
	-4	-.0010	-.0009	-.0010	-.0012	-.0012	-.0006	-.0004
	-8	+.0000	+.0000	-.0002	-.0004	-.0004	-.0008	-.0011
.95	4	+.0065	+.0047	+.0031	+.0010	-.0005	-.0020	-.0030
	0	+.0065	+.0044	+.0023	+.0008	+.0015	+.0022	+.0029
	-4	+.0038	+.0031	+.0022	+.0013	+.0022	+.0031	+.0038
	-8	+.0043	+.0010	+.0018	+.0010	+.0009	+.0007	+.0005
1.05	4	+.0014	+.0010	+.0006	+.0002	-.0001	-.0005	-.0009
	0	+.0011	+.0008	+.0006	+.0004	+.0017	+.0028	+.0044
	-4	-.0005	-.0001	+.0005	+.0007	+.0004	+.0010	+.0011
	-8	-.0017	-.0010	-.0003	+.0001	-.0006	-.0007	-.0021

ORIGINAL PAGE IS
OF POOR QUALITY

Table 9-14b. INBOARD ELEVON POWER DELTA - HINGE MOMENT COEFFICIENT
OUTBOARD ELEVON GRADIENT - δ_{E_0} GREATER THAN NOMINAL

MACH	α \ β	-6	-4	-2	0	+2	+4	+6
1.10	4	+.0018	+.0013	+.0007	+.0001	-.0008	-.0017	-.0026
	0	+.0003	+.0003	+.0003	+.0003	+.0020	+.0010	+.0013
	-4	-.0007	-.0003	+.0002	+.0007	+.0012	+.0017	+.0024
	-8	-.0028	-.0016	-.0006	+.0007	+.0013	+.0020	+.0018
1.15	4	+.0000	+.0000	+.0000	+.0001	+.0000	-.0001	-.0002
	0	+.0009	+.0005	+.0000	-.0003	-.0001	+.0001	+.0002
	-4	+.0002	+.0001	+.0001	+.0001	+.0001	+.0000	-.0001
	-8	+.0000	+.0000	-.0001	-.0001	-.0001	-.0001	-.0001
1.25	4	+.0004	+.0003	+.0002	+.0000	+.0000	+.0000	+.0000
	0	+.0000	+.0000	+.0000	+.0000	+.0001	+.0001	-.0002
	-4	-.0004	-.0003	-.0001	+.0000	+.0000	+.0000	+.0000
	-8	-.0008	-.0004	-.0002	+.0000	+.0000	+.0000	-.0001
1.40	4	-.0004	-.0003	-.0001	+.0000	+.0000	-.0001	-.0001
	0	-.0003	-.0002	-.0001	+.0000	-.0001	-.0001	+.0000
	-4	-.0001	-.0001	+.0000	+.0001	+.0000	-.0001	-.0002
	-8	+.0000	+.0000	+.0001	+.0001	+.0002	+.0003	+.0003

ORIGINAL PAGE IS
OF POOR QUALITY

Table 9-15a. INBOARD ELEVON POWER DELTA - HINGE MOMENT COEFFICIENT
OUTBOARD ELEVON GRADIENT - δ_{E_0} LESS THAN NOMINAL

MACH	α	β = -6	-4	-2	0	+2	+4	+6
.6	4	-.0002	-.0002	-.0001	-.0001	+.0000	+.0000	+.0000
	0	-.0003	-.0002	-.0001	-.0001	+.0000	+.0000	+.0000
	-4	-.0002	-.0002	-.0001	-.0001	+.0000	+.0000	+.0000
	-8	-.0003	-.0002	-.0001	+.0000	+.0000	+.0000	+.0000
.8	4	+.0001	+.0000	-.0001	-.0001	-.0001	+.0000	+.0000
	0	+.0001	+.0000	+.0000	+.0000	-.0001	+.0000	+.0000
	-4	+.0001	-.0001	-.0001	-.0001	-.0001	+.0000	+.0000
	-8	+.0000	-.0001	-.0001	-.0002	-.0002	-.0001	-.0001
.90	4	-.0027	-.0020	-.0016	-.0007	-.0009	-.0014	-.0018
	0	-.0001	+.0002	+.0004	+.0012	+.0006	+.0003	-.0005
	-4	-.0006	-.0005	-.0005	-.0004	-.0005	-.0007	-.0009
	-8	-.0009	-.0009	-.0007	-.0005	-.0006	-.0006	-.0010
.95	4	+.0002	+.0001	+.0003	+.0004	+.0002	-.0001	-.0005
	0	+.0000	+.0004	+.0006	+.0009	+.0008	+.0008	+.0007
	-4	+.0000	+.0002	+.0006	+.0009	+.0009	+.0009	+.0011
	-8	+.0002	+.0013	+.0003	+.0007	+.0009	+.0011	+.0014
1.05	4	+.0003	+.0002	+.0001	+.0000	+.0000	+.0001	+.0001
	0	+.0001	+.0001	+.0001	+.0001	+.0002	+.0005	+.0005
	-4	+.0001	+.0001	+.0001	+.0002	+.0000	-.0001	-.0002
	-8	+.0001	+.0001	+.0000	+.0000	+.0000	-.0001	+.0002

ORIGINAL PAGE IS
OF POOR QUALITY

Table 9-15b. INBOARD ELEVON POWER DELTA - HINGE MOMENT COEFFICIENT
OUTBOARD ELEVON GRADIENT - δ_{E_0} LESS THAN NOMINAL

MACH	α \ β	-6	-4	-2	0	+2	+4	+6
1.10	4	-.0005	-.0002	-.0001	-.0001	-.0002	-.0003	-.0003
	0	-.0005	-.0003	-.0001	+.0002	-.0006	+.0001	+.0000
	-4	-.0004	-.0003	-.0003	-.0002	+.0000	+.0001	+.0003
	-8	-.0004	-.0004	-.0002	-.0001	-.0001	-.0002	-.0004
1.15	4	-.0001	+.0000	+.0000	+.0001	+.0002	+.0003	+.0004
	0	-.0003	-.0005	-.0002	+.0002	-.0002	-.0003	-.0005
	-4	-.0001	-.0001	+.0000	+.0000	-.0002	-.0004	-.0005
	-8	-.0006	-.0004	-.0002	-.0001	-.0001	-.0001	-.0002
1.25	4	+.0007	+.0006	+.0003	+.0001	+.0000	-.0002	-.0003
	0	+.0001	+.0001	+.0001	+.0001	+.0001	+.0001	+.0001
	-4	+.0001	-.0002	+.0000	+.0000	+.0000	+.0000	+.0000
	-8	-.0001	-.0003	-.0002	+.0000	+.0000	+.0000	-.0001
1.40	4	+.0001	-.0002	-.0004	-.0007	-.0005	-.0004	-.0003
	0	+.0000	-.0001	-.0001	-.0002	-.0002	-.0002	-.0002
	-4	-.0001	-.0001	-.0002	-.0003	-.0002	-.0002	-.0002
	-8	-.0001	-.0001	-.0001	-.0001	-.0001	+.0000	+.0000

ORIGINAL PAGE IS
OF POOR QUALITY

Table 9-16a. VERTICAL TAIL SIDE FORCE POWER DELTA

MACH	$\delta_{e_{IO}}$	α	β -6	-4	-2	0	+2	+4	+6
.6	10/9	4	+.0339	+.0226	+.0113	+.0000	-.0113	-.0226	-.0339
		0	+.0278	+.0185	+.0093	+.0000	-.0093	-.0185	-.0278
		-4	+.0302	+.0201	+.0100	+.0000	-.0100	-.0201	-.0302
		-8	+.0249	+.0166	+.0083	+.0000	-.0083	-.0166	-.0249
.8	10/9	4	+.0129	+.0086	+.0043	+.0000	-.0043	-.0086	-.0129
		0	+.0080	+.0053	+.0026	+.0000	-.0026	-.0053	-.0080
		-4	+.0014	+.0010	+.0005	+.0000	-.0005	-.0010	-.0014
		-8	+.0015	+.0010	+.0005	+.0000	-.0005	-.0010	-.0015
.9	10/9	4	+.0170	+.0113	+.0057	+.0000	-.0057	-.0113	-.0170
		0	+.0170	+.0113	+.0057	+.0000	-.0057	-.0113	-.0170
		-4	+.0210	+.0140	+.0070	+.0000	-.0070	-.0140	-.0210
		-8	+.0158	+.0105	+.0053	+.0000	-.0053	-.0105	-.0158
.95	10/9	4	+.0689	+.0459	+.0230	+.0000	-.0230	-.0459	-.0689
		0	+.0654	+.0436	+.0218	+.0000	-.0218	-.0436	-.0654
		-4	+.0615	+.0410	+.0205	+.0000	-.0205	-.0410	-.0615
		-8	+.0566	+.0377	+.0188	+.0000	-.0188	-.0377	-.0566
1.05	10/9	4	+.0369	+.0246	+.0123	+.0000	-.0123	-.0246	-.0369
		0	+.0340	+.0227	+.0113	+.0000	-.0113	-.0227	-.0340
		-4	+.0279	+.0186	+.0093	+.0000	-.0093	-.0186	-.0279
		-8	+.0315	+.0210	+.0105	+.0000	-.0105	-.0210	-.0315

Table 9-16b. VERTICAL TAIL SIDE FORCE POWER DELTA

MACH	$\delta_{e_{IO}}$	α	β -6	-4	-2	0	+2	+4	+6
1.1	10/9	4	+.0124	+.0082	+.0041	+.0000	-.0041	-.0082	-.0124
		0	+.0007	+.0005	+.0025	+.0000	-.0025	-.0005	-.0007
		-4	+.0048	+.0032	+.0016	+.0000	-.0016	-.0032	-.0048
		-8	+.0119	+.0079	+.0040	+.0000	-.0040	-.0079	-.0119
1.15	10/5	4	+.0145	+.0097	+.0048	+.0000	-.0048	-.0097	-.0145
			+.0080	+.0053	+.0026	+.0000	-.0026	-.0053	-.0080
		-4	+.0087	+.0058	+.0029	+.0000	-.0029	-.0058	-.0087
		-8	+.0067	+.0045	+.0022	+.0000	-.0022	-.0045	-.0067
1.25	10/-2	4	+.0068	+.0045	+.0023	+.0000	-.0023	-.0045	-.0068
		0	+.0057	+.0038	+.0019	+.0000	-.0019	-.0038	-.0057
		-4	+.0057	+.0038	+.0019	+.0000	-.0019	-.0038	-.0057
		-8	+.0065	+.0043	+.0022	+.0000	-.0022	-.0043	-.0065
1.4	10/-2	4	+.0034	+.0023	+.0011	+.0000	-.0011	-.0023	-.0034
		0	-.0020	-.0013	-.0006	+.0000	+.0006	+.0013	+.0020
		-4	+.0018	+.0012	+.0006	+.0000	-.0006	-.0012	-.0018
		-8	+.0121	+.0081	+.0040	+.0000	-.0040	-.0081	-.0121

Table 9-17a. VERTICAL TAIL BENDING MOMENT POWER DELTA

MACH	$\delta_{e_{IO}}$	α	β -6	-4	-2	0	+2	+4	+6
.6	10/9	4	+.0163	+.0110	+.0055	+.0000	-.0055	-.0110	-.0163
		0	+.0139	+.0092	+.0046	+.0000	-.0046	-.0092	-.0139
		-4	+.0152	+.0101	+.0051	+.0000	-.0051	-.0101	-.0152
		-8	+.0121	+.0080	+.0040	+.0000	-.0040	-.0080	-.0121
.8	10/9	4	+.0010	+.0004	+.0016	+.0000	-.0016	-.0004	-.0010
		0	+.0070	+.0004	+.0016	+.0000	-.0016	-.0004	-.0070
		-4	+.0010	+.0004	+.0005	+.0000	-.0005	-.0004	-.0010
		-8	+.0010	+.0004	+.0005	+.0000	-.0005	-.0004	-.0010
.9	10/9	4	+.0010	+.0005	+.0005	+.0000	-.0005	-.0005	-.0010
		0	+.0052	+.0027	+.0022	+.0000	-.0022	-.0027	-.0032
		-4	+.0071	+.0047	+.0036	+.0000	-.0036	-.0047	-.0071
		-8	+.0078	+.0047	+.0036	+.0000	-.0036	-.0047	-.0078
.95	10/9	4	+.0673	+.0460	+.0270	+.0000	-.0270	-.0460	-.0673
		0	+.0690	+.0480	+.0290	+.0000	-.0290	-.0480	-.0690
		-4	+.0676	+.0460	+.0270	+.0000	-.0270	-.0460	-.0676
		-8	+.0630	+.0430	+.0240	+.0000	-.0240	-.0430	-.0630
1.05	10/9	4	+.0336	+.0160	+.0140	+.0000	-.0140	-.0160	-.0336
		0	+.0248	+.0163	+.0100	+.0000	-.0100	-.0163	-.0248
		-4	+.0182	+.0098	+.0075	+.0000	-.0075	-.0098	-.0182
		-8	+.0187	+.0010	+.0079	+.0000	-.0079	-.0010	-.0187

ORIGINAL PAGE IS
OF POOR QUALITY

Table 9-17b. VERTICAL TAIL BENDING MOMENT POWER DELTA

MACH	$\delta_{e_{IO}}$	α	β -6	-4	-2	0	+2	+4	+6
1.1	10/9	4	+.0135	+.0105	+.0063	+.0000	-.0063	-.0105	-.0135
		0	+.0013	+.0009	+.0006	+.0000	-.0006	-.0009	-.0013
		-4	+.0044	+.0031	+.0020	+.0000	-.0020	-.0031	-.0044
		-8	+.0082	+.0060	+.0040	+.0000	-.0040	-.0060	-.0082
1.15	10/5	4	+.0136	+.0042	+.0021	+.0000	-.0021	-.0042	-.0136
		0	+.0061	+.0015	+.0006	+.0000	-.0006	-.0015	-.0061
		-4	+.0060	+.0015	+.0006	+.0000	-.0006	-.0015	-.0060
		-8	+.0048	+.0012	+.0006	+.0000	-.0006	-.0012	-.0048
1.25	10/-2	4	+.0021	+.0021	+.0010	+.0000	-.0010	-.0021	-.0021
		0	+.0019	+.0019	+.0009	+.0000	-.0009	-.0019	-.0019
		-4	+.0018	+.0018	+.0009	+.0000	-.0009	-.0018	-.0018
		-8	+.0012	+.0012	+.0006	+.0000	-.0006	-.0012	-.0012
1.4	10/-2	4	+.0093	+.0066	+.0034	+.0000	-.0034	-.0068	-.0098
		0	-.0010	-.0007	-.0003	+.0000	+.0003	+.0007	+.0010
		-4	+.0006	+.0001	+.0001	+.0000	-.0001	-.0001	-.0006
		-8	+.0090	+.0050	+.0020	+.0000	-.0020	-.0050	-.0090

Table 9-18a. VERTICAL TAIL TORSION MOMENT POWER DELTA

MACH	$\delta_{e_{IO}}$	α	β -6	-4	-2	0	+2	+4	+6
.6	10/9	4	-.0055	-.0080	-.0051	+.0000	+.0051	+.0080	+.0055
		0	-.0035	-.0060	-.0045	+.0000	+.0045	+.0060	+.0035
		-4	-.0050	-.0070	-.0050	+.0000	+.0050	+.0070	+.0050
		-8	-.0041	-.0070	-.0050	+.0000	+.0050	+.0070	+.0041
.8	10/9	4	-.0030	-.0028	-.0014	+.0000	+.0014	+.0028	+.0030
		0	-.0020	-.0017	-.0008	+.0000	+.0008	+.0017	+.0020
		-4	-.0004	-.0003	-.0003	+.0000	+.0003	+.0003	+.0004
		-8	-.0004	-.0003	-.0003	+.0000	+.0003	+.0003	+.0004
.9	10/9	4	-.0013	-.0065	-.0037	+.0000	+.0037	+.0065	+.0013
		0	-.0012	-.0062	-.0035	+.0000	+.0035	+.0062	+.0012
		-4	-.0009	-.0062	-.0035	+.0000	+.0035	+.0062	+.0009
		-8	-.0017	-.0070	-.0035	+.0000	+.0035	+.0070	+.0017
.95	10/9	4	-.0522	-.0391	-.0204	+.0000	+.0204	+.0391	+.0522
		0	-.0531	-.0395	-.0212	+.0000	+.0212	+.0395	+.0531
		-4	-.0510	-.0383	-.0199	+.0000	+.0199	+.0383	+.0510
		-8	-.0498	-.0374	-.0195	+.0000	+.0195	+.0374	+.0498
1.05	10/9	4	-.0286	-.0131	-.0101	+.0000	+.0101	+.0131	+.0286
		0	-.0218	-.0098	-.0093	+.0000	+.0093	+.0098	+.0218
		-4	-.0160	-.0073	-.0068	+.0000	+.0068	+.0073	+.0160
		-8	-.0152	-.0072	-.0068	+.0000	+.0068	+.0072	+.0152

Table 9-18b. VERTICAL TAIL TORSION MOMENT POWER DELTA

MACH	$\delta_{e_{IO}}$	α	β -6	-4	-2	0	+2	+4	+6
1.1	10/9	4	-.0122	-.0091	-.0062	+.0000	+.0062	+.0091	+.0122
		0	-.0021	-.0006	-.0049	+.0000	+.0049	+.0006	+.0021
		-4	-.0047	-.0035	-.0025	+.0000	+.0025	+.0035	+.0047
		-8	-.0081	-.0060	-.0041	+.0000	+.0041	+.0060	+.0081
1.15	10/9	4	-.0132	-.0028	-.0002	+.0000	+.0002	+.0028	+.0132
		0	-.0069	-.0015	-.0000	+.0000	+.0000	+.0015	+.0069
		-4	-.0069	-.0015	-.0000	+.0000	+.0000	+.0015	+.0069
		-8	-.0049	-.0009	-.0000	+.0000	+.0000	+.0009	+.0049
1.25	10/-2	4	-.0050	-.0032	-.0016	+.0000	+.0016	+.0032	+.0050
		0	-.0028	-.0033	-.0016	+.0000	+.0016	+.0033	+.0028
		-4	-.0029	-.0018	-.0009	+.0000	+.0009	+.0018	+.0029
		-8	-.0022	-.0012	-.0006	+.0000	+.0006	+.0012	+.0022
1.4	10/-2	4	-.0017	-.0009	-.0005	+.0000	+.0005	+.0009	+.0017
		0	+.0005	+.0005	+.0003	+.0000	-.0003	-.0005	-.0005
		-4	-.0009	-.0003	-.0003	+.0000	+.0003	+.0003	+.0009
		-8	-.0060	-.0044	-.0020	+.0000	+.0020	+.0044	+.0060

Table 9-19

FOREBODY FORCE COEFFICIENT TOLERANCES - SSLV AND ELEMENTS

MACH NO.	SSLV	ORB	ET	SRB(1)
		$\pm\Delta C_A$		
.6	.0038	.0010	.0010	.0025
.8	.0038	.0010	.0010	.0025
.9	.0038	.0010	.0010	.0025
.95	.0052	.0012	.0012	.0035
1.05	.0037	.0017	.0017	.0020
1.1	.0035	.0015	.0015	.0020
1.15	.0035	.0015	.0015	.0020
1.25	.0045	.0014	.0014	.0025
1.40	.0040	.0013	.0013	.0025
		$\pm\Delta C_N$		
.6	.0068	.0060	.0030	.0010
.8	.0077	.0070	.0030	.0010
.9	.0094	.0080	.0040	.0020
.95	.0101	.0080	.0050	.0025
1.05	.0099	.0080	.0055	.0015
1.1	.0089	.0070	.0050	.0015
1.15	.0067	.0050	.0040	.0015
1.25	.0055	.0030	.0030	.0025
1.40	.0079	.0030	.0020	.0050
		$\pm\Delta C_Y$		
.6	.0083	.0080	.0005	.0015
.8	.0083	.0080	.0005	.0015
.9	.0093	.0090	.0006	.0015
.95	.0109	.0100	.0007	.0030
1.05	.0098	.0080	.0010	.0040
1.10	.0093	.0060	.0010	.0050
1.15	.0082	.0040	.0008	.0050
1.25	.0064	.0030	.0006	.0040
1.40	.0052	.0030	.0006	.0030

Table 9-20

FOREBODY MOMENT INCREMENT EQUATIONS - SSLV AND ELEMENTS

ELEMENTS

$$\Delta C_M = \sqrt{\left[\Delta C_N \left(\frac{X_N}{L}\right)\right]^2 + \left[C_N \left(\frac{\Delta X_N}{L}\right)\right]^2 + \left[\Delta C_A \left(\frac{Z_A}{L}\right)\right]^2}$$

$$\Delta C_{YN} = \sqrt{\left[\Delta C_Y \left(\frac{X_{YN}}{L}\right)\right]^2 + \left[\Delta C_A \left(\frac{Y_{ZL}}{L}\right)\right]^2}$$

$$\Delta C_\ell = \sqrt{\left[\Delta C_Y \left(\frac{Z_L}{L}\right)\right]^2 + \left[\Delta C_N \left(\frac{Y_L}{L}\right)\right]^2}$$

SSLV TYPICAL

$$\Delta C_{M_{SSLV}} = \sqrt{(\Delta C_{M_o})^2 + (\Delta C_{M_{ET}})^2 + (\Delta C_{M_{RSRB}})^2 + (\Delta C_{M_{LSRB}})^2}$$

	ORB							ET						
MACH	$\frac{X_N}{L}$	$\frac{\Delta X_N}{L}$	$\frac{X_{YN}}{L}$	$\frac{Z_L}{L}$	$\frac{Y_{ZL}}{L}$	$\frac{Y_L}{L}$	$\frac{Z_A}{L}$	$\frac{X_N}{L}$	$\frac{\Delta X_N}{L}$	$\frac{X_{YN}}{L}$	$\frac{Z_L}{L}$	$\frac{Y_{ZL}}{L}$	$\frac{Y_L}{L}$	$\frac{Z_A}{L}$
.6	-.92	.03	-.98	.42	0	0	.26	-.7	0	-.7	.03	.03	.03	.03
.8	-.93	.03	-.94	.42	0	0	.26	-.7	0	-.7	.03	.03	.03	.03
.9	.96	.03	-1.02	.43	0	0	.26	-.8	0	-.8	.03	.03	.03	.03
.95	-1.01	.03	-1.03	.44	0	0	.26	-.8	0	-.8	.03	.03	.03	.03
1.05	-.95	.04	-1.02	.45	0	0	.26	-.8	0	-.8	.03	.03	.03	.03
1.10	-.96	.03	-1.01	.45	0	0	.26	-.8	0	-.8	.03	.03	.03	.03
1.15	-.97	.02	-1.0	.44	0	0	.26	-.8	0	-.8	.03	.03	.03	.03
1.25	-.98	.02	-1.0	.44	0	0	.26	-.8	0	-.8	.03	.03	.03	.03
1.40	-.99	.02	-1.0	.44	0	0	.26	-.8	0	-.8	.03	.03	.03	.03

SRB RIGHT / LEFT

MACH	$\frac{X_N}{L}$	$\frac{\Delta X_N}{L}$	$\frac{X_{YN}}{L}$	$\frac{Z_L}{L}$	$\frac{Y_{ZL}}{L}$	$\frac{Y_L}{L}$	$\frac{Z_A}{L}$
.6	-1.15	0	-1.15	0	±.194	∓.194	.02
.8	-1.15	0	-1.15	0	±.194	∓.194	.02
.9	-1.15	0	-1.15	0	±.194	∓.194	.02
.95	-1.14	0	-1.14	0	±.194	∓.194	.02
1.05	-1.14	0	-1.14	0	±.194	∓.194	.02
1.10	-1.13	0	-1.13	0	±.194	∓.194	.02
1.15	-1.10	0	-1.10	0	±.194	∓.194	.02
1.25	-1.10	0	-1.10	0	±.194	∓.194	.02
1.40	-1.10	0	-1.10	0	±.194	∓.194	.02

NOTE: L = 1290 INCHES

Table 9-21

FOREBODY FORCE TOLERANCES — COMPONENTS

WING TOLERANCES		VERTICAL TAIL TOLERANCES
MACH	$\pm\Delta$CNW	$\pm\Delta$CYV
.6	.0050	.010
.8	.0050	.010
.9	.0050	.030
.95	.0050	.030
1.05	.0060	.030
1.10	.0065	.010
1.15	.0060	.008
1.25	.0040	.010
1.40	.0040	.006

Table 9-22

FOREBODY MOMENT EQUATIONS — COMPONENTS

WING

$$\Delta C_{BW} = \Delta C_{NW} \left(\frac{y_w}{b}\right)$$

$$\Delta C_{TW} = \Delta C_{NW} \left(\frac{x_w}{\bar{c}}\right)$$

VERTICAL TAIL

$$\Delta C_{BV} = \sqrt{\left[\Delta C_{YV} \left(\frac{Z_V}{L}\right)\right]^2 + \left[C_{YV} \left(\frac{\Delta Z_V}{L}\right)\right]^2}$$

$$\Delta C_{TV} = \sqrt{\left[\Delta C_{YV} \left(\frac{X_V}{L}\right)\right]^2 + \left[C_{YV} \left(\frac{\Delta X_V}{L}\right)\right]^2}$$

HINGE MOMENT

$$\Delta CHEI = \Delta CHEI$$

$$\Delta CHEO = \Delta CHEO$$

	WING[1]		VERTICAL[2]					
MACH	$\frac{y_w}{b}$	$\frac{x_w}{\bar{c}}$	$\frac{Z_V}{L}$	$\frac{\Delta Z_V}{L}$	$\frac{X_V}{L}$	$\frac{\Delta X_V}{L}$	$\pm\Delta CHEI$	$\pm\Delta CHEO$
.6	.091	-.22	.60	.20	.34	.10	.0050	.0020
.8	.095	-.20	.75	.20	.33	.10	.0050	.0015
.9	.098	-.27	.42	.20	.59	.17	.0100	.0040
.95	.105	-.26	1.10	.25	.84	.20	.0130	.0100
1.05	.110	-.26	.72	.30	.51	.25	.0100	.0030
1.10	.100	-.28	.91	.30	.81	.20	.0080	.0010
1.15	.110	-.32	.63	.20	.87	.20	.0070	.0010
1.25	.110	-.33	.34	.15	.78	.15	.0050	.0010
1.40	.110	-.32	.45	.30	.40	.10	.0050	.0010

1 For Wing

b = 936.68"
c = 474.81"

2 Vertical

L = 199.8 in.

Section X

CONCLUSIONS

The IA119 test resulted in an appreciable amount of good plume induced aerodynamic data. Problems with the data were very limited and the power off data compares very good with other tests.

The base pressures showed good trends when plotted versus the current similarity parameter. This trend adds confidence to the similarity parameter and the test data.

The major independent variables that change the plume induced aerodynamic characteristics are angle of attack, angle of sideslip, inboard elevon deflection and SRB and SSME power level. The base and forebody plume induced aerodynamic characteristics and tolerances have been developed into math models compatible with the forebody math models.

The orbiter base plume induced aerodynamic characteristics are the result of a complicated integration of pressure coefficients and power delta pressure coefficients, that when combined with the forebody data, produce the proper total vehicle aerodynamic characteristics.

The ET base plume induced axial force is larger than previous analyses have predicted, however, it is felt that the present results are consistent and representative of the ET base pressure environment.

The plume induced near field (base environment) and far field (orbiter forebody wing and hinge moment data) had good consistent trends when plotted versus the plume similarity parameter. The consistency of the data for both the near field and far field added confidence in the similarity parameter used.

Section XI

RECOMMENDATIONS

A computer program was developed to integrate the pressure data for all elements and components and tabulate the results and the results of the gauge data. The tabulated results and plotted power variation data represent approximately 1500 computer printout pages. Time did not permit an extensive analysis of all the data. It is recommended that additional analyses be conducted of the vertical tail data, wing data, inboard hinge moment data and orbiter fuselage data.

Section XII

REFERENCES

1. Dziubala, T. J., Marroqoin, J., "Pretest Information for Test IA119 of the 0.020-Scale 88-OTS Configuration 140 C (Modified) Integrated Space Shuttle Vehicle Test-Plume Model in the NASA/ARC UP WT 11 by 11 Foot Leg for Determination of Aspiration-Induced Effects", Document SD-77-SH-0196, Rockwell International, Space Division, September 20, 1977.

2. Informal notes and figures, some from RI memo SAS/WTO/74-367.

3. Program 7412 "Calibration of 88075 SRB and MPS Flow Through Nozzles", Test Log, Rocket Nozzle Wind Tunnel, Rocketdyne, dated 8/10/74.

4. Program 7501, "Space Program IA-19 Plume Recalibration of SRB Nozzles 88075", Test Log, Rocket Nozzle Wind Tunnel, Rocketdyne, dated 8/10/74.

5. Program 7503, "Calibration of 88075 Contoured MPS Nozzles IA-80", Test Log, Rocket Nozzle Wind Tunnel, Rocketdyne, dated 10/22/74.

6. Program 7508, "Plume Calibration of Pressure Instrumented SRB OTS", Test Log, Rocket Nozzle Wind Tunnel, Rocketdyne, dated 4/25/75.

7. Harden, R. B., Campbell, J. R. II, "Pretest Information for Test IA19 of the 0.02 Scale 88-OTS Jet Plume Space Shuttle Model in the 11x11 Foot Leg of the NASA/ARC Unitary Plan Wind Tunnel", Document 5074-SH-0276, Rockwell International Space Division, dated 3/9/74.

8. Andrews, C. D., "MSFC Input for RI/SD SSLV Wind Tunnel Tests IA119/IA138 NASA Memo ED32-77-13, dated February 23, 1977.

9. Boyle, W. W., "Plume Technology Program Base Pressure Similarity Parameters", NSI Memo M-9210-76-45, dated July 1976.

10. Boyle, W. W., Jordan, T. A., "SSLV Aerodynamic Large Model Data Analysis", TR-230-1935, Northrop Services, Inc., dated 1978.

11. Aero Sciences Staff, "Aerodynamic Design Data Book, Vol. II: Mated Vehicle", Document SD72-SH-0060-2I Rockwell International Space Division, dated December 1976.

12. Allen, E., Chee, E., Daileda, J. J., "Pretest Information for IA156A of the 0.02 Scale Model 89-OTS of the Space Shuttle Integrated Vehicle in the AEDC Propulsion Wind Tunnel (16T)", Doc. SD-77-SH-0195, Rockwell International Space Division, dated 4 August 1977.

13. Allen, E., Chee, E., Hawthorn, P., "Pretest Information for Test IA105A of the 0.03 Scale Pressure Loads Model 42-OTS of the Space Shuttle Integrated Vehicle in the 16-Ft Transonic Test Section of the Propulsion Wind Tunnel at AEDC, Rockwell International, Space Division, Document SD77-SH-0194, dated 2 September 1977.